Australian Government

Australian Fisheries Management Authority

Bass Strait Central Zone Scallop Fishery — Population biology and bed dynamics

AFMA Project 2022-0809

2025

Andrew Penney, Matt Koopman and Ian Knuckey

fishwell

© 2025 Fishwell Consulting

All rights reserved.
ISBN: 978-0-6453571-9-6

Title: Bass Strait Central Zone Scallop Fishery — Population biology and bed dynamics

AFMA Project 2022-0809

Ownership of Intellectual Property Rights

Unless otherwise noted, copyright (and any other intellectual property rights, if any) in this publication is owned by the Fishwell Consulting and the Australian Fisheries Management Authority.

This publication (and any information sourced from it) should be attributed to:

Penney, A. Koopman, M., and I. Knuckey. (2025). Bass Strait and Central Zone Scallop Fishery – Population Dynamics. AFMA Project 2022-0809. Fishwell Consulting. 148 pp.

Creative Commons licence

All material in this publication is licensed under a Creative Commons Attribution 4.0 Australia Licence, save for content supplied by third parties, logos and the Commonwealth Coat of Arms.

Creative Commons Attribution 4.0 Australia Licence is a standard form licence agreement that allows you to copy, distribute, transmit and adapt this publication provided you attribute the work. A summary of the licence terms is available from https://creativecommons.org/licenses/by/4.0/ The full licence terms are available from https://creativecommons.org/licenses/by/4.0/legalcode.en

Inquiries regarding the licence and any use of this document should be sent to: ian@fishwell.com.au

Cover photo: Jess Kube

Disclaimer

The authors do not warrant that the information in this document is free from errors or omissions. The authors do not accept any form of liability, be it contractual, tortious, or otherwise, for the contents of this document or for any consequences arising from its use or any reliance placed upon it. The information, opinions and advice contained in this document may not relate, or be relevant, to a reader's particular circumstances. Opinions expressed by the authors are the individual opinions expressed by those persons and are not necessarily those of the publisher, research provider or the AFMA.

Researcher Contact Details
Name: Ian Knuckey
Address: Fishwell Consulting
27A Hesse St Queenscliff, VIC 3225
Phone: +61 3 5258 4399
Web: www.fishwell.com.au

Contents

List of Tables

List of Figures

List of Maps

Acknowledgements

We would like to thank the owners, skippers and crews of all of the commercial scallop vessels that have undertaken the surveys from 2015 to 2023. We appreciate the hard work and dedication of the scientific observers over this time, including Russell Hudson, Jess Kube, Bryce Nurnatis, Tiffany Sih, Michael Davis and Graeme Ewing worked very hard to collect all data required to a high-quality standard. AFMA staff including Steve Hall, Daniel Corrie, Andrew Powell, Yvette Lamont, Sally Weekes (AFMA), provided the logbook data used to guide the survey design. AFMA, together with the members of ScallopRAG, ScallopMAC and the BSCZSF Co-Management Committee provided valuable input into the survey logistics and design over the years.

Executive summary

The Bass Strait Central Zone Scallop Fishery (BSCZSF) is an important component of the region's commercial fisheries, focusing primarily on harvesting the Commercial Scallop (*Pecten fumatus*). This species exhibits considerable variability in population dynamics, driven by variations in recruitment, growth rates, mortality, and abundance. Scallops in this fishery are known to be highly sensitive to changes in environmental conditions and subsequent effects on natural life cycles, which can lead to rapid shifts in spatial distribution of population biomass.

This study, undertaken by Fishwell Consulting in collaboration with the Australian Fisheries Management Authority (AFMA), presents a comprehensive analysis of scallop population biology and bed dynamics within the BSCZSF. Using data and analyses derived from biomass surveys conducted from 2015 to 2023—excluding a gap year in 2020 due to the COVID-19 pandemic—the study offers analysis and insights aimed at improving the understanding of population trends, bed connectivity, recruitment and mortality. The surveys were designed to capture variability across different regions, including King Island, Flinders Island, and Apollo Bay, while incorporating industry feedback and input from the Scallop Resource Assessment Group (ScallopRAG) to adapt survey designs to emerging population trends.

The key conclusion from this work is that scallop productivity is highly variable and unpredictable, such that most productivity assumptions used in stock assessments (e.g. regarding existence of a stock-recruit relationship, likelihood of a constant M and similar growth across regions and years), are untenable. Regular biomass surveys remain the most reliable way to obtain estimates of exploitable biomass. In particular, results of this study confirm that scallop recruitment is highly variable, both temporally and spatially. Long periods can occur without successful scallop recruitment in a region, despite there being adult populations present that spawn every year. In contrast, substantial dense settlements of recruits can suddenly appear in several beds, even across several regions. However, the distribution of recruits is typically highly patchy, often occurring only in parts of several individual survey beds.

Analyses revealed significant inter-annual and spatial variability in biomass and density across different beds and regions within the fishery. Many beds exhibited notable inter-annual changes in population dynamics, including recruitment pulses marked by the emergence of smaller scallops, together with declines in biomass due to fishing pressure and natural mortality. These fluctuations in abundance, often driven by complex interactions between biological and environmental factors, underscore the need for continuous monitoring and flexible management responses.

Within the regions defined for analyses, population structure was found to be similar across nearby survey beds, indicating that these populations resulted from a similar history of recruitment and growth, and are likely to be components of the same population. These aggregated regions span distances of some 15 – 30 km (diagonal) per region. Genetic analyses by Ovendon *et al*. (2016) indicated that populations in Bass Strait within 45 km of one another are unlikely to be genetically distinct.

An important aspect of the study was investigating the influence of Bass Strait's tidal currents on scallop distribution and bed connectivity. The region’s complex tidal currents play a critical role in shaping recruitment and dispersal patterns. Using information from the Integrated Marine Observing System (IMOS), the study explored how tidal flow and substrate conditions influence scallop settlement and population distribution, and potential for connectivity among adjacent beds.

The distribution of scallop beds is associated with areas of highest tidal current flow, between 30 – 60 m depth. Tidal currents, as modified by winds and larger oceanographic current features, are a likely candidate for dispersal of scallop larvae among smaller beds within regions, with beds being closely aligned with tidal current directions in the area to the north and east of King Island. Off King Island, the bathymetry is relatively flat, potentially facilitating settlement over a larger area compared to off Flinders Island. The situation appears to differ in the area east of the Flinders Island chain, with scallop beds being aligned north – south, across the direction of tidal flow, although still within the 30 – 60 m depth range and the area of highest tidal current velocity. Anecdotal information from industry suggests that settlement in this area is associated with “sand hills” that may act to interrupt or disrupt current flow.

Within regions of up to at least 45km extent, subject to strong current flows, cross seeding of smaller beds within those regions is likely. The widespread recruitment across much of the Apollo Bay / King Island area over 2018 – 2023, including extension of scallop beds into areas previously not considered to support commercially-viable populations, indicates widespread dispersal of larvae, perhaps resulting from favourable spawning conditions across several regions. However, such recruitment events do not occur every year, with long periods of apparent poor recruitment in some regions. It therefore remains prudent to leave components of populations across regions (~30 - 45 km in extent) unfished to allow for successful recruitment should favourable spawning conditions occur. However, this does not mean protection of populations within each and every individual survey bed in each region.

Growth and recruitment analyses provided further insights into the biological dynamics of the scallop population. Length-frequency data revealed distinct recruitment events across different beds and regions, revealing recruitment timing, strength, and regional growth variability. Growth patterns, modelled using von Bertalanffy growth curves, varied significantly across regions, reflecting differences in environmental conditions and in population densities. These findings are essential for understanding how environmental factors and spatial distribution impact growth and recruitment, and how these dynamics influence population sustainability.

Detailed morphometric data collected during the surveys further contributed to understanding the biological characteristics of scallops across different beds. Measurements of shell dimensions, weights, and gonad staging provided valuable insights into the reproductive condition and health of scallops. These data, combined with growth and recruitment analyses, offer a comprehensive view of scallop population dynamics and their response to environmental and fishing pressures.

The study also focused on mortality patterns within the fishery, distinguishing between natural and fishing-induced mortality. Mortality estimates were derived from biomass comparisons, shell condition assessments, and analysis of dead shell presence. The findings indicate that mortality events, including instances of mass natural mortality, are a significant factor influencing population dynamics. These events have varied substantially among beds and years, and may be driven by environmental stressors, predation, and other factors, necessitating close monitoring and adaptive management responses to mitigate their impact.

As has been anecdotally reported by industry, scallops do appear to be susceptible to mass mortality events at ages of around 6+ to 8+ and shell lengths of around 90mm – 120mm. Dramatic biomass declines have been observed between survey years in beds consisting primarily of adult scallops, with no recruitment and little fishing mortality. These declines have been observed in the Apollo Bay region over 2017 – 2019, Apollo Bay East over 2021 - 2022, King Island Mid over 2015 – 2018, King Island East over 2017 - 2019, Flinders Island North over 2016 – 2017 and Flinders Island South over 2022 – 2023.

Mass mortality of juvenile scallops also seems to occur following particularly dense settlements, such as that observed in the King Island – JH bed in 2019. Although the adult mass mortalities do not seem to be related to density, mass mortality of juveniles is probably density dependent, as small scallops grow to exceed the carrying capacity of the bed.

These findings underscore the importance of continuous monitoring, flexible management measures, and collaboration with industry stakeholders to ensure the long-term sustainability of the fishery. Ongoing data collection and analysis, together with technological advancements in survey and monitoring methods, will improve the fishery's management and resilience. The study’s findings on biomass and density trends highlight the importance of adaptive management measures, including area closures, rotational fishing, and biomass-based catch limits, to ensure the sustainability of the scallop stock. Responsive, adaptive management of the fishery is vital to ensure sustainability while adhering to the Commonwealth Fisheries Harvest Strategy Policy 2018 (HSP).

1. Introduction

The main target species in the Bass Strait Central Zone Scallop Fishery (BSCZSF) is the Commercial Scallop, *Pecten fumatus*. Commercial Scallops in wild populations live for between five and nine years but have been observed to die-off rapidly after only three to five years in some situations (Haddon *et al.,* 2006). The species is generally subject to high spatial and temporal variability in recruitment and abundance, variable growth and mortality, and rapidly changing meat yield and reproductive condition. This variability means that management of Commercial Scallops must adapt to short-term changes in distribution and abundance of scallops, yet still ensure protection of the resource consistent with the *Commonwealth Fisheries Harvest Strategy Policy 2018* (HSP).

Biomass surveys in scallop beds in the BSCZSF have been undertaken by Fishwell Consulting using a relatively consistent methodology since 2015 (with the exception of 2020 during which no survey was undertaken because of the COVID-19 pandemic). Additional surveys during November and April of 2021 were undertaken in limited areas during the Beach Energy BACI survey, which was also contracted to Fishwell Consulting (Koopman et al. 2022). The data collected includes operational, retained and discarded catch, gonad stage, morphometrics and size frequency, which enables estimation of biomass, densities in weight and number, potential discard rates, and catch composition. Furthermore, the data were analysed to provide a rough indication of mortality (through percent composition of dead shell), effect of recruitment/density of changes in biomass and potential recruitment connectiveness through size frequency and morphometrics. In many cases, scallop beds have been repeatedly surveyed, providing a time-series of information which is currently underutilised.

This time series contains potentially valuable information for improving understanding of population dynamics, growth, recruitment, and bed structure to inform the management of the fishery. This information would be particularly valuable in the event that an annual survey cannot be undertaken, as occurred, for example, during 2020. Such information could be used to make predictions about scallop biomass and discard rates during off years. However, results would also be valuable to discussions around management arrangements in ScallopRAG and Scallop Management Advisory Committee (ScallopMAC) meetings in those years when biomass surveys were undertaken.

2. Objectives

- Compile all BSCZSF biomass survey and Beach Energy BACI survey data including, scallop catch, density and biomass, percent composition of dead shell, density of predators, morphometric and length frequency data, as well as commercial catch by scallop bed since 2015.
- Undertake thorough analyses of those data to better understand the population dynamics, connectiveness and biological characteristics of Commercial Scallops in the BSCZSF.

3. Methods

3.1. Survey design and history

The first 2015 survey covered three beds in the King Island (KI) region and one bed in the Flinders Island (FI) region (Map 3-1 to Map 3-3). To provide greater flexibility in management arrangements regarding closures, the pre-season survey was expanded in 2016 with the addition of an extra four beds in the KI region and another bed in the FI region. In addition to extra survey sites, the boundaries of some of the 2015 beds were modified (for example northern and southern boundaries of the bed known as KI-Main in Knuckey *et al.* (2015) were brought in slightly, and the eastern and western boundaries moved east slightly to form a bed titled KI-2 in Knuckey *et al.* (2016)). The beds surveyed during 2017 were based on advice from the Scallop Research Workshop and input from ScallopRAG and the BSCZSF Co-Management

Committee. They comprised previously surveyed beds, modified beds and new exploratory beds. In 2018 two beds were added off King Island, while Apollo Bay (AB) – 3, AB – 4, FI – 3 and FI – 4 were not surveyed. In 2019 as well as the FI bed, AB 1 and 2 were surveyed, and two new beds (one stretching south-east of KI BlueDot Extended (BDE) and another called the KI – JH bed comprising high density of juvenile scallops) were added. To protect the juveniles at KI – JH, sampling intensity was reduced, and a fine mesh cover was placed over half of the dredge to improve sampling of small scallops. No survey was undertaken in 2020 because of concerns regarding the COVID-19 outbreak. Twelve beds were surveyed in 2021 when the FI – North - The Sisters and FI – North of Babel (NB) beds were added in the FI region, the KI – JH site was extended to the southeast, AB – 2 was extended to the north and AB – The Hill and AB – Five Hours sites were added in the AB region.

Significant catches were taken from an area to the north-west of the FI South – North of Babel site during 2021. Accordingly, new beds were surveyed in 2022 (FI – Wreck A together with FI – The Wreck B) to reflect that catch.

New beds introduced in 2023 included: KI – Three Hummocks East, KI – Three Hummocks West and FI – The Sisters East. The Three Hummocks beds were based on results of an FRDC funded industry survey in December 2021 that showed high densities of undersized scallops. Similarly, VMS data showed high fishing effort in a new bed east of the Sisters. Accordingly, a new bed (FI – The Sisters East) was surveyed there in 2023.

More generally, the beds surveyed in 2023 were based on previous surveys, analysis of 2022 catch and effort data and advice from the ScallopRAG and the BSCZSF Co-Management Committee.

Changes to the beds surveyed since 2015 are outlined below.

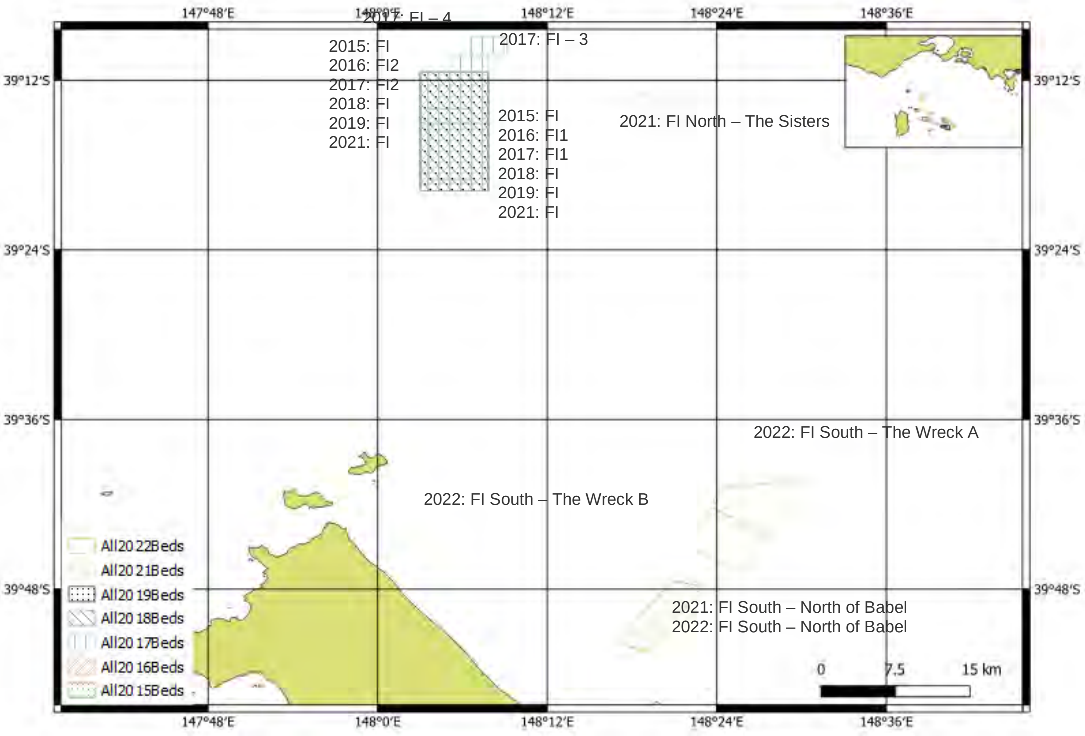

Map 3-1. History of beds surveyed off Flinders Island from 2015 to 2022.

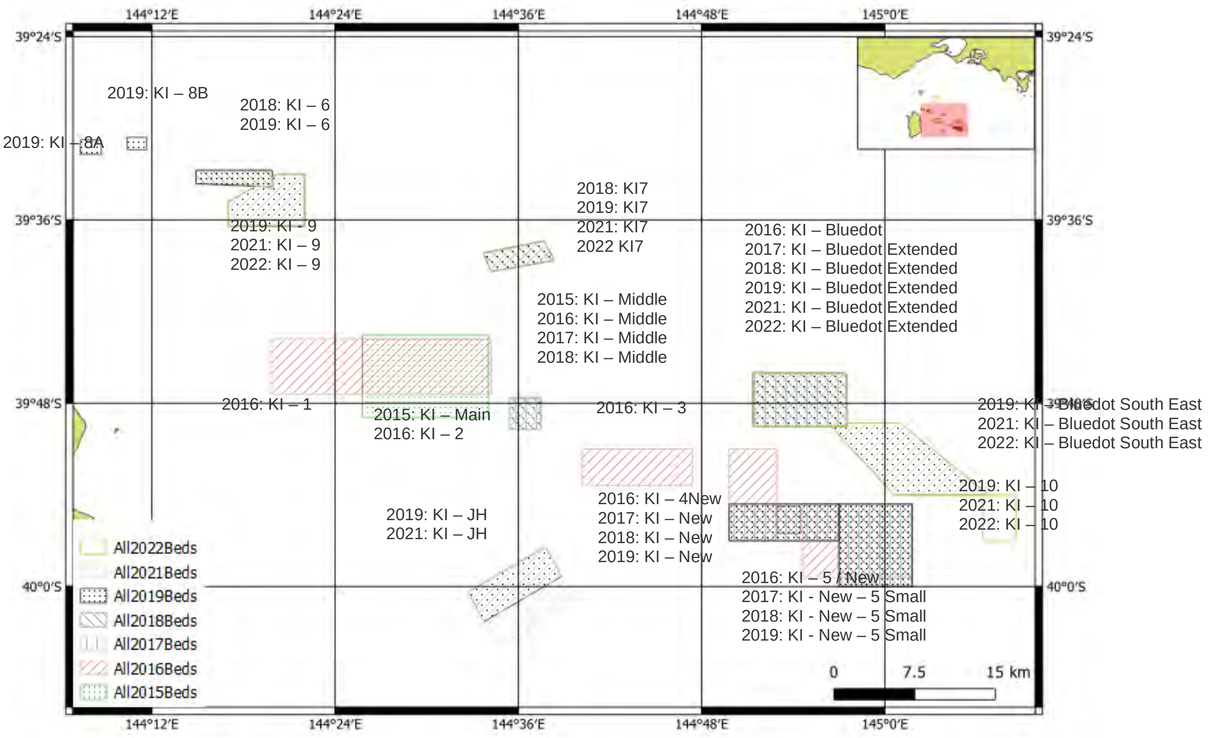

Map 3-2. History of beds surveyed off King Island from 2015 to 2022.

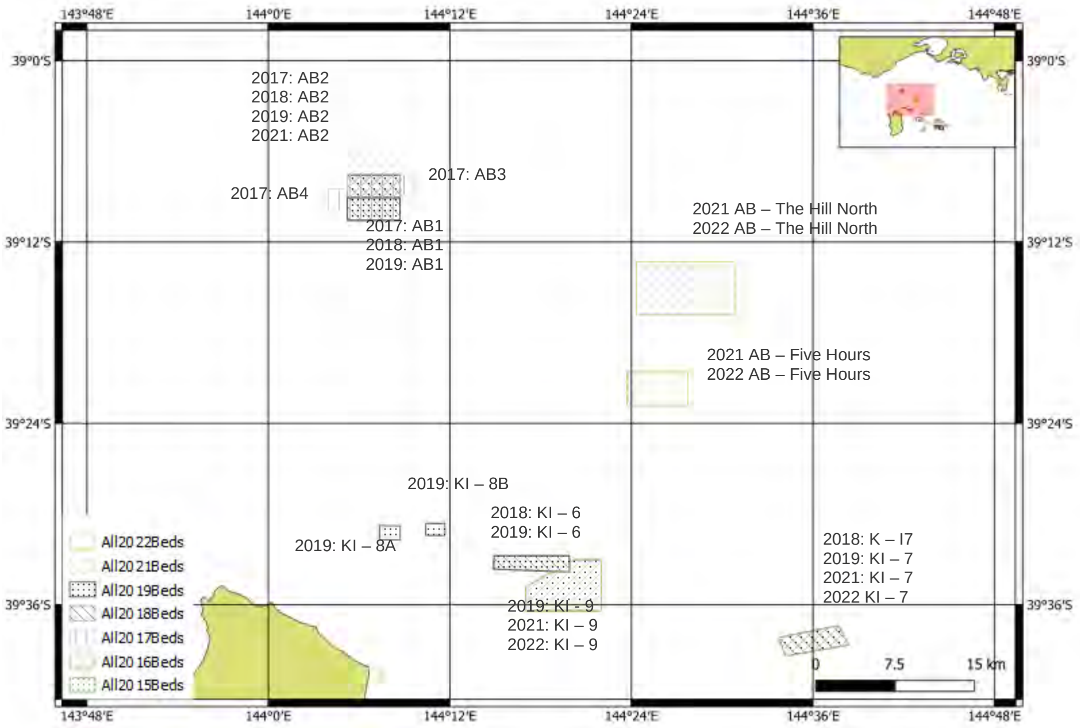

Map 3-3. History of beds surveyed off Apollo Bay and King Island from 2015 to 2022.

New beds surveyed off King Island (Three Hummocks East and Three Hummocks West) and Flinders Island (the Sisters East) in 2023 are described in Table 3-1 and shown in Figure 3-1and Figure 3-2.

Table 3-1. Description of beds surveyed since 2015 and beds new to 2023. See Map 3-1 to Map 3-3 for maps of beds.

Bed Code	Description
KI – 5S	Originally a larger area that was surveyed in 2016, KI – 5S was formed by extending the eastern boundary of KI-New south to -40˚S and including the area of KI – 5 to the east of that. This bed remained unchanged from the 2017 to 2019 when it was last surveyed.
KI – New	KI-New was a bed that was defined for management proposes (it formed the initial closure) after the 2016 survey, covering at least parts of three different beds surveyed in 2016. It comprised parts of a bed called KIEast which was surveyed during 2015, and again in 2016, together with two new adjacent beds, KI – 4 and KI – 5. KI – New remained unchanged from the 2017 to 2019 when it was last surveyed.
KI – BDE	During the TAC setting by the MAC for the 2016 season, industry provided information regarding a dense bed of small scallops that would be more suitable for closure than the KI – New bed. This bed titled King Island Blue Dot was mapped out and then surveyed during August of 2016. The area was expanded north and west to form an area closure that replaced the closure of KI – New. The boundaries of this expanded area are shown in Map 3-2. This bed remained unchanged from the 2017 to 2022 surveys.
AB – 1 and AB – 2	Seven exploratory marks in the KI region were provided by industry in 2017 to be explored and considered for additional survey beds. Only one of those showed enough promise to survey, and the skippers mapped out area, splitting it into two beds. Two additional smaller beds were added to each of the western and eastern boundaries. However, these contained low densities of scallops and were omitted from the 2018 and future surveys. The AB-1 and AB – 2 bed boundaries remained unchanged during the 2018 and 2019 surveys. For the 2021 survey, only AB – 2 was surveyed, and the northern boundary was moved north to include relatively high levels of commercial effort in that area. Neither beds were surveyed in 2022
KI – 6	Examination of 2018 commercial catch and effort data revealed significant catches in a large area at approximately longitude 144˚ 17’, latitude 39˚ 32’. The vessels mapped out this area to provide a smaller area with high density scallops with the boundaries shown in Map 3-2. The bed boundaries remained unchanged from the 2018 survey, was resurveyed in 2019, but omitted for the 2021 survey.
KI – 7	Examination of 2018 commercial catch and effort data revealed significant catches in a large area at approximately longitude 144˚ 36’, latitude 39˚ 38’. The vessels mapped out this area to provide a smaller area with high density scallops with the boundaries shown in Map 3-2. The bed boundaries remained unchanged from the 2018 survey, was resurveyed in 2019 and in 2021 as a replacement for KI – Mid (in accordance with ScallopRAG recommendations).
FI	FI-1 was named the “Flinders Island” bed during the 2015 survey. For the 2016 and 2017 surveys, the area was expanded and spilt into the two beds (FI – 1 and FI – 2). Two additional smaller beds were added to the northern boundary of FI-2 in 2017. However, because of low densities, these beds were omitted for the 2018 survey. For the 2018 survey, FI – 1 and FI – 2 were combined into a single large bed (Map 3-1). The bed boundaries remained unchanged from the 2018 survey and the bed was resurveyed in 2019, 2021 and 2023, but not in 2022.
KI – 8a and KI – 8b	Examination of 2019 commercial catch and effort data revealed significant catches in a large area at approximately longitude 144˚ 10’, latitude 39˚ 31’. Within this general area, there were three main patches of densely populated scallop beds separated by areas of low density and an underwater cable. The two largest of these small areas were selected to survey in that year. They were not surveyed in 2021 or 2022.
KI – 9	Examination of 2019 commercial catch and effort data revealed significant catches in a large area at approximately longitude 144˚ 21’, latitude 39˚ 35’. The final boundaries were set based on a combination of fishing effort by the survey vessel in the previous year and exploratory fishing. This bed was resurveyed in 2021 and 2022.
KI – JH	An industry member provided two marks that bound a line of exploratory tows that yielded relatively high densities of juvenile scallops (~50 mm). Being the most recent sign of significant recruitment, there was interest in tracking the growth of this bed. However, there was concern of potential to disturb the bed by surveying it. As a compromise, a relatively small survey area was set with only 20 survey sites. Based on advice from industry, the bed was extended to the south-east for the 2021 survey. This bed was not surveyed in 2022
KI – BDSE	Examination of 2019 commercial catch and effort data revealed significant catches in a large area at approximately longitude 145˚ 00, latitude 39˚ 49. The final boundaries were set based

	on a combination of fishing effort by the survey vessel in the previous year and exploratory fishing. This bed was resurveyed in 2021 and 2022.
KI – Mid	This bed remained unchanged from 2015, 2016, 2017 and 2018. In accordance with ScallopRAG recommendations, five exploratory tows were conducted within this bed during 2021 revealing low densities (no scallops were caught), and so KI – 7 was surveyed instead. This bed was not surveyed in 2022.
KI – 10	Significant catches were taken from an area to the south-east of the KI-BDSE site during 2020. KI – 10 is a bed that surrounds that catch and was surveyed in 2021 and 2022.
AB – The Hill North	Industry members provided marks about 17 nm to the south-east of Apollo 2 where significant amounts of scallops were caught in 2020. Based on commercial effort reported from the area, and notes made on a fishing vessel's plotter, a bed was defined and surveyed in 2021 and 2022.
AB – Five hours	Industry members provided marks about 19 nm to the south-east of AB – Apollo 2 where significant amounts of scallops were caught in 2020. Based on commercial effort reported from the area, and notes made on a fishing vessel's plotter, a bed was defined and surveyed in 2021 and 2022.
FI – North - The Sisters	Significant catches were taken from an area about 11 nm to the east of the FI site. Based on commercial effort reported from the area, and notes made on a fishing vessel's plotter, a bed was defined. This bed was surveyed in 2021, but not in 2022.
FI – South – North of Babel	Significant catches were taken from an area about 31 nm to the south-south-east of the FI site. Based on commercial effort reported from the area, and notes made on a fishing vessel's plotter, a bed was defined and surveyed in 2021 and 2022.
FI – The Wreck A	Significant catches were taken from an area to the north-west of the FI South – North of Babel site during 2021. FI – The Wreck A was a new bed in 2022 that, together with FI – The Wreck B, surrounds that catch.
FI – The Wreck B	Significant catches were taken from an area to the north-west of the FI South – North of Babel site during 2021. FI – The Wreck B was a new bed in 2022 that, together with FI – The Wreck A, surrounds that catch.
KI – Three Hummocks West	An industry-led survey in December 2021 (as part of a FRDC project) revealed high densities of undersized scallops. The bed was not surveyed in 2022 as many scallops remained undersized.
KI – Three Hummocks East	An industry-led survey in December 2021 (as part of a FRDC project) revealed high densities of undersized scallops. The bed was not surveyed in 2022 as many scallops remained undersized. The division between the two beds of the Three Hummocks (Figure 3-1) reflects a difference in depth (and size composition) of scallops.
FI – The Sisters East	For the 2023 survey, the previously agreed FI – North bed was replaced with an eastern extension to FI – North - The Sisters. This new bed is based on VMS data and commercial fisher input (Figure 3-2).

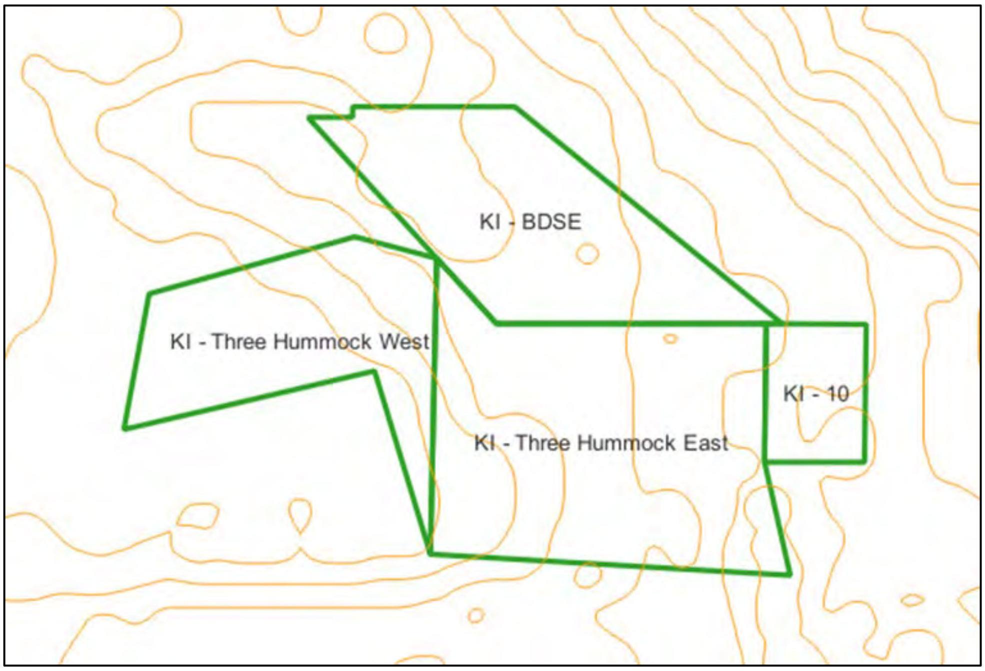

Figure 3-1. New beds surveyed in 2023 off King Island (Three Hummocks West and Three Hummocks East) in relation to historical beds. One metre incremental bathymetry is show in orange.

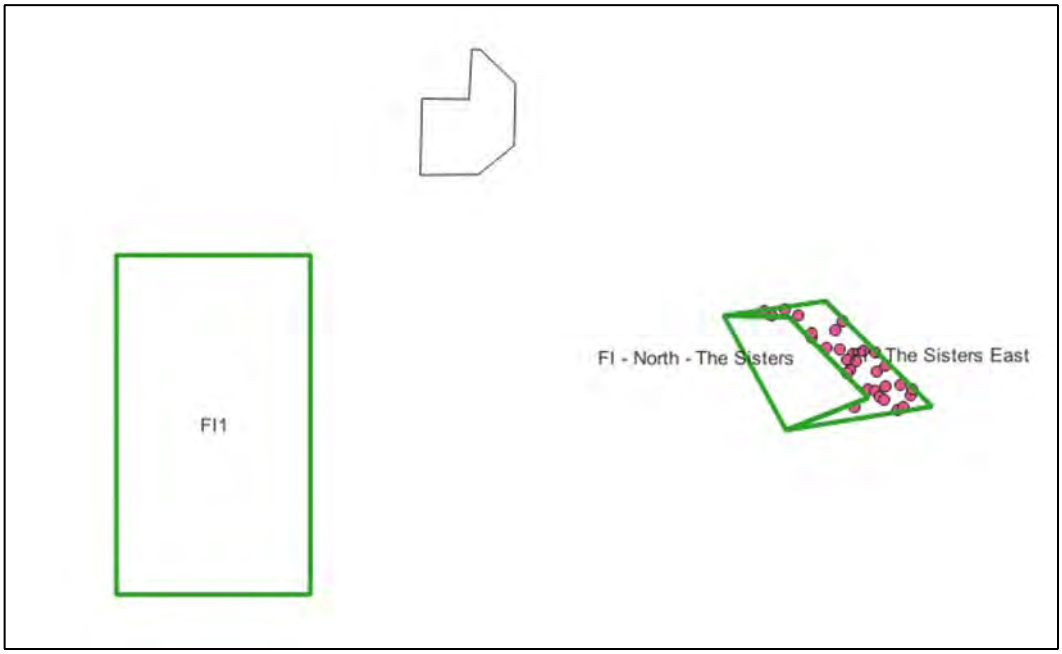

Figure 3-2. New beds surveyed in 2023 off Flinders Island – The Sisters East (with survey sites indicated) and Flinders Island – North – The Sisters (grey polygon). The FI historical survey bed is also shown. The black polygon in the north shows a bed that was proposed during the survey design based on incorrect logbook data that was subsequently moved to create the Flinders Island – The Sisters East bed

3.2. Data preparation

The data used in the analyses presented in this report were the data collected during the annual scallop dredge surveys conducted from 2015 – 2023 (2020 excluded due to COVID-19 restrictions) (see survey reports by Knuckey *et al.* (2015, 2016, 2017, 2018); Koopman *et al.* (2019, 2021) and Koopman and Knuckey 2022). Data collected by observers during each scallop dredge survey were collated and converted into standard format data files during each survey, suitable for subsequent analysis in R analysis software (R Core Team 2024).

Spatial data

All length-frequency, density and biological data were recorded together with the accurate start and end position of each dredge tow in longitude and latitude. Scallop survey beds were selected and geo-spatially specified in consultation with industry before each annual survey, modified when necessary following initial dredge tows to exclude areas with low scallop density, or expanded to include adjacent areas with significant scallop densities (see previous survey reports for details). Polygon shapefiles for each survey bed in each year were prepared in QGIS® geospatial mapping software (QGIS.org 2024) and subsequently also imported into Arcview® for further analyses. Seabed areas (km^2) of scallop beds surveyed in each year were calculated from these shapefiles.

Survey catch data

In addition to other data used to calculate some of the catch data, pre-prepared catch data included the following main fields:

Bed	Region	Survey Num	Set Num	Day	Month	Year	Lon	Lat	Green Wt	Area Swept	Scallop Density	Selected Density
KI - BDSE	KI	1	1	17	5	2023	144.9951	-39.8245	1	2606.83	0.000376	0.001140
KI - BDSE	KI	21	2	17	5	2023	144.9772	-39.8415	2	2606.83	0.000766	0.002320

Bed is a unique bed code allocated to each survey bed in each year, Survey Num is a unique number for each random shot in each bed (the tow number), Set Num is a sequential number of the shot for each trip, Day, Month and Year are extracted from the Start Date for each tow, Lon/Lat is the midpoint of the tow, between two start and end positions calculated from the tow start and end positions, Green Wt is the approximate total weight (measured onboard) of the total catch for the tow, Area Swept is the swept area of the dredge tow calculated from tow distance and dredge width, Scallop Density is the total number of scallops in the tow divided by the swept area (in kg.m^{-2}) and Selected Density is the density of scallops adjusted for dredge selectivity.

Survey length frequency data

Pre-prepared length-frequency data are contained the following fields:

Bed	Survey Num	Year	Sample Wt	Length	Size Limit	Green Wt	Area Swept	No. of Scallops	Weighted Freq	Lon	Lat
AB - 1	1	2017	4.8	108	over	214	2319.22	2	89.17	144.1366	-39.1424
AB - 1	1	2017	4.8	103	over	214	2319.22	5	222.92	144.1366	-39.1424

Data for each tow were split into separate records, one for each scallop length class found in each tow, with other tow-specific fields (Bed, Survey Num, Year, Sample Wt, Green Wt, Area Swept, Lon and Lat) being duplicated across records for each tow. Bed is a unique bed code allocated to each survey bed in each year, Survey Num is a unique number for each random shot in each bed (the tow number), Sample Wt is the approximate weight (measured onboard) of the sample taken from the total catch for the dredge tow, Length is the length class (shell height in mm) for the scallops in this record, Green Wt is the approximate total weight (measured onboard) of the total catch for the tow, Area Swept is the calculated swept area of the dredge tow, calculated from tow distance and dredge width, No. of Scallops is the total number of scallops of the length class for this record recorded in the sampled weight, Weighted Freq is the number scallops measured raised by the ration of Catch Wt / Sample Wt, and Lon/Lat is the midpoint of the tow, between two start and end positions.

Survey biological data

Biological data recorded for each biologically sampled scallop included the following fields:

Bed	Survey Num	Year	Lon	Lat	Length	Height	Width	Weight	Stage	Flesh Wt	Meat Wt	Gonad Wt
AB - 1	2	2019	144.10219	-39.17494	101.7	83.3	22.9	83	3	38	14	24
AB - 1	2	2019	144.10219	-39.17494	108.4	88.7	24.3	108	3	46	14	32

Bed is a unique bed code allocated to each survey bed in each year, Survey Num is a unique number for each random shot in each bed (the tow number), Lon/Lat is the midpoint of the tow, between two start and end positions, Length is the shell length (mm), Height is the shell height (mm), Width is the shell width (mm), Stage is the maturity stage of the gonad as determined by observers) (see Shell measurement and gonad staging), Flesh Wt is the total weight of the scallop flesh, gonad plus meat, Meat Wt is the weight of the gonad meat only, Gonad Wt is the weight of the gonad only.

Survey data filtering and coding

Data collected in individual scallop surveys has been analysed and reported separately for each survey. Analysis methodology (such as R coding) has been increasingly standardised over the years, but this report is the first time that data from all years have been merged and analysed. Inevitably, some inconsistencies were found such as the exact codes used for different scallop beds in different years. There are also many data records that cannot be used in certain analyses (such as length-frequency analysis) due to missing data, e.g. no scallops caught, or measured for a tow, or the positional data missing for some tows.

Data filtering

The main consolidated data file used for trend and length-frequency analysis was the length-frequency data file, which contains all but the biological sampling data. The initial data set contained 50,453 records. Of these, 23 records were deleted due to missing catch weight, sample weight, or tow position. Many records with NA in fields that should appropriately be 0 (number of scallops, sample weight, catch weight) were changed to zero for calculation purposes. Some records had missing Area Swept or Lon/Lat in the consolidated data file and these were sourced from individual survey data files. Apparent duplicate tow numbers resulting from missing additional attributes (such as Beach Energy Before/After surveys) were allocated unique tow number suffixes.

Standardisation of scallop bed codes

Initial analyses, particularly a comparison of bed codes used in data records and the codes of geospatial scallop bed polygons mapped using GIS, showed inconsistencies in how some beds were coded between the spatial and length-frequency data, or for the same beds in different years. Since the first survey, scallop beds have been allocated a code to be used in analyses. This has generally, but not always, included region prefix for the Apollo Bay (AB) King Island (KI) and Flinders Island (FI) regions of the Strait, followed by an abbreviation of the bed name, or a number indicating a particular bed.

Bed boundaries have also changed between surveys, and these changes have sometimes been indicated by addition of a letter indicating the change, such as South (S) or Extended (E), and sometimes by a different number. For example, the BlueDot survey bed added to the King Island region in 2016 (KI – BD) was extended and renamed to KI – BDE for the 2017 – 2022 surveys, and an adjacent bed to the south (KI – BDSE) was added for 2019 – 2023. The FI bed in 2015 became the FI - 1 bed from 2016 onwards. In some cases, the code itself has not changed, but has been expressed differently, such as KI-6 vs. KI – 6.

All retained length-frequency data records (with positional data) were plotted in Arcview against the scallop bed polygons for each year. GIS bed polygons were first checked to ensure that bed polygons were included for each surveyed area in each year, and these were then allocated a standardised bed code consistent with the codes used across years. An additional column of standardised bed codes was added to each length-frequency data record, matching the codes of the surveyed beds in each year. Bed codes for 3,147 records were standardised and checked to ensure that all data records were consistently allocated to the correct scallop beds for each survey.

Commercial catch and effort data

Commercial logbook catch and effort data submitted to AFMA were obtained for the period 2002 – 2023. After deletion of fields not used in analyses, the logbook data contained the following fields:

Operation_No	Date	Trip_ID	Boat_ID	Longitude	Latitude	Depth	No_shots	Catch_Wt
386259	13/09/2002		7308	148.4333	-39.5667	39	48	500
416732	14/12/2002		7308	148.4333	-39.5667	40	18	1,200

The initial data contained 5,180 records. Of these, 61 were deleted due to not having any catch, or having missing or invalid position data. Four records with positive latitude were converted to negative latitude.

There is a remarkable range in the number of shots and the catch weight reported by (supposedly daily) record. Figure 3-3 shows frequency distribution histograms of the reported numbers of shots and catch (kg) per record. The number of shots (supposedly per day) mainly ranges from 0 – 100, but there are records with 660 shots, 1,200 shots and 1,600 shots. These larger numbers of shots are clearly not daily records but are probably records summed across entire trips.

Similarly, catch per record mainly ranges from 5 kg – 15 t, but there are records of up to 55 t. These records are also likely to be summed catch across an entire trip. There may also be simple data-entry errors in the numbers of shots or the catch, but these were not checked and no corrections were made to reported numbers. It is also notable that both the numbers of shots and the catches are reported in rounded numbers or categories – more likely to be multiples of 10 shots, and multiples of 1,000 kg for catch.

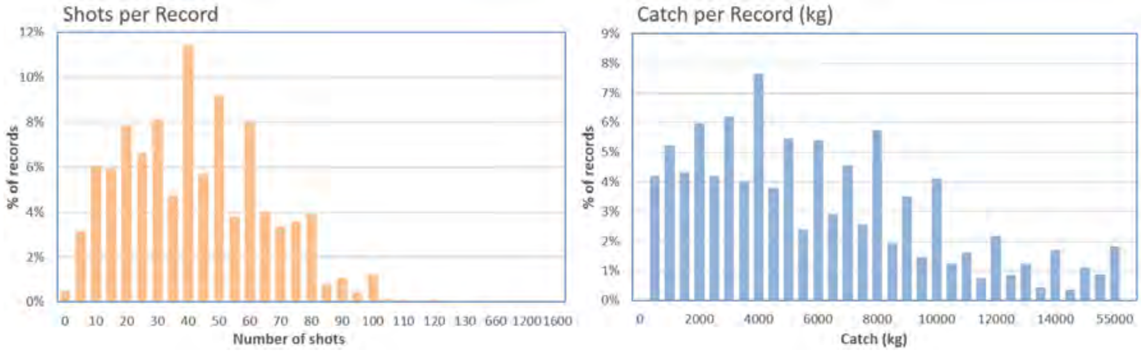

Figure 3-3. Frequency distributions of the percentage of shots (left) and the reported catch (kg, right) per record in scallop fishery logbook records over the period 2002 - 2023.

No CPUE analysis was conducted as part of this report, so no further attention was given to reviewing the accuracy of the numbers of shots or catch per record. For the purpose of spatial plotting of scallop catches and comparison with depth and current patterns, it was assumed that all of the retained catch and effort data were correct.

3.3. Commercial catches

The purpose of this project was to evaluate scallop bed dynamics, and so didn’t focus on analysis of commercial catches. The main purpose of incorporating catch data in analyses was to estimate catches for selected beds for which mortality analyses were conducted (see section on Fishing and natural mortality estimation).

A few analyses of overall catch trends by year and region were conducted in Excel® to provide some general context for the fishery. These analyses showed that, in some years, a significant proportion of the commercial catch was taken outside of the survey areas, providing information on scallop distribution beyond that provided in survey data. In addition to using spatial plots of reported catches to allocate catches to beds for mortality analysis, spatial distribution of catches was used to produce overall catch heat maps in QGIS, for comparison with IMOS-predicted tidal current maps (see section on Bass Strait tidal currents). These overlays were used to inform consideration of how tidal currents may influence observed scallop distribution patterns and therefore, how recruitment may be influenced by tidal currents.

3.4. Bass Strait tidal currents

Being a shallow area partially separated by islands from adjacent deeper areas to the west and east, Bass Strait is subject to particularly strong tidally induced currents. Griffin *et al.* (2021) developed a barotropic tidal current model for the Australian continental shelf. They show that this model (COMPAS v1.3.0 rev6631) has predictive value for much of the 79% of Australia's shelf seas where tides are a major component of the total variability in current velocity, with the Bass Strait being one of the two regions (with the Kimberley) with the lowest relative model error compared with observed tidal current and amplitude data. Bass Strait contains several tidal depth and current gauges that contribute to the reliability of this predictive morel in this region.

This current model has been adopted by IMOS as the basis for providing advice on tidal patterns and resulting tidal currents. Specific predictions are provided for Bass Strait (https://oceancurrent.aodn.org.au/tides/Bass_spd/2024/) using a version of the model optimised for the region, with hourly maps of predicted tidal current direction and velocity available for the period December 2023 to August 2024. The scallop dredge surveys have generally been conducted in late May or into early June. Therefore, hourly or two-hourly tidal current prediction maps were downloaded from the website for the period 01-05- 2024 to 14-05-2024 to visualise the distribution and velocity of tidal currents in Bass Strait under neap and spring tide conditions. Selected frames were overlaid with polygons of the scallop survey regions and with heat maps of commercial scallop catches using QGIS GIS software (QGIS.org 2024) to explore how ebb and flow tidal currents might influence scallop beds.

Identification of regions

Trends in length-frequency distributions and modes across years provide useful information on occurrence of recruitment events through appearance of modes of small scallops, and on growth as modal lengths progress across years. However, surveys have not been conducted on all beds in each survey region in each year, reducing options for tracking modal progression across missing years in individual scallop beds, raising the question of whether beds can be combined to obtain better length-frequency coverage across years. This can potentially be justified if there is evidence that recruitment has occurred at the same time in different beds, and subsequent growth has been similar, such that length-frequency distributions in the beds are similar, suggesting that they may constitute the same population.

The easiest approach to comparing length-frequency distributions between beds is simple visual comparison of the length-frequency distributions shown in Appendix 8.5 for nearby beds in the same year. Two approaches were taken in comparing length-frequencies between pairs of beds. In the first approach, the length-frequency distribution plots shown in Appendix 8.5 were graphically overlaid in Excel, using partial transparency to allow both distributions to be seen. Pairs of nearby beds were chosen in geospatial regions and length-frequency plots for the same year overlaid. This provides a quick and simple way to compare length-frequency distributions.

The second approach involved producing plots of the cumulative length frequency distributions for the chosen pairs of beds and overlaying these. The individual bed scallop density data used to produce the plots in Appendix 8.5 were converted to relative cumulative densities by dividing each value by the sum of densities across length classes and accumulating these. The resulting cumulative densities span the range from 0 – 1 for each length-frequency distribution, providing cumulative proportions (or percentages) of scallops by length class. The resulting plots provide an alternative way of visually assessing whether comparable length-frequency distributions are similar (the cumulative density plot lines overlay one another) or are different (the cumulative density plots lines are substantially separated).

Having produced cumulative density plots, the difference between these can be evaluated by calculating the maximum distance in the density axis (y-axis) between the two curves. This maximum distance is the Kolmogorov-Smirnov D statistic. The Kolmogorov–Smirnov test (KS test, see description in https://en.wikipedia.org/wiki/Kolmogorov%E2%80%93Smirnov_test) is a non-parametric test of the equality of continuous one-dimensional probability distributions that can be used to test whether a sample came from a given reference probability distribution, or whether two samples came from the same distribution. Formally, the KS-test calculates a maximum distance statistic on the cumulative density axis between two cumulative density functions (CDFs) using the formula:

$$D_x = max_x |F_1(x) - F_2(x)|$$

where D_x – the KS distance statistic
max_x – the maximum absolute difference between two functions
$F_1(x)$ and $F_2(x)$ – two functions evaluated across a range of values of x

The KS test is typically used to compare a sample distribution against a mathematical distribution, such as the normal distribution, to evaluate whether the sample is normally distributed. When comparing length-frequencies there are no mathematical distributions, and the comparison is between two empirical cumulative density functions (eCDFs). For the scallop length-frequencies, the cumulative density reflects the actual scallop density in the beds. How this is applied is illustrated in Figure 3-4, which shows the overlaid relative cumulative density plots for length-frequencies from the KI – 6 and KI – Mid beds in 2018. The dashed black line shows the maximum difference between the two cumulative density plots, being 0.721, or ~72% of the total range in cumulative density. This indicates substantially different length-frequency distributions on these two beds in 2018.

The formal KS test allows for the estimation of a ‘probability’ (p) using the estimated D and the numbers of measures in the two distributions, compared with the Kolomogorov-Smirnov distribution. However, this probability differs from the conventional concept of a probability, being the probability of seeing a test statistic as high or higher than the one observed if the two samples were drawn from the same distribution. It is not the probability that var1 = var2. High p -values suggest similar distributions, but low p -values (< 0.05) suggest that the distributions significantly differ from the Kolomogorov-Smirnov distribution and that the observed cumulative density distributions are different between beds. For the large numbers of scallops measured in these surveys, and given that these are converted to densities before being summed across tows, this p value is not meaningful when comparing the eCDFs, and therefore no attempt was made to estimate p values. Instead, estimates of D distances across all pairs of beds compared were summarised to evaluate what range of D distances might indicate similarity between length-frequencies on different beds.

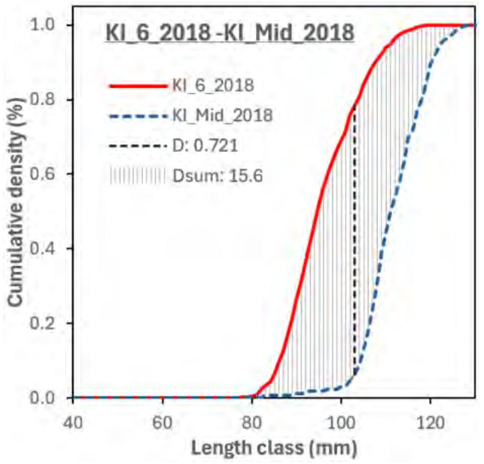

Figure 3-4. Overlay of the cumulative density plots for length-frequencies from the King Island KI – 6 and KI – Mid scallop beds in 2018, showing the maximum separation distance (D) and the sum of density differences.

As an alternative, or additional, measure of difference between the two eCDFs, the sum of vertical distances between the two curves provides an approximation of the area between the curves, potentially a better measure of the difference between the curves. This is illustrated by the grey vertical hatching in Figure 3-4, which shows all the vertical distance lines for each 1 mm size class. The true area between the curves cannot be (easily) mathematically calculated, as the length-frequencies are empirical and do not conform to mathematical relationships that can be integrated. The sum of distances is a useful approximation of the area between the curves.

Examples of applying the length-frequency distribution overlay, the cumulative density function overlay and the calculation of the maximum D value between eCDFs are shown in Figure 3-5 – Figure 3-7. Figure 3-5 shows the comparison between length-frequencies in Apollo Bay beds AB – 1 and AB – 3 in 2017. These length-frequencies are almost identical, consisting of one closely similar adult mode with D = 0.04 (4%). These two beds can be combined in a region for the purposes of tracking length modes across years.

In contrast, the comparison between King Island beds KI – 6 and KI – Mid in 2018 (Figure 3-6, also used in the example in Figure 3-4) shows that length-frequencies are clearly different, with different modes and length ranges and D = 0.721 (72.1%). These two beds seem to support different populations and should not be combined in a region for the purposes of tracking length modes across years.

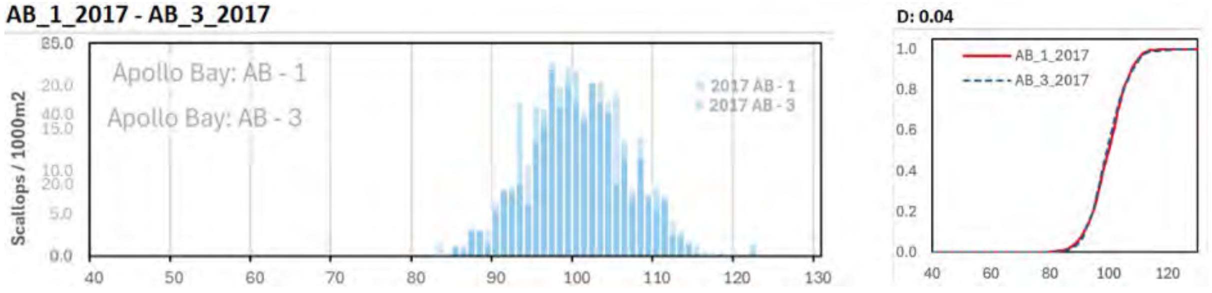

Figure 3-5. Graphic overlay of length-frequency distributions for Apollo Bay beds AB – 1 and AB – 3 in 2017 (left panel) and eCDFs (right panel). The maximum vertical distance D value the eCDFs is shown.

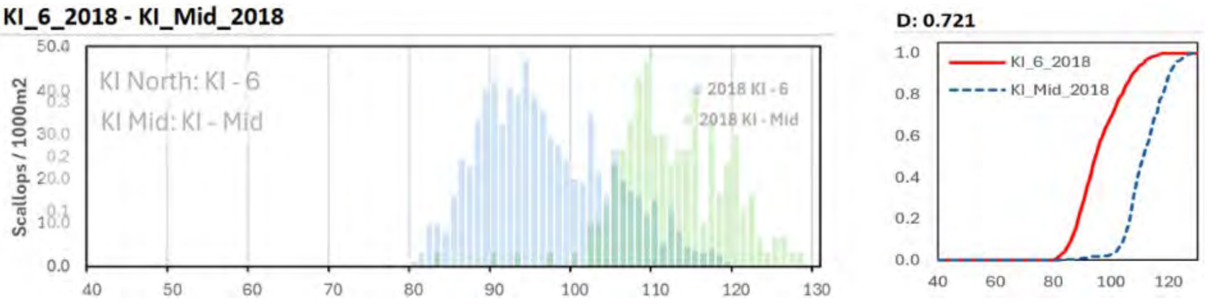

Figure 3-6. Graphic overlay of length-frequency distributions for King Island beds KI – 6 and KI – Mid in 2018 (left panel) and eCDFs (right panel). The maximum vertical distance D between the eCDFs is shown.

However, there are situations where the length-frequency distributions differ, and have substantial D separation distances for the eCDFs, but could usefully be combined. This would apply when both beds have very similar adult modes, but there is a mode of smaller recruits present only, or predominantly, in one of the beds, resulting in different eCDFs. Recruitment is known to be patchy, often occurring in one bed, or only part of a bed, or parts of adjacent beds.

Figure 3-7 shows an example of closely similar adult modes in King Island beds KI – BDSE and KI – 10 in 2021, but with a strong mode of smaller recruits in KI – BDSE, only slightly apparent in KI – 10. The eCDFs have a maximum separation distance D = 0.237 (~24%) which would seem to indicate a substantial difference between the populations, but this is entirely due to the presence of the smaller mode. These two beds could usefully be combined in a region to track the mode for recruiting scallops.

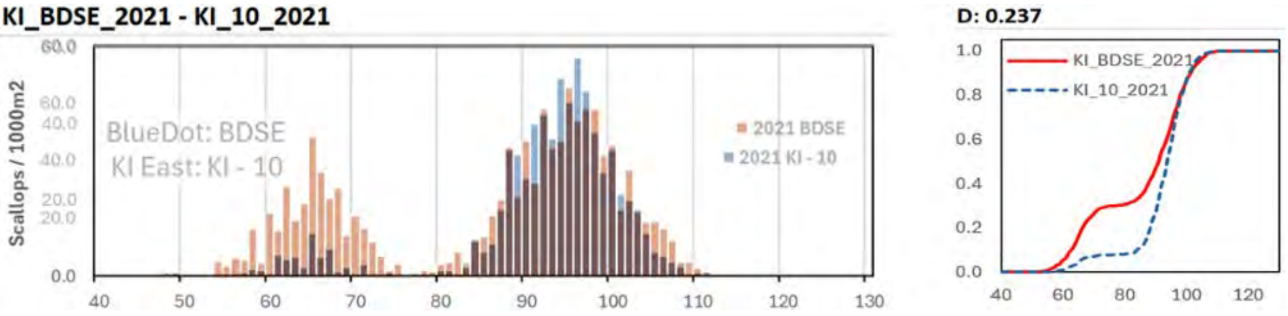

Figure 3-7. Graphic overlay of length-frequency distributions for King Island beds KI – BDSE and KI – 10 in 2021 (left panel) and eCDFs (right panel). The maximum vertical distance D between the eCDFs is shown.

Survey selectivity

The scallop dredge used in surveys is the same design and construction as commercial scallop dredges used in the fishery, and therefore has the same size-selectivity for scallops. This dredge selectivity will influence the length-frequency distribution of survey catches, allowing for the escape of smaller scallops, potentially upwards biasing the modal and mean size of the smallest recruiting scallops. This could, in turn, upwards bias the estimation of early growth rates of scallops using modal progression.

The 2019 survey of the King Island Extended KI – JH bed used a dredge that was specifically modified to catch small scallops, in response to industry reports of an apparent massive settlement of small scallops in the area. The dredge used was the standard survey dredge, but divided in half, with half of the dredge unmodified (JH – Large) and half of the dredge covered by a finer mesh (JH – Fine) to retain small scallops, in a controlled experiment that provided data that can be used to determine selectivity of the standard dredge section, compared with the finer mesh section.

The weighted frequencies of scallops caught per 1mm size class in the JH – Large mesh dredge section were expressed as ratios of the frequencies of scallops caught in the JH – Fine mesh dredge section, to calculate the increasing proportion of scallops in the large mesh section as scallop size increased. A selectivity curve was fitted to these proportions by 1mm size class using the GRG Nonlinear option in the Excel Solver function:

$$S = \frac{1}{1 + e^{-k(L - L_{50})}}$$

Where S – selectivity
k – the logistic increase rate; the steepness of the curve
L – a length for which selectivity is to be calculated
L_{50} – the length at 50% selectivity

Similar curves were fitted to the aggregated scallop length frequency data across all beds for each survey year and compared with the JH – Large experimentally determined selectivity curve.

Effect of selectivity on recruiting juvenile modal length

The purpose of determining a selectivity curve for the survey dredge is to allow for evaluation of whether the modal length of recruiting juvenile scallops caught in surveys has been biased upwards by dredge selectivity. The effect of selectivity was evaluated by simulating a normally distributed mode of scallops with a mean length increasing from 57 mm to 81 mm, applying the selectivity curve to the resulting length frequency distributions, and determining the mean length of the remaining scallops after the length-frequencies had been modified by selectivity. A 2° polynomial function was fitted to the relationship between the two mean lengths for the full and selected length-frequencies and this was used to apply a correction factor for recruiting juvenile modes of < 80 mm, after which scallops are fully recruited. The corrected juvenile modal lengths were used in growth curves determined from modal progression.

3.5. Scallop bed dynamics

Spatial analysis was conducted in ESRI Arcview® and QGIS. Analyses of scallop length-frequency data were conducted mainly in MS Excel® with some analyses for growth modal separation conducted in R®. Final graphics were prepared in Excel®, Arcview® and QGIS.

Trends in biomass

Scallop biomass estimates by bed are available in individual annual survey reports (Knuckey *et al.* 2015, 2016, 2017, 2018; Koopman *et al.* 2019, 2021; Koopman and Knuckey 2022) and were sourced from those reports for plotting of trends in biomass by individual beds across the survey years. These biomass estimates were summed by year across beds in the defined regions to generate charts of inter-annual trends in biomass by region.

Trends in density and size

The first step in the analysis of trends in length-frequency data was the preparation of a summary of data by tow, starting with the allocation of a unique ID to each tow, by concatenating the Year, Bed Code (after standardisation of codes across the data) and tow number (or survey number), after addition of suffixes to separate out tows with same number where necessary. The resulting summarised tow data file had the following fields

Uniq Id	Year	Region	Bed Code	Lon	Lat	Samp Wt	Ctch Wt	Freq	U_Freq	L_Freq
2015_FI_13	2015	Flinders Island North	FI	148.08347	-39.24375	3.4	40	52	17	35
2015_FI_14	2015	Flinders Island North	FI	148.08278	-39.26889	4.2	80	50	8	42

P_Undr	P_Legl	Wt_Freq	Under Wt_Freq	Legal Wt_Freq	Wtd Len	Avg Len	Area Swept	Dens	U_Dens	L_Dens
0.33	0.67	611.8	200.0	411.8	4468	85.9	4722.6	129.5	42.3	87.2
0.16	0.84	952.4	152.4	800.0	4577	91.5	4722.6	201.7	32.3	169.4

Trends in the mean size, overall density, density of undersize and legal-size scallops and proportion of undersize and legal-size scallops of the populations in beds across survey years were determined by analysis of the by-tow summarised length-frequency data.

The length-frequency data do not include 0's for scallop lengths that did not occur in the samples, requiring caution in determining average lengths across different beds or regions. The numbers of scallops are also aggregated by length-class, requiring scallop lengths to be weighted by the numbers in each size class before they can be averaged to determine mean lengths. The first step in this process was to calculate the weighted length for each data record by multiplying the length class by the number of scallops measured in each record:

$$\hat{L}_{l,t} = l_t \times N_{l,t}$$

where $\hat{L}_{l,t}$ – the weighted length of length class l in tow t
l_t – a length class l in tow t
$N_{l,t}$ – the number of scallops of length class l in tow t

The average length of scallops in any grouping of tows, beds or regions can then be calculated by dividing the sum of the weighted lengths by the sum of the number of scallops in those groups:

$$\bar{L}_{(t,B,R)} = \left(\sum_{l=1}^{n} \hat{L}_{l\ (t,b,R)}\right) / \left(\sum_{l=1}^{n} N_{l\ (t,B,R)}\right)$$

where $\bar{L}_{(t,B,R)}$ – the mean length of scallops across tows, beds or regions
$\hat{L}_{l\ (t,B,R)}$ – the weighted lengths of all length classes l across tows, beds or regions
$N_{l\ (t,B,R)}$ – the numbers of scallops of all length classes l across tows, beds or regions

Trends in average lengths of scallops by bed and by region were calculated in this way using the sums of weighted lengths and of numbers of scallops across the chosen stratum (Bed or Region).

Trends in the proportion of legal size and undersize scallops by bed or region were obtained using Excel pivot tables to summarise the data in the by-tow summarised data file, producing summary tables and plots of inter-annual trends in mean size, proportions of undersized and legal-size scallops and density of undersize and legal-size scallops.

Length-frequency distributions

The scallop beds surveyed differ each year, with different beds being surveyed in different years, and boundaries and areas of certain beds changing among surveys. Some beds may be surveyed in several years, although their boundaries may change among years. The boundaries of some beds have remained consistent over time but may not only have been surveyed in some years. There are therefore gaps in the data for beds across years, and the actual area of some beds has changed among survey years.

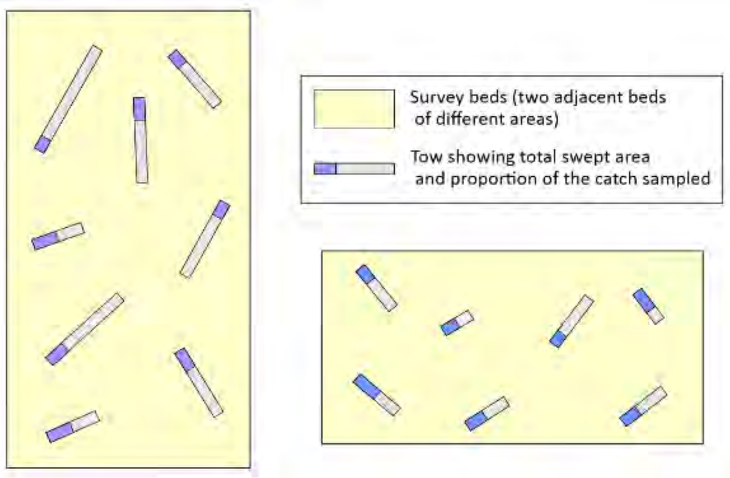

Figure 3-8. Diagram of stylised scallop survey beds showing two beds of different areas, each subject to a different number of dredge tows of differing length (and so of differing area swept) and direction. The blue shading in tows represents the differing proportion (not actual area) of the total catch from each tow that was sampled for scallop length frequencies.

Survey tows within beds are of different lengths, and so of different swept areas. The total catch made during a tow is the sample of the population existing in that tow path (given dredge selectivity). The sample weight is a (random, representative) sample of the catch made during that tow, and the proportion of total tow catch sampled differs among tows. The numbers of scallops measured (per length class) is therefore a sample of the total number of scallops (per length class) in the total catch of each tow. A diagrammatic depiction of the differing survey bed areas, tow swept areas and proportion of tow catch sampled, is shown in Figure 3-8.

Because the proportion of tow catch that is sampled differs among tows, the numbers of scallops measured in each tow cannot be added across tows without first raising the numbers measured to the total catch weight per tow. Long tows with small sample sizes would be under-represented, and small tows with large sample sizes would be over-represented, when sample numbers are summed across tows. The first step before summing sample numbers across tows is to raise each individual tow sample (~per length class) by the ratio of Catch.Wt / Sample.Wt for each tow.

$$\widehat{N}_{l,t} = N_{l,s} * C_t / C_s$$

where $\widehat{N}_{l,t}$ – the raised number of scallops in length class l in tow t
$N_{l,s}$ – the number of scallops in length class l in sample s for the tow
C_t – the total catch weight in each tow
C_s – the sampled weight from each tow

The raised number of scallops by length-class by tow was calculated as above and added to each record in the length-frequency datafile. The resulting raised numbers of scallops (~per length class) can be summed across tows in a bed, with the resulting summed numbers being representative of the summed swept area, representing a sample of the population across the bed.

$$\widehat{N}_B = \sum_{t=1}^{n} \widehat{N}_t$$

where $\widehat{N}_B$ – the raised number of scallops (in total, or per length class) in bed B
$\widehat{N}_t$ – the raised number of scallops in tow t (from the above equation)
n – the number of tows conducted in the bed concerned.

There are different numbers of tows per bed in each year, and each bed has a different area from other beds, sometimes differing from the same bed in a different year. Further standardization of scallop numbers per length class is therefore required before they can be added across different beds, by raising the scallop numbers to individual bed areas. Before this can be done, the numbers of scallops summed across tows in a bed must be expressed as a density in that bed:

$$D_B = N_B \,/\, \sum_{t=1}^{n} A_{t,B}$$

where D_B – the density of scallops per sampled m^2 in bed B

N_B – the raised number of scallops (in total, or per length class) in bed B

$A_{t,B}$ – the swept area in tow t in bed B

n – the number of tows conducted in the bed concerned.

This provides estimates of the densities of scallops across all tows in each bed in each year. These densities can be raised to the total area of a bed to get the estimated total numbers of scallops in the bed, and these estimated total numbers per bed can be summed across beds to get estimates of the total numbers of scallops across multiple beds in a region. These can then be divided by the sum of the areas of the aggregated beds in a region:

$$D_R = \sum_{B=1}^{n} (D_B \times A_B) \,/\, \sum_{B=1}^{n} A_B$$

where D_R – the density of scallops summed across beds in a region

D_B – the density of scallops in bed B

A_B – the total area of bed B

n – the number of beds across which scallop densities are being summed

3.6. Population biology

Growth

Haddon *et al.* (2006) evaluated growth rates of several Tasmanian scallops in beds to the east of Flinders Island, extending down from ~39.6°S to ~40.4°S. They observed clear progression of modes of newly recruited juvenile scallops in some beds that could be tracked across years to provide estimates of growth of three cohorts (settled in 1999, 2000 and 2001) among years in these beds. Haddon *et al.* (2006) identified the peaks of these modes using modal separation, given that these modes conformed well to normal distributions. The modes identified are summarised in Table 3-2.

Table 3-2. Mean values from identifiable modes in the length frequency of scallops from different strata progressing through several years (from Haddon *et al.* 2006)

Cohort	Stratum	2002	2003	2004	2005
Cohort 1999	**Age**	**2+**	**3+**	**4+**	**5+**
	TIS	80.26	90.36	95.60	98.70
	TIN	75.74	88.16	91.91	
	T2	71.64	80.60	88.08	92.03
	T3	72.75	84.95	89.49	94.22
	C2	83.15	101.83	102.41	106.72
	C3	80.70	98.48		
Cohort 2000	**Age**	**1+**	**2+**	**3+**	**4+**
	C2	49.62	88.08	84.64	90.27
Cohort 2001	**Age**		**1+**	**2+**	**3+**
	C2			68.52	75.80
	TIS		42.00	73.97	83.00
	TIN		44.25	74.84	87.00
	C4XMain			77.81	82.93

C4XSouth	85.83	97.85

Haddon *et al.* (2006) plotted the growth between these modes as straight lines superimposed on length-frequency distributions but did not generate growth curves. An overlay of those partial growth curves is shown in Figure 3-9.

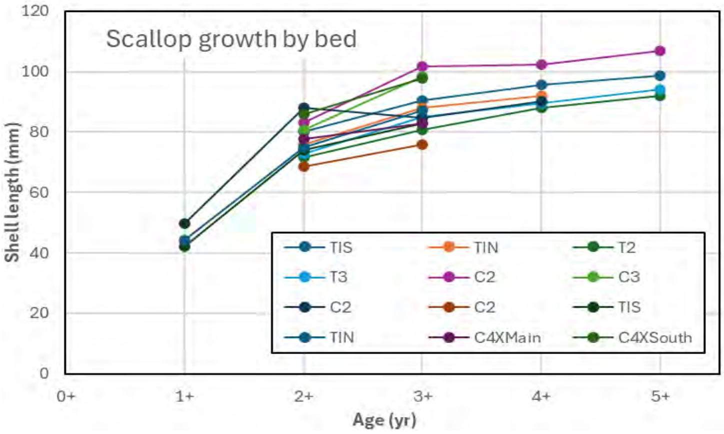

Figure 3-9. Overlay of partial growth curves on modes found by Haddon *et al.* (2006) for 12 Tasmanian scallop beds in the Flinders Island region.

A von Bertalanffy growth curve fitted to the modes found by Haddon *et al.* (2006) (Table 3-2) is shown in Figure 3-10. This illustrates the ranges of length-at-age found for modal progression growth in this region, as summarised in Table 3-3 and used as guidance in allocating assumed ages to modes found in BSCZSF length-frequency data.

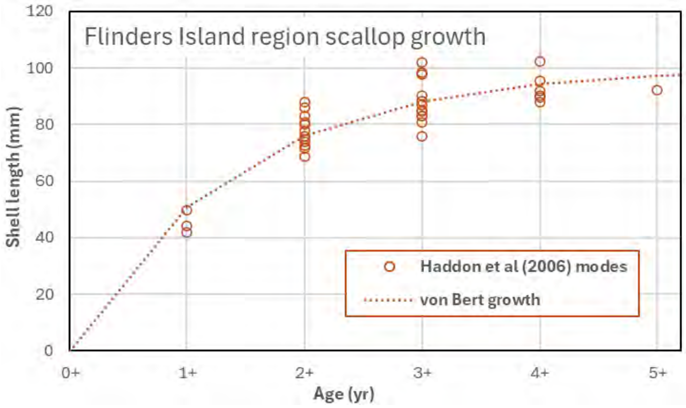

Figure 3-10. von Bertalanffy growth curve (t_0 = 0) fitted to length modes found by Haddon *et al.* (2006) across 12 Tasmanian scallop beds in the Flinders Island region.

Their main conclusion was that scallops showed marked differences in growth (cohort progression) in different beds, and in different years, as shown in Figure 3-9. The differences between modes at different ages on different beds can be used to provide guidelines on the minimum and maximum expected length of scallops of different ages (Table 3-3).

Koopman *et al.* (2018) conducted an age and growth study as part of a survey of the scallop fishery in Victoria state waters in 2017 – 18. Scallops in this study were directly aged using various parts of the scallop shell and hinge ligament. 101 scallops ranging in shell length from 31.4 – 104.8 mm were aged, found to range from 3+ to 9+ years of age. A plot of the age data with a fitted von Bertalanffy growth curve (L_∞ = 108.57. K = 0.2972, t_0 set to 0) is shown in Figure 3-11.

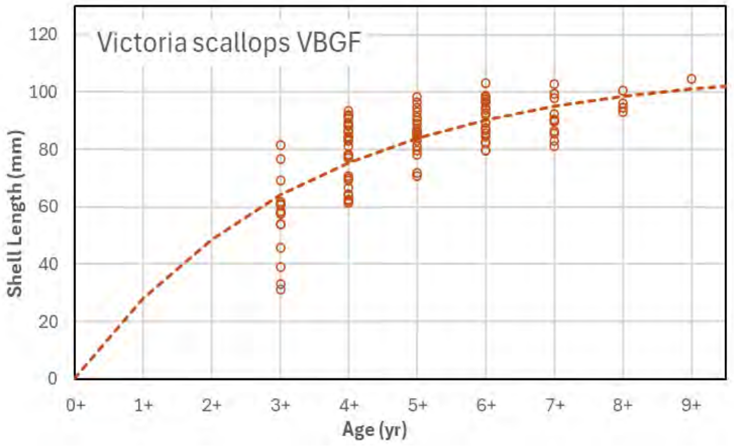

Figure 3-11. Age reading data and fitted von Bertalanffy growth curve for scallops from the Victoria state waters fishery (from Koopman *et al.* 2018).

The minimum and maximum ages per length class for these previous growth studies of Tasmanian scallop (Haddon *et al.* 2006) and Victorian scallop (Koopman *et al.* 2018) are summarised in Table 3-3. The age results for these two studies only overlap in the 3+ to 5+ range. Haddon *et al.* (2006) found smaller 1+ and 2+ modal lengths that the Koopman *et al.* (2018) dredge survey did not capture, likely due to dredge selectivity. Koopman *et al.* (2018) found ages for large scallops which were not tracked to those ages in the Haddon *et al.* (2006) modal progressions.

There are differences, particularly in the minimum age per length class, between lengths-at-age in these two studies. The maximum lengths by age class by Koopman *et al.* (2006) fall within the ranges for those ages by Haddon *et al.* (2006) over 3+ to 5+. However, the minimum ages in Koopman *et al.* (2018) lie well below those for Haddon *et al.* (2006), being two to three years older than ages for similar minimum lengths in Haddon *et al.* (2006). This may be due to slower growth in Victoria state waters, or scallops in the modes tracked by Haddon *et al.* (2006) being older than assumed, or a combination of these possibilities. Notably, the same dredge, with the same selectivity, was used for the Victorian scallop surveys as was used in the Commonwealth surveys but was able to catch scallops as small as 31.4 mm, showing that the dredge is able to catch small numbers of small scallops below the selected sizes.

Table 3-3. Summary of minimum and maximum observed cohort modal lengths of scallops of different ages in Tasmanian scallop beds (summarised from Table 3-2).

Age	1+	2+	3+	4+	5+	6+	7+	8+	9+
Tasmania fishery (Haddon *et al.* 2006)									
Min (mm)	42.00	68.52	75.80	88.08	92.03	-	-	-	-
Max (mm)	49.62	88.08	101.83	102.41	106.72	-	-	-	-
Victoria fishery (Koopman *et al.* 2018									
Min (mm)	-	-	31.4	61.4	70.6	79.5	81.1	93.2	104.8
Max (mm)	-	-	81.7	93.6	98.4	103.2	102.6	100.6	104.8

A similar approach to that taken by Haddon *et al.* (2006) was taken to evaluating growth of scallops across years in the BSCZSF surveys. Length-frequency distributions by region were inspected to identify regions that showed clear modes as well as apparent modal progression among years (see Methods and Results for length-frequency analysis). Length-frequency data for regions showing apparent progression of length modes were subject to further analysis to separate and identify peaks of these modes, noting that clear modes in the BSCZSF data appear to conform to normal distributions, as found by Haddon *et al.* (2006).

Following initial trial analyses using length-frequency data aggregated to various length bin sizes (1mm, 2mm, 3mm) it was decided to aggregate length data to 2mm bins for modal analysis. This resulted in clearer modes with less empty bins compared with 1mm bins, but with a low risk of obscuring modes using larger bins. Where multiple modes were present in length-frequency data for a region/year, modal separation analysis was conducted using the 'normalmixEM' routine in the R 'mixtools' package (Benaglia *et al.* 2009). Where only single modes were present (such as a single mode of large adult scallops), no modal separation was required, and the mode was simply determined to be the weighted average length of scallops in that mode.

Having identified modes and their progression across years, exploratory growth curves were fitted to the modes. This required a subjective choice of what age each mode represents, or exploration of alternative age assignments to modes. Initial assumptions made in specifying the ages represented by each mode identified in length-frequency data, and the justification for these decisions, were:

- The length at age+ found by Haddon *et al.* (2006) (Table 3-3) were used as guidelines to the expected ranges of length to be found for each age,
- Haddon *et al.* (2006) report that scallops in southern Tasmania spawn over the period August to October. Results of gonad staging analysis of scallops sampled in BSCZ surveys indicates that spawning can occur over August – February, with spawning in November/December being common. For convenience, a standard birth date of 1 January was assumed for all cohorts, with t_0 being fixed at 0 for growth curve exploration.

Exploratory von Bertalanffy growth curves were fitted to modal estimates for regions showing apparent modal progression, using the 'Solver' function in Excel with the GRG Nonlinear solving method, unconstrained variables allowed to be negative. Alternative age assignments were explored where modes straddled the ranges found by Haddon *et al.* (2006) for different ages. This guided the fitting of ages to lengths in modal analysis. The range of lengths around each mode typically spans the range that might be expected to result from the extended spawning season, but there is inevitable uncertainty around the actual ages of scallops comprising each mode.

Spawning and recruitment

Having assigned assumed ages to modes observed in length-frequency distributions for each region, the years in which spawning would have occurred to produce those modes at those ages can be back-calculated as:

$$Y_S = Y_A - A$$

where Y_S – year of spawning
Y_A – year at age A
A – age

Given that ages were assumed for modes observed in each year, there is increasing likelihood that ages have been incorrectly assumed for larger scallops, particularly where the adult mode cannot be linked to preceding juvenile modes. Modes of large adult scallops could contain scallops of similar size but differing age, merged into a single adult mode. The back calculation of years of spawning will be more accurate for juvenile modes where the assumed age is more likely to be correct, so the back calculation of spawning years was limited to an assumed maximum age of six.

An overview of the spatial and temporal distribution of recruitment into the fishery is provided by the analysis of trends in smaller (< 85 mm shell length) scallops by bed and year (see section above on 'Trends in density and size'). Fine-scale spatial distribution of recruitment was evaluated by mapping the proportion of scallops < 85 mm shell length by individual tow across beds and years.

Morphometrics

Analysis of shell length to shell height and flesh weight has been conducted and presented in the individual survey reports for each annual survey (see survey reports by Knuckey *et al.* (2015, 2016, 2017, 2018) Koopman *et al.* (2019, 2021) and Koopman and Knuckey (2022)). To investigate the similarities or differences between morphometric relationships at a region level, scatterplots of Length:Height, Length:Width and Length:Weight (see Appendix 8.1 for diagrams of measurements) were produced, aggregated across all survey years 2015 – 2023. To these, linear trendlines were fitted in Excel® to $L{:}H$ and $L{:}W$ data, and power curves to $L{:}Wt$ data. Scatterplots and trendlines were overlaid for: the Apollo Bay and

Apollo Bay East regions; the King Island North and King Island NorthMid regions; the King Island MainMid, King Island East and King Island FarEast regions; and the Flinders Island North and Flinders Island South regions.

Inspection of these overlaid scatterplots for the above region pairings indicated that the L:Wt relationships were similar across the compared regions, with the trendlines coinciding over much of the range in the data. For use in converting changes in length (due to growth) to changes in weight as part of mortality estimation (see next section), aggregated L:Wt scatterplots and trendlines were produced for the Apollo Bay, King Island and Flinders Island areas, aggregating all beds in those broader areas. For these, empirical confidence intervals were added by holding the intercepts constant and adjusting the exponents to achieve symmetrical upper and lower relationships (assuming that variance is normally distributed around the overall power curve) that encompassed 68.2% of the data points (one standard deviation) and 95% of the data points (95% confidence interval). These upper and lower curves were used to provide probability intervals around the L:Wt conversions used in mortality estimation.

Fishing and natural mortality estimation

Some of the scallop beds show a single mode of large adult scallops over periods of several consecutive years, without evidence of recruitment. Substantial declines in survey-estimated biomass over those years are evident in a number of these beds, allowing for mortality to be estimated from the decline in biomass, after accounting for catches and growth. If these areas have been commercially fished then the decline in biomass can be separated into natural and fishing mortality, although the two would then likely be confounded as a result of cryptic discard mortality being considered to be natural mortality, whereas it should be fishing mortality.

To simplify the mortality analyses as far as possible, survey biomass estimates were chosen only for beds that showed a single mode of adult scallops that could be reasonably well approximated using a normal distribution. Growth is slow for large scallops, reducing mortality estimation errors resulting from incorrect growth estimation. Selection of beds for mortality estimation was further restricted to those that showed substantial interannual declines in biomass, well in excess of any catches that could be allocated to those beds, and with no evidence of recruitment. This ensured that, when attributing changes in biomass among years to fishing and/or natural mortality, recruitment could be considered to be zero. A simple approach was then taken to estimating natural mortality between two years:

Expected biomass in year 2: $\mathrm{B_{expected} = B_{y1} - C_{y1:y2} * G}$

Deaths (biomass loss): $D_{y1:y2} = B_{expected} - B_{y2}$

Natural mortality: $M = -ln\,(1 - (D_{y1:y2} / B_{y1}))$

Fishing mortality: $F = -ln\,(1 - (C_{y1:y2} / B_{y1}))$

where B – biomass (expected, year 1 or year 2)
C – catch (over year 1 to year 2)
G – ratio of scallop mean weights in year 2 / year 1
D – deaths, or biomass loss not attributable to fishing

The death rate (d) can be calculated from M to obtain a simple proportion of biomass lost per year as:

$$d = -(e^{-M} - 1)$$

Harvest rate (h) can be similarly calculated from fishing mortality.

The growth ratios between years were obtained by converting the mean lengths of scallops in year 1 and year 2 (from the actual length-frequency data for the individual beds and years) to weights using the aggregated L:Wt relationship for each of the three areas and dividing mean weight in year 2 by mean weight in year 1. Regarding the sequence of subtracting catches and adding growth, an initial analysis of the seasonality of commercial scallop catches showed that catches over 2015 – 2023 have almost entirely been taken in the second half of the year, after the surveys are conducted (Figure 3-12).

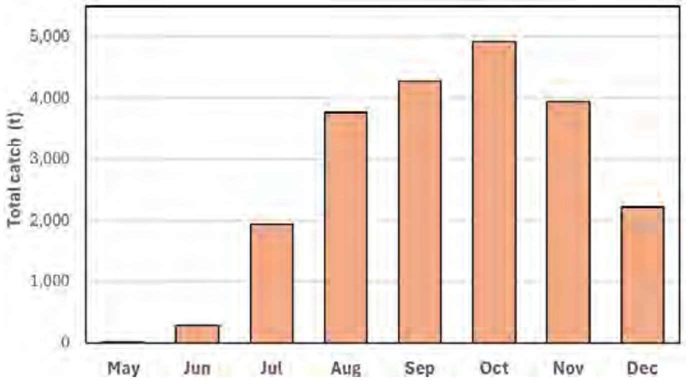

Figure 3-12. Monthly distribution of commercial scallop catches summed over the period 2015 – 2023.

Estimation of variance around mortality estimates

Applied just to the modes (or means, assuming all distributions to be normal) results in single deterministic (no variance) estimates of M and F. However, the variance around survey estimates of biomass are calculated and reported in annual survey reports, and the variance around mean lengths of adult mode scallops can be estimated from the length-frequency data for individual beds and years. The variance around $L{:}Wt$ relationships can be estimated from the scatterplots for each region or area.

Biomass variance, as reported in individual surveys reports, is assumed to be normally distributed, with symmetrical 95% CIs reported for each median biomass estimate. Standard deviations (SD) can be calculated from these as SD = 95% CI / 1.96. Assuming the adult modes in length-frequency data to be normally distributed (as found by Haddon *et al.* 2006, and in modal analyses in the present study), allows the variance around adult modal lengths to be estimated from the mean and standard deviation for the adult mode length-distributions. As described under the section on Morphometrics above, it was further assumed that variance around the $L{:}Wt$ relationships for each area is normally distributed, with standard deviations for the $L{:}Wt$ exponent estimated from upper and lower power curves encompassing 68.2% of the points in the aggregated scatterplots. Variance can then be estimated using normally distributed probabilities, rather than single mode estimates, by applying a Monte-Carlo approach to randomly sample from each of the probability distributions and repeating the above calculation for each of the samples[1].

The mean and standard deviation were calculated or obtained from survey reports for biomass, adult modal length and $L{:}Wt$ conversion for each of the beds and years used in each of the inter-annual comparative analyses. The normal distributions defined by these means and standard deviations were randomly sampled in Excel® using the formula:

Sample (B, L or G) = NORM.INV(Rand(), Mean, StDev)

2,500 random samples of B, L and $L{:}Wt$ exponent were drawn for each analysis. Three alternative estimates of combined variance around M were calculated from these samples:

- No variance - deterministic estimate using only the mean values (only for illustrative and checking purposes).
- Addition of Biomass and Length variance, applying the SDs around biomass estimates and the mean lengths in adult modes (these being the two main and known sources of variance).

---

[1] Monte Carlo methods are a broad class of computational algorithms that rely on repeated random sampling to obtain numerical results. The underlying concept is to use randomness to solve problems that might be deterministic in principle (Wikipedia 2024, https://en.wikipedia.org/wiki/Monte_Carlo_method).

- Further addition of $L\text{:}Wt$ variance applying the SD around the exponent of the $L\text{:}Wt$ relationships for each area, potentially adding substantial variance resulting from the different gonad stages and weights in different beds during surveys.

Linked or independent probabilities

In applying the randomly sampled probabilities from the normal distributions, consideration needs to be given to whether these are independent or linked among years. Is it to be expected that the variance among biomass estimates is completely independent among surveys. However, it is possible that there is some linkage (such as a constant bias) among biomass estimates, such that the probability of a lower estimate in one year is linked to the probability of a lower estimate in the following year. This is considered to be unlikely, so it was assumed that variance around biomass estimates is independent among years. Assuming this to be linked would reduce the variance among estimates of M but should not change the modal value.

It is unlikely that variance around the $L\text{:}Wt$ relationships is linked between years. This variance results largely from differences in gonad weight for different scallops in different beds and years, and these differences will be dependent on specific local and annual conditions at the times of surveys. It was therefore assumed that variance around the $L\text{:}Wt$ relationships is independent among years.

The situation is different for variance around the length of adult modes. Scallops have individual growth rates that would be expected to persist among years, with individual lengths also being related to when in the spawning season they were spawned. It is to be expected that scallops that are smaller than the mean in one year would also be smaller than the mean in the following year. Similarly, scallops that are larger than the mean in one year would also be larger than the mean in the following year. It would not be expected that a smaller scallop in one year could suddenly become a larger scallop in the following year and then revert to being a smaller scallop the year after.

The probabilities of being small or large (compared with the mean) are therefore linked among years. This was implemented by generating 2,500 random samples of a normal probability distribution and then applying the probability for each sample to all the sample length estimates across years in each bed analysis, rather than using independent probabilities for each sample in each year.

Allocation of catches to survey beds

No variance was added to estimates of catches made in the surveys beds among years used for mortality estimation. This could, in principle, be done if there is some basis for estimating a CV on reported catches. It is likely that unobserved and unknown discard mortality is more of an issue regarding fishing mortality. However, there are challenges associated with determining which catches to allocate to which beds to be subtracted from bed biomass when estimating natural mortality. Putting aside errors in position reporting, these challenges relate to the resolution at which catch positions are reported in logbooks. Catch latitudes and longitudes are reported to the nearest whole minute, apparently the nearest whole minute below, ignoring any seconds in catch positions (see next section on Commercial catches). This means that catch positions are essentially ‘gridded’ in whole minutes, so that the actual catch may have been taken within a 1,852 m (latitude) or ~1,500 m (longitude) radius around the reported position, or more likely up to 1,852 m further south or ~1,500 m further east.

The rounding of catch positions can be accounted for by including a 1,852m buffer around survey beds, and including all catches within this buffered area. However, where surveys beds lie closely adjacent to one another, or overlap one another, a reported catch position could potentially fall within either of the adjacent beds. Figure 3-13 shows catch positions reported in or near the Apollo Bay region beds in one year.

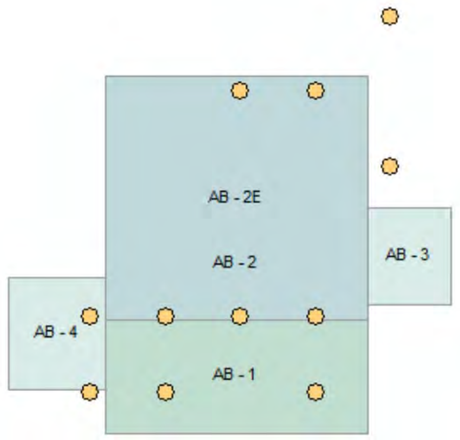

Figure 3-13. Map of scallop beds in the Apollo Bay region showing catch positions reported to the nearest 1 minute, probably the nearest 1 minute below.

After applying a 1,852 m buffer, the northern-most four catch positions can probably be allocated to bed AB – 2E (the extension of bed AB – 2). The southern-most three catch positions can probably be allocated to bed AB – 1, if the south-western catch position was reported to the nearest longitude position below and so would be in AB – 1 rather than AB – 4. The difficulty is in deciding to which bed the central four catch positions should be allocated. The catch positions have been reported within AB – 2 but, if they were reported to the nearest latitude minute below, could actually lie in AB – 1.

Allocation of catch positions to beds was done in Arcview®, after separating reported catches into separate files for each year. For each year, a 1,852m buffer was applied to all surveyed beds across all years (whether surveyed in a particular year or not) and all catch positions lying within these buffers marked as being 'Near beds'. These 'Near beds' catches were then manually selected and allocated to the beds within which they lay, or were nearest to, such that each reported 'Near bed' catch was allocated to only one bed. In the example in Figure 3-13, because mortality analyses were only undertaken for beds AB – 1 and AB – 2E, the northern and central eight positions were all allocated to bed AB – 2E and the southern four positions were allocated to bed AB – 1.

There were numerous catches reported in the central four positions and so this allocation decision could result in under-estimation of catches and fishing mortality for bed AB – 1, and in over-estimation of natural mortality for this bed. However, for the beds chosen for natural mortality analysis, *F* was very low in comparison with *M*, so analyses using alternative catch allocations to beds were not done.

Interannual trends in dead scallop shell catches

In addition to recording the weight and number of live scallops caught in survey tows, surveys since 2015 have recorded the catch of dead scallop shells in each tow, in four categories of time since death:

- Clappers – fresh dead scallops with upper and lower valves still attached by the hinge, no discolouration.
- New Single – single scallop valves, no longer attached, but still visibly fairly recently dead, with little discolouration or attached growth.
- Old Single – single scallop valves, not attached, and visibly dead for some time, probably more than a year, with noticeable discolouration and attached growth.

The quantity and time since death of dead scallop shells caught in survey dredge tows provides an indication of scallop mortality preceding the survey tow, with large numbers of dead shells indicating earlier substantial scallop mortality. Where rapid and substantial declines in scallop abundance are observed in the absence of fishing, concomitant increases in quantities of dead shell provides confirmation of natural mortality in the area.

This was investigated by graphically comparing interannual trends in the abundance of live scallops in surveyed beds with interannual trends in the abundance of clappers, new single and old single dead shells, particularly for beds chosen for natural mortality analysis (see section on ‘Fishing and natural mortality estimation’). These beds were chosen as showing rapid and substantial interannual declines in scallop abundance, with little or no fishing on those beds. Reciprocal increases in the catch of dead shells as the abundance of live scallops declined would provide some confirmation that localised natural mortality had occurred on the beds concerned.

4. Results

4.1. Identification of Regions

Results of the paired graphic comparison of beds by region and year are shown in Appendix 8.6 for all the comparisons conducted. D scores for each paired comparison are summarised in Table 8-2. The $Dmax$ and $Dsum$ results are plotted against each other in Figure 4-1, showing that these two measures are correlated, with $Dsum$ being a power function of $Dmax$, as would be expected moving from a length ($Dmax$) to an area ($Dsum$). As the separation between eCDF curves increases, there is increasing variability of $Dsum$ over $Dmax$, showing that the area between the curves does provide additional information on differences between length-frequency distributions. Nonetheless, use of the Kolmogorov-Smirnov D seems to provide an adequate measure of differences, and so this was the main measure used in identifying beds that could be combined into regions.

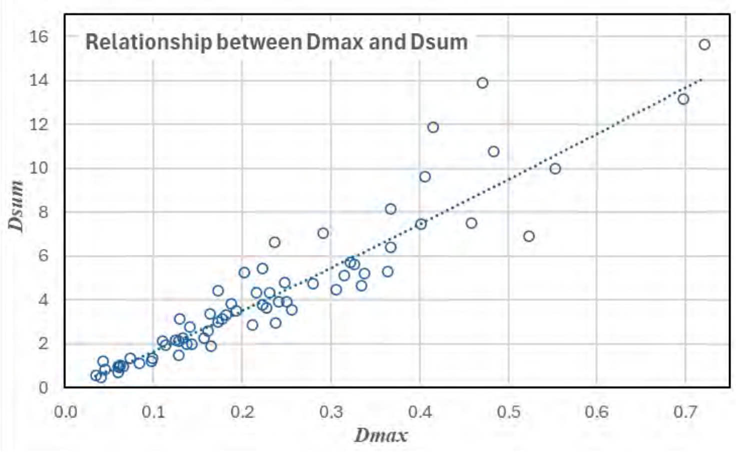

Figure 4-1. Relationship between KS test D ($Dmax$) and the sum of D distances between curves ($Dsum$) for the paired bed comparisons conducted, from Table 8-2.

The D statistic results of comparisons between beds summarised in Table 8-2 are plotted in Figure 4-2, grouped by Region, with difference scores ranked within each region from lowest D (highest similarity) to highest D (greatest difference) between beds.

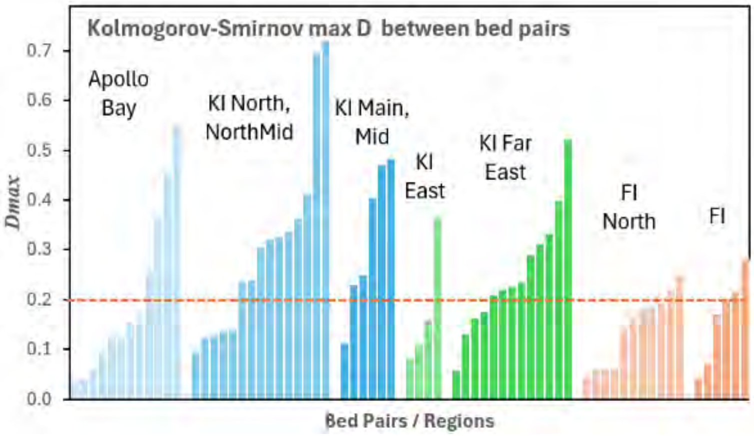

Figure 4-2. Overview of D scores ($Dmax$) measuring the separation between pairs of beds, grouped by Region, ranked from minimum to maximum difference between beds. The red dashed line shows the 20% difference level, as an illustrative level below which beds appear to be supporting similar populations.

In evaluating whether beds are similar enough to be grouped into regions, or are different enough that they appear to support different populations, the D score level is relevant. A visual scan of the overlaid length-frequency distributions in Appendix 8.6 indicates that bed pairs with a D separation score of 0.1 (10%) or less are closely similar, typically supporting populations consisting of a single and similar mode of adult scallops. In contrast, there are several bed pairs with D scores > 0.2 (20%) which show clear differences in length-frequency distributions. A D score of 0.2 is shown on Figure 4-2 as an illustrative guideline indicating those beds that appear to support similar populations. This provides a useful first indication of whether beds are similar enough to be grouped, or whether further evaluation is required to determine the reasons for differences between beds.

The comparisons in Appendix 8.6 were used to evaluate bed similarity and to draw the following conclusions regarding which beds appear to be similar enough in terms of length-frequency composition to be grouped into the following regions.

Apollo Bay

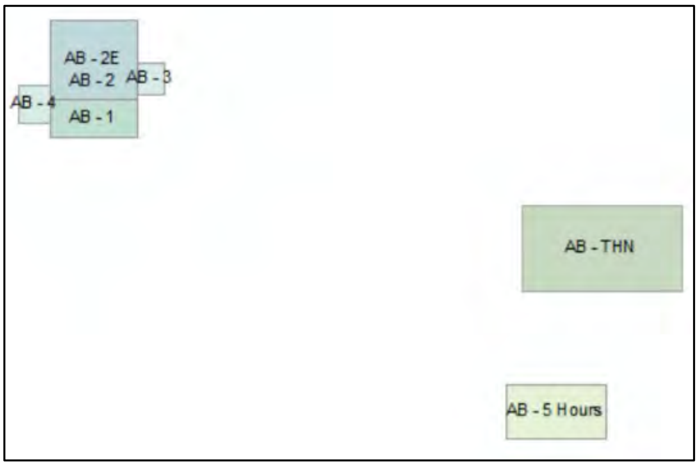

Apollo Bay northern beds AB – 1, AB – 2 and AB – 2E, AB – 3 and AB – 4 are all closely similar (D: 0.04 – 0.26) in all years for which data are available for bed pairs, supporting a single mode of adult scallops. This is not surprising given that these beds overlap to some extent. Apollo Bay eastern beds AB – THN and AB – 5Hours are also similar to each other in 2021 (D: 0.17), with a single mode of adults. AB – THN and AB – 5Hours are similar in 2022 in terms of the predominant adult mode. However, AB – THN shows a mode of small scallops 65mm – 85mm that is only weakly represented in AB – 5Hours (D: 0.37). Nonetheless, it appears that beds in Apollo Bay and in Apollo Bay East can be combined into regions. In contrast, beds AB – 2E and AB – THN, and AB – 2E and AB – 5Hours, differ substantially (D: 0.46, 0.55), with clearly different adult modes, indicating that the Apollo Bay and Apollo Bat East regions should not be combined.

King Island North, NorthMid, Mid

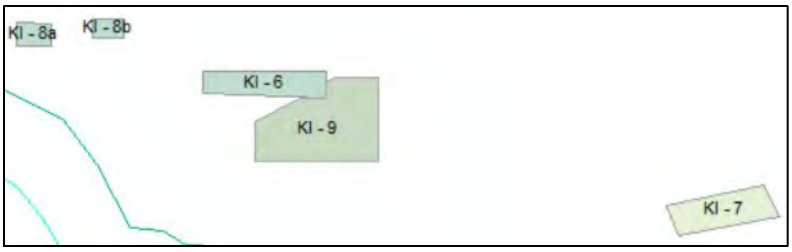

The scallop beds lying between the Apollo Bay region and the main beds surveyed to the east of King Island lie widely spread between 39.5°S – 39.65°S, from 144.12°E to 144.64°E, spanning a distance of ~47 km. Beds KI – 8a and KI – 8b lie close to one another in the west, beds KI – 6 and KI – 9 partially overlap in the centre of this area, and bed KI – 7 lies alone in the east of the area. Bed KI – Mid lies to the south of KI – 7, between the King Island Main and East and was included in these comparisons to evaluate whether there was any similarity between KI – 7 and KI – Mid, both of which are rather isolated, solitary beds.

The closest similarity is between KI – 8a and Ki – 8b in 2019 (D: 0.097), the only year in which both these beds were surveyed. There is also close similarity between KI – 6 and KI – 9 in 2019 (D: 0.137), as would be expected given their overlap. However, there is low similarity between beds KI – 6 or KI – 9 and beds KI – 8a or KI – 8b in 2019(D: 0.32 – 0.36). There is close similarity between KI – 6 and KI – 7 in 2019 (D: 0.125), but less so in 2018 (D: 0.237). In both these years, bed KI – 6 has a mode of smaller scallops, with the similarity being over the tail of larger scallops from the KI – 7 adult mode onwards. There is moderate similarity between beds KI – 9 and Ki – 7 in 2019 (D: 0.237), and low similarity between these beds in 2021 and 2022 (D: 0.31 – 0.42). Unexpectedly, there is close similarity between the widely separated KI – 8b and KI – 7 and KI – 8a and KI – 7 beds (single adult modes, D: 0.13 – 0.14), despite their substantial separation.

It therefore appears that beds KI – 8a and Ki – 8b can be combined, as can beds KI – 6 and KI – 9. It is less clear whether these four beds can be combined. However, the KI – 8a and KI – 8b beds were only surveyed in 2019, so were combined with KI – 6 and KI – 9 to evaluate modal progression across these beds. Despite the similarity, given the substantial spatial separation, bed KI – 7 should probably not be combined with beds KI – 8a and KI – 8b, and differs from bed KI – 9, and therefore should not be combined with any of these beds.

There are substantial differences between KI – 7 and Ki – Mid, and between KI – 6 and KI – Mid in 2018 (widely separated adult modes, D: ~0.7) when these beds were surveyed, indicating the KI – Mid should not be combined with the KI North beds.

King Island Main, Mid

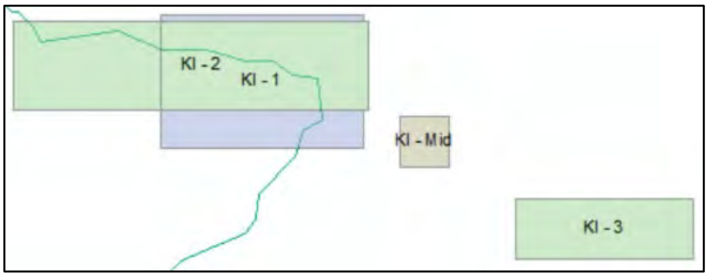

The KI – 1 and KI – 2 beds were among the first surveyed in 2015, but have not been surveyed since 2016, survey effort shifting steadily eastwards since then. The closest similarity is between KI – 2 and KI – Mid in 2016 (D: 0.114), with moderate similarity between KI – 1 and KI – 2, and KI – 1 and KI – Mid in 2016 (D: 0.231 – 0.251). There appears to be low similarity between beds KI – 2 and KI – 3, between KI – 1 and KI – 3, and between KI – Mid and KI – 3, but these differences result from an additional mode of small scallops in KI – Mid. There is similarity between a mid-size mode and a larger adult mode between these beds, indicating that recruitment occurred in the KI – Mid area, but not in the other beds. All of these King Island Mid area beds can usefully be combined to track these various modes.

King Island East

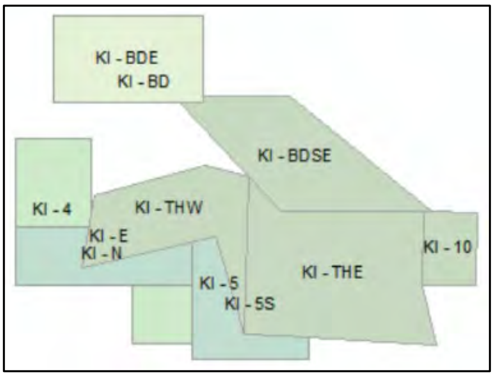

The region lying to the east of the King Island Main region is the most complex in evaluating length composition in the various beds. This region has been heavily and consistently surveyed, but the surveys in this region have steadily extended eastwards and northwards as beds were extended, or additional beds were added to surveys.

Initial inspection of length-frequency distributions indicated that these were different for the BlueDot, The Hill and KI – 10 beds from those further west, and therefore this region was divided into separate King Island East and King Island FarEast regions, notwithstanding that some of the beds overlap across these regions. The beds constituting the KI East region are KI – 4, KI – 5, KI – 5S, KI – E and KI – N. There is close similarity between beds KI – N and KI – 5S in 2017, 2018 and 2019 (D: 0.08 – 0.16). What appears to be a substantial difference between KI – 4 and KI – 5 in 2016 results from the presence of a mode of smaller scallops in KI – 4, but there are similar adult modes in both beds. These beds can usefully be combined.

King Island FarEast

The beds in the area designated the "FarEast" region are contiguous, and some of them partially overlapping, including with beds in the King Island East region (see map under King Island East above). Initial inspection of length-frequencies indicated that those in the BlueDot, The Hill and KI – 10 beds differed in length composition from those in the KI East region, prompting their separation into the region designated FarEast.

Comparisons among these beds are somewhat conflicting, differing among years. In 2023 there is close similarity between KI – 10 and KI – THW, KI – 10 and KI – BDSE and KI – BDSE and KI – THW (D: 0.06 – 0.165), all supporting single adult modes. There is also close similarity between KI – 10 and KI – BDE in 2022 (D: 0.177), although whereas KI – 10 has a single adult mode, KI – BDE has a wide and possibly bi-modal distribution spanning the KI – 10 adult mode. There is moderate similarity between KI – BDSE and KI – BDE in 2019, between KI – BDSE, KI – BDE and KI – 10 in 2021 and between KI – BDSE and KI – THE in 2023 (D: 0.211 – 0.237). These beds all support a similar adult mode in those years, with more or less of a mode of smaller scallops. An apparently lesser similarity between KI – BDE and KI – BDSE in 2021 also results from the occurrence of a mode of smaller scallops in KI – BDSE that is not present in KI – BDE.

These comparisons indicate that all these beds could be combined. There are greater differences among KI – 10 and KI – THE and KI - BDSE, between KI – THW and KI – THE, and between KI – BDE and KI – BDSE over 2022 – 2023, but these appear to result from differences in the proportion of smaller scallops recruiting into the adult mode. For the purpose of tracking modal progression across 2019 – 2023 these FarEast beds were combined.

Flinders Island North

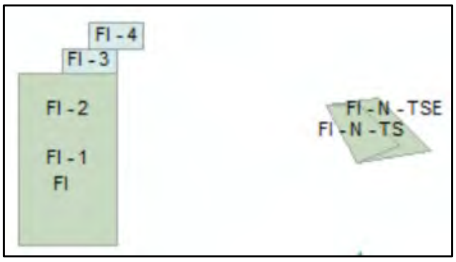

The Flinders Island North beds FI, FI – 1, FI – 2, FI – 3 and FI – 4 were all highly similar in all comparisons (D: 0.04 – 0.22), with slight differences resulting from tails of larger scallops in some beds/years. The one year with data allowing a comparison of FI – TS and FI – TSE shows these to be also highly similar (D: 0.07). Although the FI – TS beds are somewhat separated and further east from the other northern beds, they are still similar to the main FI – 1 bed (D: 0.16 – 0.25). Thus, all these northern Flinders Island beds can be grouped into a region.

Flinders Island South

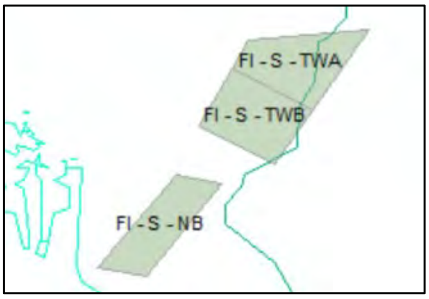

The Flinders Island South beds are all closely similar (D: 0.04 – 0.28) although with differences resulting from the presence of modes of smaller scallops in some beds / years. There is also a slight difference in the adult mode in 2022 which needs to be considered if data for this region are used to track modal progression up to 2022. These beds were grouped into a Flinders Island South region.

Based on the above analysis, beds were grouped into the regions shown in Map 4-1 and Map 4-2.

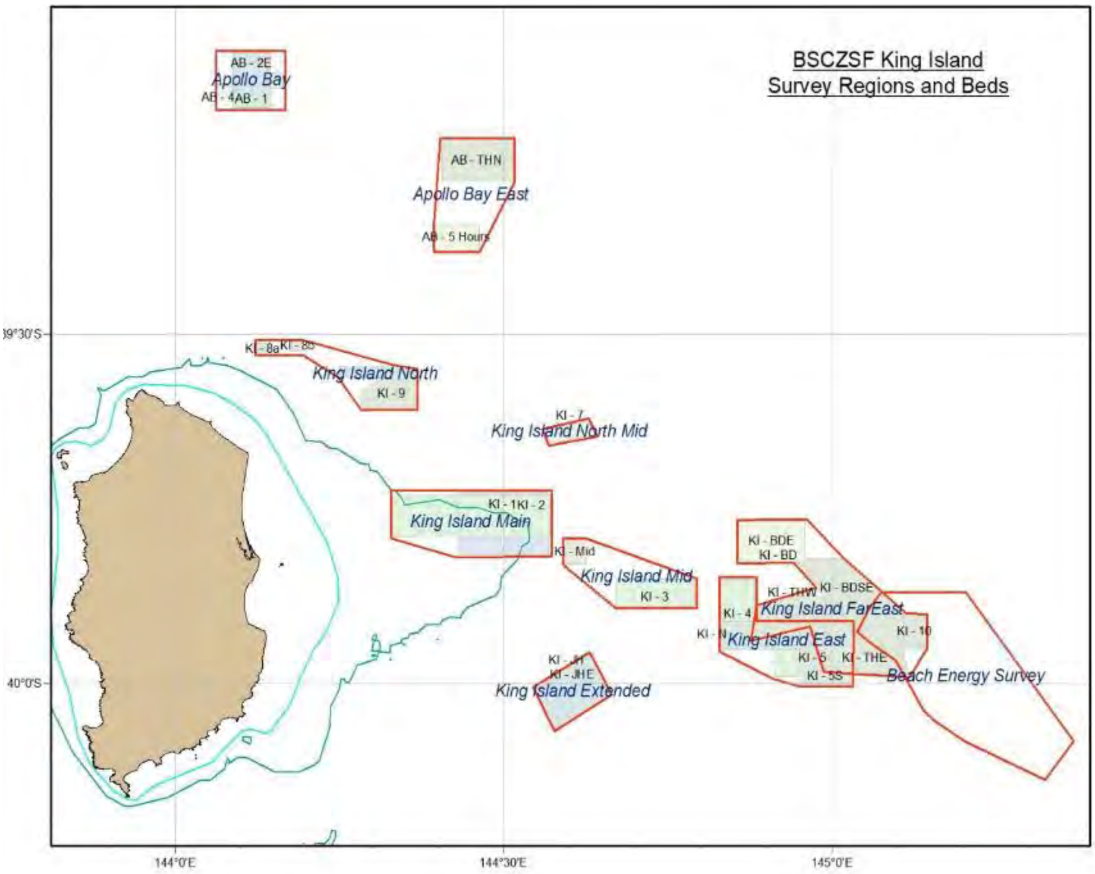

Map 4-1. Map showing the overlaid survey beds surveyed over 2015 – 2023 (shaded, with bed codes) in the Apollo Bay and King Island areas, with bounding polygons (red, with region names) showing the regions into which survey beds and data were grouped for the purpose of region-level analysis. Also shown are the 20m and 40m depth contours.

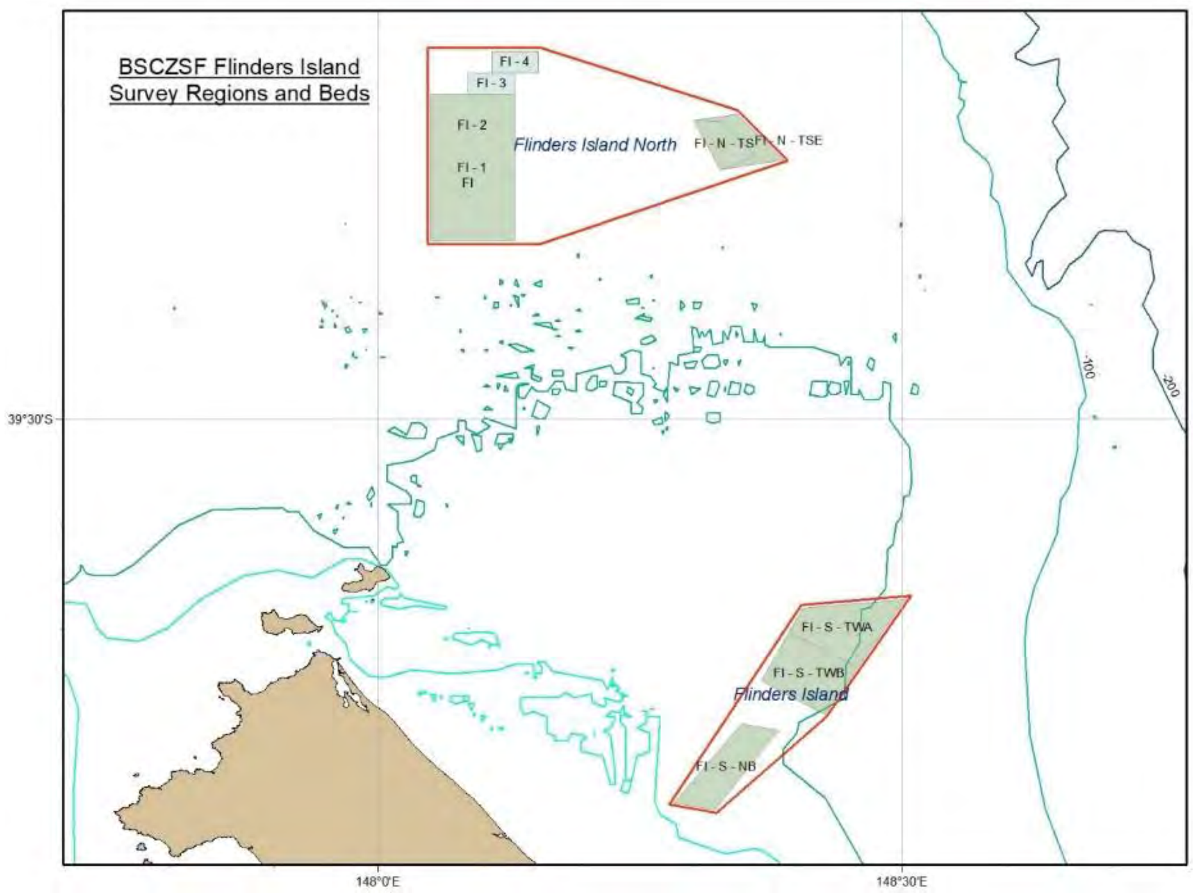

Map 4-2. Map showing the overlaid survey beds surveyed over 2015 – 2023 (shaded, with bed codes) in the Flinders Island area, with bounding polygons (red, with region names) showing the regions into which survey beds and data were grouped for the purpose of region-level analysis. Also shown are the 20m, 40m, 100m and 200m depth contours.

4.2. Commercial catches

The total logbook reported commercial catch over 2002 – 2023 was 30,378 tons. There were a few records with invalid catch positions (either on land or in deep water well to the west, east or south of Bass Strait). Records with invalid positions reported 346.1 t of catch, or 1.1% of the total. Some of these are likely transcription or data entry errors, but no attempt was made to correct these, or other potential position reporting errors.

Of the catch reported within Bass Strait, 18,668 t (61.5% of the total) was reported within or near survey regions in the west (Apollo Bay and King Island area), and 6,497 t (21.5%) was reported within or near survey regions in the East (Flinders Island area) (Figure 4-3). A further 835 t (2.8%) was reported outside of the survey regions in the West, and 4,032 t (13.3%) outside survey regions in the East. A breakdown of annual reporting by these broad position categories is shown in Figure 4-4.

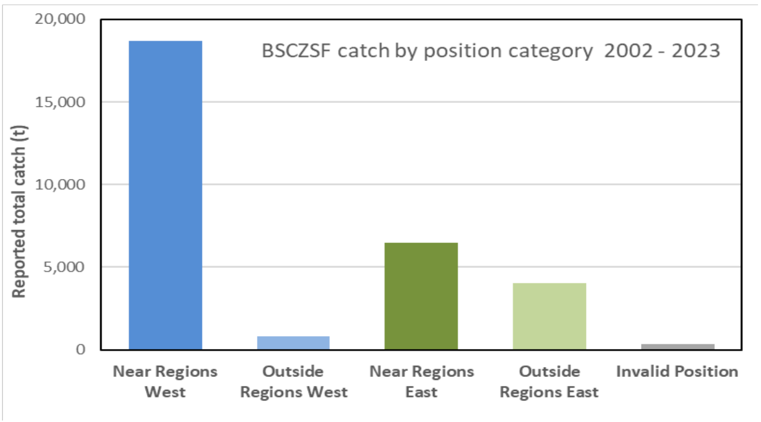

Figure 4-3. Total logbook reported BSCZSF scallop catches over the period 2002 – 2023, grouped by broad positions categories: West (Apollo Bay and King Island area), East (Flinders Island area) and with invalid positions.

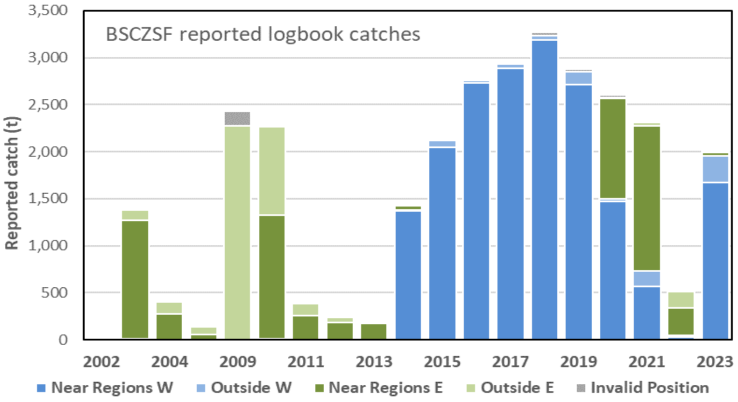

Figure 4-4. Annual total reported BSCZSF catches grouped by broad positions categories: West (Apollo Bay and King Island area), East (Flinders Island area) and with invalid positions.

Over the period of surveys from 2015 – 2023, these catches have all been taken in the second half of the year, mainly from June – December (Figure 3-12), after the annual survey results have become available to set TACs for the season.

More importantly, for the purpose of allocating catches to specific survey beds for mortality estimation, 85% of the total catch reported over the period 2015 – 2023, over which surveys were conducted, could be allocated to surveys beds after application of a 1,852 m spatial buffer to survey beds (Figure 4-5). Only in 2023 was most (67%) of the catch taken outside previously surveyed beds, with industry apparently locating and fishing new areas. The breakdown of total reported catches over the 2015 – 2023 period to individual beds (some aggregated where these overlap) is shown in Figure 4-6.

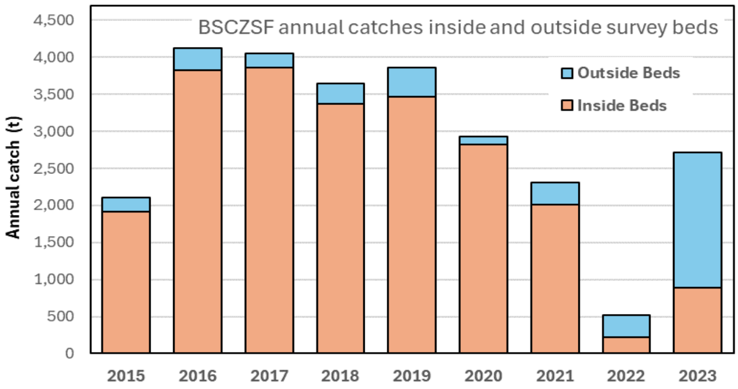

Figure 4-5. Annual proportions of total reported commercial scallop catch that could be allocated to survey beds (after application of a 1,852 m buffer) or which lay outside buffered survey bed areas.

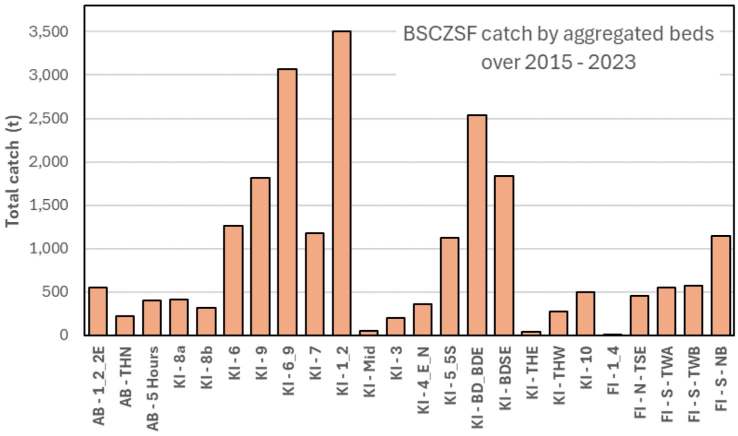

Figure 4-6. Total reported commercial scallop catch over the period 2015 – 2023 that could be allocated to survey beds (after application of a 1,852 m buffer). Some of the overlapping survey beds have been aggregated.

4.3. Bass Strait tidal currents

Selected images chosen from the series of IMOS Bass Strait tidal current prediction maps are shown in Map 4-3, showing predicted inflowing and outflowing tidal current directions and velocities over a spring tide in relation to the position of the scallop survey regions shown in Map 4-1 and Map 4-2.

The scallop beds identified and fished by industry, and so chosen for surveys, are all located in areas of moderate to high tidal current flows. In particular, the series of scallop beds extending south-eastwards from King Island North to King Island East and The Hill appear to be aligned with the direction of current flow, in areas of about 0.5 $m.s^{-1}$ maximum flow. These currents will be instrumental in conveying particulate food across these areas, explaining the persistence of scallops in these regions. The current directions are also such that it is feasible for larvae from scallop beds in at least the King Island regions to be transported to other beds in that area. In contrast, there is an area of permanently low current flow extending north-south down the centre of the Strait from Wilson’s Promontory to Tasmania around 146° E that may act as a barrier to transport of larvae between east and west, at least by tidal currents.

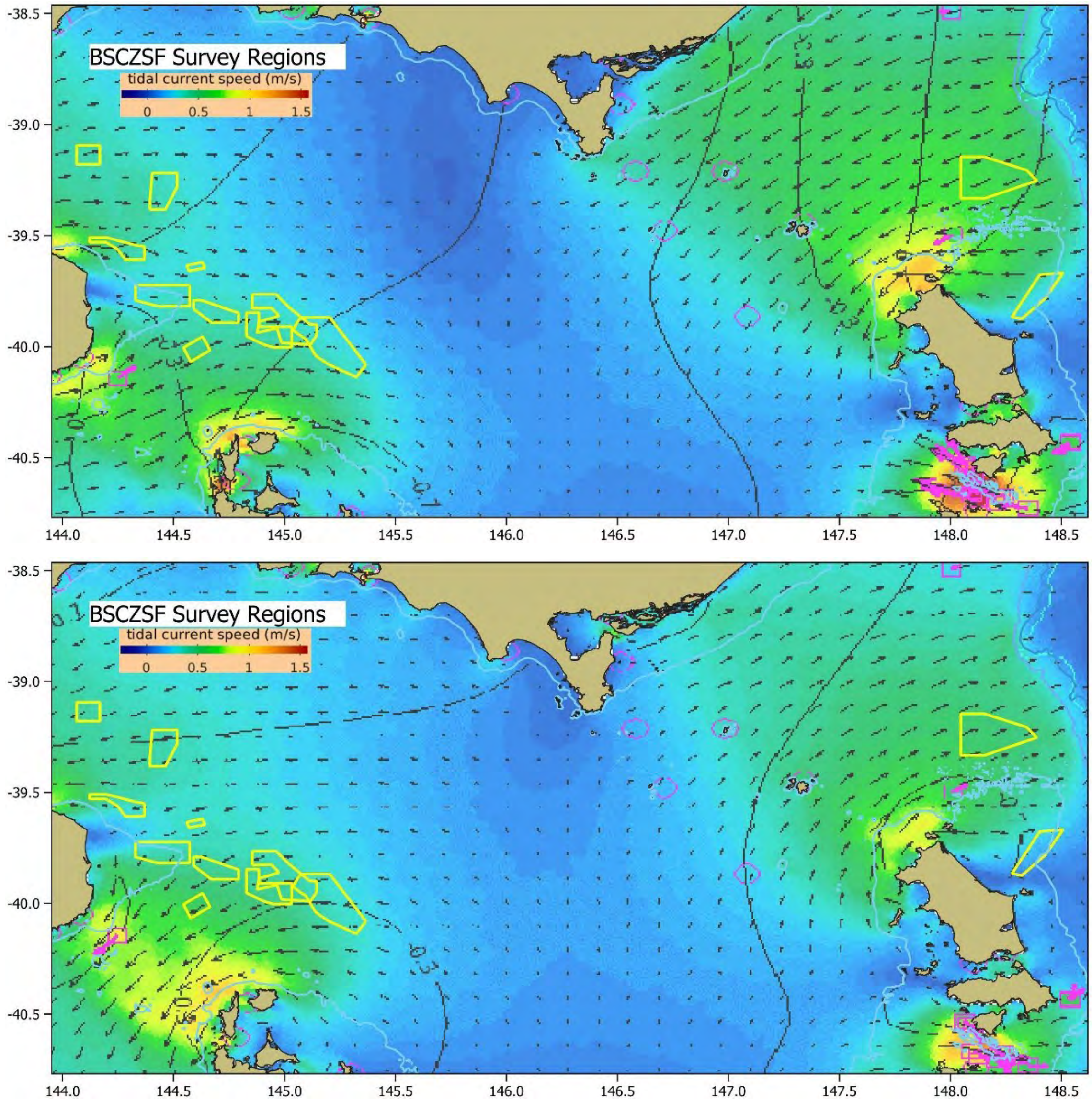

Map 4-3. Tidal current prediction maps from the IMOS Ocean Currents website for Bass Strait for spring tide conditions showing inflowing currents on the rising tide (top panel) and outflowing currents on the ebb tide (bottom panel). Arrows and colours indicate current velocity and yellow polygons show the overlayed positions of scallop survey regions.

Influence of tidal currents on scallop distribution

It appears from the above overlay of scallop survey regions with IMOS-predicted tidal current maps that there is some relationship between tidal currents and the distribution of surveyed scallop beds, particularly in the King Island area. This was further explored by plotting a heatmap of total reported commercial scallop catches summed over 2015 – 2023 on IMOS predicted current maps (Map 4-4 and Map 4-5).

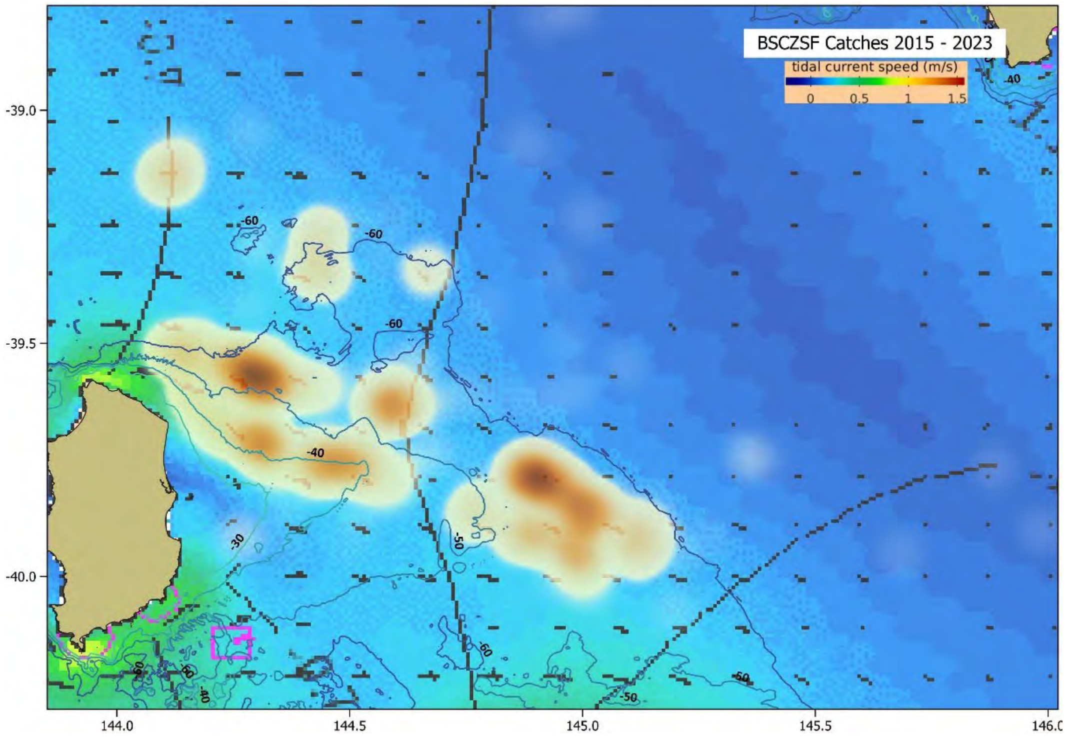

Map 4-4. Map of the Apollo Bay and King Island area showing a heatmap of total reported commercial scallop catches over 2015 – 2023 (red-brown shading) overlaid on an IMOS tidal current prediction map showing moderate (neap tide) inflowing tidal currents. The light blue line shows the 40m depth contour.

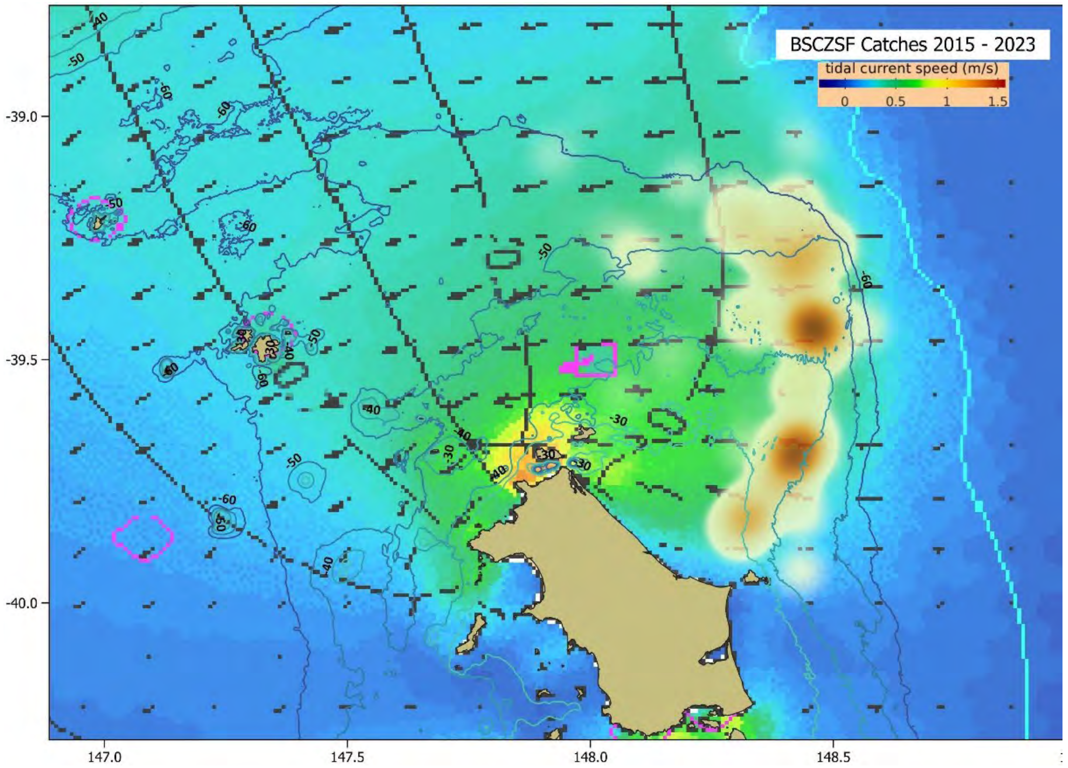

Map 4-5. Map of the Flinders Island area showing a heatmap of total reported commercial scallop catches over 2015 – 2023 (red-brown shading) overlaid on an IMOS tidal current prediction map showing moderate (neap tide) inflowing tidal currents. The light blue line shows the 40m depth contour.

Several important observations can be made from these maps:

- Scallop distribution in the eastern and western areas occurs near the western and eastern boundaries of Bass Strait, not extending into the central area of the Strait. These are the areas that would first receive particulate food transported into the Strait from productive areas to the west and east. In these areas scallops primarily occur in the 35 – 60 m depth range.
- Under conditions of moderate inflowing tidal currents, there is a striking relationship in the Apollo Bay / King Island area between the directions of these currents and the distribution of scallops, which appear to be strongly aligned with inflowing and outflowing currents (Map 4-4).
- Under moderate flow conditions, the tidal currents flow around the north of King Island and track seabed bathymetry as they flow into Bass Strait, following e.g. the 40m depth contour, running along the line of scallop beds from KI – Main to KI – Mid, KI – East and KI – 10. Under stronger flow incoming tide conditions, the currents push more directly eastwards, along the more northern scallop beds from KI – 8a and KI – 8b to KI – 6, KI – 9 and KI – 7.
- In the Apollo Bay / King Island area, the alignment of scallop bed distribution with current flows indicates that it is likely that larvae can be transported along these beds, with recruitment potentially coming from any of the beds aligned with the currents. This extends to sporadic catches of scallops made towards central Bass Strait, which are also aligned with the current direction from the main King Island beds.
- The situation appears to be different in the Flinders Island area, where the 40m depth contour lies east of Flinders Island, such that the currents do not flow around islands or bathymetry, and largely flow directly East – West.
- These beds also occur in the 35m – 60m depth range and will similarly receive particulate food from deeper areas to the East. However, other than some larval exchange between the Flinders Island North eastern and western beds, there seems to be less likelihood that the Flinders Island beds will receive recruitment from beds to the North or South.

4.4. Trends in biomass, mean size and proportion undersize

Interannual trends in biomass by survey bed are shown in Figure 8-2 in Appendix 8.4. Trends in mean length by bed are shown in Figure 8-3 and trends in proportion of undersize (< 85 mm shell length) are shown in Figure 8-4 in Appendix 8.4. These data were further summed (for biomass) or averaged (for mean length and proportion undersize) to generate tables and figures of trends by region for biomass (Figure 4-7), mean length (Figure 4-8) and proportion of undersized scallops (Figure 4-9) by region.

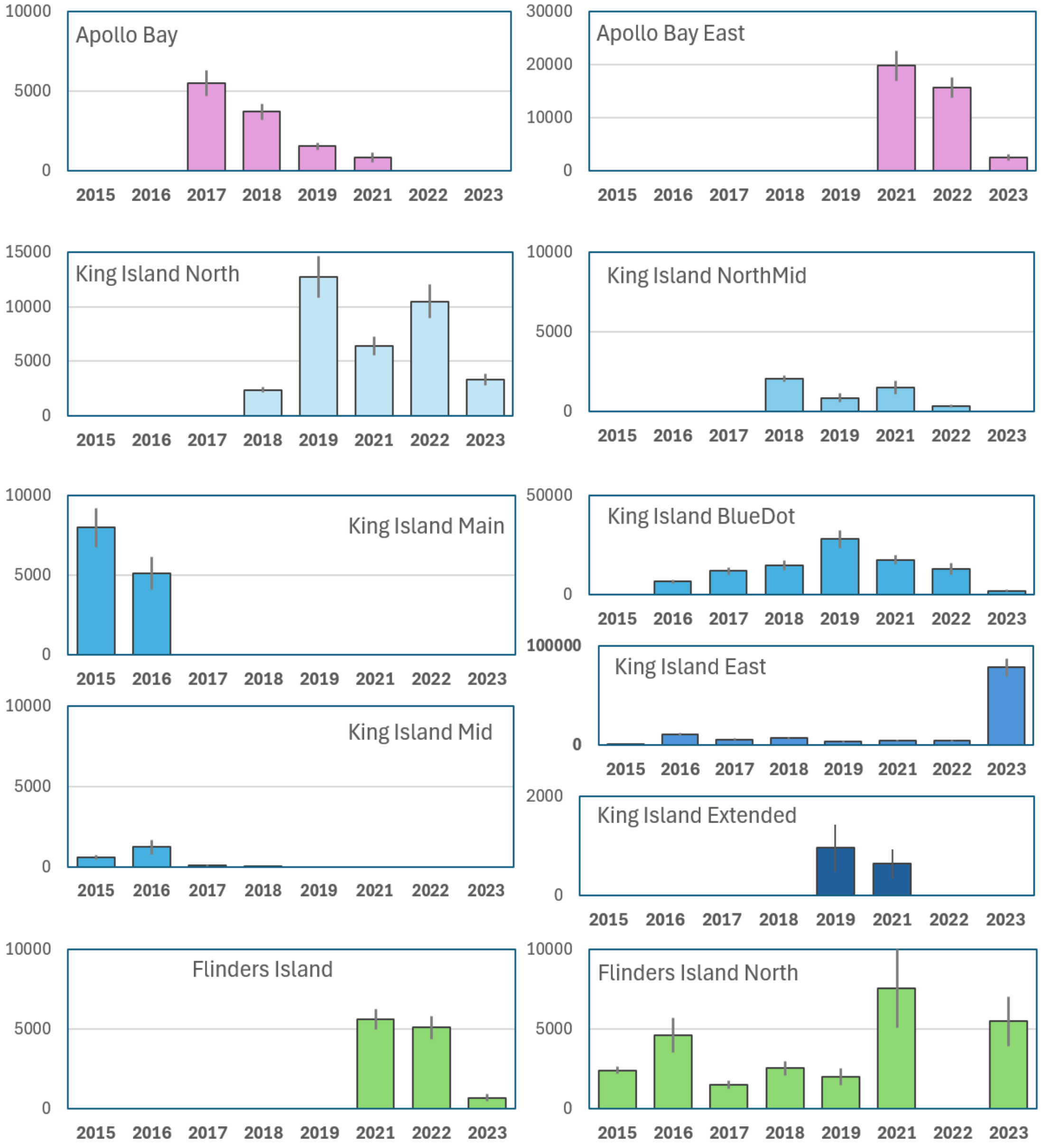

Figure 4-7. Interannual trends in total survey estimated biomass (t) summed across beds in regions. (Error bars show summed std.devs across beds. Note that the y-axis scales differ by region). KI – JH 2019 survey biomass estimated from the uncovered half of dredge only.

Figure 4-8. Interannual trends in the mean length of scallops (shell length mm) across regions. Error bars show standard deviations. KI – JH 2019 estimates from the covered and uncovered parts of the dredge combined.

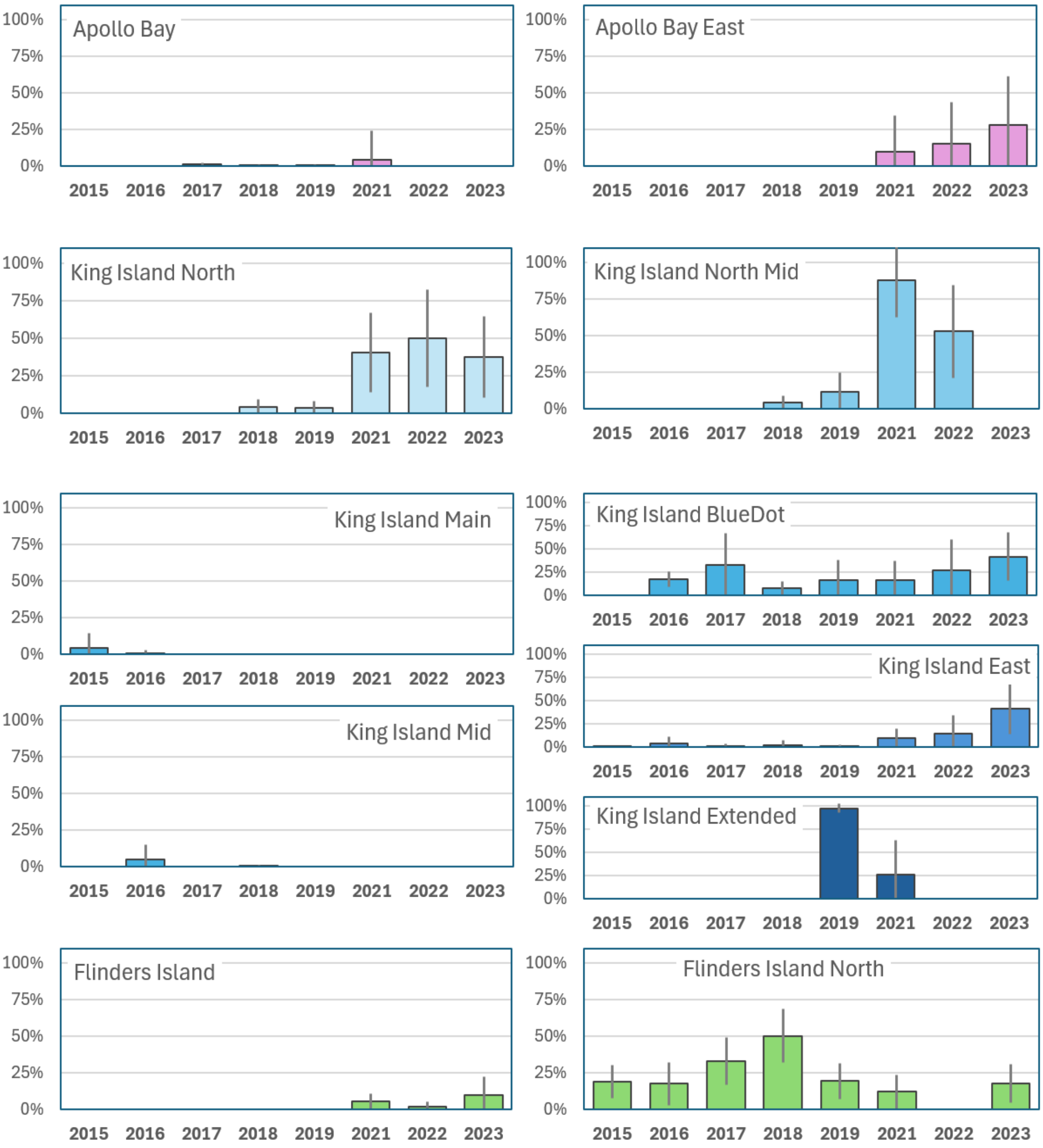

Figure 4-9. Interannual trends in the proportion of undersize (< 85 mm shell length) scallops in regions. Error bars show standard deviations. KI – JH 2019 estimates from the covered and uncovered parts of the dredge combined.

4.5. Length-frequency distributions

Length-frequency distributions of the densities of scallops per individual bed (number of scallops per 1,000 m^2) are shown in Figure 8-5 to Figure 8-22 in Appendix 8.5. These length-frequency distributions were visually compared across beds in each region and year to evaluate whether the distributions were similar enough to justify grouping beds into a region, or whether they should be separated into separate regions. Initial analysis suggested the region groupings shown in Map 4-1and Map 4-2, although region grouping in the King Island East area is less apparent. Despite being in close proximity, and even partially overlapping, some of the beds in the King Island East area appear to show different length compositions.

The individual bed length frequencies (densities) shown in Appendix 8.5 were then raised to the total area of each bed and summed across regions to obtain estimated, merged length-frequencies for each of the defined regions, shown below in Figure 4-10 to Figure 4-16.

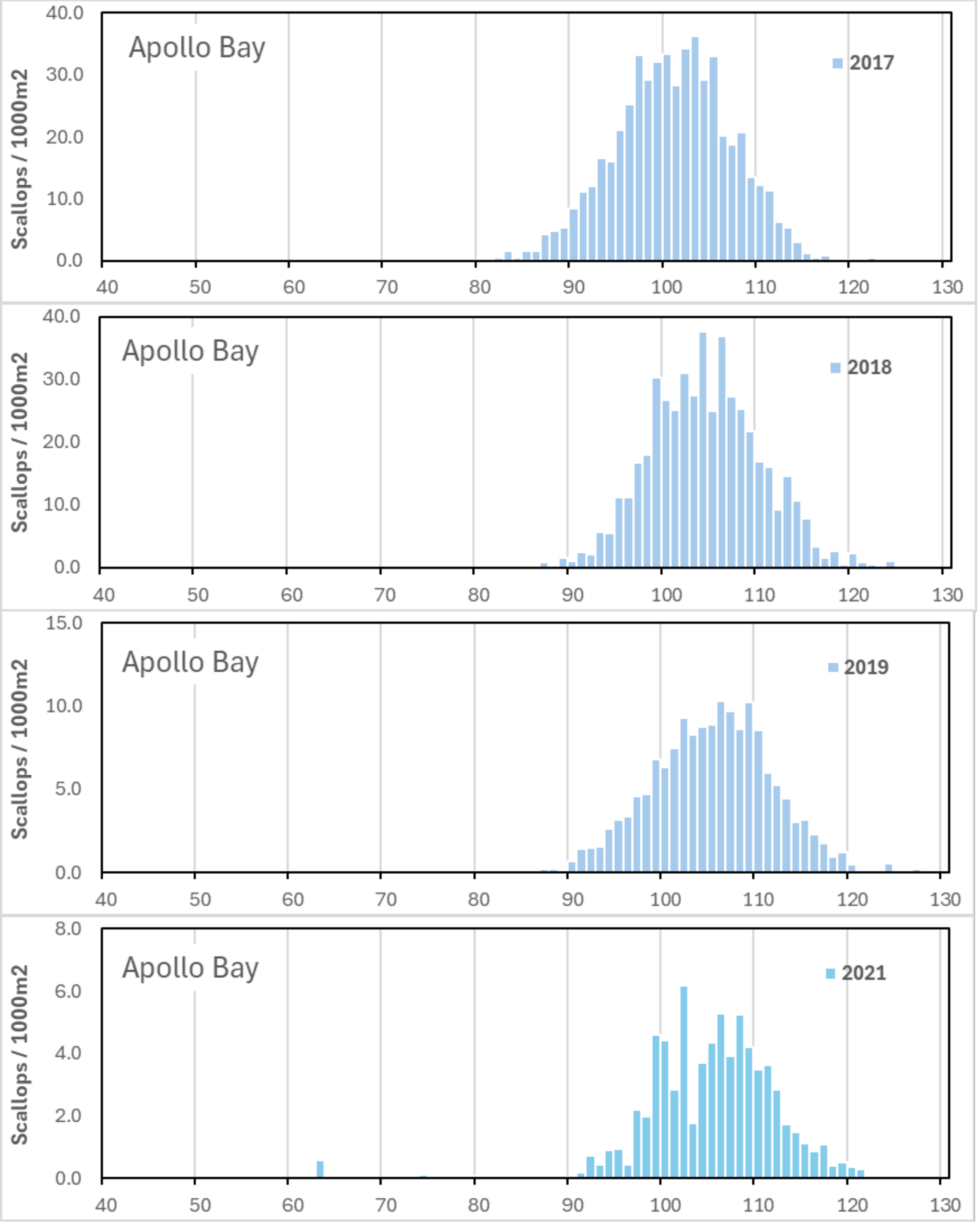

Figure 4-10. Comparative summed length-frequencies of scallops across beds constituting the Apollo Bay region from 2017 to 2021.

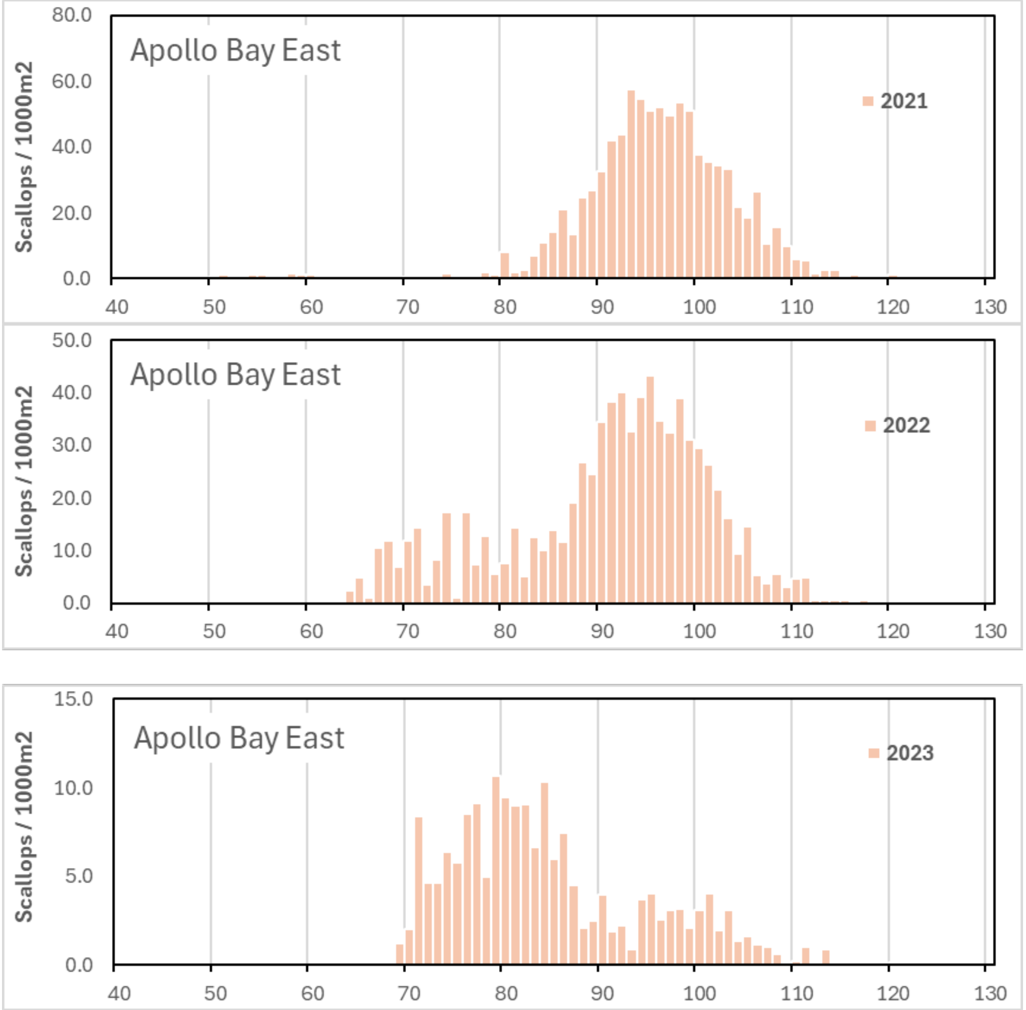

Figure 4-11. Comparative summed length-frequencies of scallops across beds constituting the Apollo Bay East region from 2021 to 2023.

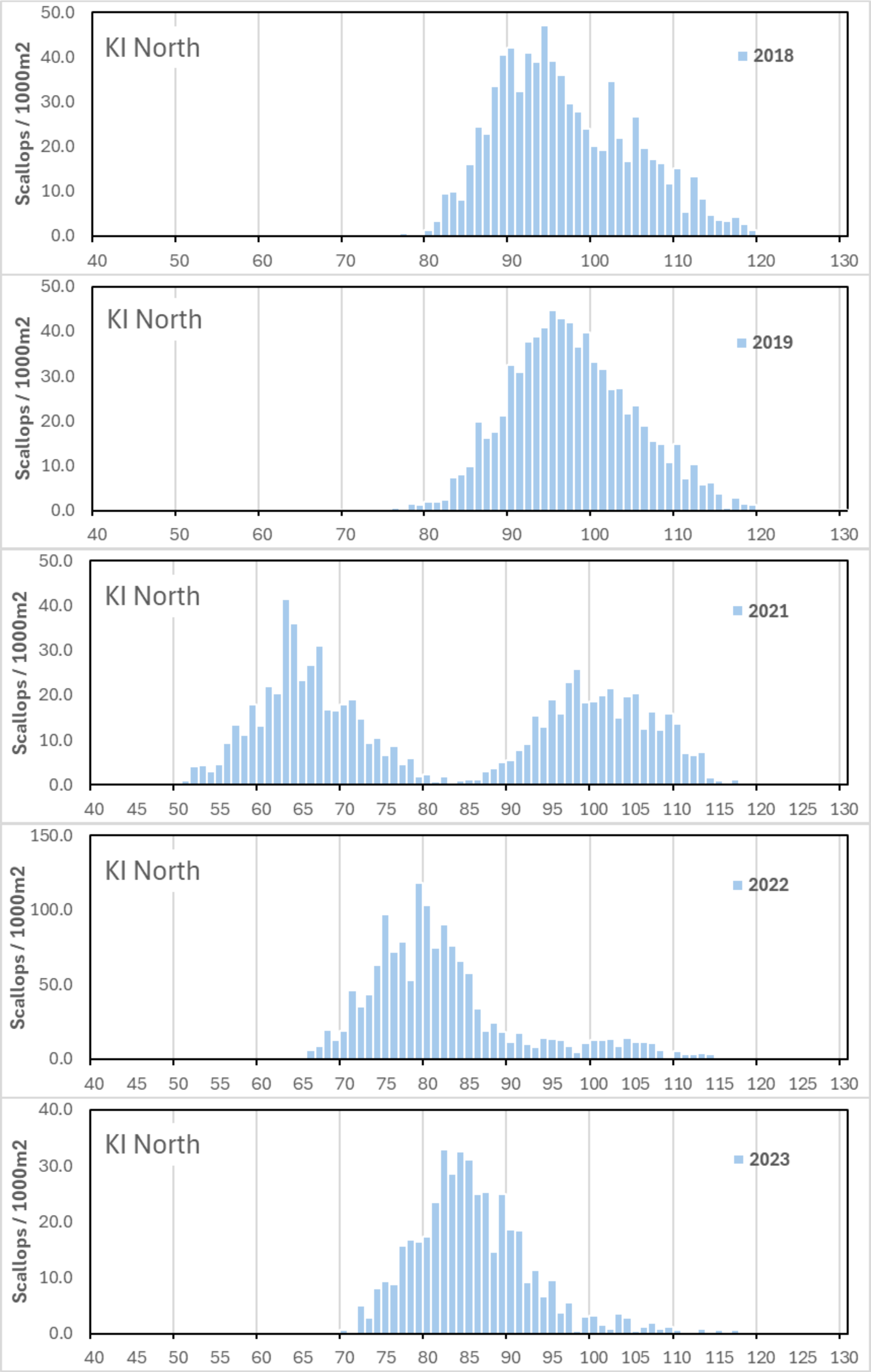

Figure 4-12. Comparative summed length-frequencies of scallops across beds constituting the King Island North region from 2018 to 2023.

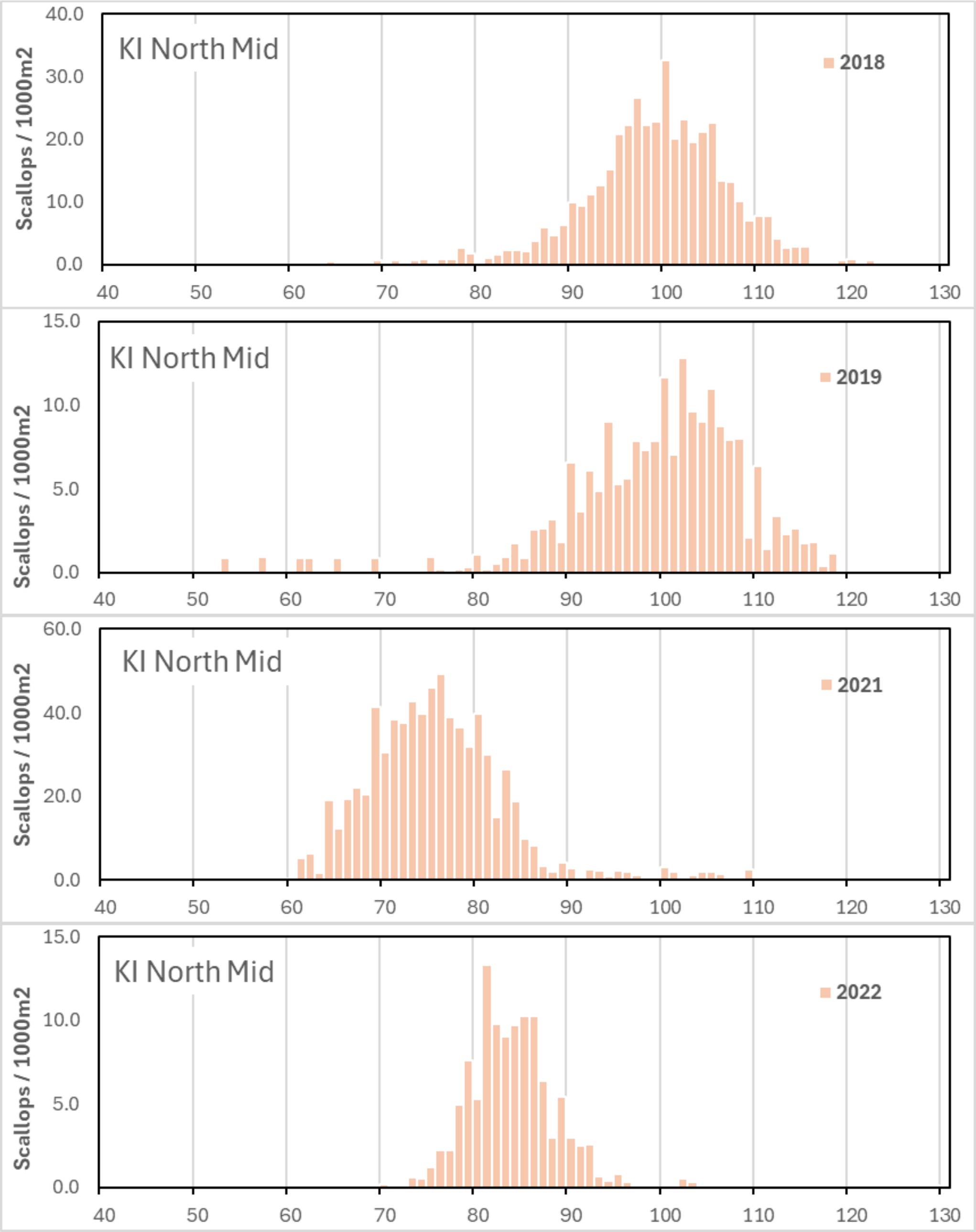

Figure 4-13. Comparative summed length-frequencies of scallops across beds constituting the King Island North Mid region from 2018 to 2022.

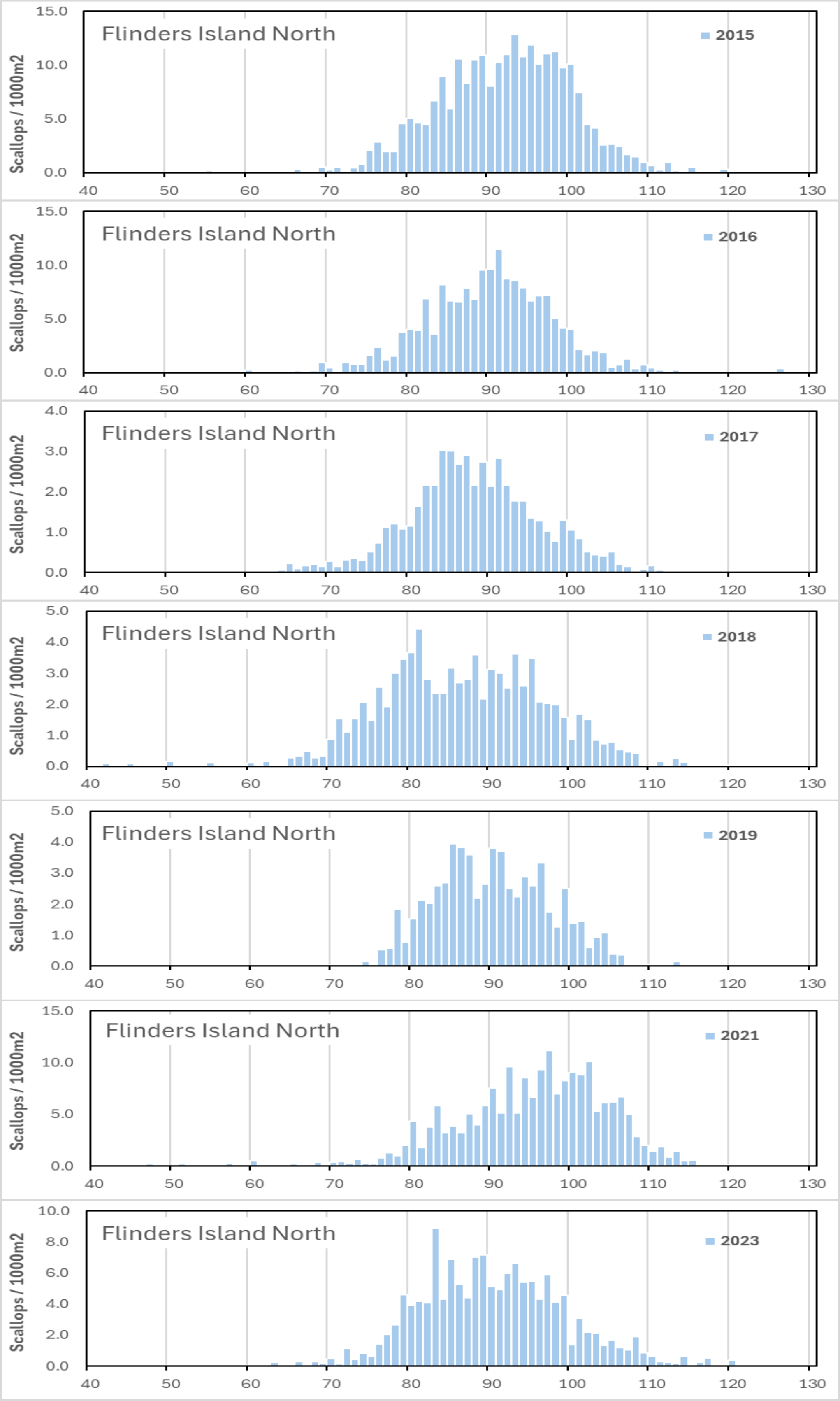

Figure 4-14. Comparative summed length-frequencies of scallops across beds constituting the Flinders Island North region from 2015 to 2023.

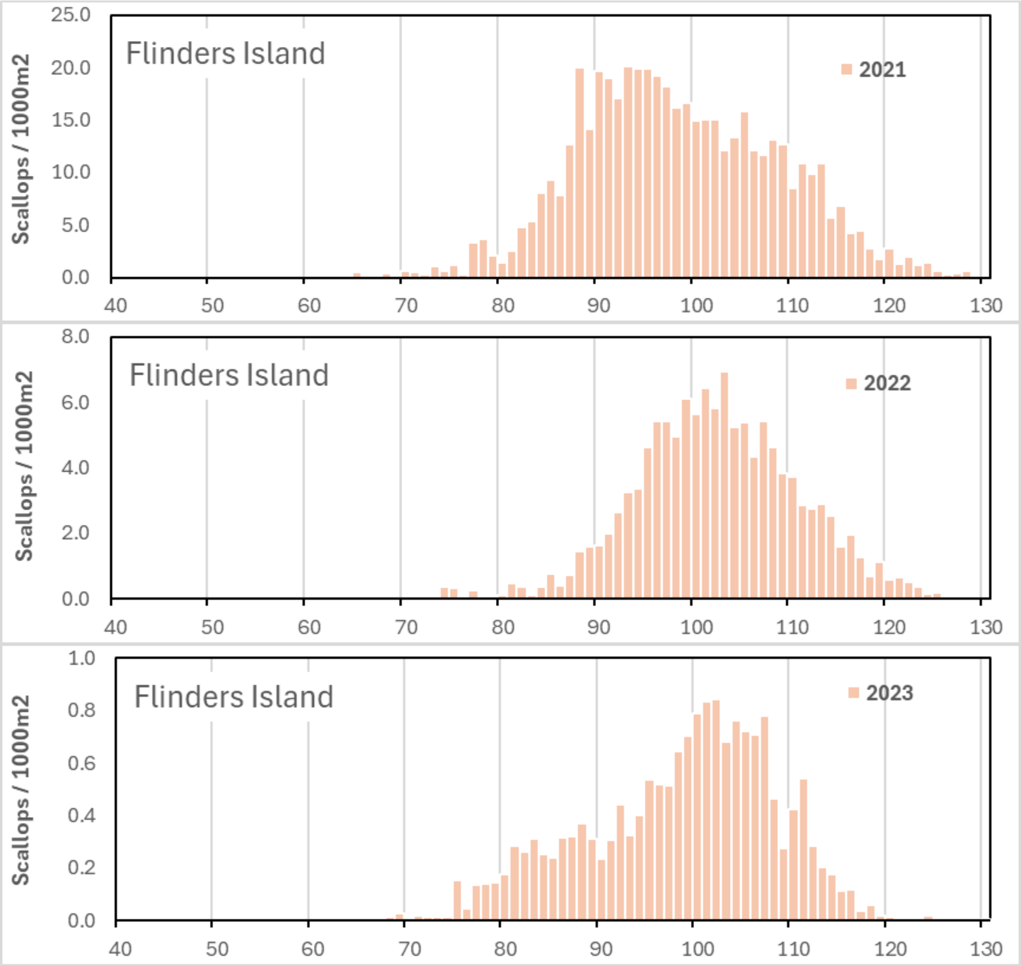

Figure 4-15. Comparative summed length-frequencies of scallops across beds constituting the Flinders Island (south) region from 2021 to 2023.

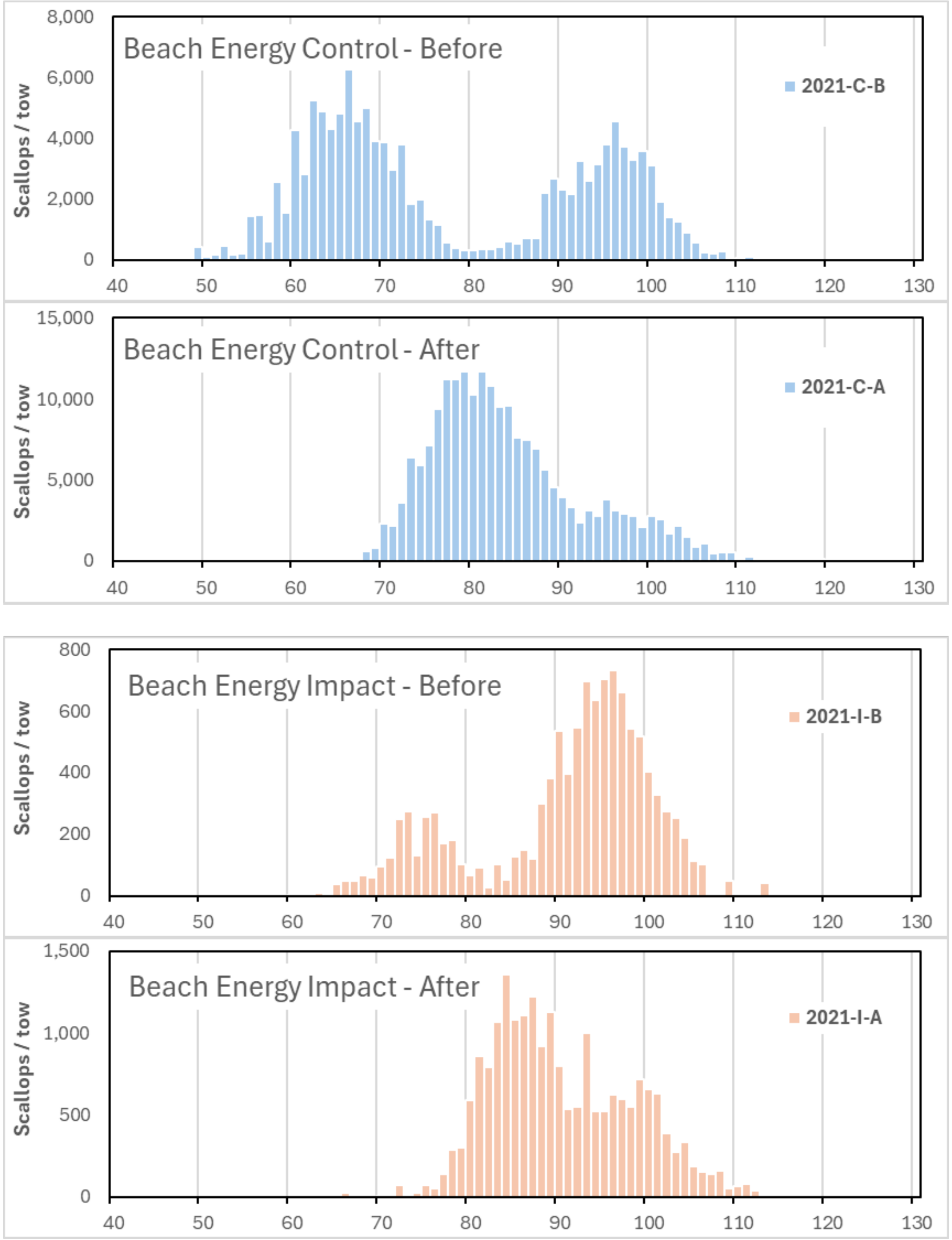

Figure 4-16. Comparative summed length-frequencies of scallops across beds surveyed in the Beach Energy control/impact survey in 2021.

These merged length-frequencies per region were used in modal separation analysis for use in growth analyses for regions showing modal progressions, particularly in regions showing apparent recruitment and modal progression of small scallops. Fairly clear modal progressions are apparent in length frequencies for King Island North, King Island North Mid, and for the Beach Energy Before and After surveys, with less obvious modal progression in data for Apollo Bay, Apollo Bay East and Flinders Island (south).

4.6. Selectivity

The comparison of the catch of scallops by length class in the Fine mesh and Large mesh portions of the 2019 survey of the KI – JH bed shows an increasing proportion of scallops caught by the Large mesh as scallop size increases, from zero < 57 mm to 77% of the small mesh portion at 73 mm. Above that size the numbers of scallops per size class in the Large mesh portion exceeded those in the Fine mesh portion of the dredge, and were assumed to be 100%. There seemed to be some aspect of the fine mesh portion that excluded large scallops > 73 mm, possibly a back-pressure bow wave resulting from clogging of the fine mesh by large numbers of small scallops. The observed numbers by length class in the Fine mesh and Large mesh dredge portions are shown in Figure 4-17 (top and middle panels) with a selectivity curve fitted to the Large mesh proportions (bottom panel), with k = 0.4177 and L_{50} = 70.17 mm.

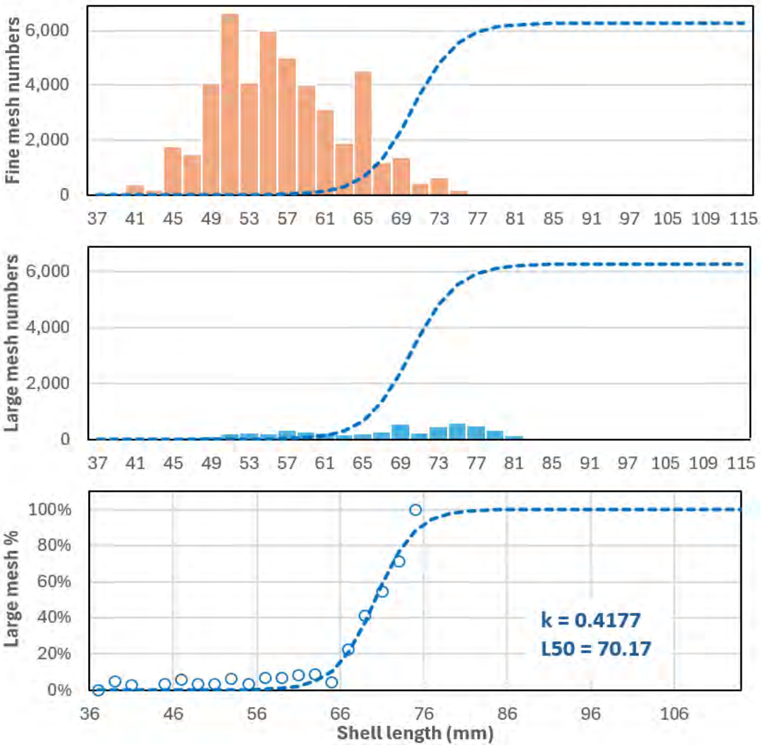

Figure 4-17. Length-frequency distributions of scallops caught in the 2019 survey of the KI – JH bed, showing the numbers of scallops by length in the Fine mesh portion of the dredge (top), the numbers by length in the Large mesh position (middle) and the relative proportions by length caught in the Large mesh compared with the Fine mesh (bottom). The selectivity curve fitted to the Large mesh proportions (L_{50} = 70.17 mm) is overlaid on the three plots.

Selectivity curves were then also fitted to the aggregated length-frequency data per year, summed across all beds surveyed in each year from 2015 – 2023, to compare with the experimental KI – JH selectivity curve. The resulting curves (Figure 4-18) show that scallops caught in surveys over 2015 – 2018 were generally far larger than the size at 50% selectivity, with L_{50} ranging from 84.2 to 89.7, and therefore not biased by selectivity. In 2019 the selectivity curve fitted to the aggregated survey data continues to exceed the JH selectivity curve (L_{50} 88.0), but with the first sign of significant numbers of small scallops appearing in survey catches, down to as small as 36 mm in shell length, and certainly affected by selectivity.

Over 2021 – 2023 the proportion of small scallops increased in survey catches, showing a substantial and eventually dominant mode of recruiting scallops progressing over 2021 – 2023. L_{50} values of selectivity curves fitted to these years range from 74.1 to 77.8.

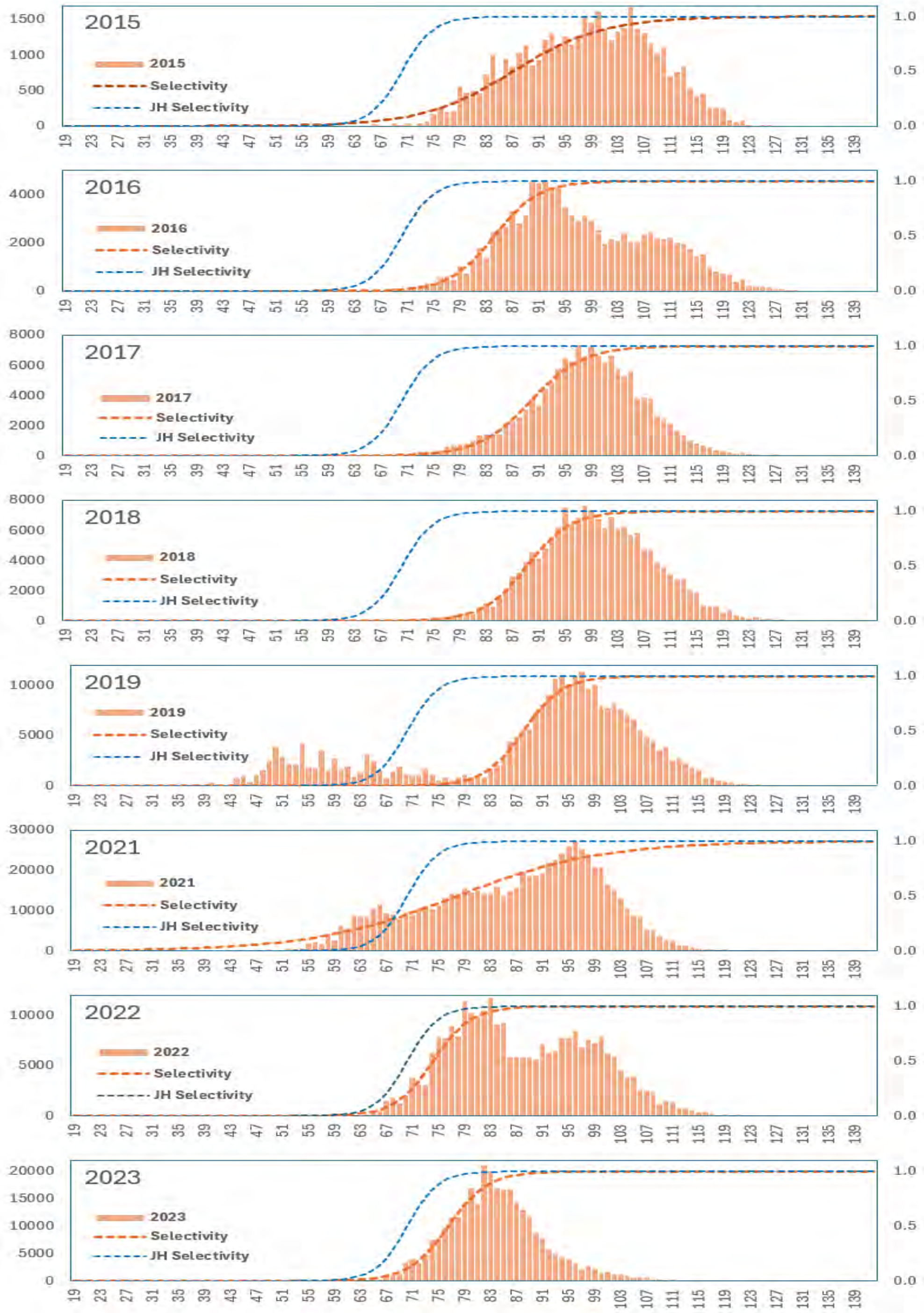

Figure 4-18. Aggregated annual length-frequency distributions summed across all beds surveyed in each year from 2015 – 2023 showing overlaid selectivity curves fitted to the survey data (red dashed lines), and the selectivity curve experimentally determined using the 2019 KI – JH Fine and Large mesh data (blue dashed lines).

Aggregating these length frequencies across years 2015 – 2019 and 2021 – 2023 (Figure 4-19) emphasises the differences in length distributions between these two periods. The 2015 – 2019 data are considerably greater than the JH L_{50} of 70.17 mm, apart from the tail of small scallops caught in 2019, with a L_{50} of 82.2 mm. In contrast, the length distributions of scallops caught over 2021 – 2023 show a selectivity curve similar to that experimentally determined from the JH data, with a L_{50} of 72.6 mm. The mean length of recruiting scallops caught over 2021 – 2023 would have been affected by the dredge selectivity.

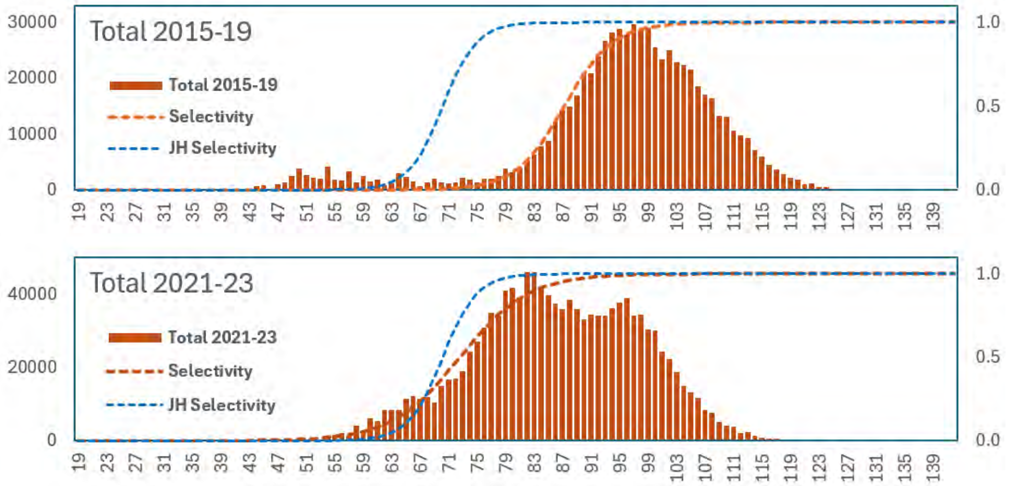

Figure 4-19. Aggregated length frequency distributions of survey catches across all beds surveyed over the periods 2015 – 2019 (top) and 2021 – 2023 (bottom), with overlaid fitted selectivity curves for the survey data (red dashed lines) compared with the experimental JH selectivity curve (blue dashed lines).

Effect of selectivity on mean length of recruiting scallops

The effect of dredge selectivity was explored by simulating normally distributed modes of small scallops ranging from 57 mm (below which selectivity is estimated to be zero) and 81 mm (about the size at 100% selectivity in the JH selectivity curve), with a standard deviation of 5.5 mm, as determined from application of the R Mixtools modal separation analysis to a number of recruiting juvenile modes. The JH selectivity curves was then applied to these simulated distributions to estimate what the length-frequencies would be after removal of non-selected scallops. The results are shown in Figure 4-20.

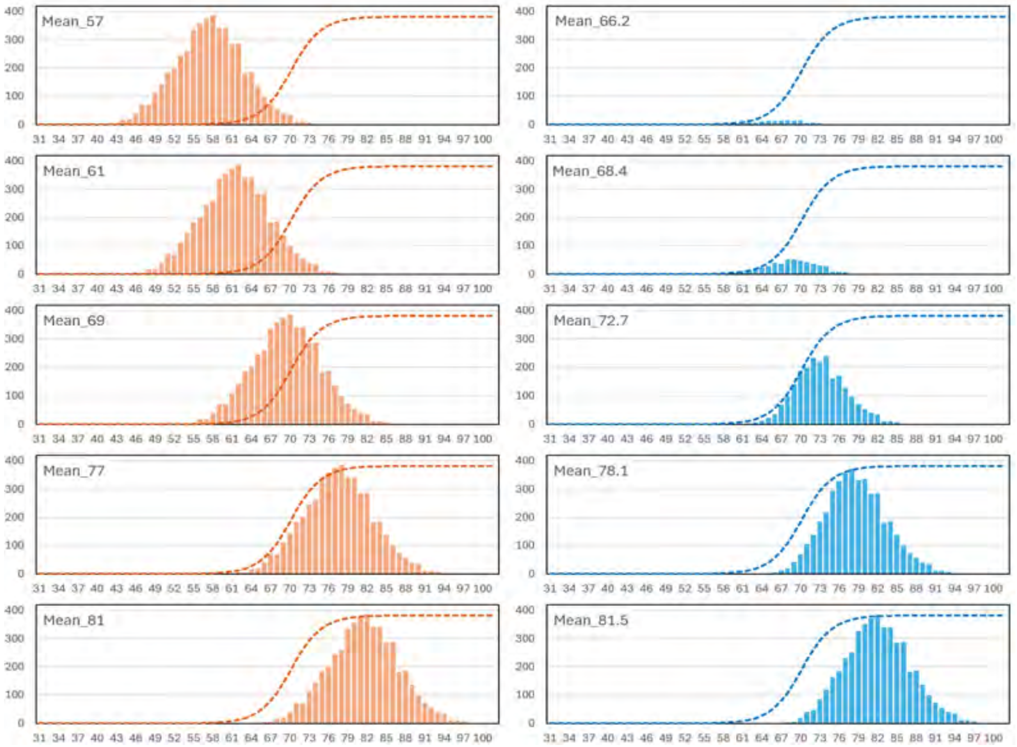

Figure 4-20. Comparison of the ‘True’ length frequency of a mode of simulated juvenile scallops ranging in mean size from 57 mm to 81 mm (left), and the observed Sample length-frequency (right) after application of the JH selectivity curve (red and blue dashed lines) to the ‘true’ data.

The application of the JH selectivity curve to scallops with a mean length of 57 mm results in exclusion of almost all scallops from the catch, with only 2% being retained. With a true mean length of 69 mm, 46% of scallops are retained, and with a true mean length of 81 mm, 95% of scallops are retained. The retained scallops are the larger ones that exceed the selectivity curve, therefore the mean size of selected scallops is greater than the true mean size, and increasingly so for smaller scallops. The mean sizes resulting from application of the selectivity curve are shown on the sample distributions in Figure 4-20. The relationship between the Sample and True mean lengths can be well fitted using a polynomial curve, either to the Sample vs. True mean lengths, or to the Sample mean lengths vs the True/Sample length ratios. The resulting curves are shown in Figure 4-21, with the mode ratio plateauing after about 80 mm.

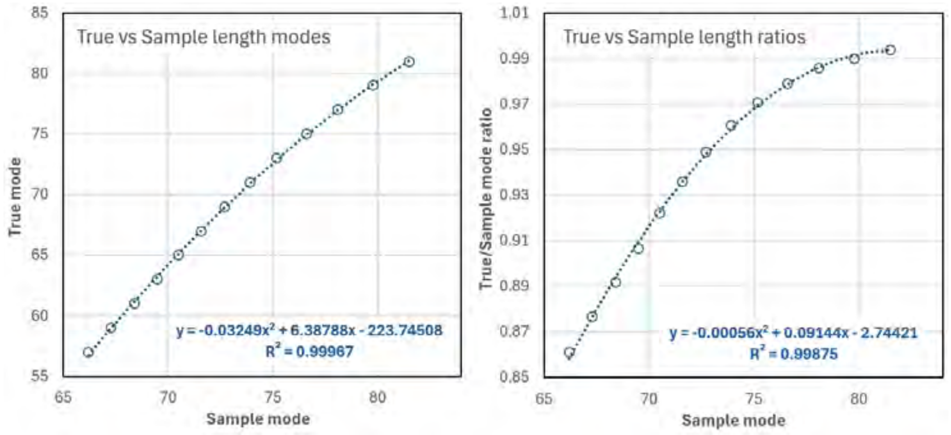

Figure 4-21. Polynomial relationships fitted to the Sample vs. True modes (left) and the Sample modes vs. the True/Sample mode ratios, for simulated recruiting scallops ranging from 57 mm to 81 mm in mean/modal length.

The True vs Sample mode relationship shown in Figure 4-21 (left) was used to apply a correction factor to the survey catch modes of small scallops < 80 mm in mean/modal length for use in modal progression growth analysis.

4.7. Morphometrics

Morphometric comparisons of shell length, height, width and weight data collected during each scallop survey are reported in the individual survey reports (Koopman *et al.* 2015 – 2022), including statistical comparison of differences among morphometric relationships between beds surveyed in each year.

Having identified regions of aggregated beds with similar length-frequency composition (see section on Identification of Regions), morphometric comparisons were conducted for morphometric measurements in these regions, aggregated across all years and beds in each region for which morphometric data were available (noting that not all beds were surveyed in all years). Overlaid scatterplots of length : height, length : width, and length : whole weight were plotted for the defined regions in four main areas: Apollo Bay and Apollo Bay East; King Island North and NorthMid; King Island Main, Mid, East and Fareast; and Flinders Island North and South (Figure 4-22). Best fit trendlines were fitted in Excel to each of these scatterplots, linear fits with the intercept set to zero for $L:H$ and $L:W$, and power curves for $L:Wt$.

Length : Height and Length : Width relationships

Within each of the four areas, there are no apparent differences in $L:H$ relationships between the beds in each region. There are also no differences in $L:H$ relationships across any of the four areas, with relationships being closely similar among all the survey beds and regions. Given the lack of difference between $L:H$ relationships among all beds and regions, it is surprising to note that there are differences between $L:W$ relationships among regions in the Apollo Bay and the Flinders Island areas. The Apollo Bay $L:W$ line lies above the Apollo Bay East line, with Apollo Bay scallops apparently having greater width than those from Apollo Bay East, despite there being no differences in the $L:H$ relationships between these two regions. Residuals for the Apollo Bay East region lie more closely aligned with those for Apollo Bay, above most of the Apollo Bay East points. These data were from the 2021 survey, and it is unclear why the scallops should suddenly be wider in that region in that year.

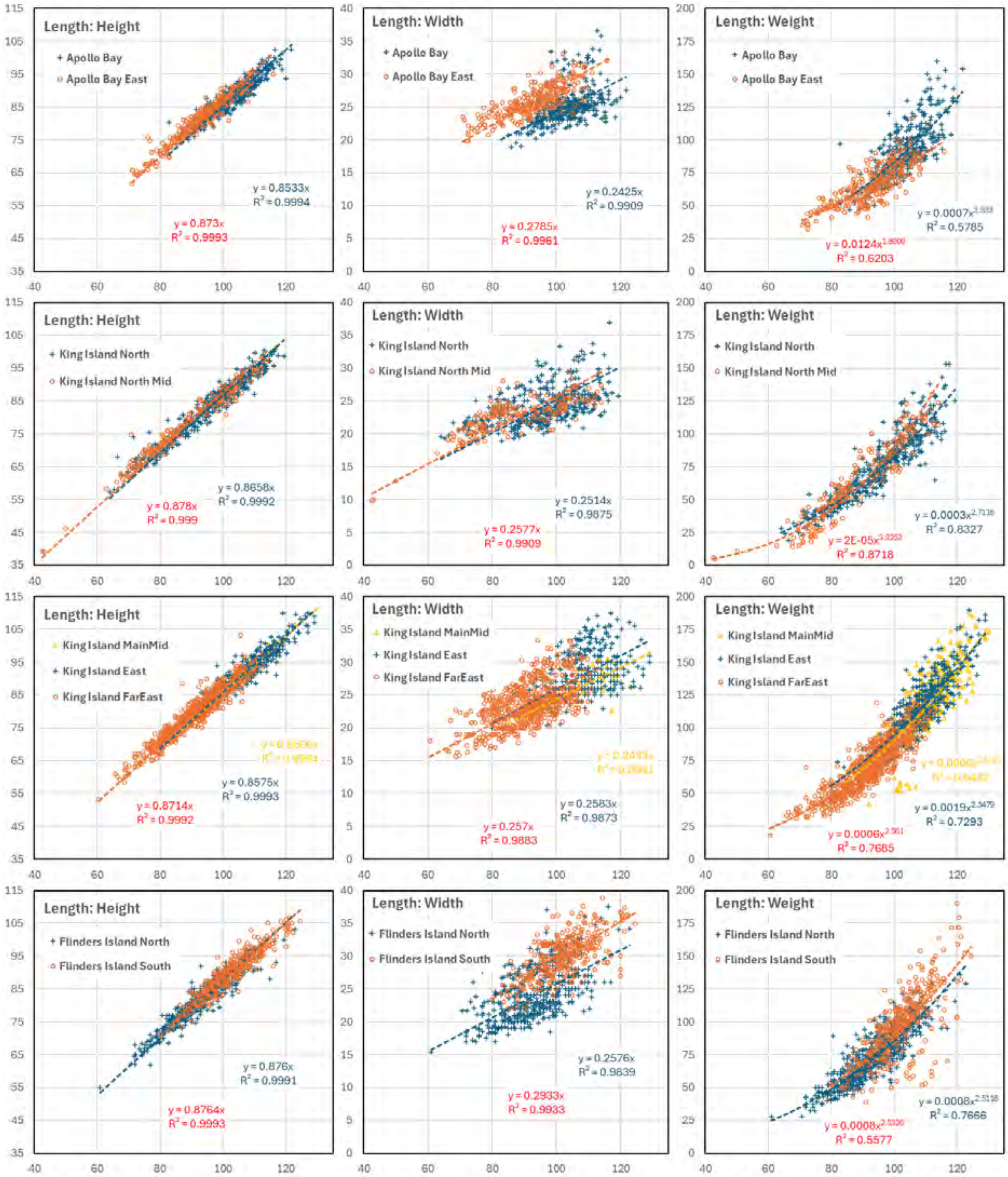

Figure 4-22. Morphometric scatter plots with best fit trendlines for length : height, length : width and length : weight relationships for scallops in four main areas: Apollo Bay; King Island North/NorthMid; King Island Main/Mid/East/FarEast; and Flinders Island. Separate scatterplots for regions in each area are overlaid, with separate trendlines and equations for each region.

The situation is similar in the Flinders Island area, where the $L{:}W$ line for Flinders Island South lies above that for Flinders Island North, although less clearly than for the Apollo Bay area. The separation is less clear between these areas, with the $L{:}W$ points for the Flinders Island North region appearing to consist of two groups of residuals, one of which is more aligned with the Flinders Island South $L{:}W$ line.

There are no substantial differences between the $L{:}W$ relationships for individual regions within the King Island North/NorthMid and the King Island Main/Mid/East/FarEast areas, or between these areas themselves. The $L{:}W$ relationships in these areas coincide quite closely with the lower $L{:}W$ lines for Apollo Bay and for Flinders Island North.

Length : Weight relationships

The scatter of residuals around $L{:}Wt$ relationships is substantial in all regions. This is to be expected, given that these are whole weights, including gonad weight, and the surveys coincide with the start of the protracted spawning season when some scallop gonads have not yet started to develop whereas others may have developed substantial gonad mass in preparation for spawning. Weights are difficult to measure onboard and are affected by the amount of water retention within the shell. There are also differences in the size ranges sampled in different regions, with larger scallops having larger and more variable gonad weight.

There are no substantial differences in $L{:}Wt$ relationships for regions in the most heavily fished and surveyed King Island Main/Mid/East/FarEast area. The differences in size range sampled in other areas appear to have contributed to minor differences in the $L{:}Wt$ curves among regions in the Apollo Bay area, and to a lesser degree the King Island North and Flinders Island areas. However, the residual distribution around all of these relationships indicates that these differences in the fitted trendlines among regions within areas are swamped by the variability of individual data.

Aggregated L:Wt curves for use in mortality estimation

For natural mortality estimation, $L{:}Wt$ relationships are required to convert changes in length to changes in weight between years. The similarity and wide scatter of $L{:}Wt$ residuals among regions within the four main areas indicates that results for regions could be combined within each area to provide single $L{:}Wt$ curves for each region. There were no beds identified as being suitable for natural mortality estimation (i.e. showing single adult modes and substantial biomass declines) in the King Island North/NorthMid area, therefore aggregated $L{:}Wt$ curves were constructed across all beds and years only for the Apollo Bay, King Island Main/Mid/East/FarEast and Flinders Island areas (Figure 4-23).

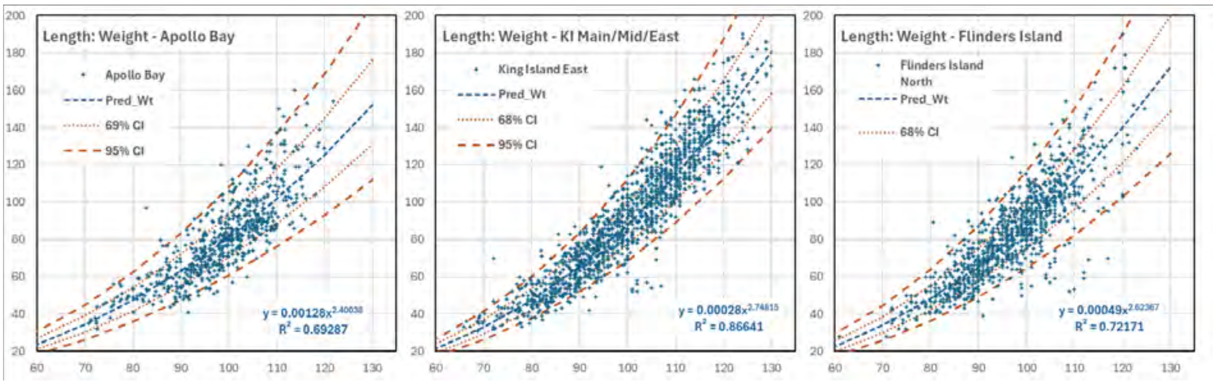

Figure 4-23. Aggregated length : weight curves across all beds and years for the Apollo Bay., King Island Main/Mid/East/FarEast and Flinders Island areas. Empirical confidence intervals showing one standard deviation (68.2 % CI) and the 95% CI are shown around the best-fit trendline.

Confidence intervals showing one standard deviation (68.2 % CI) and the 95% CI are shown around the best-fit trendline for each area (see *Methods: Morphometrics*). The best fit weight for any length plus the 68.2% standard deviation were used to generate normally distributed random samples of a $L{:}Wt$ conversion around changes in mean length among years for each area.

Once aggregated, the $L{:}Wt$ curves for King Island Main/Mid/East and for Flinders Island North/South are similar in terms of the best fit relationship, with slightly wider confidence intervals for the Flinders Island area. Both show larger weights at length than the $L{:}Wt$ curve for Apollo Bay, with the King Island and Flinders Island best fit curves aligning almost with the upper 68% CI of the Apollo Bay curve.

4.8. Growth

Length-frequency data for regions showing apparent modal progression, particularly of juvenile scallops, were aggregated into 2mm length classes by region, and subject to modal separation analysis. For regions or years showing single modes, the modal peaks were calculated as the weighted average length in each mode. As explained in the above section on selectivity, a correction factor was applied to correct for the upwards biasing of modes of recruiting scallops < 80 mm in modal length.

Apollo Bay growth curve

Length frequency distributions for the Apollo Bay area only show a single adult mode in all years sampled, but with clear (albeit slight) progression across the years 2017 – 2021 (Figure 4-24).

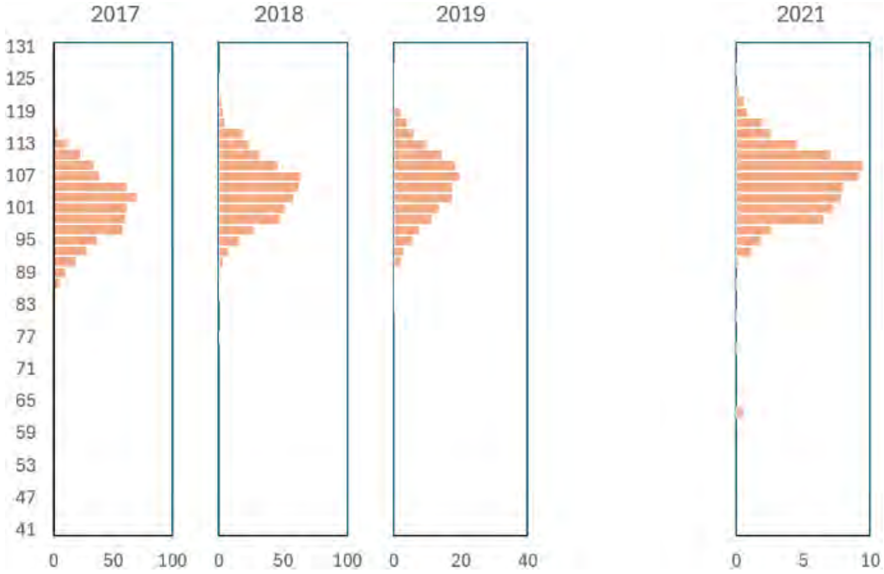

Figure 4-24. Length-frequency distributions for the Apollo Bay region (2mm size classes) from 2017 – 2021

The position of the modes in each year were determined as the weighted average length across the length classes present and are summarised in Table 4-1. Assigning ages to these modes is inevitably subjective, given how similar they are. Assuming a maximum age for scallops in these samples of 9+, ages were assigned as shown in Table 4-1. A von Bertalannfy growth curve (t_0 = 0, L_∞ = 106.9, K = 0.61) fitted to these modes is shown in Figure 4-25.

Table 4-1. Modal peaks determined from the annual weighted average length for the Apollo Bay region over 2017 – 2021, with ages assigned to each mode.

Year	Mode 1	Age
2017	101.19	5
2018	104.71	6
2019	105.56	7
~~2020~~		
2021	105.89	9

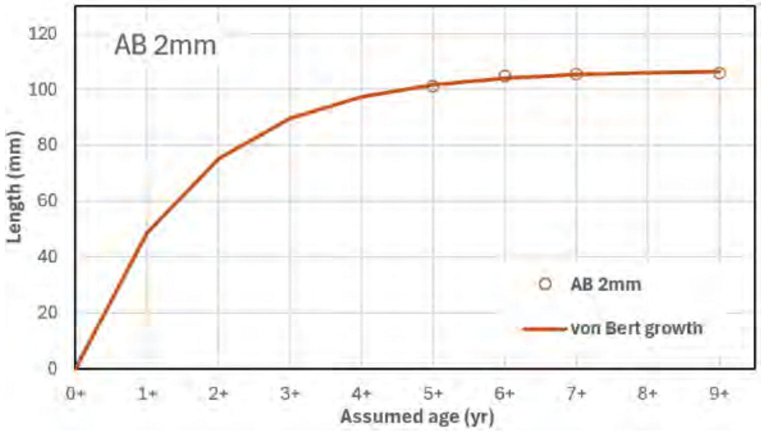

Figure 4-25. Von Bertalanffy growth curve (t_0 = 0, L_∞ = 106.9, K = 0.61) fitted to modes in length-frequency data for the Apollo Bay region over 2017 – 2021, assuming the ages for each mode shown in Table 4-1.

Apollo Bay East growth curve

The length-frequency data for the Apollo Bay East region over 2021 – 2023 show multiple modes (Figure 4-26). ‘Mixtools’ was therefore used to estimate the modes, assuming two normal modes per distribution. The resulting modes are summarised in Table 4-2 and shown in Figure 4-27.

Table 4-2. Modal peaks determined using ‘mixtools – normalmixEM’ modal separation analysis for the Apollo Bay East region over 2021 – 2023.

Year	Mode1	Mode2
2021	58.85	96.72
2022	73.83	95.14
2023	79.94	98.67

Ages assumed for the detected modes are summarised in Table 4-3.

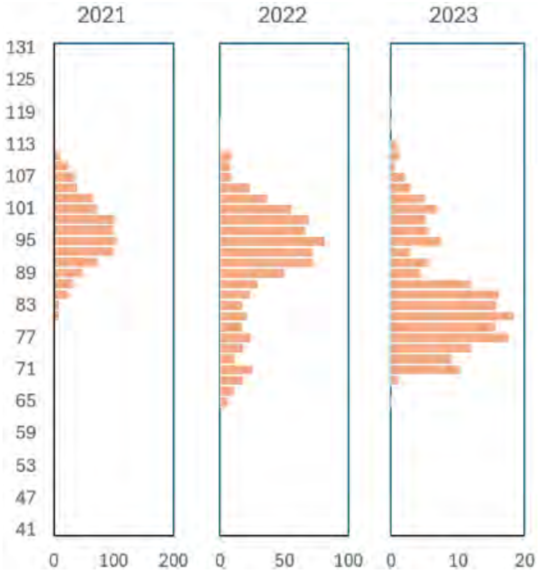

Figure 4-26. Length-frequency distributions for the Apollo Bay East region (2mm size classes) from 2021 – 2023.

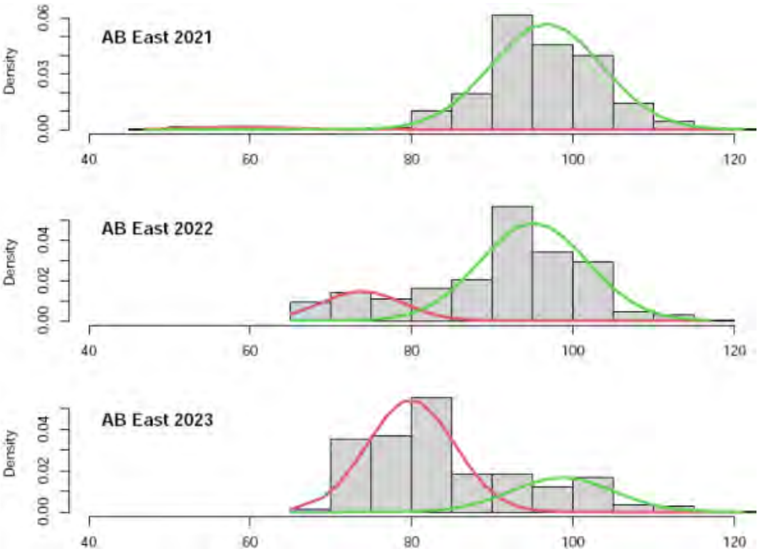

Figure 4-27. Modal separation for Apollo Bay East length-frequency data (2mm size classes) over 2021 – 2023, determined using the R 'mixtools - normalmixEM' routine.

Table 4-3. Ages assumed for each of the modes detected for Apollo Bay East length frequency data over 2021 – 2023, using the age ranges identified by Haddon *et al.* (2006) (Table 3-3) as guidance. (The red number shows the 3+ mode after application of a selectivity correction factor.)

Age	Mode
2	58.85
3	73.83 (70.8)
4	79.94
5	
6	96.72
7	95.14
8	98.67

A von Bertalanffy growth curve ($t_0 = 0$, $L_\infty = 105.6$, $K = 0.36$) fitted to the assumed ages for these modes is shown in Figure 4-28.

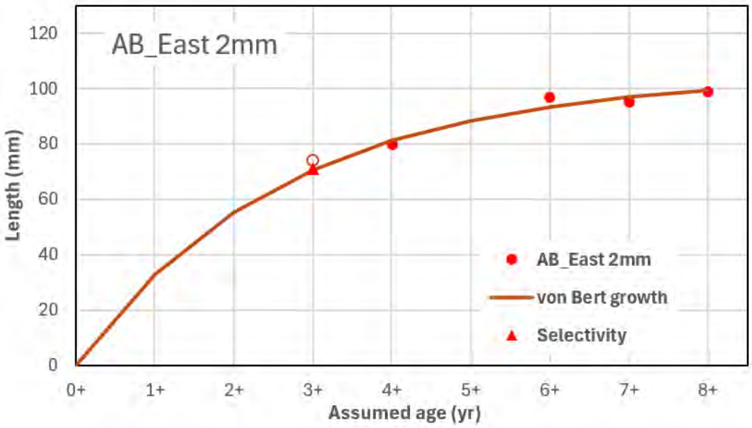

Figure 4-28. Von Bertalanffy growth curve ($t_0 = 0$, $L_\infty = 105.6$, $K = 0.36$) fitted to modes in length-frequency data for the King Island North region over 2018 – 2023, assuming the ages for each mode shown in Table 4-3. The red triangle shows the 3+ mode after application of the correction factor for selectivity.

The application of a correction factor for the 3+ mode made little difference to this growth curve.

King Island North growth curve

The region showing the clearest separation and progression of modes, with clear modes for juvenile and adult scallops, is King Island North. The modal peaks determined using modal separation analysis for this region are summarised in Table 4-4 and the modal separation analysis results are shown in Figure 4-29.

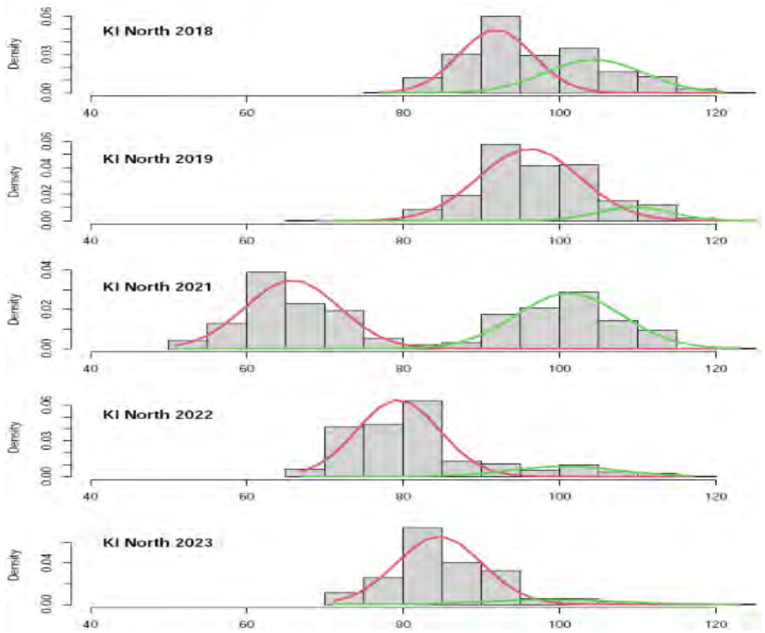

Figure 4-29. Modal separation for King Island North length-frequency data (2mm size classes) over 2018 – 2023, determined using the R 'mixtools - normalmixEM' routine.

Table 4-4. Modal peaks determined using 'mixtools – normalmixEM' modal separation analysis, for the King Island North region over 2019 – 2023.

Year	Mode 1	Mode 2
2018	91.87	104.46
2019	96.16	109.58
~~2020~~		
2021	65.83	101.23
2022	79.37	100.74
2023	84.62	98.98

An overlay of a manually drawn growth curve on the 2mm length-frequency histograms for King Island North is shown in Figure 4-30. A von Bertalanffy growth curve was fitted to the modes in Table 4-4 (t_0 = 0, L_∞ = 105.9, K = 0.43) using the assumed ages in Table 4-5. The resulting growth curve is shown in Figure 4-31.

Table 4-5. Ages assumed for each of the modes detected for King Island North length frequency data over 2018 – 2023, using the age ranges identified by Haddon *et al.* (2006) (Table 3-3) as guidance. (The red number shows the 2+ mode after application of a selectivity correction factor.)

Age	Mode
2	65.83 (55.97)
3	79.37
4	84.62
5	91.87
6	96.16
7	101.23
8	104.46

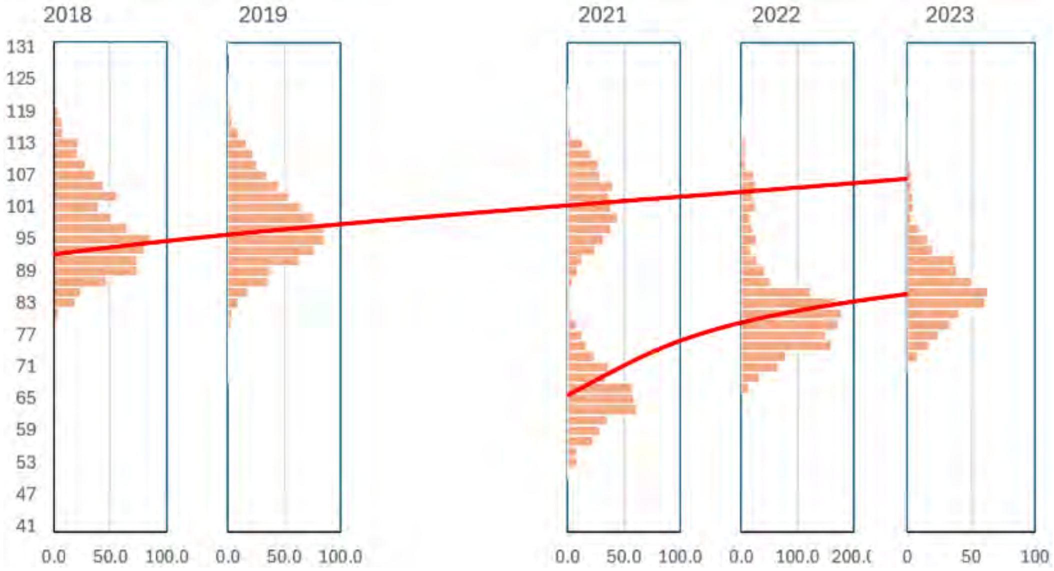

Figure 4-30. Length-frequency distributions for the King Island North region (2mm size classes) from 2018 – 2023 with growth curve drawn through modes determined using normal modal separation.

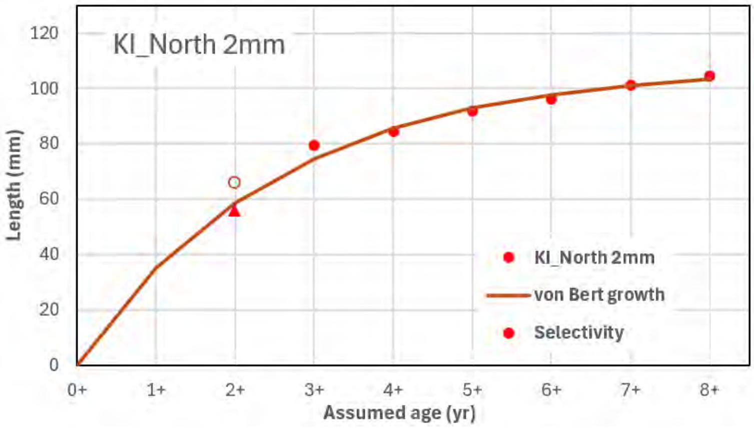

Figure 4-31. Von Bertalanffy growth curve (t_0 = 0, L_∞ = 105.9, K = 0.43) fitted to modes in length-frequency data for the King Island North region over 2018 – 2023, assuming ages for each mode in Table 4-5. The red triangle shows the 2+ mode after application of the correction factor for selectivity.

Application of a selectivity correction factor to the 2+ mode resulted in a 9.9 mm decrease in the estimated size of this mode, resulting in a slight decrease in K and an increase in L_∞. from 104.1 mm to 108.1 mm.

King Island NorthMid growth curve

The King Island NorthMid region consists of a single spatially isolated bed (KI – 7) surveyed in 2018 – 2022. The length-frequency distributions for the region are different before and after 2020, with a single adult mode in 2018 – 2019, and a recruiting smaller scallop mode in 2021 – 2022 (Figure 4-32). There is a long tail of a few small scallops evident in 2019, probably the first indication of the recruiting smaller scallop mode apparent in 2021. There is also a tail of a few large scallops in 2021, presumably the remnants of the adult mode apparent in 2019. No survey was conducted in 2020.

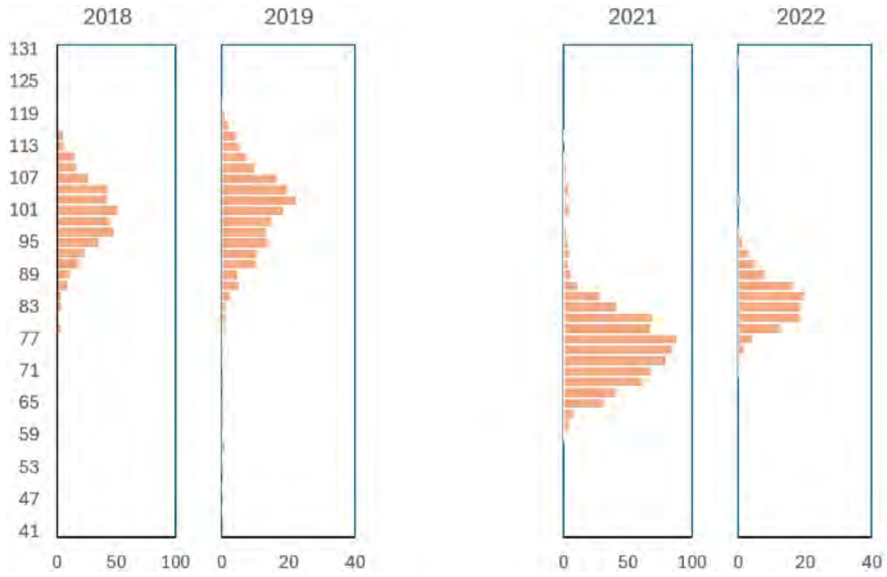

Figure 4-32. Length-frequency distributions for the King Island NorthMid region (2mm size classes) over 2018 – 2022.

Use of modal separation analysis to detect multiple modes in these length-frequency distributions is challenging, given that there is one dominant mode in each year, and identification of other modes will be informed by small numbers of scallops in the tails of the distribution. Given the long tail of small scallops in 2019, the analysis was specified to fit three modes in 2019, to allow for the addition of a mode of small scallops to the two larger modes progressing from those fitted in 2019, but only two modes in the other years. The resulting modes are summarised in Table 4-6 and the modal separation plots are shown in Figure 4-33.

Table 4-6. Modal peaks determined using 'mixtools – normalmixEM' modal separation analysis, for the King Island NorthMid region over 2018 – 2022. (The red number shows the 3+ mode after application of a selectivity correction factor.)

Year	Mode1	Mode2	Mode3
2018	81.20	100.34	
2019	61.81	92.55	103.34
~~2020~~			
2021	75.24 (72.95)	101.02	
2022	84.01	104.89	

The dominant smaller scallop modes in 2021 and 2022 were chosen, followed by the large adult modes in 2018 – 2021. The resulting ages assigned to modes are summarised in Table 4-7 and a von Bertalanffy growth curve (t0 = 0, L_∞ = 116.9, K = 0.32) fitted to those ages and modes is shown in Figure 4-34.

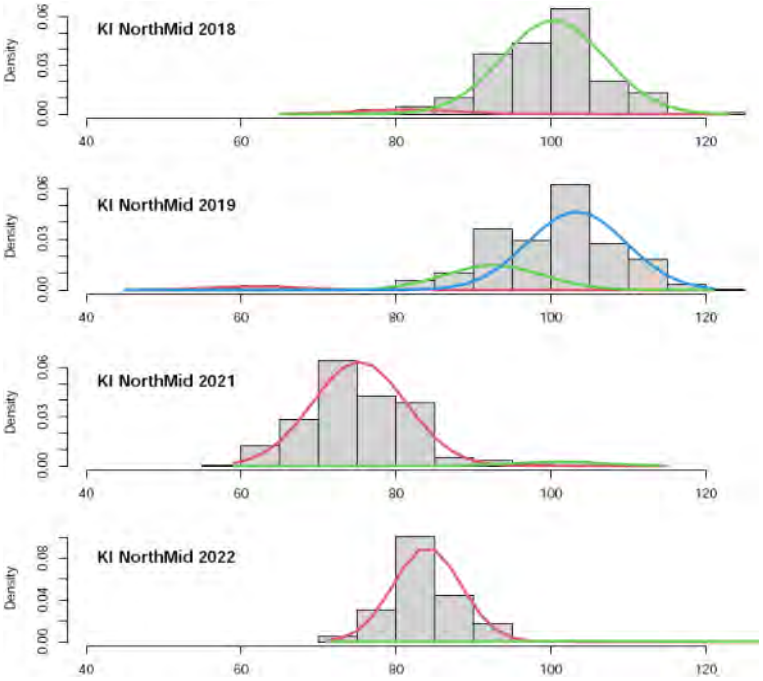

Figure 4-33. Modal separation for King Island NorthMid length-frequency data (2mm size classes) over 2018 – 2022, as determined using the R 'mixtools - normalmixEM' routine.

Table 4-7. Ages assumed for each of the modes detected for King Island NorthMid length frequency data over 2018 – 2022, using the age ranges identified by Haddon *et al.* (2006) (Table 3-3) as guidance.

Age	Mode
3	75.24
4	84.01
5	92.55
6	101.02
7	104.89

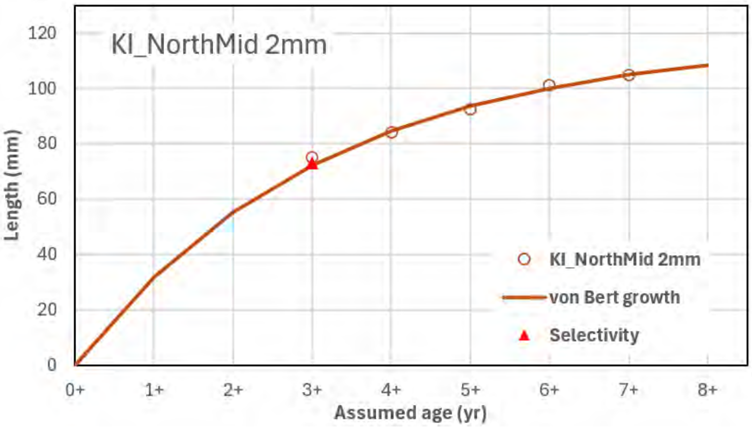

Figure 4-34. Von Bertalanffy growth curve ($t_0 = 0$, $L_\infty = 116.9$, $K = 0.32$) fitted to modes in length-frequency data for the King Island NorthMid region over 2018 – 2022, assuming ages for each mode in Table 4-7. The red triangle shows the 3+ mode after application of the correction factor for selectivity.

Application of a selectivity correction factor to the 3+ mode made negligible difference to this growth curve.

King Island Main, Mid region growth curve

The combined King Island Main and Mid regions shows an adult mode clearly progressing over 2015 – 2018. Furthermore, there is evidence of another mode of smaller scallops in a tail of smaller scallops in 2015 and 2016 increasingly merging into the adult mode (Figure 4-35).

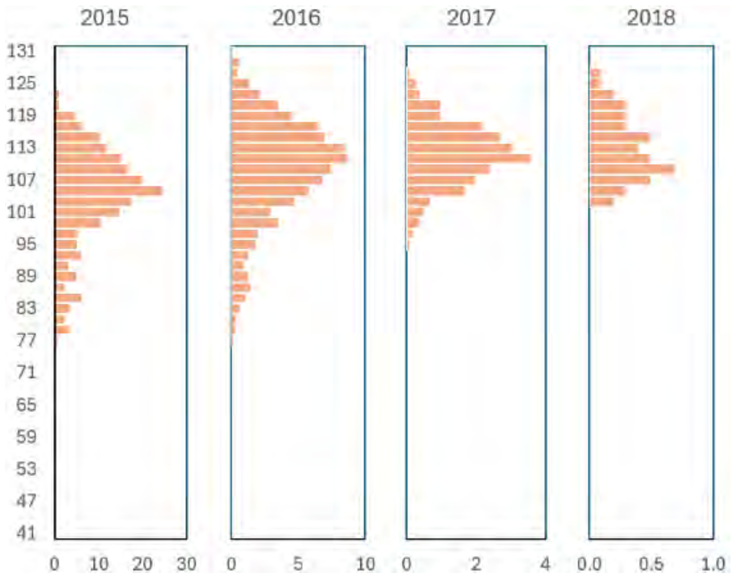

Figure 4-35. Length-frequency distributions for the King Island Main, Mid region (2mm size classes) over 2015 – 2018.

Modal separation analysis was used to fit two normal modes to these distributions, resulting in the modal separation plots shown in Figure 4-36 and the modes summarised in Table 4-8.

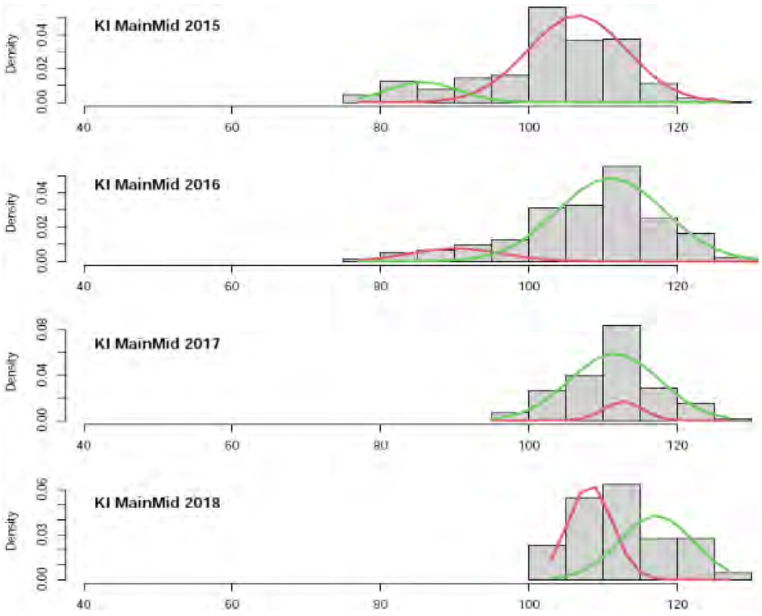

Figure 4-36. Modal separation for King Island Main, Mid length-frequency data (2mm size classes) over 2015 – 2018, as determined using the R 'mixtools - normalmixEM' routine.

Table 4-8. Modal peaks determined using 'mixtools – normalmixEM' modal separation analysis, for the King Island Main, Mid region over 2015 – 2018.

Year	Mode1	Mode2
2015	85.72	106.56
2016	90.12	111.05
2017	111.60	112.70
2018	108.26	117.18

Assumed ages at modal length are summarised in Table 4-9 and a von Bertalanffy growth curve (t_0 = 0, L_∞ = 122.9, K = 0.38) fitted to these is shown in Figure 4-37.

Table 4-9. Ages assumed for each of the modes detected for King Island Main, Mid length frequency data over 2015 – 2018, using the age ranges identified by Haddon *et al.* (2006) (Table 3-3) as guidance.

Age	Mode
3	85.72
4	90.12
5	106.56
6	111.05
7	112.70
8	117.18

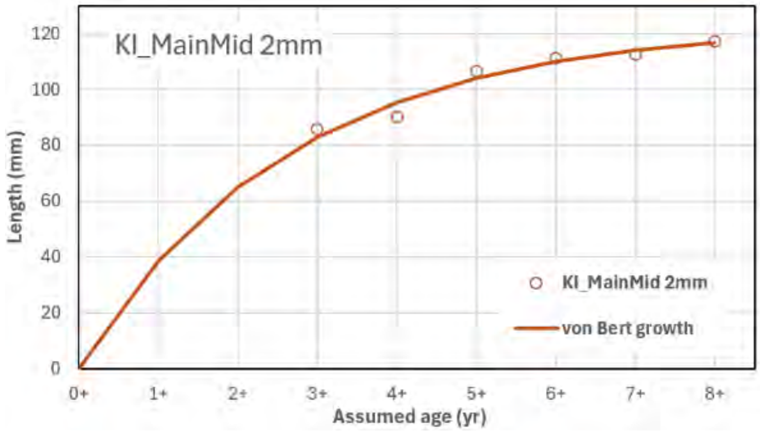

Figure 4-37. Von Bertalanffy growth curve (t_0 = 0, L_∞ = 122.9, K = 0.38) fitted to modes in length-frequency data for the King Island Main, Mid region over 2015 – 2018, assuming ages for each mode in Table 4-9.

King Island East region growth curve

The King Island East region (excluding beds designated as FarEast) shows an adult mode over 2016 – 2019 clearly progressing over the period. Furthermore, there is evidence of mode of smaller scallops in 2016, merging into the adult mode thereafter (Figure 4-38).

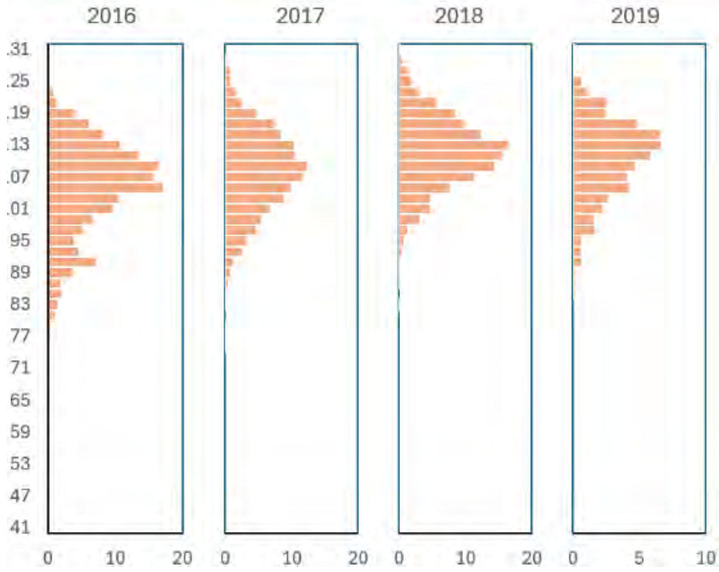

Figure 4-38. Length-frequency distributions for the King Island East region (2mm size classes) over 2016 – 2019.

Modal separation analysis was used to fit two normal modes to these distributions, resulting in the modal separation plots shown in Figure 4-42 and the modes summarised in Table 4-12.

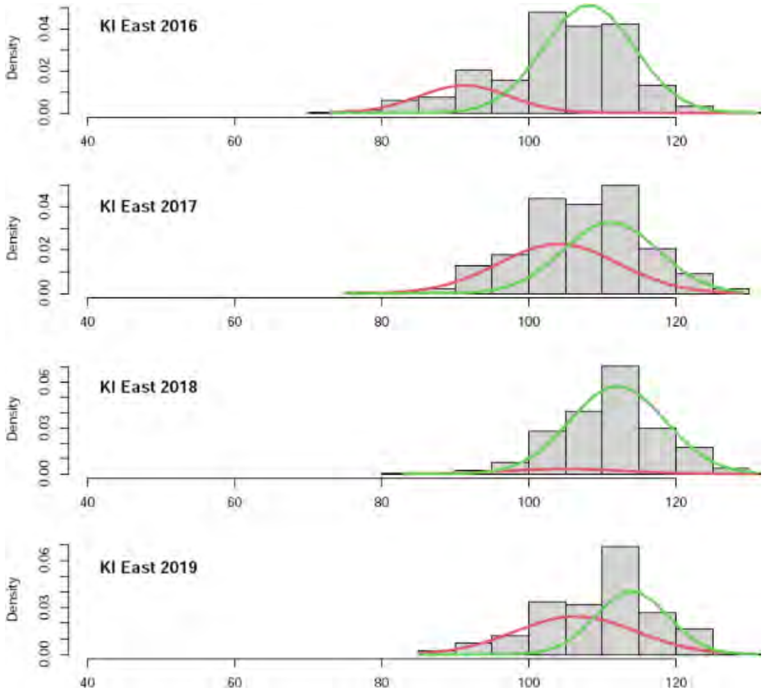

Figure 4-39. Modal separation for King Island East length-frequency data (2mm size classes) over 2016 – 2019, as determined using the R 'mixtools - normalmixEM' routine.

Table 4-10. Modal peaks determined using 'mixtools – normalmixEM' modal separation analysis, for the King Island East region over 2016 – 2019.

Year	Mode1	Mode2
2016	91.22	108.19
2017	104.03	111.14
2018	105.04	112.05
2019	106.40	113.99

Assumed ages at modal length are summarised in Table 4-9 and a von Bertalanffy growth curve ($t_0 = 0$, $L_\infty = 115.6$, $K = 0.54$) fitted to these is shown in Figure 4-37.

Table 4-11. Ages assumed for each of the modes detected for King Island East length frequency data over 2015 – 2018, using the age ranges identified by Haddon *et al.* (2006) (Table 3-3) as guidance.

Age	Mode
3	91.22
4	104.03
5	108.19
6	111.14
7	112.05
8	113.99

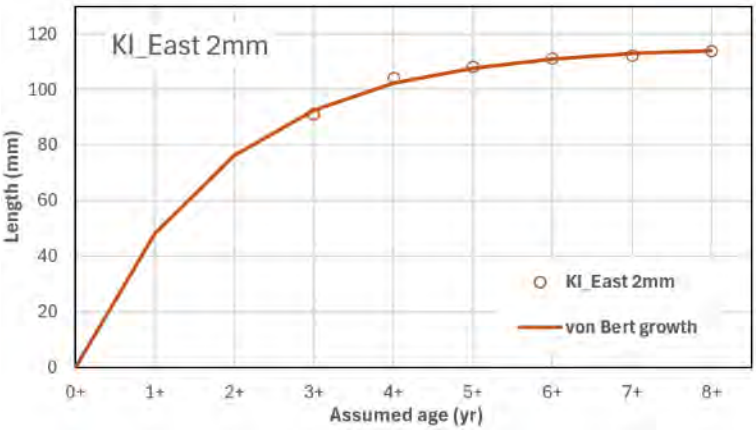

Figure 4-40. Von Bertalanffy growth curve ($t_0 = 0$, $L_\infty = 115.6$, $K = 0.54$) fitted to modes in length-frequency data for the King Island East region over 2015 – 2018, assuming ages for each mode in Table 4-13.

King Island FarEast region growth curve

The region designated as King Island FarEast has been surveyed in every survey over 2016 – 2023, providing one of the longest series of length data to track modal progression. Length-frequencies show a clear adult mode progressing over 2016 – 2022, and a mode of smaller scallops that first appears in 2019 and which progresses clearly over 2021 – 2023 as the adult mode disappears (Figure 4-41).

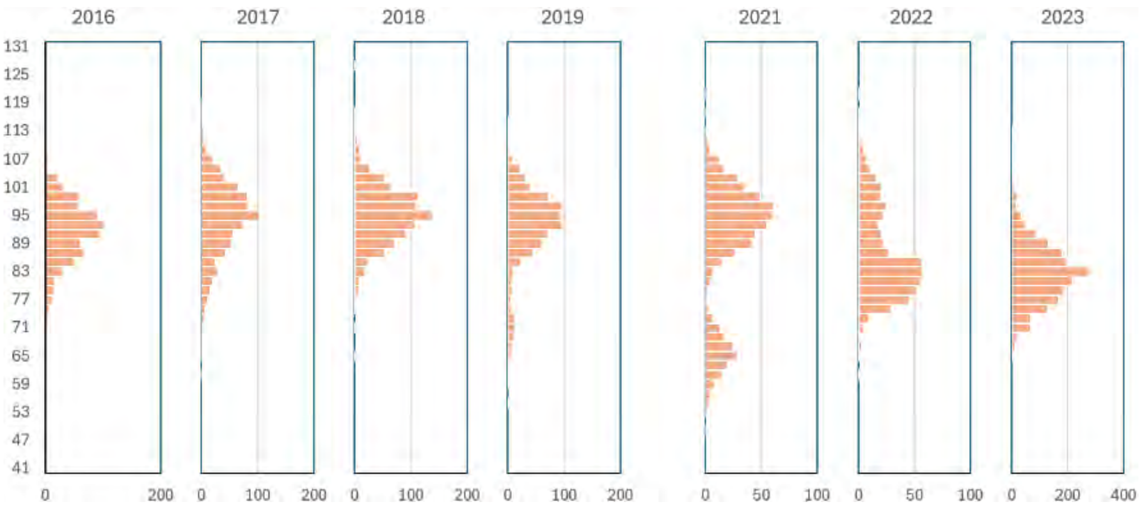

Figure 4-41. Length-frequency distributions for the King Island FarEast region (2mm size classes) over 2016 – 2023.

Modal separation analysis was used to fit two normal modes to these distributions, resulting in the modal separation plots shown in Figure 4-42 and the modes summarised in Table 4-13.

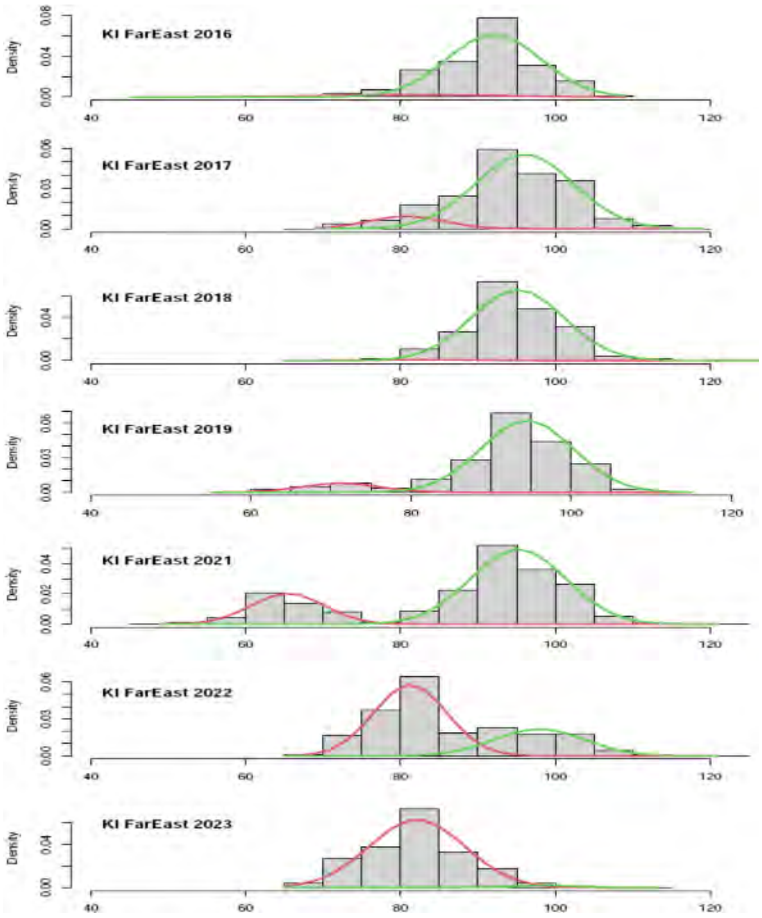

Figure 4-42. Modal separation for King Island FarEast length-frequency data (2mm size classes) over 2016 – 2023, as determined using the R 'mixtools - normalmixEM' routine.

Table 4-12. Modal peaks determined using 'mixtools – normalmixEM' modal separation analysis, for the King Island FarEast region over 2016 – 2023. (The red number shows the 2+ mode after application of a selectivity correction factor.)

Year	Mode1	Mode2
2016	81.6	92.1
2017	80.8	96.0
2018	82.7	95.2
2019	71.2	94.5
~~2020~~		
2021	65.5 (55.2)	95.2
2022	81.3	98.0
2023	82.1	98.7

Assumed ages at modal length are summarised in Table 4-13 and a von Bertalanffy growth curve ($t_0 = 0$, $L_\infty = 98.1$, $K = 0.52$) fitted to these is shown in Figure 4-43.

Table 4-13. Ages assumed for each of the modes detected for King Island FarEast length frequency data over 2016 – 2023, using the age ranges identified by Haddon *et al.* (2006) (Table 3-3) as guidance.

Age	Mode
2	65.45
3	81.28
4	82.14
5	92.05
6	96.03
7	95.15
8	94.51

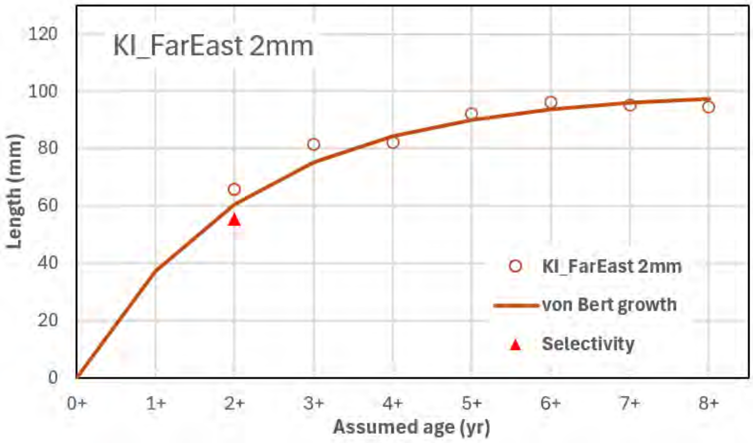

Figure 4-43. Von Bertalanffy growth ($t_0 = 0$, $L_\infty = 98.1$, $K = 0.52$) curve fitted to modes in length-frequency data for the King Island FarEast region over 2016 – 2023, assuming ages for each mode in Table 4-13. The red triangle shows the 2+ mode after application of the correction factor for selectivity.

Application of a selectivity correction factor to the 2+ mode results in a 10.3 mm decrease in estimated size of this mode, resulting in a decrease in K and an increase in L_∞ from 96.8 mm to 99.7 mm. It appears that the adult modes over 2016 – 2019 underestimate the L_∞ for this region, given that the adult mode in 2023 is estimated to be 98.7mm, whereas the maximum length reached ~120mm.

Flinders Island North region growth curve

The Flinders Island North has been surveyed over 2016 – 2023 (excluding 2020 and 2022), providing one of the longest series of length data to track modal progression. However, adult length-frequencies only show an adult mode, albeit with some evidence of that consisting of several merged modes in 2018 – 2023. There is little evidence of modal progression over 2015 – 2018, but some progression over 2018 – 2021 (Figure 4-44). There is not enough separation to use normal modal separation analysis, therefore single modes were assumed and approximate modes were calculated as the weighted mean length over the length class ranges in each year. The resulting modes are summarised in Table 4-14.

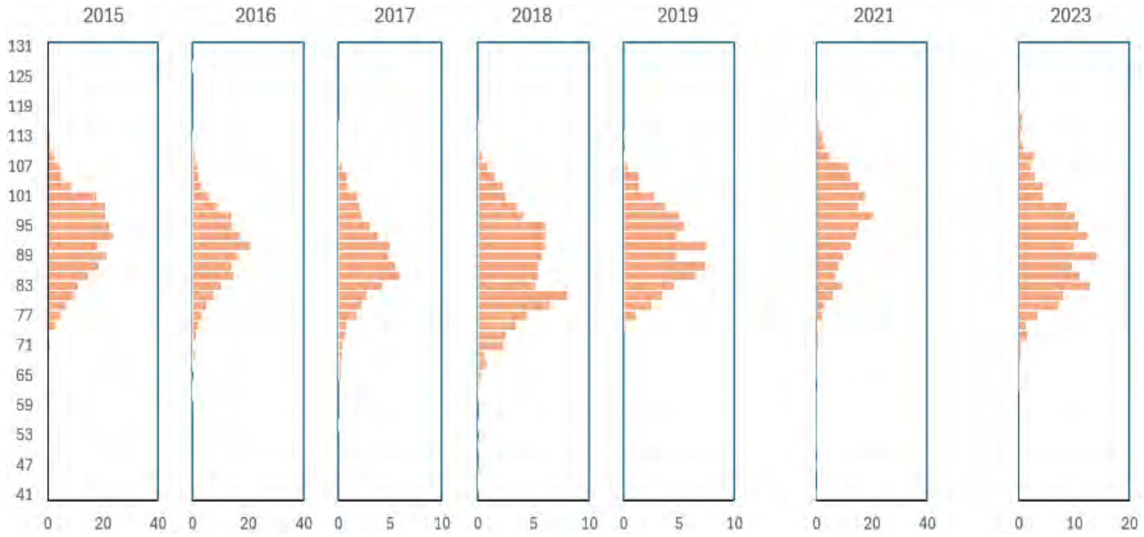

Figure 4-44. Length-frequency distributions for the Flinders Island North region (2mm size classes) over 2015 – 2023.

Table 4-14. Modal peaks determined using 'weighted average length for the Flinders Island North region over 2015 – 2023.

Year	Mode
2015	92.3
2016	90.5
2017	88.4
2018	86.9
2019	90.5
~~2020~~	
2021	95.4
~~2022~~	
2023	90.7

Assumed ages at modal length are summarised in Table 4-15 and a von Bertalanffy growth curve (t_0 = 0, L_∞ = 97.1, K = 0.56) fitted to these is shown in Figure 4-45.

Table 4-15. Ages assumed for each of the modes detected for Flinders Island North length frequency data over 2016 – 2023, using the age ranges identified by Haddon *et al.* (2006) (Table 3-3) as guidance.

Age	Mode
4	86.92
5	90.54
6	
7	95.38

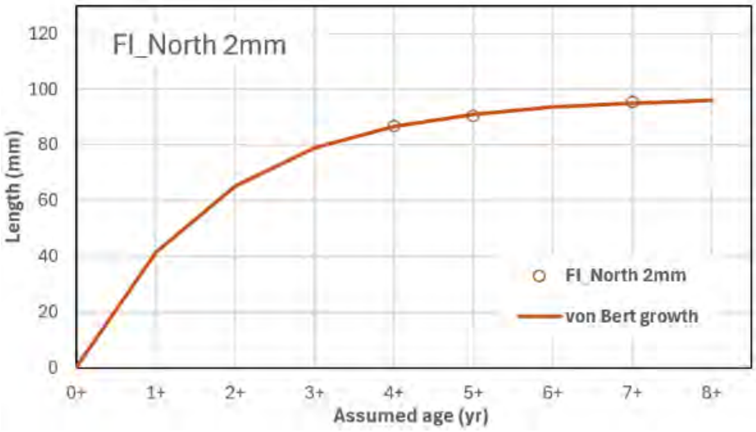

Figure 4-45. Von Bertalanffy growth curve ($t_0 = 0$, $L_\infty = 97.1$, $K = 0.56$) fitted to modes in length-frequency data for the King Island FarEast region over 2015 – 2023, assuming ages for each mode in Table 4-15.

Given the apparent lack of modal progression over 2015 – 2018 and the few assumed ages used, this is a rather tenuous growth curve. It also under-estimates L_∞ in this region by using modes of rather wide length call distributions when the maximum length in this region reaches ~115 – 120 mm.

Flinders Island South region growth curve

The Flinders Island South region has only been surveyed over 2021 – 2023. Length-frequencies apparently consist of a number of merged modes, with earlier recruiting cohorts merging more or less into an adult cohort (Figure 4-46).

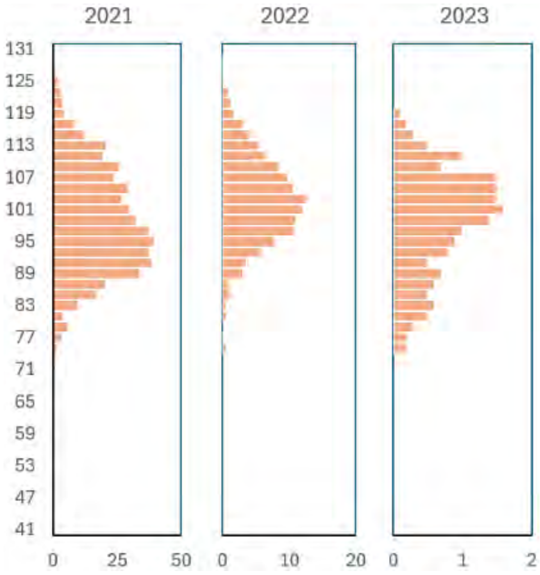

Figure 4-46. Length-frequency distributions for the Flinders Island South region (2mm size classes) over 2021 – 2023.

Modal separation analysis shows progression of a mode from 2021 – 2023, the appearance of a mode of smaller scallops in 2023, and a mode of larger scallops in 2021 (Figure 4-47). The resulting modes are summarised in Table 4-16.

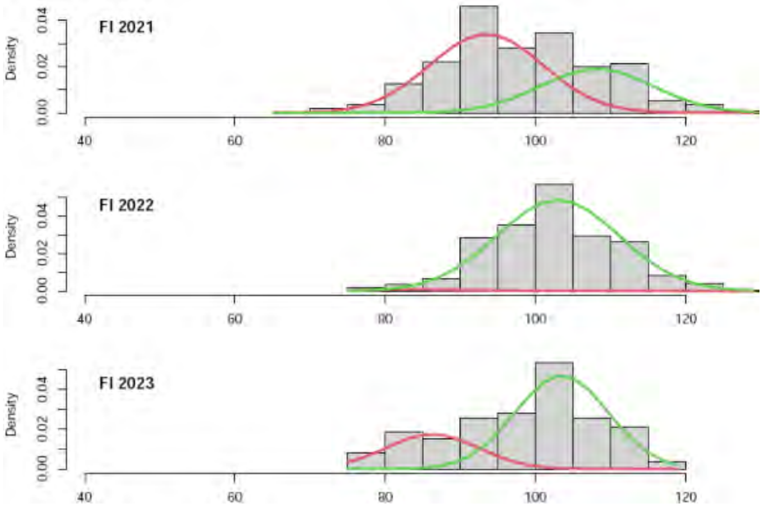

Figure 4-47. Modal separation for Flinders Island South length-frequency data (2mm size classes) over 2021 – 2023, as determined using the R 'mixtools - normalmixEM' routine.

Table 4-16. Modal peaks determined using 'mixtools – normalmixEM' modal separation analysis, for the Flinders Island South region over 2021 – 2023.

Year	Mode 1	Mode 2
2021	93.47	108.16
2022	82.72	103.01
2023	86.27	103.50

Assumed ages at modal length are summarised in Table 4-17 and a von Bertalanffy growth curve ($t_0 = 0$, $L_\infty = 103.0$, $K = 0.72$) fitted to these is shown in Figure 4-48.

Table 4-17. Ages assumed for each of the modes detected for Flinders Island South length frequency data over 2021 – 2023, using the age ranges identified by Haddon *et al.* (2006) (Table 3-3) as guidance.

Age	Mode
2	82.72
3	86.27
4	93.47
5	103.01
6	103.50

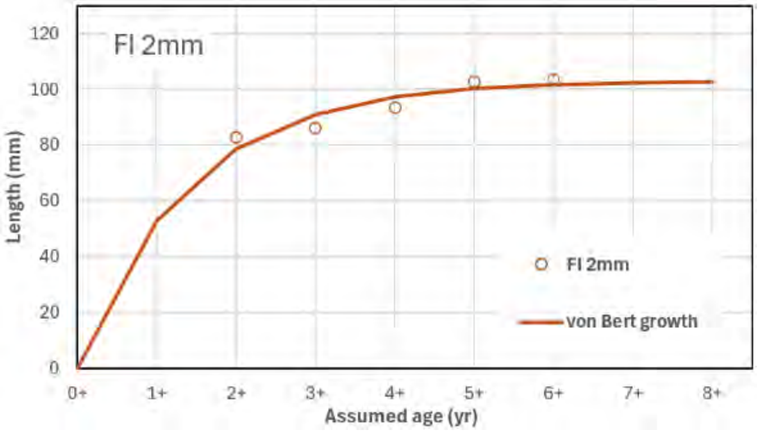

Figure 4-48. Von Bertalanffy growth curve fitted to modes in length-frequency data for Flinders Island South region over 2021 – 2023, assuming ages for each mode in Table 4-17.

Beach Energy Survey growth

The Beach Energy Before/After – Control/Impact survey (conducted in 2021/22 to evaluate the impacts of a gas field seismic survey) provides an opportunity to evaluate short-term changes in scallop length-frequency distributions. The Before and After surveys were conducted seven months apart, in September 2021 (before the November/December seismic survey), and in April 2022.

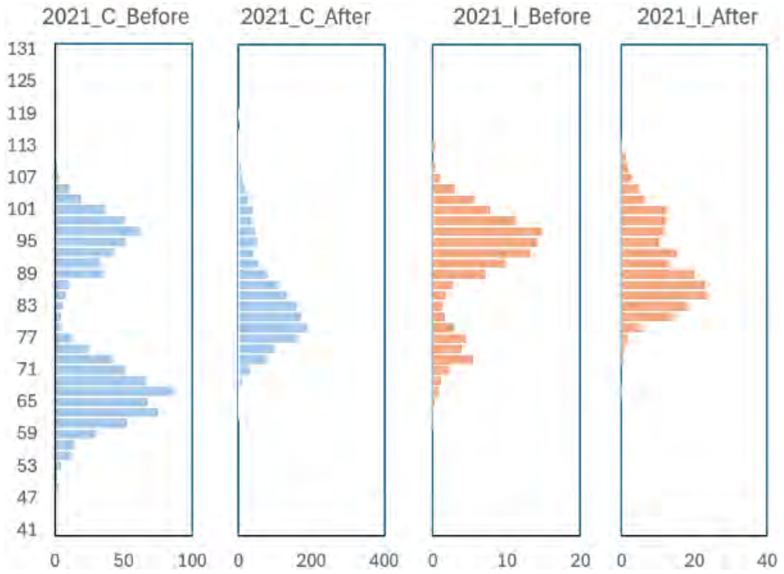

Figure 4-49. Length-frequency distributions for the Beach Energy Before/After – Control/Impact survey (2mm size classes) in 2021/22.

There is good separation between apparent adult and juvenile modes in the survey data, with rapid progression in the juvenile mode in the seven months between the Before and After surveys. Modal separation analysis results are summarised in Table 4-18 and shown in Figure 4-50.

Table 4-18. Modal peaks determined using 'mixtools – normalmixEM' modal separation analysis, for the Beach Energy Before/After – Control/Impact survey in 2021/22.

Survey		Mode1	Mode2
Control	Before	66.26	95.62
	After	80.39	95.87
Impact	Before	74.81	95.69
	After	84.70	94.13

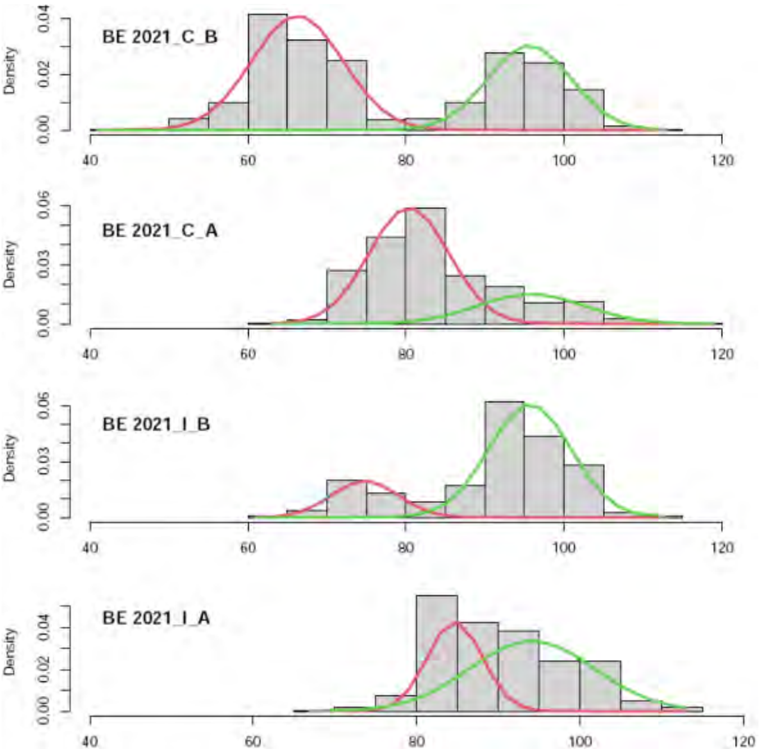

Figure 4-50. Modal separation for the Beach Energy Before/After – Control Impact survey length-frequency data (2mm size classes) in 2021/22, as determined using the R 'mixtools - normalmixEM' routine.

The ages of After modes were being calculated as the Before survey modal length plus 0.58 years (seven months). The resulting assumed ages at modal length are summarised in Table 4-19 and a von Bertalanffy growth curve ($t_0 = 0$) fitted to these is shown in Figure 4-51.

Table 4-19. Ages assumed for each of the modes detected for Flinders Island South length frequency data over 2021 – 2023, using the age ranges identified by Haddon *et al.* (2006) (Table 3-3) as guidance. (The red numbers shows the 2+ modes after application of a selectivity correction factor.)

Age	Control	Impact
2	66.26 (56.88)	74.81 (72.30)
2.58	80.39	84.70
4		
5	95.62	95.69
5.58	95.87	94.13

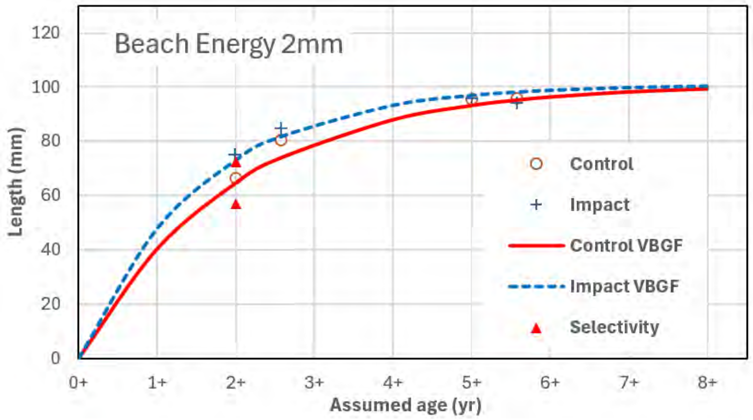

Figure 4-51. Von Bertalanffy growth curve fitted to modes in length-frequency data for The Beach Energy - Before and After surveys in 2021/22, assuming ages for each mode in Table 4-17. The red triangles show the 2+ mode after application of the correction factor for selectivity.

The progression in the juvenile modes in the Control and Impact surveys show that scallops grew substantially in the intervening seven months. Scallops from the Control sites grew more rapidly than can be fitted with a standard von Bertalanffy growth curve. This suggests that there may be a seasonal effect on growth rate, with more rapid growth in summer. Without monthly length-frequency data it is not possible to fit a seasonally oscillating growth curve.

Comparison of growth curves across regions

The growth curves fitted to BSCZSF length-frequency modes for the King Island North, King Island North Mid and King Island Mid regions are compared in Figure 4-52 with the growth curve fitted to modes found by Haddon *et al.* (2006) for Tasmanian scallop beds and by Koopman *et al*. (2018) for Victorian beds.

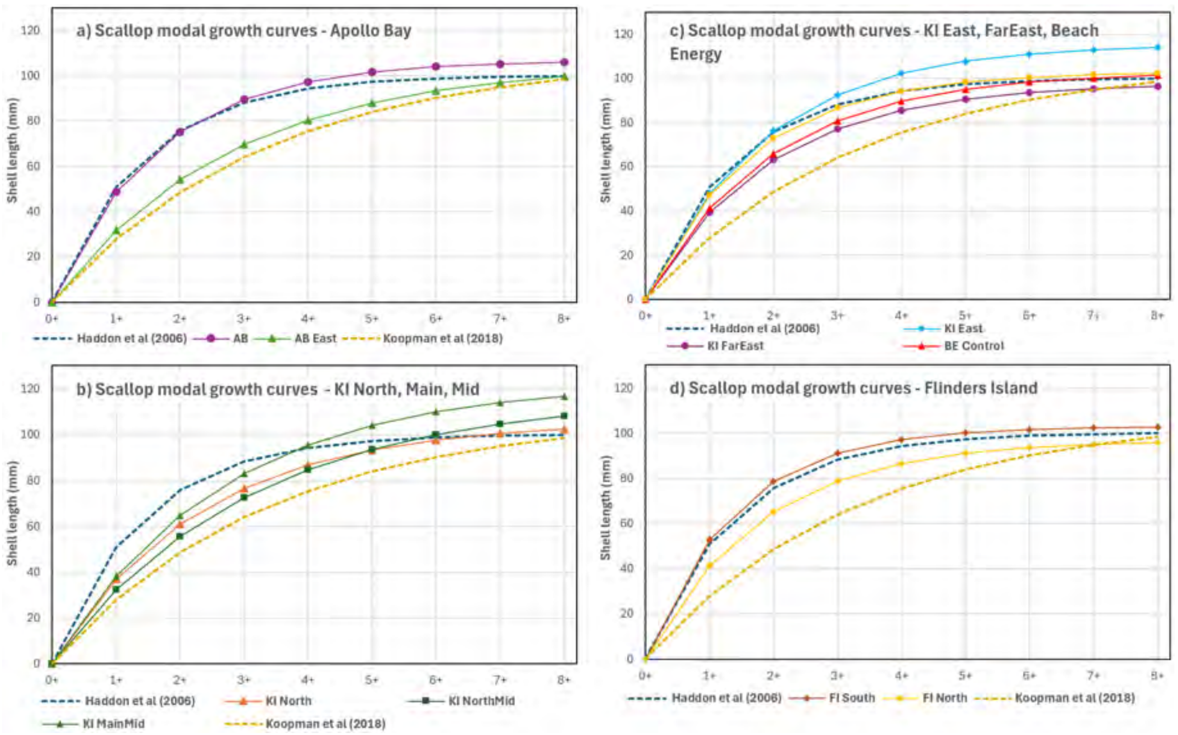

Figure 4-52. Comparison of von Bertalanffy growth curves fitted to length mode data for each of the regions in this study, compared with the growth curve fitted to modes found by Haddon *et al.* (2006).

Noting from Figure 4-52 that these are exploratory growth curves using assumed but plausible ages, there is similar variation among these curves (in K and L_∞) as found by Haddon *et al.* (2006) for Tasmanian scallops. This variation occurs within each region, with little evidence of similarity among growth curves in each region. Growth in the Apollo Bay region differs from that in Apollo Bay East, as does growth in King Island East and King Island FarEast, and Flinders Island South and North. The curves for King Island North and King Island NorthMid are similar, and both reveal somewhat slower growth than the average across the Haddon *et al.* (2006) modes. However, the growth for King Island Main/Mid indicates slower initial growth than the average across the Haddon *et al.* (2006) modes, but with a higher L_∞ and size-at-age for scallops older than assumed 4+.

4.9. Spawning and recruitment

The years in which spawning is estimated to have occurred in the various regions, back-calculated from the assumed ages for modes in the length-frequency distributions and the resulting growth curves for those regions, are summarised in Table 4-20. This shows the years in which clear juvenile modes were present in length-frequency data. These are compared in Table 4-21 with the years in which the various regions were surveyed.

Table 4-20. Back-calculated years in which recruitment is estimated to have occurred in various regions, given assumed ages of modes in length-frequency distributions in the years listed.

Region	Year	Age	Recruited
Apollo Bay	2017	5	2012
Apollo Bay East	2021	🟦 2	2019
Apollo Bay East	2021	6	2015
King Island North	2021	🟦 2	2019
King Island North	2018	5	2013
King Island NorthMid	2021	🟦 3	2018
King Island NorthMid	2019	5	2014
King Island MainMid	2015	3	2012
King Island MainMid	2015	5	2010
King Island East	2016	3	2013
King Island East	2016	5	2011
King Island FarEast	2016	5	2011
King Island FarEast	2021	🟦 2	2019
Flinders Island North	2018	4	2014
Flinders Island South	2022	🟦 2	2020
Flinders Island South	2021	4	2017
	Juvenile mode	🟦	

Table 4-21. Back-calculated years of recruitment of modes seen in length-frequency data compared with the years in which the regions were surveyed.

Region	2010	2011	2012	2013	2014	2015	2016	2017	2018	2019	2020	2021	2022	2023
Apollo Bay			?					🟦	🟦	🟦		🟦		
Apollo Bay East						?				✓		🟦	🟦	🟦
King Island North				?					🟦	🟦 ✓		🟦	🟦	🟦
King Island NorthMid					?				🟦 ✓	🟦		🟦	🟦	
King Island MainMid	?		?			🟦	🟦	🟦	🟦					
King Island East		?		?		🟦	🟦	🟦	🟦	🟦				
King Island FarEast		?					🟦	🟦	🟦	🟦 ✓		🟦	🟦	🟦
Flinders Island North					?							🟦	🟦	🟦
Flinders Island South						🟦	🟦	🟦 ?	🟦	🟦	✓	🟦		🟦

Surveyed 🟦 Possible recruitment ? Likely recruitment based on juvenile mode ✓

Increasing elapsed time between when a region was surveyed (and a mode observed in length-frequency data) and the back-calculated year of spawning is associated with increasing uncertainty regarding the assumed age of the mode, and of the back-calculated year of spawning. The assumed age of large adult scallops could be over- or under-estimated by one or more years, resulting in a similar error in the back-calculated year of spawning. The age of small, fast-growing scallops is likely to be more accurately assumed, resulting in more accurate estimates of the year of spawning. The years and regions in which clear juvenile modes were observed in the length-frequency data are shown in Table 4-20 and Table 4-21. There would have been earlier years of strong spawning and recruitment that resulted in the adult modes seen in the length-frequency data on all beds, but these can only be inferred from the assumed ages for those adult modes which are less reliable.

A high proportion of undersize (< 85 mm) scallops in a bed provides an indication of a recent recruitment event to that bed. Interannual trends in the proportion of undersize scallops are summarised by region in (Figure 4-9). This shows substantial differences in recruitment among regions. The Apollo Bay region shows a negligible proportion of small scallops across the entire time series, indicating little or no recruitment to this region over the period. In contrast, the King Island North and King Island NorthMid regions show no substantial recruitment before 2018, show first signs of recruitment in 2018 and 2019, and then show substantial recruitment in 2021, reaching 50% of the selected population in King Island North and 88% of the selected population in King Island North. The high proportion of small scallops then decreases as they grow greater than 85 mm shell length.

The King Island BlueDot region shows apparent extended recruitment with two peaks, in 2017 and 2023. Flinders Island North similarly shows two peaks in recruitment, in 2018 and 2023, with extended recruitment from 2015 – 2018. Flinders Island South only shows signs of limited recruitment over 2021 – 2023. The proportion of undersize scallops in the King Island Extended bed in 2019 shows the effect of dredge selectivity on the size-composition of surveyed scallops. The back-pressure caused by the fine mesh appeared to also prevent some percentage of the larger scallops from entering the dredge, resulting in most of the scallops caught (98%) being undersize.

Finer-scale detail on trends in the proportions of small scallops by individual survey bed is provided in Figure 8-4 in Appendix 8.4. The absence of recruitment in Apollo Bay occurs across all beds in that region. In Apollo Bay East, moderate recruitment starting in 2021 occurs in both the AB – 5 Hours and AB – THN beds. In the King Island North region, the substantial recruitment occurring from 2019 – 2023 occurs almost entirely in the KI – 9 and KI – 7 beds, although with slight recruitment in 2019 in the KI – 6, KI – 8a and KI – 8b beds. Recruitment in the BlueDot region is moderate and spread across 2016 – 2022 in the KI – BD/BDE bed, and increases steadily in the KI – BDSE bed over 2019 – 2023. There is little apparent recruitment in the King Island East region, but increasing recruitment from 2021 – 2023 in the King Island FarEast region in beds KI – 10, KI – THE and KI – THW, coincident with recruitment in the KI – BDSE bed. In the Flinders Island North region, moderate recruitment occurred in the FI, FI – 1, FI – 3 and FI – 4 beds (which partially overlap) over 2015 – 2021. Moderate but more widespread recruitment occurred in bed FI – 1, the Flinders Island North FI – TS and FI – TSE beds, and in all the Flinders Island South beds, in 2023.

The maps of proportion of undersize scallops by individual bed and survey year in Appendix 8.3 show that recruitment, even when it occurs across a number of beds in a region, does not necessarily occur across entire beds. Recruitment often occurs only partially across one or more beds in a region, or in one bed and not an adjacent bed. In 2015, high proportions of small scallops were seen in the northern half of bed FI – 1, but not the southern half of the bed (Map 8-9). This is even more pronounced in 2016, with a high proportion of small scallops across bed FI – 2 and the northern part of bed FI – 1, but few small scallops in the southern half of bed FI – 1 (Map 8-10). Similarly, in 2017, recruitment is evident in beds FI – 2, FI – 3 and FI – 4, but scant in FI – 1. In the King Island area, there were high proportions of small scallops in the KI – BDE bed, but not in the Apollo Bay, King Island Mid or King Island East beds (Map 8-11). However, recruitment was substantial across the whole of Flinders Island bed FI – 1 in 2018 (Map 8-12).

The 2019 survey of the KI – JH bed in the KI Extended region, which used a fine mesh cover on half of the dredge, clearly shows the very high proportion of small scallops in this bed when using a fine mesh dredge, obviously suggesting that higher proportions of small scallops would be seen, and would be seen earlier, if fine mesh dredges were used elsewhere. However, there were also high proportions of small scallops in the western part of KI – BDE, the northwest corner of KI – BDSE, and to a lesser extent in the KI – 7, KI – 6 and KI – 9 beds (Map 8-13). Although a fine mesh cover net was not used in the KI – JHE beds in 2021, there was still a high proportion of small scallops caught in this bed in that year. This was the year that the Beach Energy survey was conducted in the Control (C1 – C8) and Impact (I1 – I8) sites and it is striking to note the very high proportions of small scallops across almost all of these additional survey beds, lying to the southeast of the King Island East and FarEast regions. In 2021 there were also high proportions of undersize scallops caught in the KI – 7 and KI – 9 beds together with parts of the AB – 5 Hours, AB – THN and AB – 2E beds (Map 8-14). There was clearly a widespread spawning event across much of this region in 2018 – 2019 which, with no survey conducted in 2020, appeared as widespread recruitment across much of this area in 2021.

The widespread recruitment of small scallops across the King Island regions remained evident in 2022, even though growth would have resulted in a proportion of small scallops caught in 2019 and 2020 growing over 85 mm shell length (Map 8-15). A high proportion of small scallops was also apparent in the King Island FarEast beds KI – BDE, KI – BDSE, KI – THW, KI – THE and part of KI – 10 into 2023, together with bed KI – 9 and the southeast part of bed AB – THN (Map 8-16).

There was a low proportion of small scallops in the Flinders Island South region in 2022 (Map 8-15). However, a moderate proportion of small scallops appeared across the Flinders Island South beds and parts of the Flinders Island North beds in 2023 (Map 8-16).

4.10. Fishing and natural mortality estimates

Beds for use in estimation of natural mortality were selected based on whether they showed a single mode of adult scallops, with little or no evidence of smaller recruits, together with a substantial decline in survey estimates of biomass across two or more years. Beds meeting these criteria and selected for mortality analysis are detailed in Table 4-22, with information on the years for analysis and the mean survey biomasses and shell lengths in each year. Histograms of the annual biomass estimates for these beds are shown in Figure 8-2 in Appendix 8.4 and length-frequency distributions are shown in Appendix 8.5.

Table 4-22. Scallop beds selected for natural and fishing mortality analysis, showing the years used for analyses, the survey median biomass estimates in those years, and the mean length of the adult mode in those years.

Region / Bed	Years	Biomass (t)	Mean length (mm)
Apollo Bay AB – 1	2017, 2018, 2019	2856.1, 1892.3, 631.3	100.3, 104.0, 104.7
Apollo Bay AB – 2	2017, 2018, 2019	2182.0, 1803.8, 886.1	101.6, 104.4, 105.3
Apollo Bay AB – 5 Hours	2021, 2022	3627.0, 1037.0	97.8, 98.4
King Island KI – Mid	2015, 2016, 2017, 2018	578.4, 600.7, 92.0, 16.3	107.6, 109.2, 111.4, 112.1
King Island KI – 5S	2017, 2018, 2019	3059.2, 3529.4, 1612.1	108.0, 111.3, 108.8
Flinders Island FI – 2	2016, 2017	2304.6, 585.1	89.3, 85.9
Flinders Island FI – S – TWA	2022, 2023	1578.0, 249.0	100.7, 100.9

Variance was added around the mean estimates of biomass and length in Table 4-22 using Monte-Carlo random sampling of normal distributions around these median estimates, using standard deviations published for survey biomass estimates and calculated for adult scallop modes in those beds and years. Additional variance was added using randomly sampled normal distributions around the $L{:}Wt$ conversion relationships for each area (See *Methods: Population biology: Fishing and natural mortality estimation*).

Histograms were produced of the samples drawn from normal distributions around mean biomass and length for each bed in each year. For pairs of years across which some catch was reported and allocated to each bed, a frequency distribution of fishing mortality rate (F) was produced, using the reported catch (with no CV) over the samples of estimated biomass in the first year of each year pair. Two alternative frequency distributions of M were then produced for each bed for each pair of years from the samples of B and L:

- Applying variance in only B and L, with no $L{:}Wt$ variance (i.e. only the best fit $L{:}Wt$ curve for each area used to convert L to Wt).
- Applying variance in B, L and $L{:}Wt$ using normally distributed samples drawn from the best fit $L{:}Wt$ curves plus standard deviations for the three areas (as shown in Figure 4-23).

For the Apollo Bay AB – 1 bed, additional frequency distributions of M were produced applying only variance in B, with no L or $L{:}Wt$ variance, to illustrate how the frequency distribution of estimated M changes as sources of variance are sequentially applied. This showed a relatively small decrease in mean and modal M from excluding variance in L as a result of the probabilities in L being linked across years (see *Methods: Population biology: Fishing and natural mortality estimation*). Therefore, this additional analysis was not done for the other beds. Frequency distributions of fishing mortality and natural mortality estimates with variance are summarised in Table 4-23.

Apollo Bay AB – 1

The Apollo Bay AB – 1 bed shows a dramatic decline in survey estimated biomass over 2017-18 (34%) and over 2018-19 (67%). There were no catches allocated to this bed in 2017 and only 15.65 t in 2018, resulting in a mean F of 0.009 over 2018-19 (Figure 4-53). Length increased from 100.3 mm to 104.0 mm to 104.7 mm over the period, with assumed ages assigned to these modes of 5+, 6+ and 7+ (see Growth results).

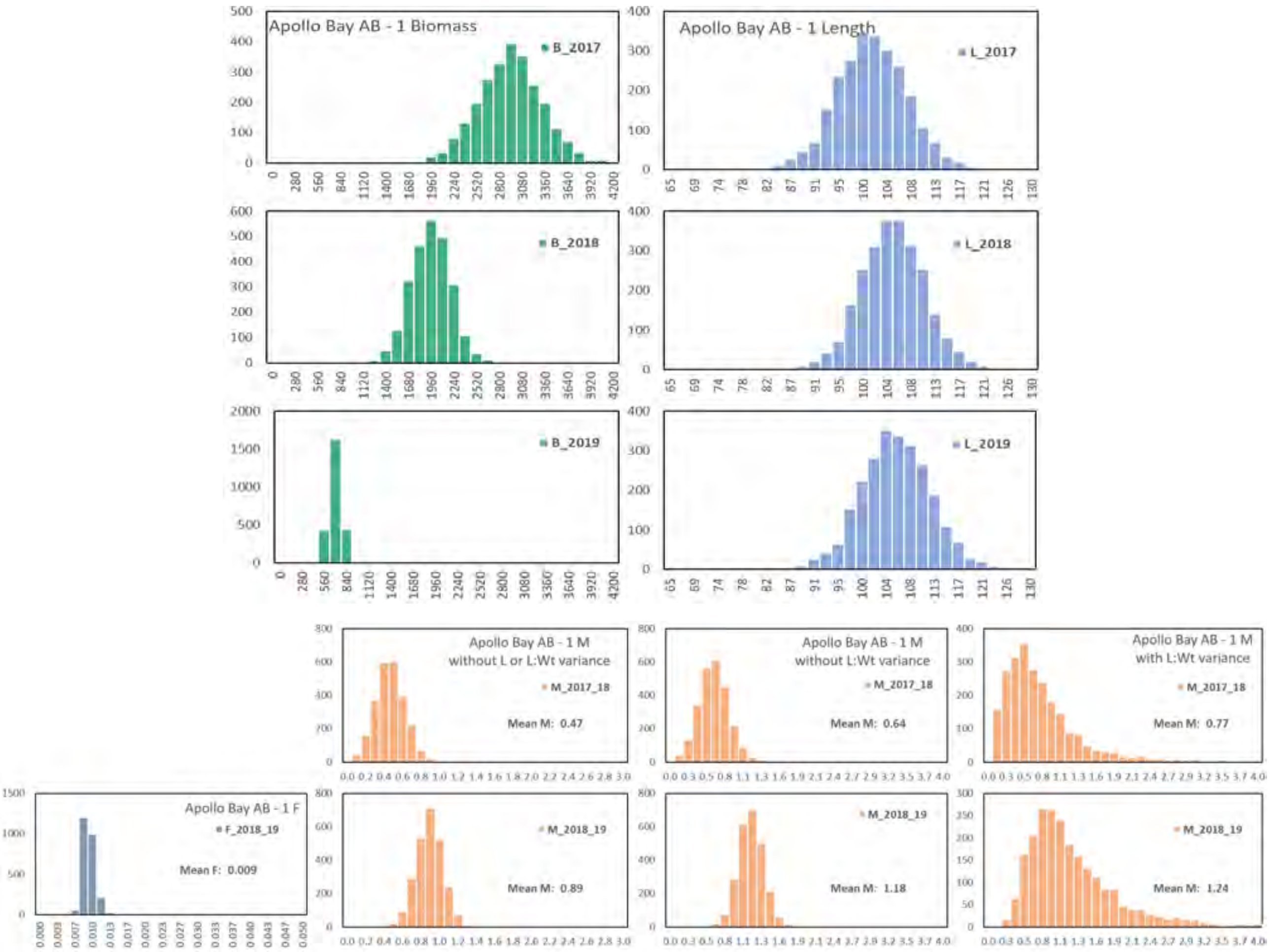

Figure 4-53. Frequency histograms of biomass (B), mean adult mode length (L) fishing mortality (F) and natural mortality (M) for the Apollo Bay AB – 1 bed over 2017-18 and 2018-19.

Estimated M averaged 0.47 (d: 37.5%) over 2017-18 with no L or $L:Wt$ variance, 0.64 (d: 47.3%) with L variance, and 0.77 (d: 53.7%) with L and $L:Wt$ variance. Mean M values over 2018-19 were 0.89, 1.18 and 1.24 (d: 71.1%) (Figure 4-53). Note that the frequency distributions for B and L are normally distributed (sampled from normal distributions), whereas those for F and M are log-normally distributed, after application of a power curve $L:Wt$ conversion. As sources of variance are added, the mode of the M distribution remains relatively stationary, but the distribution has an increasing tail of high M values to the right of the mode, resulting in an increase in mean M. For bed AB – 1, this results in M potentially reaching a 95% CI level of up to ~2.7 (d: 93.3%).

Apollo Bay AB – 2

The Apollo Bay AB – 2 bed shows a similar decline in B to the AB – 1 bed over 2017 – 2019. There were no catches allocated to this bed in 2017, but there was a catch of 194.1 t in 2018, resulting in a mean F of 0.121 over 2018-19. Length increased from 101.6 mm to 104.4 mm to 105.3 mm over the period, with assumed ages assigned to these modes of 5+, 6+ and 7+.

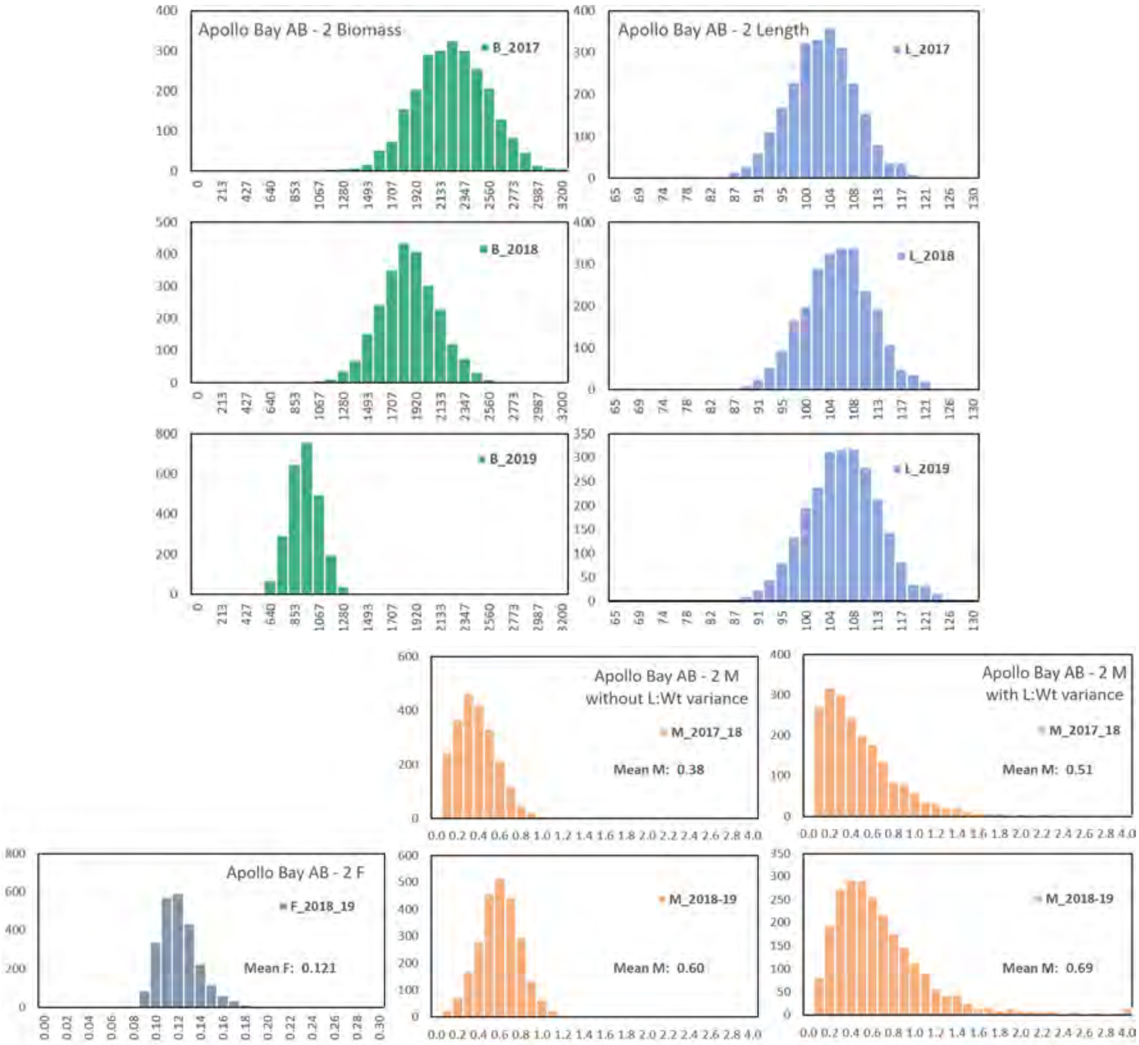

Figure 4-54. Frequency histograms of biomass (B), mean adult mode length (L) fishing mortality (F) and natural mortality (M) for the Apollo Bay AB – 2 bed over 2017-18 and 2018-19.

No M distribution without L variance was done for this bed. Estimated M average 0.38 (d: 31.6%) over 2017-18 with L variance, and 0.51 (d: 40.0%) with L and $L:Wt$ variance. Mean M values over 2018-19 were 0.60 and 0.69 (d: 49.8%). With L and $L:Wt$ variance, the 95% CI of the M distribution reaches an M of up to ~1.5 (d: 77.7%) over 2018-19 (Figure 4-54)

Apollo Bay AB – 5 Hours

The Apollo Bay AB – 5 Hours bed shows a substantial decline in survey estimated biomass by 71.4 % over 2021-22. Allocated catch in 2021 was 276.8 t, resulting in a mean F of 0.089 over 2021-22 (Figure 4-55). Scallops were smaller in this bed with length increasing from 97.8 mm to 98.4 mm over the period, with assumed ages for these modes of 7+ and 8+, suggesting slower growth (Figure 4-55).

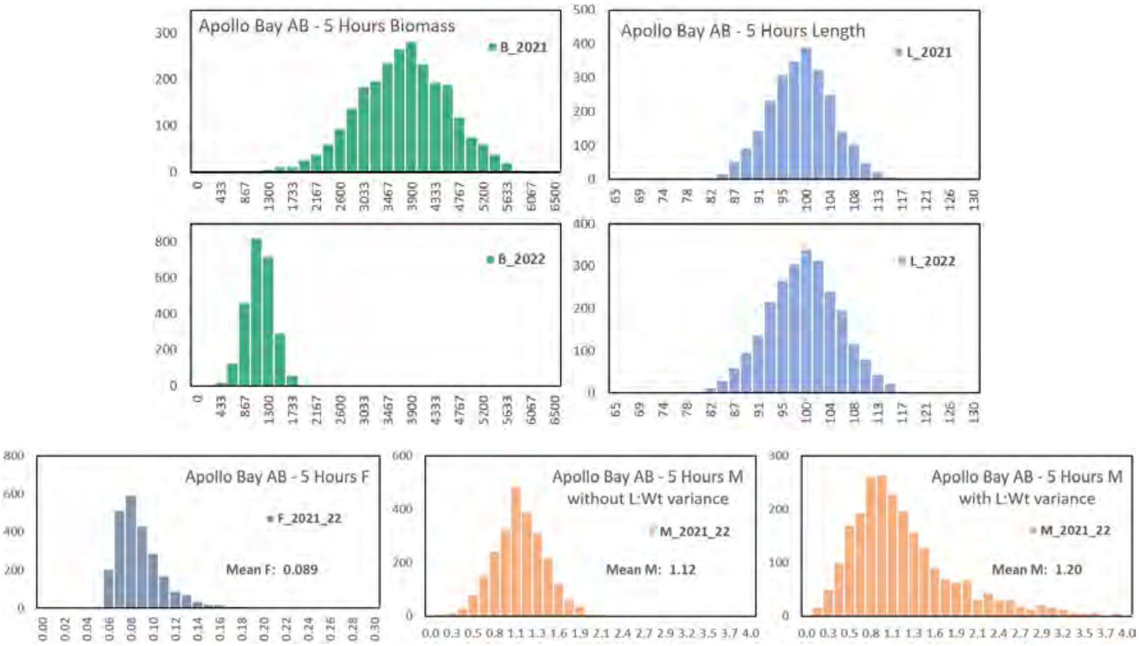

Figure 4-55. Frequency histograms of biomass (B), mean adult mode length (L) fishing mortality (F) and natural mortality (M) for the Apollo Bay East AB – 5 Hours bed over 2021-22.

Estimated M averaged 1.12 (d: 67.4%) over 2021-22 with L variance, and 1.20 (d: 69.9%) with L and $L{:}Wt$ variance. With L and $L{:}Wt$ variance, the 95% CI of the M distribution reaches up to ~2.5 (d: 91.8%) over 2021-22.

King Island KI – Mid

Survey estimated biomass in the King Island KI – Mid bed increases over 2015 – 2016, but 2015 was kept in this comparison because it provides an interesting example of a single adult mode that shows biomass increase (due to growth), with no apparent mortality, followed by sudden and substantial biomass decline in the following two years. This is a small scallop bed and actual median biomass estimates are low, increasing from 578.4 t in 2015 to 600.7 t in 2016. Thereafter median biomass decreased substantially to 92 t in 2017 and 16.3 t in 2018 (Figure 4-56).

The mean length of the adult mode increased from 107.6 mm in 2015 to 109.2 mm, 111.4 mm and 112.1 mm. These large scallops were assumed to be 5+, 6+, 7+ and 8+ years of age, showing moderate growth rate when young but reaching a large L_∞ and maximum size A catch of 24 t was assigned to this bed in 2015, 4.52 t in 2016 and zero catch in 2017, giving estimates of F of 0.049 over 2015-16 and 0.047 over 2016-17.

Expectedly, the modal estimate of M is 0 over 2015-16, although the incorporation of variance around biomass estimates in 2015 and 2016 does result in a 95% CI in possible estimates of M out to ~0.8. Estimated M was high in subsequent years, averaging 2.07 (d: 87.4%) over 2016-17 with L variance, and 1.76 (d: 82.8%) with L and $L{:}Wt$ variance. Over 2017-18 M averages 1.64 (d: 80.6%) and 1.55 (d: 78.8%). The 95% CI in M estimates extends out to ~3.2 (d: 95.9%) in 2016-17 and 2017-18 (Figure 4-56).

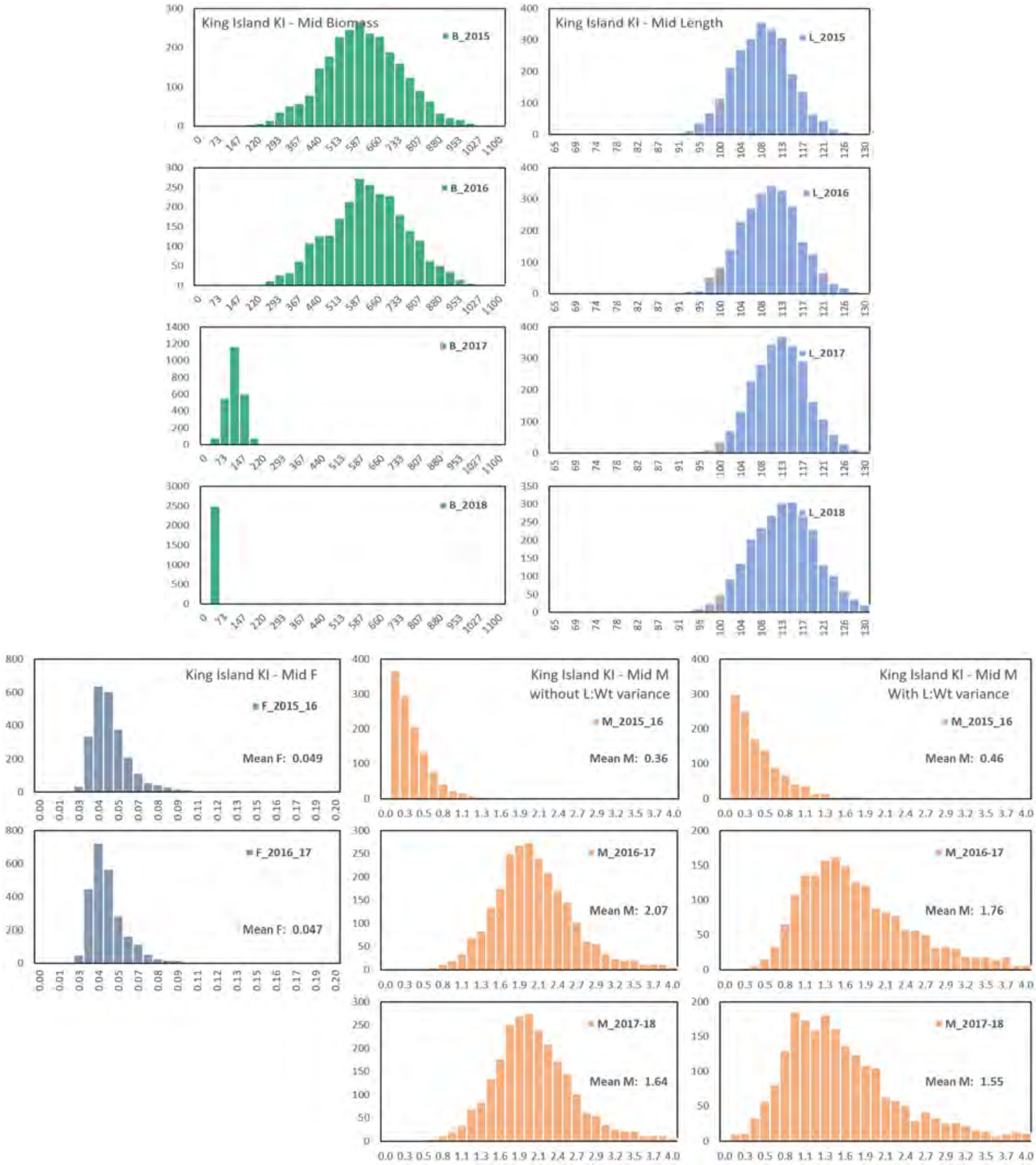

Figure 4-56. Frequency histograms of biomass (B), mean adult mode length (L) fishing mortality (F) and natural mortality (M) for the King Island KI – Mid bed over 2015-16, 2016-17 and 2017-18.

King Island KI – 5S

As with KI – Mid, median survey estimated biomass in the King Island KI – 5S bed increases from 3,059.1 t in 2017 to 3,529.4 t in 2018, but then decreases to 1612.1 t in 2019. Catches allocated to this bed were 7 t in 2017, 5 t in 2018 and zero in 2019, giving very low estimates of F of 0.0024 over 2017-18 and 0.0015 over 2018-19 (Figure 4-57).

The mean length of the adult mode increased from 108.0 mm in 2017 to 111.3 mm in 2018, but then decreased to 108.8 mm in 2019. This is not the case for modal lengths, which increased from 109 mm to 110 mm to 113 mm. The mean length in 2019 was brought down by a tail of smaller scallops, so that this was not strictly a totally adult mode. However, there was also an apparent decrease in the proportion of the largest scallops which may be the result of age-dependent mortality (senescence) of the largest scallops associated with the decline in biomass. The modes were assigned ages of 6+, 7+ and 8+ in the modal progression growth analysis.

As expected, the modal estimate of M over 2017-18 is zero, although variance in biomass estimates does result in 95% CIs in estimated M out to ~0.4 or ~1.0. Estimated M was moderately high over 2018-19, averaging 0.73 (d: 51.8%) with L variance, and 0.82 (d: 56%) with L and $L{:}Wt$ variance, with the 95% CI extending out to ~1.7 (d: 81.7%) in 2018-19 (Figure 4-57).

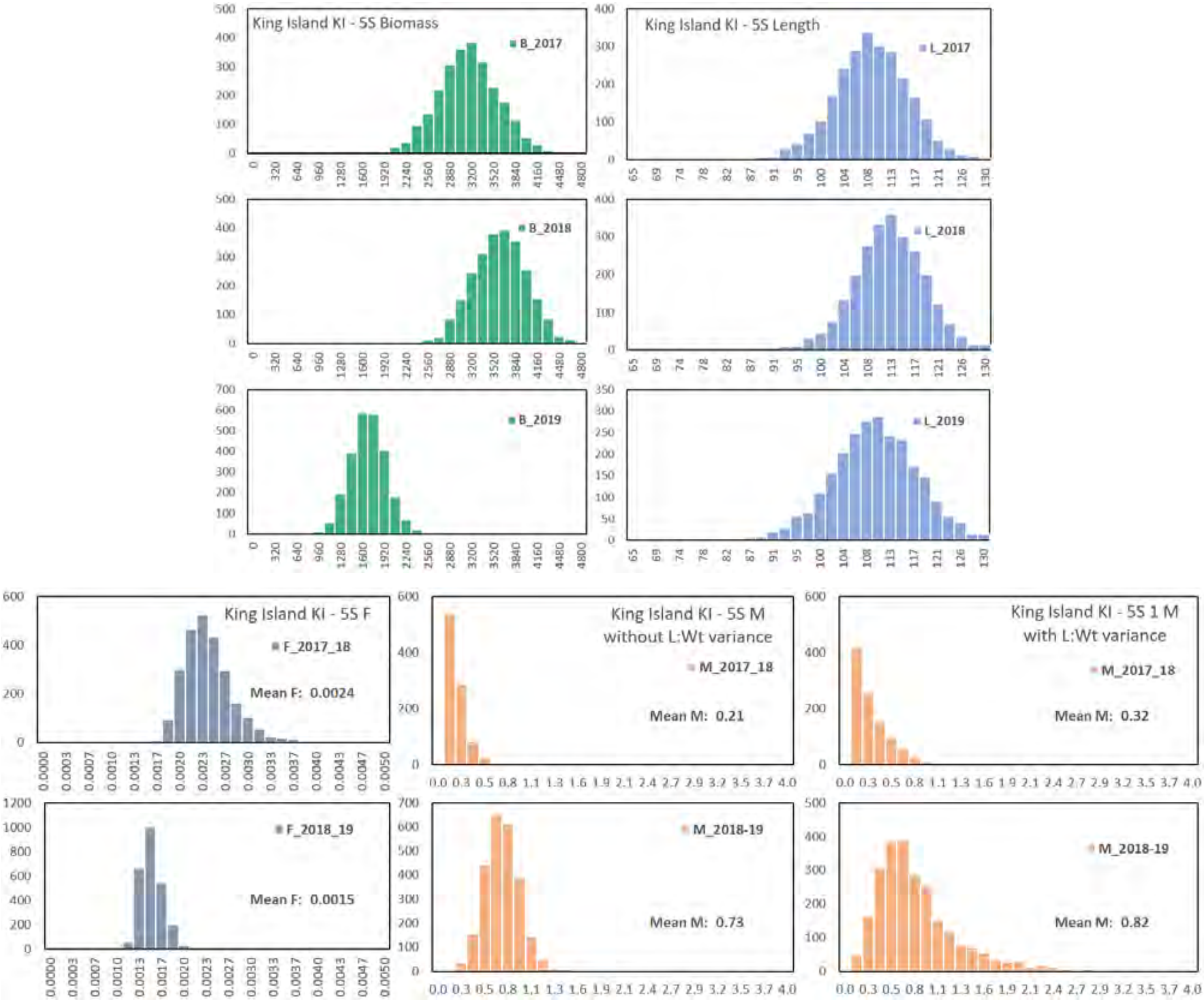

Figure 4-57. Frequency histograms of biomass (B), mean adult mode length (L) fishing mortality (F) and natural mortality (M) for the King Island KI – 5S bed over 2017-18 and 2018-19.

Flinders Island North FI – 2

Biomass in the Flinders Island North FI – 2 bed was estimated to be 2,304.6 t in 2016 with wide variance, decreasing substantially to 585.1 t in 2017, a 75% decrease. No catch was assigned to this bed over that period (Figure 4-58). The mean length of the adult mode decreased from 89.3 mm – 85.9 mm, with modal length decreasing similarly. There is wide variance around the adult modal length, with tails of both smaller and larger scallops. Reduction in the tail of larger scallops contributes to the decline in mean and may be the result of age-dependent mortality (senescence) associated with the substantial mortality over 2016-17.

Estimated M averaged 1.07 (d: 65.7%) over 2016-17 with L variance, and 1.16 (d: 68.7%) with L and $L{:}Wt$ variance. With L and $L{:}Wt$ variance, the 95% CI of the M distribution reaches an M of ~2.5 (d: 91.8%) over 2016-17 (Figure 4-58).

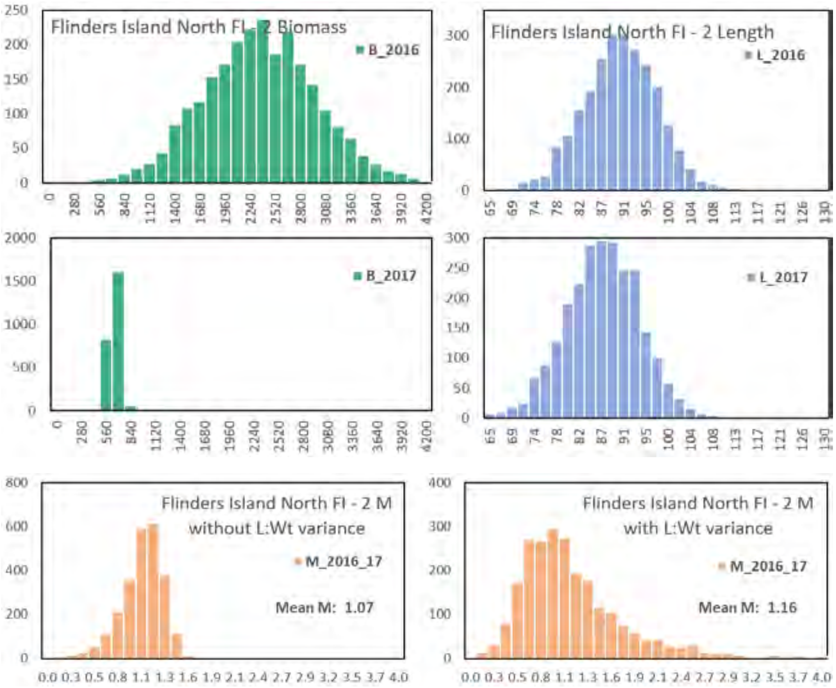

Figure 4-58. Frequency histograms of biomass (B), mean adult mode length (L) fishing mortality (F) and natural mortality (M) for the Flinders Island North FI - 2 bed over 2016-17 (Note: There were no catches made in FI – 2 over 2016-17.)

Flinders Island FI – S – TWA

Survey estimated biomass in the Flinders Island South FI – S – TWA bed declined from 1,578 t in 2022 to 249 t in 2023. Mean length of the adult mode remained almost unchanged, increasing slightly from 100.7 mm – 100.8 mm (Figure 4-59). Growth assigned to these modes is unclear and appears to have plateaued, ranging anywhere from 5+ - 8+ years of age.

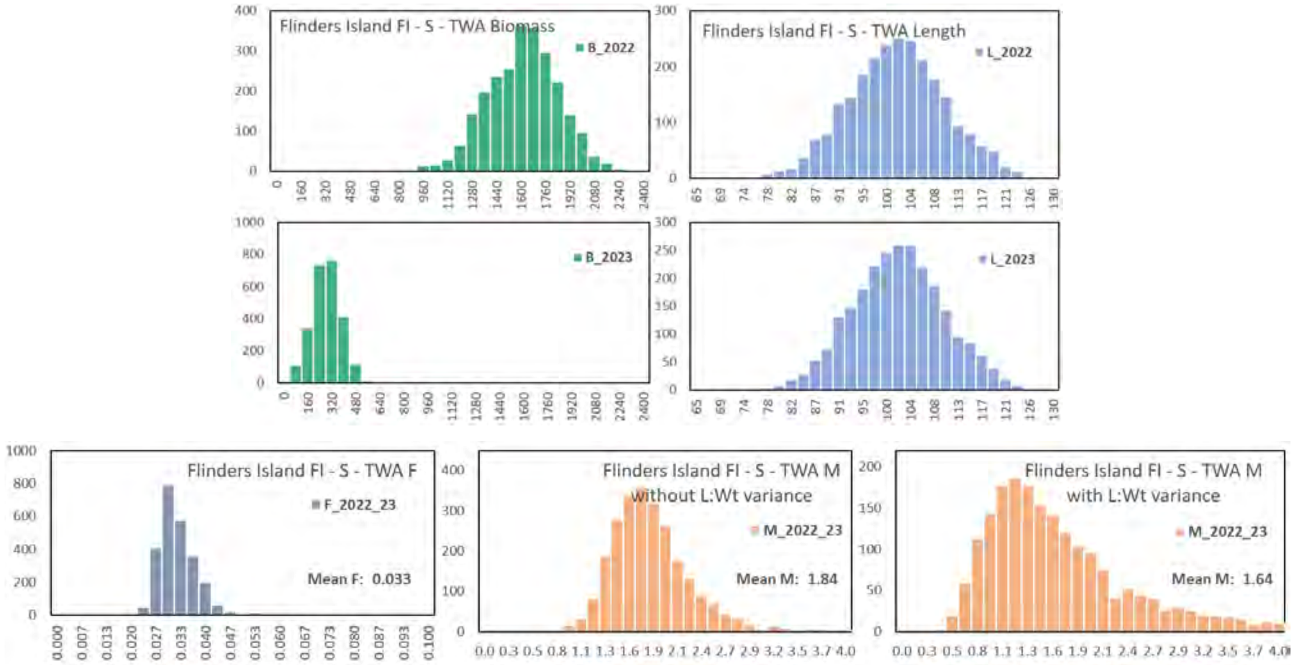

Figure 4-59. Frequency histograms of biomass (B), mean adult mode length (L) fishing mortality (F) and natural mortality (M) for the Flinders Island South FI – S - TWA bed over 2022-23.

A catch of 46.8 t was assigned to this bed in 2022, giving an estimated mean *F* of 0.033, ranging from about 0.025 – 0.047. Estimated M averaged 1.84 (d: 84.1%) over 2022-23 with L variance, and 1.64 (d: 80.6%) with L and $L:Wt$ variance. With L and $L:Wt$ variance, the 95% CI of the M distribution reaches an M of ~3.3 (d: 96.3%) over 2016-17 (Figure 4-59).

Summary of fishing and natural mortality

The mean fishing mortality and mean natural mortality with addition of various sources of variance from the above analyses for individual beds are summarised in Table 4-23 (noting that values may differ slightly from those shown on the above figures due to re-calculation of the randomised sample draws each time the spreadsheet is altered or saved).

Table 4-23. Summary of mean fishing mortality (F) and natural mortality (M) estimates for the survey beds and years chosen as showing substantial M on adult modes. Four estimates of M are shown for each comparison: No variance applied (deterministic, mean values only); addition of variance in biomass and mean length; addition of variance on the $L:Wt$ conversion – mean M; and addition of variance on the $L:Wt$ conversion – modal M.

Region	Bed	Years	F	Average Natural Mortality				
				No var	No L:Wt var	With L:Wt var Mean	With L:Wt var Mode	Max 95% CI
Apollo Bay	AB - 1	2017 - 2018	-	0.56	0.64	0.77	0.53	1.90
		2018 - 2019	0.009	1.12	1.18	1.26	0.93	2.70
	AB - 2	2017 - 2018	-	0.28	0.37	0.53	0.30	1.30
		2018 - 2019	0.122	0.55	0.60	0.70	0.50	1.50
	AB - 5 Hours	2021 - 2022	0.089	1.03	1.12	1.19	0.93	2.50
King Island	KI - Mid	2015 - 2016	0.049	0	0.36	0.45	0.00	1.20
		2016 - 2017	0.046	1.97	2.07	1.78	1.50	3.30
		2017 - 2018	-	1.57	1.64	1.53	1.10	3.20
	KI - 5S	2017 - 2018	0.0024	0	0.21	0.33	0.00	0.80
		2018 - 2019	0.0015	0.66	0.73	0.83	0.50	1.70
Flinders Island N	FI - 2	2016 - 2017	-	1.05	1.08	1.20	0.93	2.50
Flinders Island S	FI - S - TWA	2022 - 2023	0.032	1.70	1.83	1.66	1.20	2.70

Although there is uncertainty around exactly which reported catches to allocate to which individual beds (see *Methods: Fishing and natural mortality estimation*), catches available to be assigned to these beds were low and fishing mortality rates were extremely low over the observed periods of rapid biomass decline. The highest F values were 0.12 (harvest rate h: 11.5%) for bed AB – 2 over 2018 – 2019 and 0.09 (h: 8.6%). Otherwise, F is below 0.05 for all beds in which rapid biomass declines were observed.

In contrast, natural mortality rates over years when rapid biomass declines were observed are extremely high, despite scallops generally continuing to grow (albeit slowly for adult scallops) in length and weight. Without added variance, M ranges from 0.55 – 1.97 (d: 43% – 86%) over periods of biomass decline. With added variance, mean M ranges from ~0.6 – 2.0 (d: 45% – 87%), with 95% CIs extending out to an M of up to ~3.3 (d: 96%). The modal M values including L and $L:Wt$ variance are similar to, but slightly lower, than the deterministic no-variance values, due to the distributions being skewed to the left (Table 4-23).

These observed declines in biomass appear to be mass mortality events occurring in some beds over periods of one to two years, at approximate estimated ages of 6+ to 8+. The causes are unknown but could be related to episodic food shortage for large scallops with high reproductive energetic demand under certain environmental conditions, or perhaps to age-related senescence.

Interannual trends in dead scallop shell catches

Interannual trends in the catches of live scallops, and of dead shells in the categories Clappers, New Single and Old Single, are shown below in Figure 4-60 through Figure 4-63 for selected survey beds and years over which marked declines in scallop abundance occurred despite low or no fishing mortality on those beds over those years.

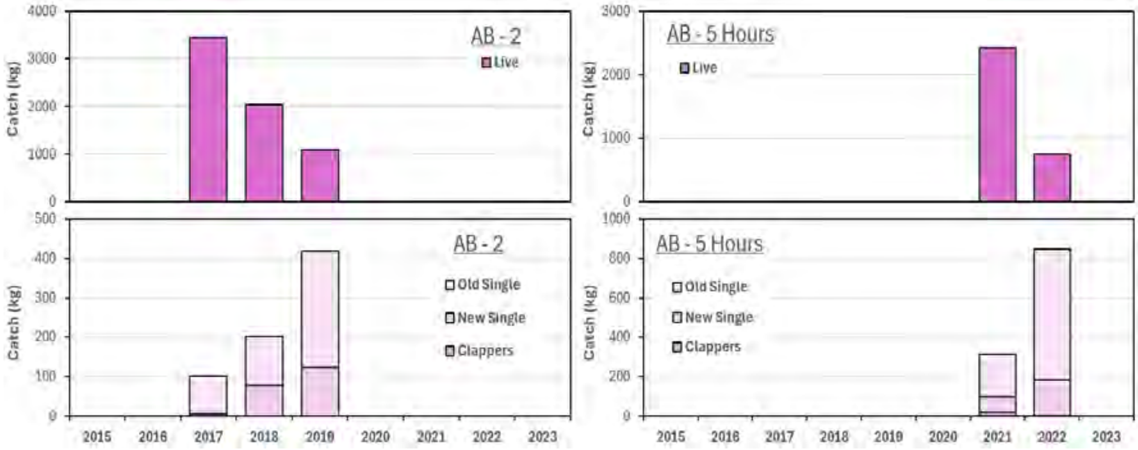

Figure 4-60. Interannual trends in the catch of scallops in surveys of the AB – 2 (2017 – 2019) and AB – 5 Hours (2021 – 2022) scallop beds showing declines in the catch of live scallops (top panels) compared with increases in the catches of dead Clappers, New Single and Old Single shells (bottom panels).

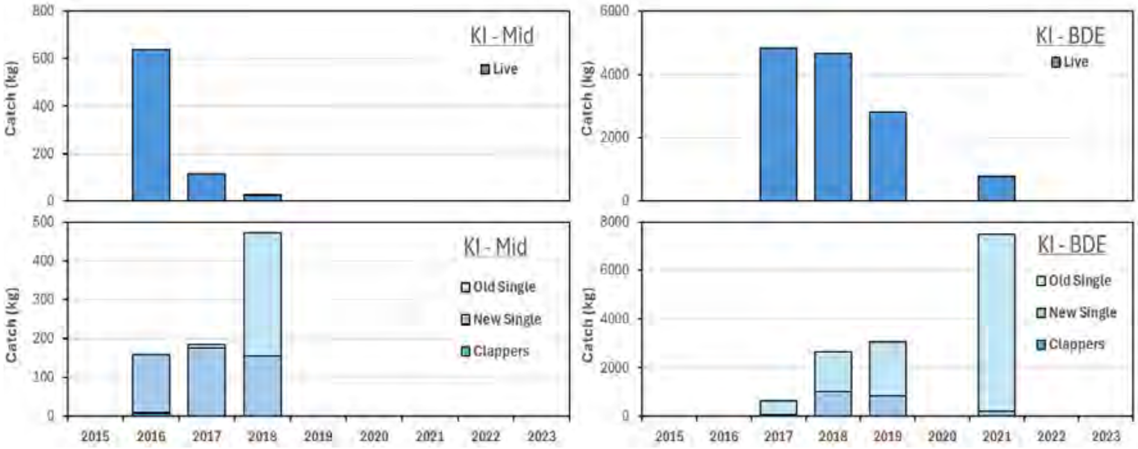

Figure 4-61. Interannual trends in the catch of scallops in surveys of the KI – Mid (2016 – 2018) and KI – BDE (2017 – 2021) scallop beds showing declines in the catch of live scallops (top panels) compared with increases in the catches of dead Clappers, New Single and Old Single shells (bottom panels).

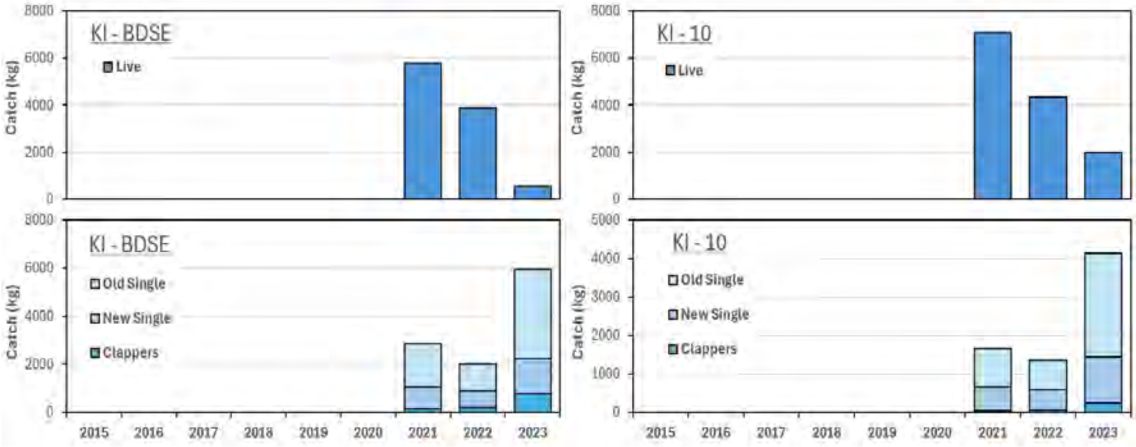

Figure 4-62. Interannual trends in the catch of scallops in surveys of the KI – BDSE (2021 – 2023) and KI – 10 (2021 – 2023) scallop beds showing declines in the catch of live scallops (top panels) compared with increases in the catches of dead Clappers, New Single and Old Single shells (bottom panels).

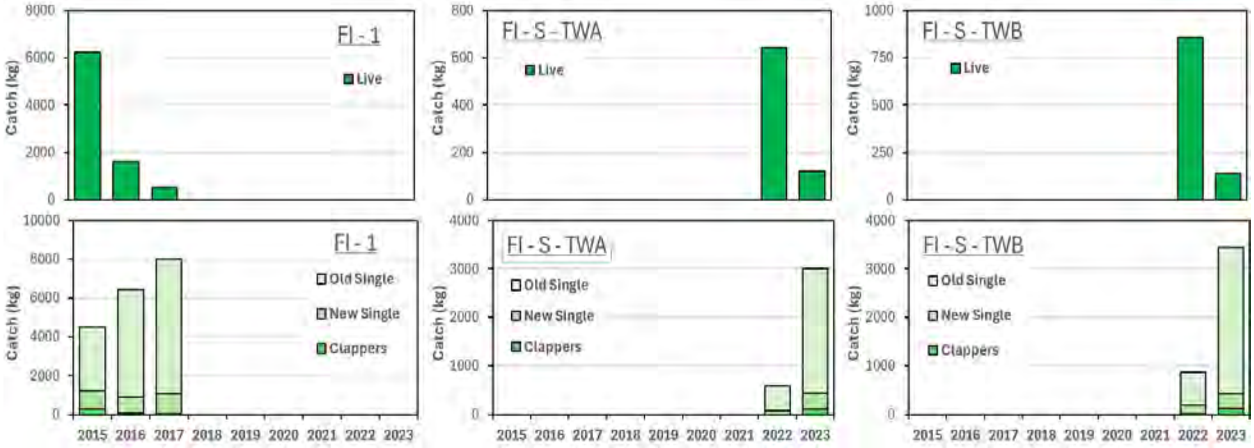

Figure 4-63. Interannual trends in the catch of scallops in surveys of the FI – 1 (2015 – 2017), FI – S – TWA (2022 – 2023) and FI – S – TWB (2022 – 2023) scallop beds showing declines in the catch of live scallops (top panels) compared with increases in the catches of dead Clappers, New Single and Old Single shells (bottom panels).

For these selected beds and years, there is a clear inverse relationship between declines in live scallop catches across years and increases in catches of dead shells. This inverse relationship is not clear in the catches of Clappers, of which few are caught. The relationship is more evident in catches of New Single shells but is particularly clear in catches of Old Single shells. The visual distinction between new and old dead shells is subjective and will depend on the rate of shell discolouration and encrustation in different areas. However, once shells have discoloured to the point of being identified as Old Single, they will remain in that category and accumulate to provide a better measure of accumulated mortality. For these selected beds, increasing quantities of dead shells, summed across all dead shell categories, provides confirmation of substantial natural mortality events occurring within those beds across those years.

This inverse relationship is evident in all beds in which rapid and substantial declines in abundance occur over periods of 2 – 4 years. However, it is not evident on beds with fluctuating abundance and evidence of multiple recruitment events. In such cases, quantities of dead shells observed fluctuate, with no clear relationship to the abundance of live scallops.

Evidence for mortality of dense juvenile recruitments

The 2019 survey of the KI – Extended JH bed was conducted in response to industry reports of unusually high densities of juvenile scallops in the area. A fine-mesh cover was used over half of the dredge to sample small individuals. The covered portion of the dredge was effective in catching small scallops at very high densities, but was apparently ineffective at catching large scallops, likely due to clogging of the dredge and back-pressure excluding the larger, more active scallops (Figure 4-64). The uncovered half of the dredge also caught small scallops, but at very low numbers, expectedly catching scallops mostly above the 70 mm size at 50% selectivity (see selectivity curve in Figure 4-17).

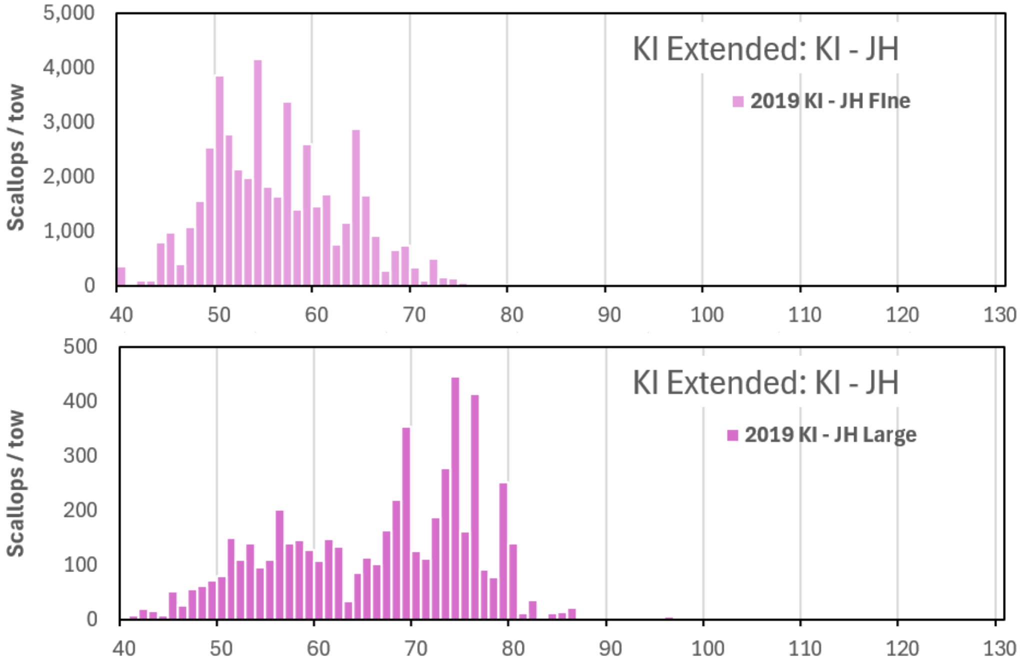

Figure 4-64. Scallop length-frequency distributions sampled by the 2019 survey of the KI – Extended JH – Fine (fine-mesh cover) and JH – Large (uncovered) halves of the dredge.

It could be expected that this exceptional recruitment in 2019 would result in a large biomass of adult scallops in the JH bed as these juveniles grew to harvestable size. However, biomass estimated in the 2021 JH – E survey in 2021 was lower than the estimates in 2019 using either the covered or uncovered halves of the dredge, despite the area surveyed increasing by 80% (JH: 34.09 km^2; JH – E: 62.85 km^2) (see Figure 4-7, Figure 8-2 and survey biomass estimates in Koopman *et al*. 2019 and Koopman *et al*. 2021). Estimated biomass in the JH bed in 2019 was 4,615 t using the covered half of the dredge, and 965 t using the uncovered half of the dredge (although highly uncertain). Estimated biomass in the JH – E survey in 2021 using an uncovered dredge was only 633 t.

This biomass that might have been expected to have resulted in 2021 from growth of the scallops present in 2019 can be approximately estimated if the growth rate and length : weight relationships for scallops in this area are known or can be assumed. A separate growth curve or length : weight relationship was not estimated for the JH bed due to limited data and differences in dredge specifications for part of the 2019 survey. For illustrative purposes, the growth rate (Figure 4-37) and length : weight relationship (Figure 4-23) for the KI – MainMid area were used for the JH area, this being the closest area to the JH beds. The methods described in Section 3.6 on ‘Fishing and natural mortality estimation’ were used.

The mean length of scallops sampled in 2019 in the JH bed using the covered portion of the dredge was 55.92 mm and the estimated biomass using the covered dredge samples was 4,615 t. Applying the KI – MainMid growth curve and *L*:*Wt* relationship to this mean size and biomass, and applying a 1.8x scaling factor to account for the larger survey area in 2021, yields a biomass of ~31,920 t in 2021 in the absence of natural mortality. The 2021 biomass estimate of 633 t implies a natural mortality rate of 3.9 (*d: 98.0%*) for the scallops present in 2019, given the assumed growth.

The mean length of scallops sampled in 2019 in the JH bed using the uncovered portion of the dredge was 66.26 mm (although using a single mean length for this multi-modal distribution is crude, see Figure 4-64), and the estimated biomass using the covered dredge samples was 965 t. Applying the KI – MainMid growth curve and *L*:*Wt* relationship to this mean size and biomass, and applying a 1.8x scaling factor to account for the larger survey area in 2021, yields a biomass of ~4,830 t in 2021 in the absence of natural mortality. The 2021 biomass estimate of 633 t implies a natural mortality rate of 2.0 (*d: 86.9%*) for the scallops present in 2019, given the assumed growth.

There was an apparent substantial natural mortality of the dense juvenile settlement observed on the JH bed in 2019, with the expected large adult biomass not eventuating. Although the high natural mortalities evident on adult beds described in Section 4.10 did not seem to have resulted from density-dependent mortality, this was apparently not the case for JH beds as the scallops grew to exceed the carrying capacity of the area consistent with anecdotal reports from industry.

As observed in other areas with high natural mortality events, this mortality of juvenile scallops in the JH bed was associated with an increase in the proportion of dead shells in the catch (see Figure 4-65).

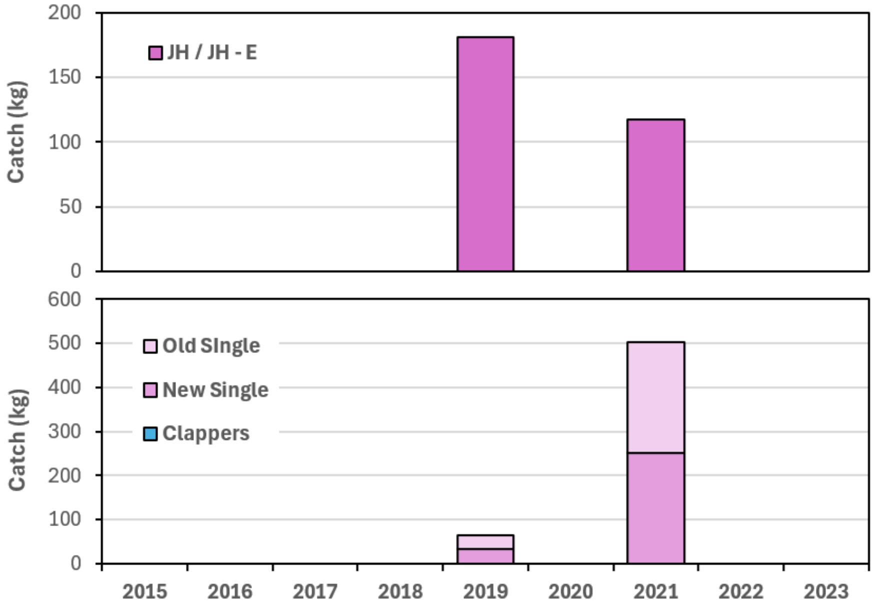

Figure 4-65. Interannual trends in the catch of scallops in surveys of the JH and JH – E beds (combined) in 2019 and 2021 showing declines in the catch of live scallops (top panel) compared to increases in the catches of dead Clappers, New Single and Old Single shells (bottom panels).

5. Discussion

Similarities in population structure within regions

The substantial quantity of length-frequency data collected during annual scallop surveys over 2015 – 2023 provides a valuable resource for comparison of population structure within and among beds and regions. Given the rapid early growth of this species (potentially attaining ~40mm in one year) and short life span (up to 9+ years), length composition data provide information on scallop recruitment events, growth by modal progression, relative proportion of age classes and longevity on beds.

Scallop beds defined for the purpose of surveys are not separated from adjacent beds by areas with no scallops. Particularly where beds are reasonably close to one another, scallops occur across areas separating the beds, as evident by reported catches among survey beds. Scallop beds showing similar length and age composition are likely to have experienced similar histories of scallop recruitment, growth and survival, and probably form components of the same population, derived from the same spawning events. At least, such population components would need to be derived from synchronous spawning and settlement events. Subsequent similar growth rates would be expected in closely adjacent beds with similar temperature and current-driven food provision regimes.

Comparisons of length-frequency distributions (see *Results: Identification of Regions*) show close similarity between adjacent survey beds lying within 10 – 30 km of each other. These similarities indicated that these beds probably contained components of the same populations and so they were grouped into Regions for subsequent analysis (Map 4-3). Ovenden *et al.* (2016) similarly found that there was no genetic distinction between scallops from locations within regions that were spaced < 45 km apart, although they did not have samples from the King Island area.

Comparisons also showed that there were beds that were dissimilar, despite being nearby or directly adjacent (such as the King Island East and FarEast Regions). In some cases, this was due to a newly recruited cohort of small scallops in one bed only, with the adult cohort being similar among beds. These could also be components of a linked population and could be assigned to a Region. However, in some cases, the length-frequency distributions of adult scallops differed substantially among beds, indicating a different history of recruitment and/or growth. Such beds were defined as separate regions, or independent and not part of an aggregated Region.

Within the defined aggregated Regions, it appears that scallops in beds within each region probably form components of a single or linked population, derived from the same or synchronous recruitment events in the Region, and with similar subsequent growth, despite patchiness of the original recruitment and the subsequent scallop distribution. Differences in growth and morphometrics among Regions suggest that these probably constitute separate populations, derived from different recruitment events and with different subsequent growth, although not necessarily genetically distinct.

Trends in biomass, mean size and proportion undersize

The following observations regarding key aspects of scallop bed dynamics can be drawn from trends in biomass, mean size and proportion undersize shown in Section 3.5 and in Appendix 4.4:

- Estimated biomass can differ substantially (by an order or magnitude) among different beds in different years, even those in the same region.
- The mean length of scallops in beds dominated by large adults, with no recruitment, expectedly remains steady, or increases slightly due to slow adult growth.
- The mean length declines in some beds following recruitment of juvenile scallops. This can be seen strongly in the Flinders Island (south) beds and King Island BlueDot Extended, and moderately in King Island North (bed KI – 9) and King Island North Mid (bed KI – 7).
- Evidence for recruitment is provided by the trends in percent undersize scallops by bed across years. This can be seen in appearance of an increased proportion of small scallops in the King Island

North beds in about 2021, the King Island BlueDot beds from 2017 onwards (bed KI – BDE) or 2019 onwards (bed KI – BDSE), King Island East in 2023, Flinders Island North over most of 2016 – 2023 and Flinders Island (south) in 2023. These indicate a widespread recruitment event starting in 2018 and extending through to 2021 across many of the Apollo Bay / King Island beds.

- The results of the King Island Extended beds survey (bed KI – JH), which used a fine mesh cover over half the dredge to target juvenile scallops reported to have settled in that region, show very large numbers of small scallops in 2019, confirming a substantial recruitment in that bed.
- Maps of the proportion of undersize scallops by tow show that recruitment can occur in only a part of a bed. Recruitment patterns are complex and unpredictable, with small scallops appearing in parts of bed KI – BDE in 2017, part of bed KI – BDE, bed KI – JH and part of bed KI – 7 in 2019, and in parts of many Apollo Bay, KI North, KI North Mid, KI – THE and Beach Energy survey beds in 2021, 2022 and 2023.
- In the Flinders Island area, sporadic recruitment appears to have occurred in parts of the Flinders Island North beds, and less frequently in the Flinders Island South beds in several years. There is an increase in biomass across 2017 - 2021 in the Flinders Island North region (bed FI – 1) associated with recruitment and growth of juvenile scallops.
- There have been rapid declines in biomass in several beds that predominantly consisted of large adult scallops with little evidence of recruitment. These declines are predominantly a result of substantial natural mortality in beds that were not fished.

Morphometric differences between Regions

There were no apparent differences between Length : Height relationships for scallops within different Regions, or between different Regions. It is therefore surprising that there are apparent differences in Length : Width relationships for Apollo Bay and Apollo Bay East, together with those for Flinders Island North and South. It is unclear how $L{:}W$ can differ without $L{:}H$ differing, and whether these differences are real or perhaps due to differences in how scallop width was measured on different surveys.

There were differences among Length : Weight relationships within some Regions, perhaps due to different size ranges of scallops in different beds, but the high variability in $L{:}Wt$ obscures these differences. When $L{:}Wt$ curves are aggregated into regions (for use in converting length to weight for mortality estimation), there is a difference between the curve for the aggregated Apollo Bay area and those for either the King Island or the Flinders Island areas, with the King Island and Flinders Island median curve coinciding with the Apollo Bay upper 68% CI curve (Figure 4-23). This lower weight at length in the Apollo Bay area appears to coincide with slower growth, at least in the Apollo Bay East beds (see Results: Growth variability between Regions), and may indicate lower productivity in this area.

Growth variability between Regions

It is unfortunate that the opportunity was not taken to collect length-stratified samples of scallop shells from the various beds surveyed over 2015 – 2023 for the purposes of age determination. Ageing using ring counts on whole shells is quick and reasonably accurate (Koopman *et al.* 2018) and could have provided data on apparent age and growth differences among beds and Regions. Nonetheless, there are substantial length composition data available, and for this fast-growing species these probably provide a reasonable estimation of growth rates using modal progression. These data certainly provide an accurate measure of maximum sizes observed on surveyed beds.

Modal progression growth rate analysis did indicate some differences in growth rate K and estimated L_∞ among regions, with fitted growth curves straddling the modal progression growth curve fitted to the Haddon *et al.* (2006) modal length-at-age results for Tasmanian scallops (Figure 4-52). All fitted growth curves showed more rapid growth than found for Victorian scallops by Koopman *et al.* (2018), although the modal progression curve for Apollo Bay East is close to that for Victoria. L_∞ values range from 97 – 123 mm, but the lower values for some regions appear to be underestimated when compared with observed maximum lengths. There is less certainty around assumed ages for larger lengths, which could be out by a year either way. However, the slower growth at larger lengths results in age-assumption error having a minor effect on estimates of L_∞.

The fitted growth curves for some Regions that lie reasonably close to one another differ in early growth rate, although less so in L_∞. For example, early growth rates appear to differ between Apollo Bay and Apollo Bay East, between Flinders Island North and Flinders Island South, and between King Island East and King Island FarEast (Figure 4-52). It is not clear whether these apparent early growth rate differences are real (resulting e.g. from differential food availability or density-dependent effects) or result from limitations in the data. Direct scallop shell ageing results could have addressed this.

Occurrence of mass natural mortality events

After accounting for fishing mortality and growth, natural mortality rates estimated from rapid declines in biomass in several beds consisting of adult scallops indicate the occurrence of repeated mass mortality events of large (age 6+ to 8+) scallops. This has occurred at various times in several beds across all areas, including the Apollo Bay area, the central and eastern King Island areas, Flinders Island North and Flinders Island South. Although fishing mortality was low during these events (averaging 0.044, range 0.002 – 0.12) , estimates of mean natural mortality M are extremely high, averaging > 1.1 (equivalent to 67% of scallops dying in one year), ranging from 0.3 (26%) – 2.0 (87%). When all sources of variance are considered, the 95% CI on M ranges as high as 3.3, implying a mortality of 96% of scallops in one year.

Inverse increasing trends in catches of dead shells on beds and over years in which substantial natural mortality seems to have occurred provides confirmation that observed declines in abundance resulted from local natural mortality on those beds.

This adult mortality is unlikely to have resulted from density effects such as overcrowding by recruiting small scallops, as the beds concerned were chosen to have little or no evidence of juvenile recruitment. The density and biomass of adults differed across the beds that showed declines, and these beds all clearly supported growth from recruitment to age 6+. Therefore, adult over-crowding seems unlikely.

It is possible that food shortage resulting from changed current patterns could have contributed to mortality. However, mortality events have been observed across individual areas and over years ranging from 2015 – 2023, with no such mortality in other years or areas, so this seems unlikely to be a direct cause. Food limitation could potentially contribute to mortality as the high energetic requirement of large scallops producing large gonads eventually results in little energy being left for somatic maintenance. Alternately, senescence could occur as a result of scallops simply dying of old age.

Industry have previously made anecdotal reports of substantial natural mortality of juvenile scallops following dense settlements in some areas. Results for the dedicated juvenile survey on the KI – JH bed in 2019 and follow-up survey in 2021 show that a juvenile mass mortality event did occur in this bed, with the expected large adult biomass expected from the substantial juvenile settlement observed in 2019 not eventuating. This juvenile mass mortality was likely density-dependent, as the unusually high settlement of small scallops grew to exceed the carrying capacity of the bed. It is likely that density dependence contributes to mortality of juveniles following any unusually dense settlement.

Effect of Bass Strait tidal currents on distribution patterns

Scallops are benthic resident filter feeders and broadcast spawners, dependent on near-seabed currents to provide a supply of particulate food, and both seabed and near surface currents to distribute their pelagic larvae. An overview of the predominant current patterns in the Bass Strait, and how these are spatially related to the positions of the various scallop beds surveyed and fished, is useful in informing how these currents might contribute to location of these beds, and to potential connectivity through larval transport.

Early current modelling work for the Bass Strait suggested a general eastwards nearshore flow along the Victoria and New South Wales coast, interrupted in the Bass Strait by a counterclockwise gyre down to the Tasmania north coast and back up to New South Wales (Greer *et al.* 2008). Particle distribution modelling simulating dispersal of pelagic starfish (*Asterias amurensis*) larvae (Hirst *et al.* 2013) indicated that larvae could be transported eastwards along the coast of Victoria in this nearshore drift for ~136 km in 33 days at a speed of about 4.7 cm.s^{-1}.

Hammond *et al.* (1994) extended predictive current modelling to the entire Bass Strait area and presented results showing that tidal currents are rapid near the entrances to the Strait, reaching speeds of up to 1 m/s, an order of magnitude greater than the predictions by Greer *et al.* (2008) and Hirst *et al.* (2013). However, they concluded that the net tidal circulation over scallop beds was relatively small, and that tides would be expected to have little influence on the net pelagic dispersal of the larvae throughout the exposed sections of the Strait. They therefore primarily modelled predicted larval dispersal using wind-driven and coastal-trapped wave forcing (see e.g. Hammond *et al.* (1994) Figure 22.8a). Resulting predicted circulation indicates currents flowing northwards along West and East Tasmania, into Bass Strait between Tasmania and King Island and Flinders Island, and then clockwise along the Victorian coast an up the Eastern New South Wales Coast, at speeds of up to perhaps 0.25 m/s.

Hammond *et al.* (1994) conclude from larval dispersal by predicted currents that scallop beds appear to be aligned along the dominant flow directions, and that recruitment to the beds is a mixture of self- and cross-seeding, concluding that 'self-seeding' is the dominant mechanism in scallop 'beds'. The definition of scallop 'beds' by Hammond *et al.* (1994) imply that "self-seeding is by far the most likely outcome". They use eight modern 'sites' located around Bass Strait as the basis for release of larvae from scallop 'beds' (see Hammond *et al.* (1994) Figure 1.1). The predicted integrated larval abundances spawned over a season and transported by the predicted currents cover substantial distances from these release sites, up to 115 km along western King Island, 110 km along northern Tasmania, 100 km along the Victorian coast, and 60 – 100 km east of Southern and Northern Flinders Island, although larval distribution is highly variable depending on winds. The conclusion that self-seeding is the dominant mechanism for larval recruitment therefore refers to large (up to 100 km) regions, within which cross-seeding is likely, but between which cross-seeding is unlikely. Such large regions would cover all of the King Island beds, or all of the Flinders Island beds described in the present study.

More recent modelling of tidal currents (Griffin *et al.* 2021) shows that the eastwards drift predicted by Greer *et al*. (2008) is minor compared to the diurnal tidal currents generated by the inflow and outflow of tidally driven water from the east and west of the Strait. Under spring tide conditions, these currents can reach at least 1 $m.s^{-1}$, creating a diurnal pulse of water moving into and out of the Strait funnelled between King Island and Tasmania and the mainland in the West, and Flinders, Cape Barren, Clark and many smaller islands extending in an arc down from Wilson's Promontory on the mainland to Cape Portland in Tasmania (Map 4-3). These twice-daily currents are instrumental in transporting particulate food back and forth across areas of high current velocity and provide a mechanism for daily back-and-forth larval transport, potentially able to retain larvae in the general vicinity of the adult scallop beds, or to distribute larvae to adjacent beds. It is striking to note that the main scallop beds fished and surveyed all lie within areas of high current velocity, particularly east of King Island, where beds appear to be aligned with the general direction of tidal currents (Map 4-4).

The genetic relationship between scallops from different regions within the Bass Strait was investigated by Ovendon *et al.* (2016) using high resolution analysis of micro-satellite loci for samples from scallop 'beds' along a north-south axis from Lakes Entrance, down along eastern Flinders Island and Tasmania to D'Entrecasteaux Channel, as well as from Port Phillip Bay (see Ovendon *et al*. (2016) Figure 1). Unfortunately, no samples were included from the important area east of King Island. Again, it is important to understand the definition of 'beds' used in this study. The authors state that "Samples were taken from regional beds that were spaced > 100 km apart and from locations within regions that were spaced < 50 km apart". The terms 'beds' and 'regions' is used inter-changeably and it is clearer to refer to the broad sample locations as 'regions', within which 'beds' (undefined) lying within 50 km of each other were sampled.

Genetic similarities between sample regions were compared using fixation index F_{ST} values which range from 0 to 1, where 0 means complete sharing of genetic material and 1 means no sharing. As expected, the closed scallop populations in D'Entrecasteaux Channel in south-eastern Tasmania and Port Phillip Bay in southern Victoria were genetically distinct from scallop beds in all other capture locations. Other than these distant and isolated regions, Ovendon *et al.* (2016) concluded that "*Pecten fumatus* displayed no fine-scale population genetic structure. Genetic variation (F_{ST}) did not differ between scallops from adjacent collection locations separated by < 45 km, nor were size classes within individual scallop beds genetically distinct" (see Ovendon *et al*. (2016) Table 3). Although Ovendon *et al*. (2016) did not publish their size distribution data, this last conclusion supports results of length-frequency analysis in this report, indicating close similarity between many adjacent beds within aggregated regions.

Self-seeding vs cross-seeding of scallop beds

There has been substantial but conflicting discussion in past publications regarding the prevalence of self-seeding vs. cross-seeding as a mechanism for recruitment to scallop beds. This has contributed to potentially contradictory advice to managers regarding the need to maintain substantial proportions of unfished scallops in all 'beds', because they are reliant on self-seeding. Confusion has arisen as a result of different definitions applied to the term 'bed' in different studies.

This can be clarified by instead looking at the distances represented by, or between, these 'beds'. Predictive larval dispersion modelling by Hammond *et al.* (1994) predicted that larvae could be dispersed some 50 – 100 km along the direction of current flow, noting that the direction of current flow depends on the models used. Within these relatively large areas, cross-seeding between small, individual scallop beds is likely, but a large region can be reliant on 'self-seeding' within that region. Ovendon *et al*. (2016) found no genetic differences among regions within 45 km of one another, confirming that cross-seeding sufficient to maintain genetic homogeneity, occurs within regions that extend to at least 45 km.

The scallop 'beds' defined for the purpose of dredge surveys only extend for some 5 – 15 km and do not cover the full extent of scallops occurring in a region. They are defined to cover what is assumed (from trial fishing) to cover the highest density of a detected scallop population. The 'beds' provide for reasonable estimates of the exploitable biomass for the setting of a TAC, but to are small enough to be feasibly surveyed. These regions are smaller than the extent of regions or larval distribution predicted by Hammond *et al.* (1994), and of regions found by Ovendon *et al*. (2016) to show genetic similarity.

Particularly in the King Island area, surveyed and commercially fished scallop beds are closely aligned with areas and directions of highest tidal current flow between the 30 – 60 m depth contours. After a long period of little recruitment, widespread recruitment was observed to occur across much of this area over 2017 – 2021, resulting in extension of commercially viable scallop fishing areas along the direction of tidal current flow. It seems clear that cross-seeding can and has occurred across this entire King Island fishing areas, and it would have been useful to have had genetic samples from this area to confirm this.

6. Conclusions

The key conclusion from this work is that scallop productivity is highly variable and unpredictable, such that most productivity assumptions used in stock assessments (e.g. regarding existence of a stock-recruit relationship, likelihood of a constant M and similar growth across regions and years), are untenable. Regular biomass surveys remain the most reliable way to obtain estimates of exploitable biomass, at least in surveyed areas.

In particular, results of this study confirm that scallop recruitment is highly variable, both temporally and spatially. Long periods can occur without successful scallop recruitment in a region, despite there being adult populations present that spawn every year. In contrast, substantial dense settlements of recruits can suddenly appear in several beds, even across several regions, although the distribution of recruits is typically highly patchy, often occurring only in parts of several individual survey beds.

Within the regions defined for analyses here, population structure was found to be similar across several separate survey beds, indicating that these populations resulted from a similar history of recruitment and growth, and are likely to be components of the same population. These aggregated regions span distances of some 15 – 30 km (diagonal) per region. Genetic analyses by Ovendon *et al*. (2016) indicated that populations in Bass Strait within 45 km of one another are unlikely to be genetically distinct from one another.

The distribution of scallop beds is associated with areas of highest tidal current flow, between 30 – 60 m depth. Tidal currents, as modified by winds and larger oceanographic current features, are a likely candidate for dispersal of scallop larvae between smaller beds within regions, with beds being closely aligned with tidal current directions in the area to the north and east of King Island. Off King Island, the bathymetry is relatively flat, potentially facilitating settlement over a larger area compared to off Flinders Island (Stuart Richey, pers. comm.). The situation appears to differ in the area east of the Flinders Island chain, with scallop beds being aligned north – south, across the direction of tidal flow, although still within the 30 – 60 m depth range and the area of highest tidal current velocity. Anecdotal information from industry suggests that settlement in this area is associated with “sand hills” that may act to interrupt or disrupt current flow (Stuart Richey, pers. comm.). These Flinders Island beds are not genetically distinct from one another and may be aligned with wind and oceanographic currents running northwards along eastern Flinders Island.

Within regions of up to at least 45km extent, subject to strong current flows, cross seeding of smaller beds within those regions is likely. The widespread recruitment across much of the Apollo Bay / King Island area over 2018 – 2023, including extension of scallop beds into areas previously not considered to support commercially viable populations, indicates widespread dispersal of larvae, perhaps resulting from favourable spawning conditions across several regions. However, such recruitment events clearly do not occur every year, with long periods of apparent poor recruitment in some regions. It therefore remains prudent to leave components of populations across regions (~30 - 45 km in extent) unfished to allow for successful recruitment should favourable spawning conditions occur. However, this does not mean protection of populations within each and every individual survey bed in each region.

As has been anecdotally reported by industry, scallops are susceptible to mass mortality events at ages of around 6+ to 8+ and shell lengths of about 90mm – 120mm. Dramatic biomass declines have been observed between survey years in beds consisting primarily of adult scallops, with no recruitment and little fishing mortality. These declines have been observed in the Apollo Bay region over 2017 – 2019, Apollo Bay East over 2021 - 2022, King Island Mid over 2015 – 2018, King Island East over 2017 - 2019, Flinders Island North over 2016 – 2017 and Flinders Island South over 2022 – 2023.

Mass mortality of juvenile scallops, also anecdotally reported by industry, also seem to occur following particularly dense settlements, such as that observed in the KI – JH bed between 2019 and 2021. Although the adult mass mortalities observed in some beds are not likely due to density dependent effects, juvenile mortalities evidently are as small scallops grow to exceed the carrying capacity of the bed.

7. References

Benaglia T, Chauveau D, Hunter DR, Young D (2009). “mixtools: An R Package for Analyzing Finite Mixture Models.” *Journal of Statistical Software*, **32**(6), 1–29. https://www.jstatsoft.org/v32/i06/.

Fishwell (2023). 2023 BSCZSF Survey. Operation and Procedures Manual. Fishwell Consulting 28 pp.

Greer, D., Black, K., Harrison, S., and Bosserelle, C. (2008) South-east Australian (SEA) Hydrodynamic model: Calibration and Validation. ASR Limited Marine Consulting and Research.

Griffin D.A. Herzfeld M., Hemer M. and Engwirda D. (2021) Australian tidal currents – assessment of a barotropic model (COMPAS v1.3.0 rev6631) with an unstructured grid. *Geosci. Model Dev*., 14, 5561–5582.

Haddon, M., Harrington, J.J. and Semmens, J.M. (2006). Juvenile Scallop Discard Rates and Bed Dynamics: Testing the Management Rules for Scallops in Bass Strait. Tasmanian Aquaculture and Fisheries Institute, Taroona, Tasmania.

Hammond LS, Black KP, Jenkins GP and Hodgkinson RS (1994) The influence of water circulation patterns in Bass Strait on recruitment success and stock differences in scallops. Victorian Institute of Marine Sciences, Final report to FRDC Project 87/117, October 1994, 233 pp.

Harrington, Semmens & Haddon (2008). 2008 Commonwealth Bass Strait Central Zone Scallop Fishery Survey. Survey Final Report. Tasmanian Aquaculture and Fisheries Institute. University of Tasmania.

Hirst, A., Bott, N., and R. Lee (2013) Plankton survey of *Asterias amurensis* larvae in Victorian coastal waters - Final Report. Fisheries Victoria Technical Report No. 178, Department of Primary Industries, Queenscliff, Victoria, Australia. 16 pp.

Knuckey, I., Koopman, M., and Davis, M. (2015). Bass Strait and Central Zone Scallop Fishery - 2015 Survey. AFMA Project 2015/001291. Fishwell Consulting 22pp.

Knuckey, I., Koopman, M., and Davis, M. (2016). Bass Strait and Central Zone Scallop Fishery - 2016 Survey. AFMA Project 2016/0804. Fishwell Consulting. 30pp

Knuckey, I., Koopman, M., Hudson, R., Davis, M., and A. Sullivan (2017). Bass Strait and Central Zone Scallop Fishery - 2017 Survey. AFMA Project 2016/0806. Fishwell Consulting. 42pp.

Knuckey, I., Koopman, M. and, Hudson, R., (2018). Bass Strait and Central Zone Scallop Fishery - 2018 Survey. AFMA Project 2017/0822. Fishwell Consulting. 44pp.

Koopman M, Knuckey I, Harris A and Hudson R (2018) Eastern Victorian Ocean Scallop Fishery - 2017-18 Abundance Survey. Fishwell Consulting, VFA Project 17/646976, 43 pp.

Koopman, M., Knuckey, I., Sih, T. and Kube, J. (2019). Bass Strait and Central Zone Scallop Fishery - 2019 Survey. AFMA Project 2019-0812. Fishwell Consulting. 39 pp.

Koopman, M., Knuckey, I., Kube, J., Davis, A. and Sullivan, A. (2021). Bass Strait and Central Zone Scallop Fishery - 2021 Survey. AFMA Project 2019-0812. Fishwell Consulting. 39 pp.

Koopman, M., Millar, R., and I. Knuckey. (2022). Effect of the Prion Marine Seismic Survey on densities of proximate scallop populations. Fishwell Consulting, 31pp. 2022. CC BY 3.0]

Koopman, M., and Knuckey, I. (2022). Bass Strait and Central Zone Scallop Fishery - 2022 Survey. AFMA Project 2019-0807. Fishwell Consulting. 39 pp.

Ovenden J. R., Tillett B. J., Macbeth M., Broderick D., Filardo F., Street R., Tracey S. R. and Semmens, J. (2016) Stirred but not shaken: population and recruitment genetics of the scallop (*Pecten fumatus*) in Bass Strait, Australia. *ICES Journal of Marine Science*, 73(9), 2333–2341. doi:10.1093/icesjms/fsw068

Pebesma, E. (2018). Simple Features for R: Standardized Support for Spatial Vector Data. The R Journal 10 (1), 439-446, https://doi.org/10.32614/RJ-2018-009

QGIS.org (2024). QGIS Geographic Information System. Open Source Geospatial Foundation Project. http://qgis.org

R Core Team (2023). R: A language and environment for statistical computing. R Foundation for Statistical Computing, Vienna, Austria. URL https://www.R-project.org/.

Semmens, J.M., Mendo, T., Jones, N., Keane, J., Leon, R., Ewing, G. and Hartmann, K. (2018). Determining when and where to fish: Linking scallop spawning, settlement, size and condition to collaborative spatial harvest and industry in-season management strategies, Institute for Marine and Antarctic Studies and University of Tasmania, Hobart, June. CC BY 3.0

Semmens, J. and Jones, N. (2014). Draft 2014 BSCZSF survey report. Institute for Marine and Arctic Studies. July 2014.

8. Appendices

8.1. Shell measurement and gonad staging

Shell measurements

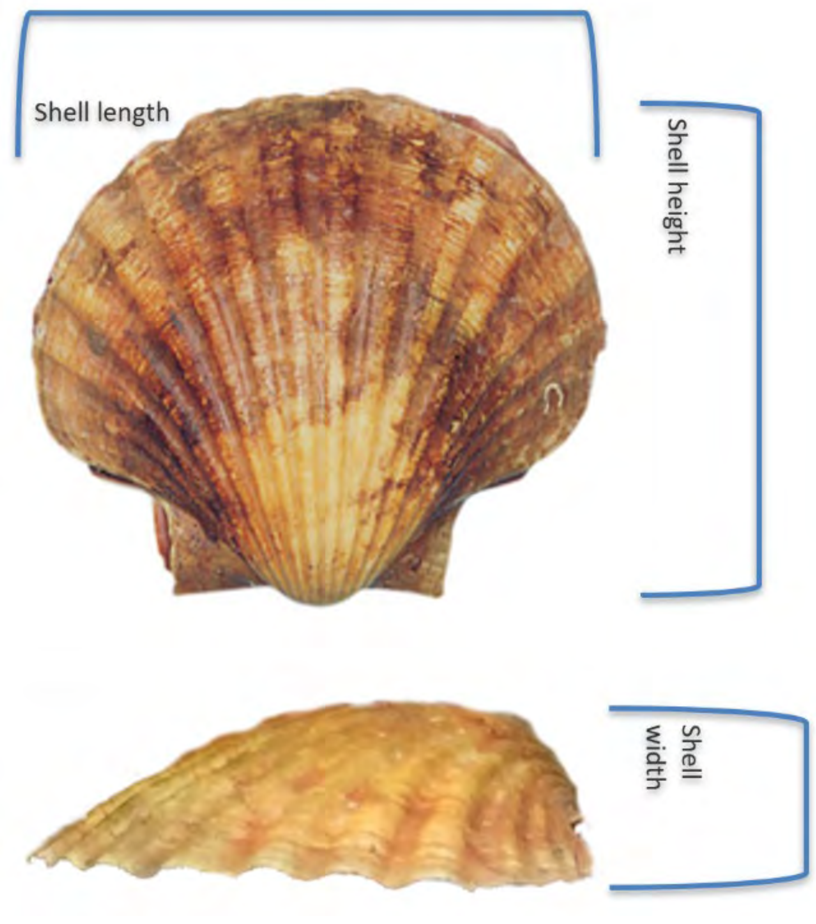

Figure 8-1. Scallop width, length and height measurements.

Gonad Staging

Table 8-1. Gonad maturation scheme for macroscopic field staging of scallops (modified from Semmens *et al*., 2019).[2]

Stages	Description
1 Developing or spent	Gonad is small, thin, translucent, brownish colour. Intestinal loop usually visible. Ovarian and testicular tissues difficult to differentiate. 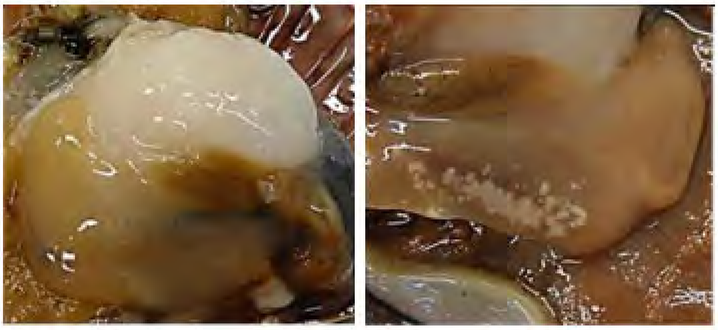
2 Maturing or atretic (reabsorbing eggs as spawning is delayed)	Separate acini clearly visible, male (white) and female (orange) part of gonad distinguishable. Gonad increases in turgor (rigidity) and becomes less granular in appearance as acini begin to fill until ovarian tissue appears uniform in colour. 
3 Partially spawned	Gonad reduced in size compared to previous stage. Ovary appears mottled, presumably due to some acini being voided. Intestinal loop usually visible, ovarian tissue uniform in colour, but interspersed with isolated specs of translucent (void) acini. Testicular tissues turn paler in colour. 

---

[2] Semmens, J.M., Mendo, Jones, Keane, Leon, Ewing, Hartmann., Institute for Marine and Antarctic Studies, 2019, Determining when and where to fish: Linking scallop spawning, settlement, size and condition to collaborative spatial harvest and industry in-season management strategies, University of Tasmania, Hobart, June. CC BY 3.0

8.2. Maps of mean size of scallops by bed and year

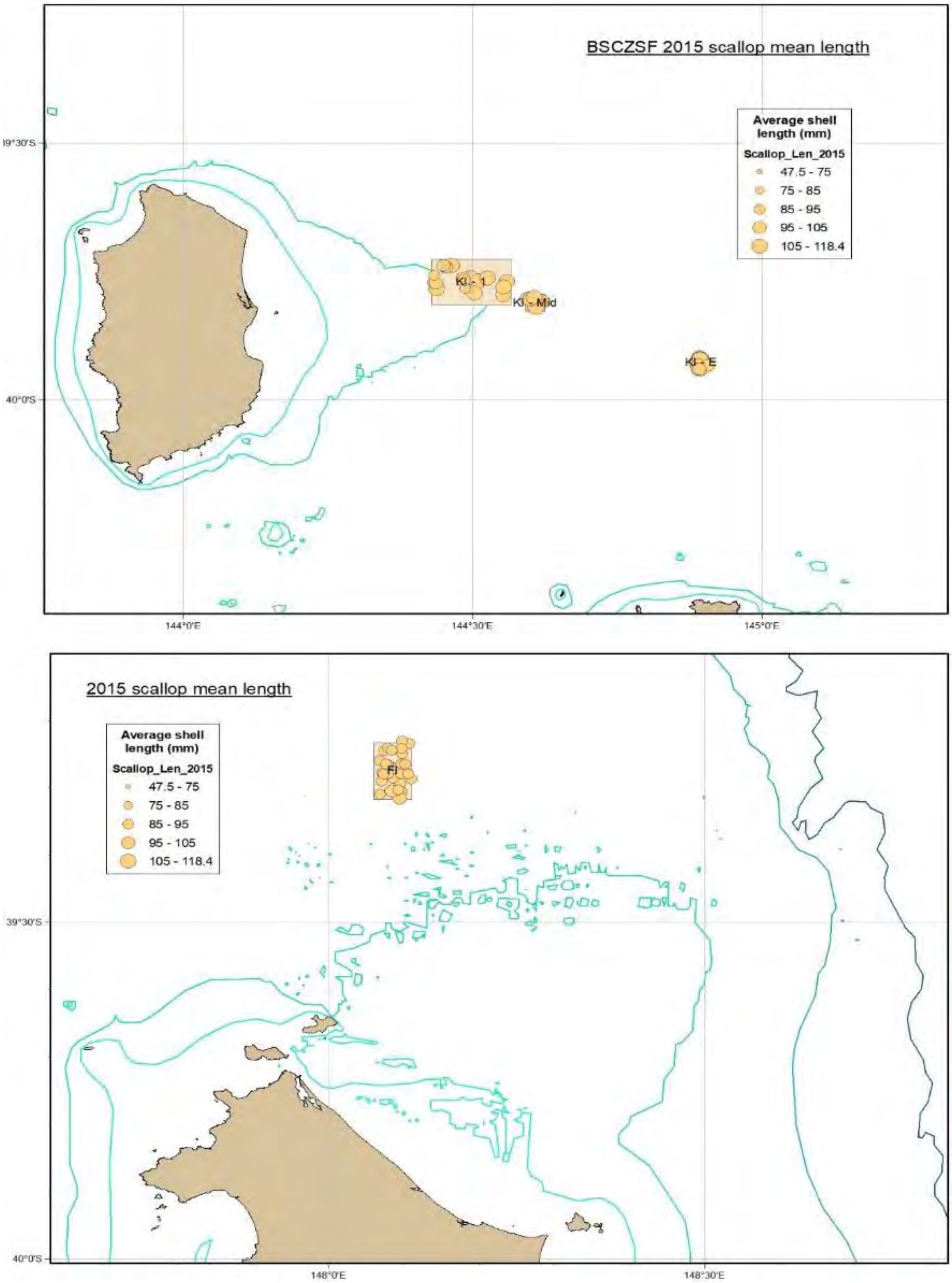

Map 8-1. Maps showing the mean size of scallops (shell length, mm) by tow in the beds surveyed in 2015 in the King Island (top) and Flinders Island (bottom) regions. Graduated symbols show the midpoint tow positions and mean size of scallops in each tow. Also shown are the 20m, 40m, 100m and 200m depth contours.

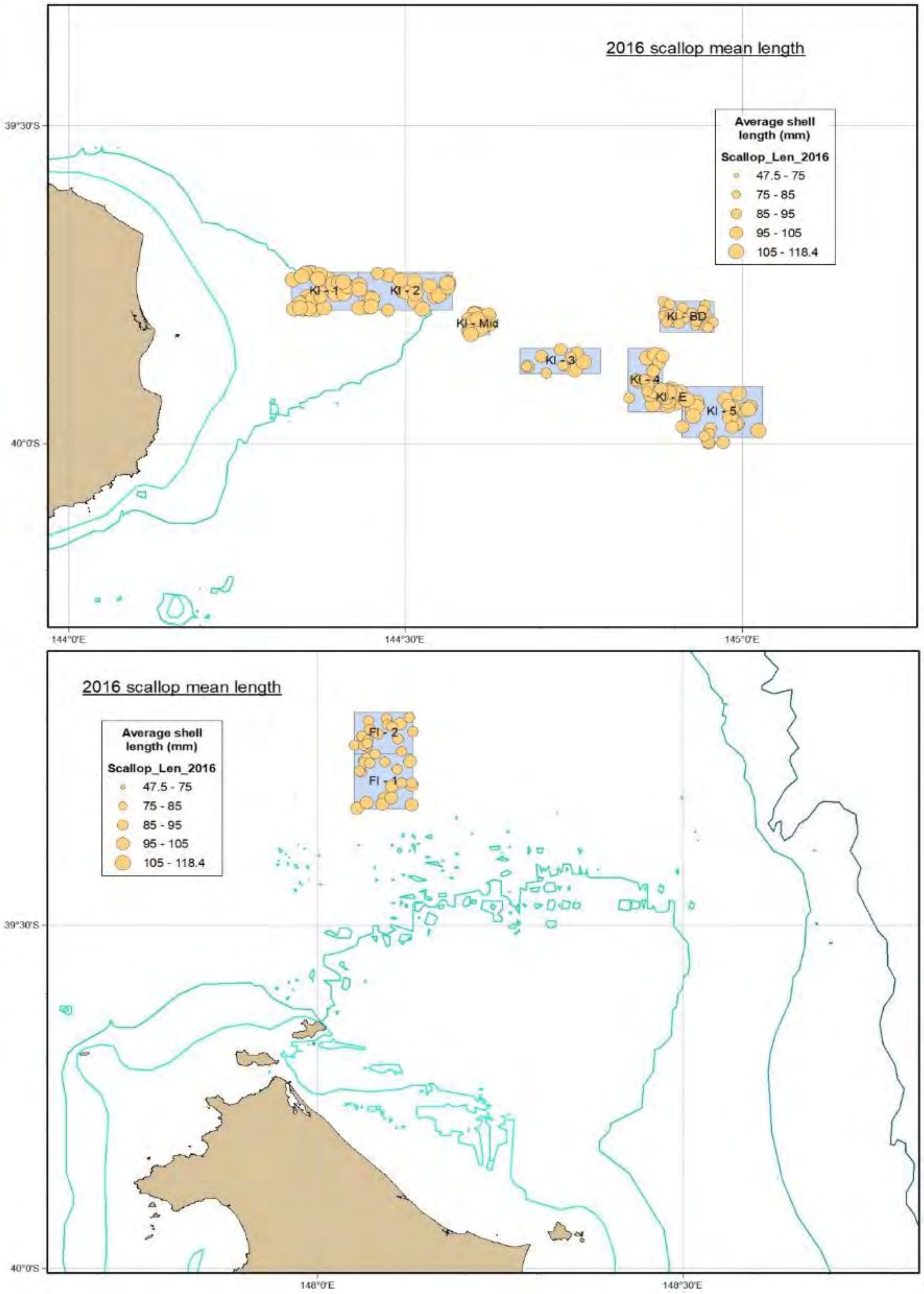

Map 8-2. Maps showing the mean size of scallops (shell length, mm) by tow in the beds surveyed in 2016 in the King Island (top) and Flinders Island (bottom) regions. Graduated symbols show the midpoint tow positions and mean size of scallops in each tow. Also shown are the 20m, 40m, 100m and 200m depth contours.

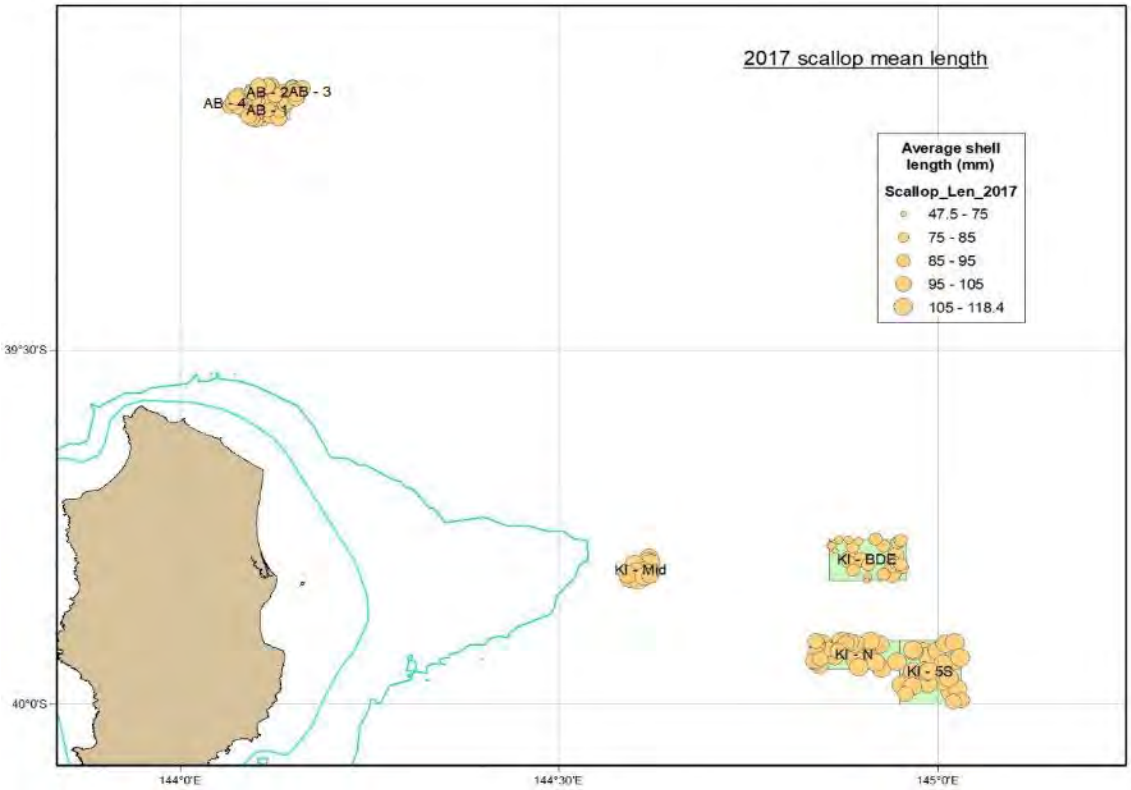

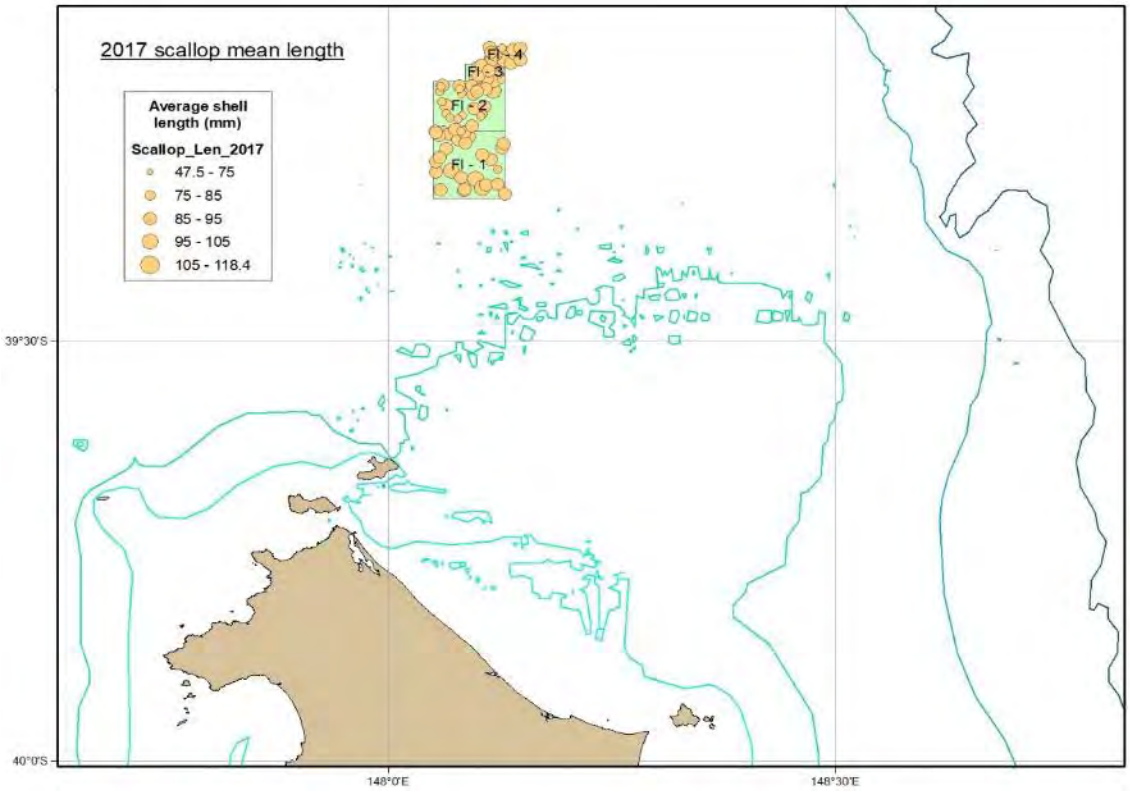

Map 8-3. Maps showing the mean size of scallops (shell length, mm) by tow in the beds surveyed in 2017 in the King Island (top) and Flinders Island (bottom) regions. Graduated symbols show the midpoint tow positions and mean size of scallops in each tow. Also shown are the 20m, 40m, 100m and 200m depth contours.

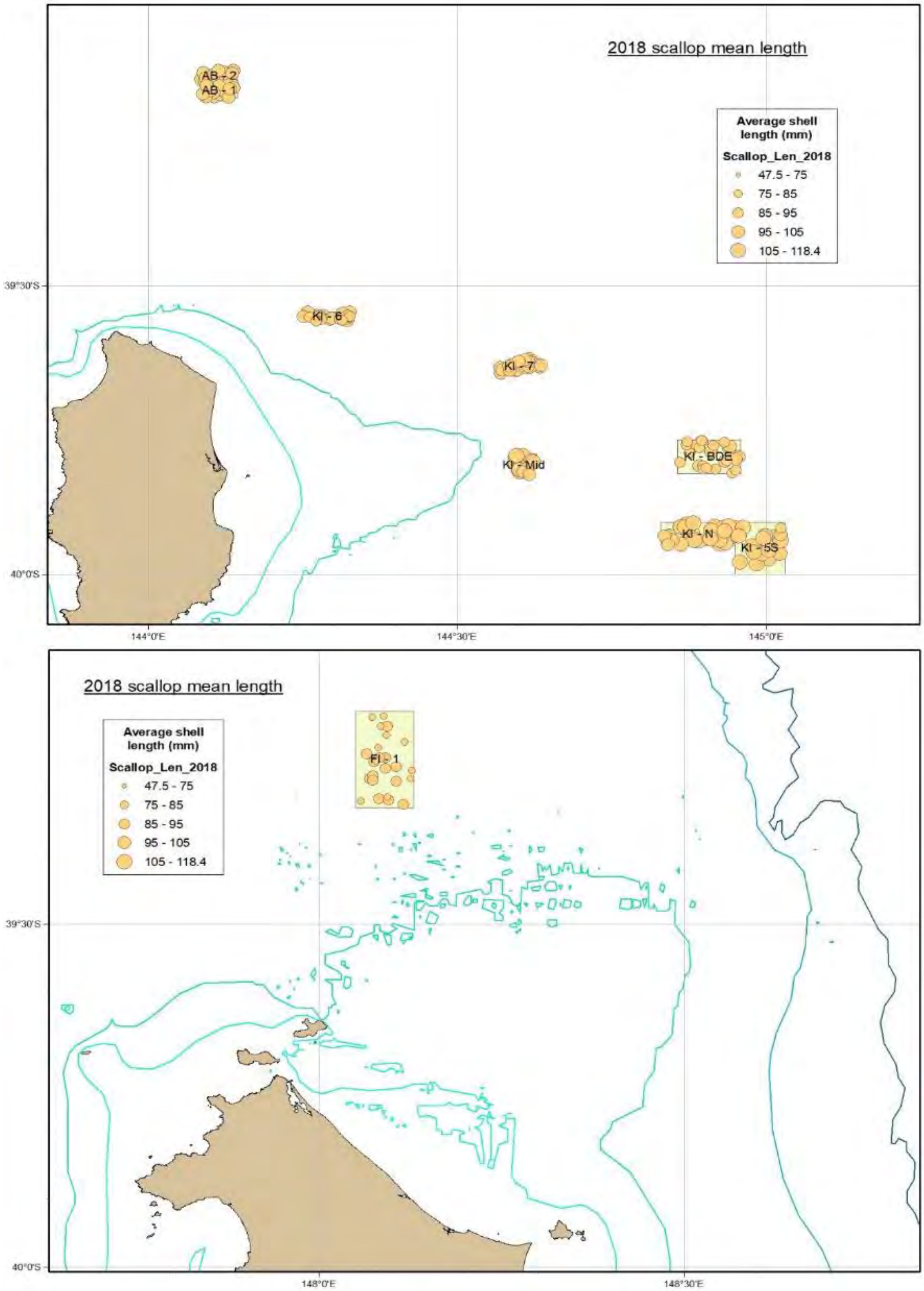

Map 8-4. Maps showing the mean size of scallops (shell length, mm) by tow in the beds surveyed in 2018 in the King Island (top) and Flinders Island (bottom) regions. Graduated symbols show the midpoint tow positions and mean size of scallops in each tow. Also shown are the 20m, 40m, 100m and 200m depth contours.

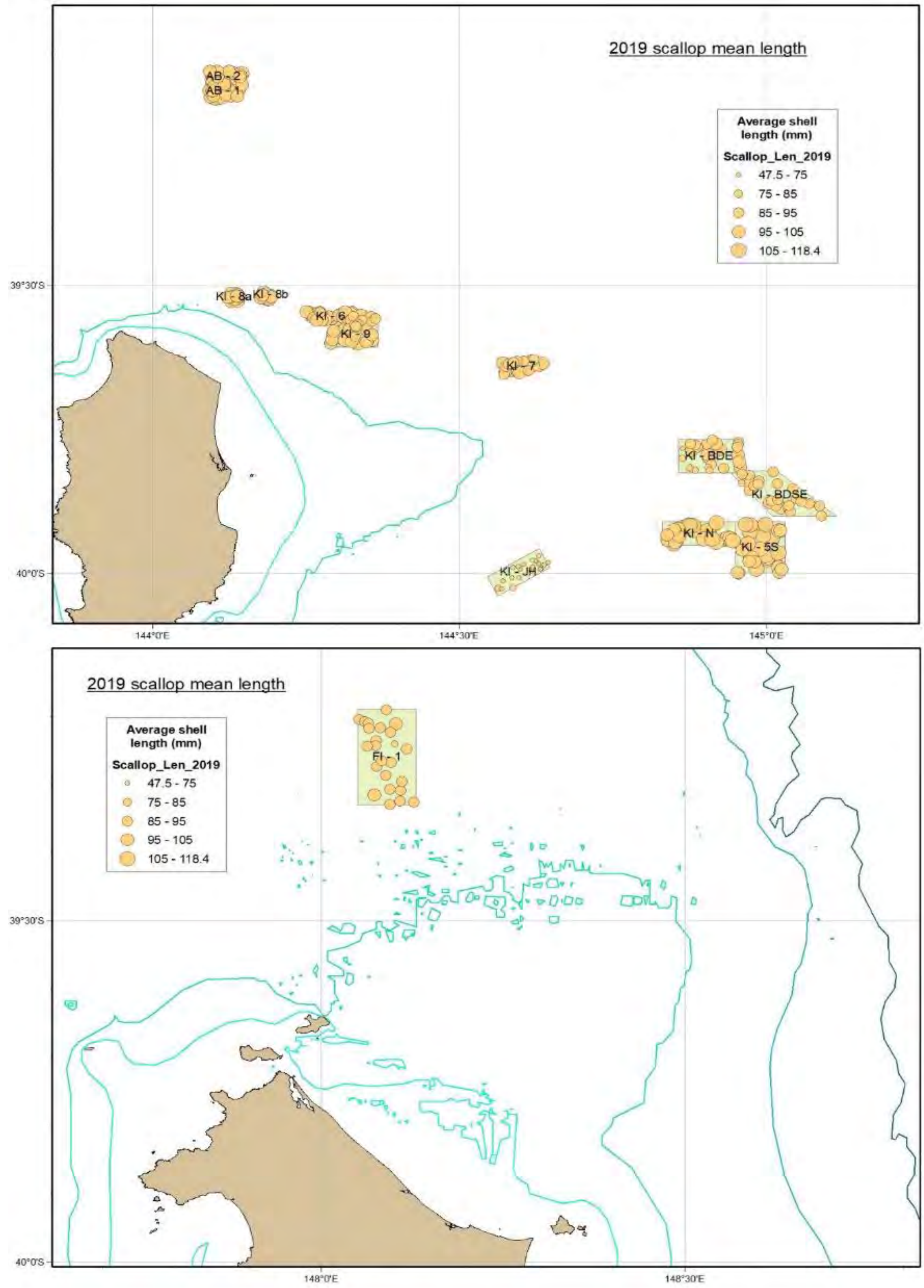

Map 8-5. Maps showing the mean size of scallops (shell length, mm) by tow in the beds surveyed in 2019 in the King Island (top) and Flinders Island (bottom) regions. Graduated symbols show the midpoint tow positions and mean size of scallops in each tow. Also shown are the 20m, 40m, 100m and 200m depth contours.

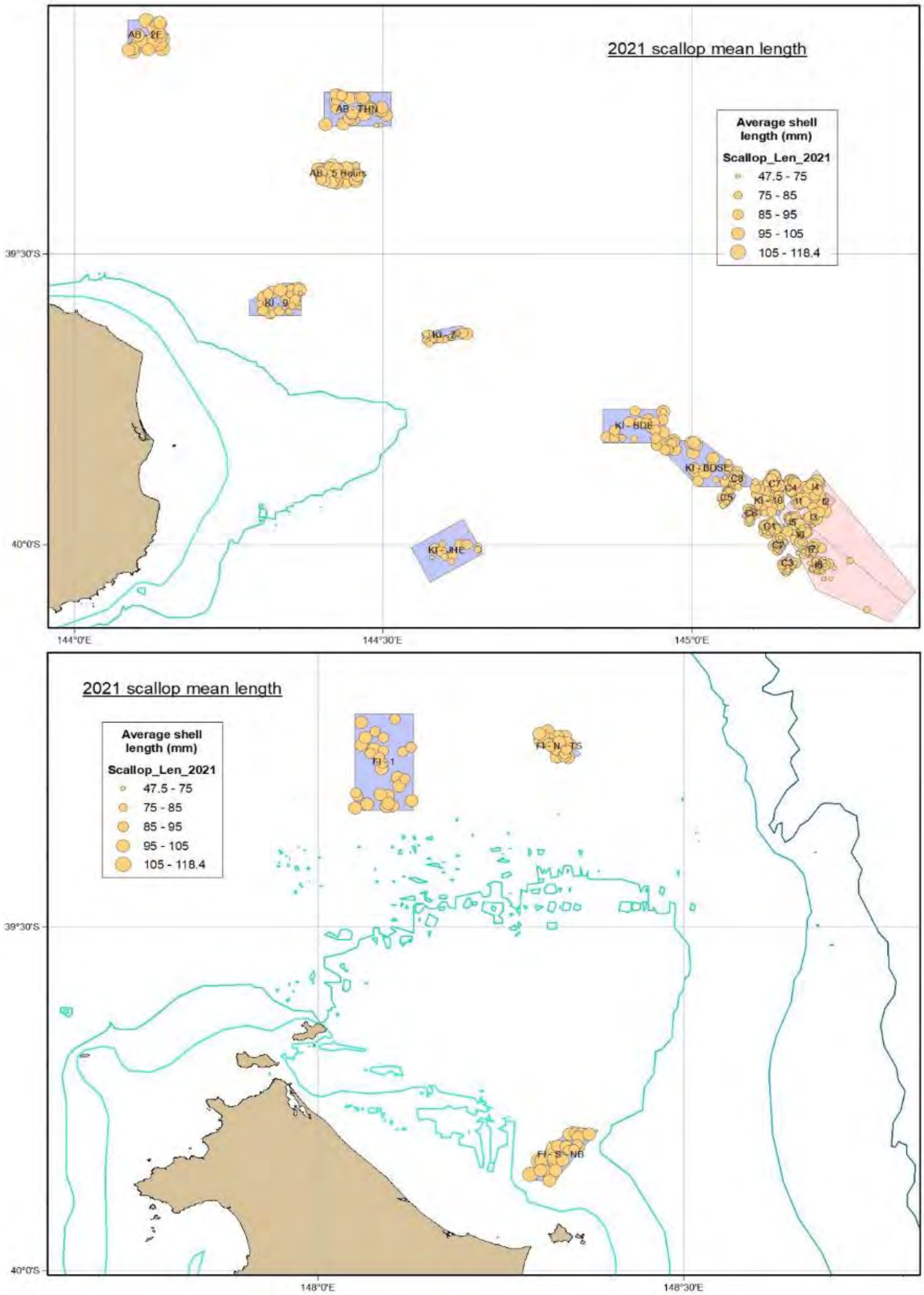

Map 8-6. Maps showing the mean size of scallops (shell length, mm) by tow in the beds surveyed in 2021 in the King Island (top) and Flinders Island (bottom) regions. Additional beds surveyed in the Beach Energy control/impact survey are shown to the southeast of the King Island East beds. Graduated symbols show the midpoint tow positions and mean size of scallops in each tow. Also shown are the 20m, 40m, 100m and 200m depth contours.

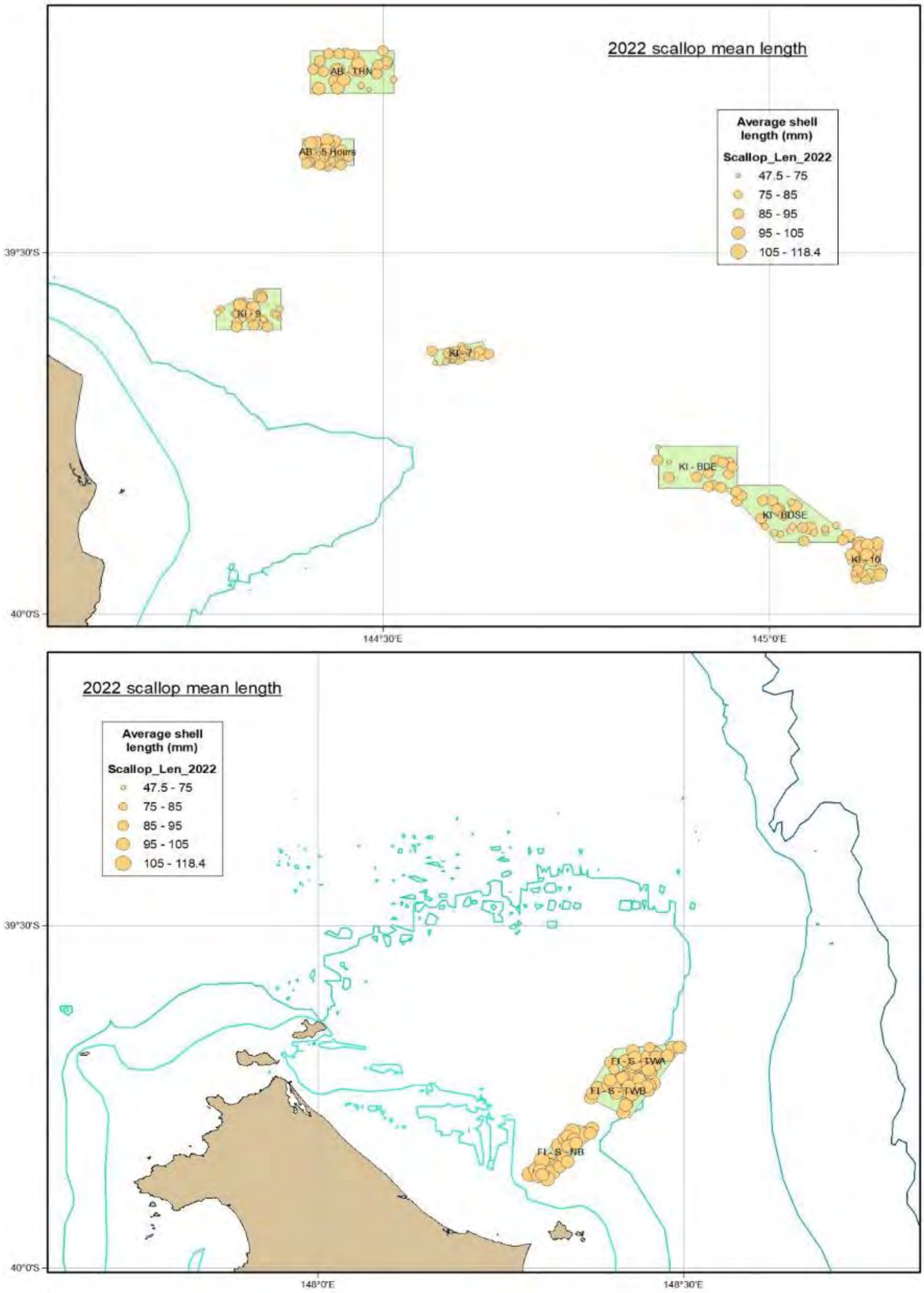

Map 8-7. Maps showing the mean size of scallops (shell length, mm) by tow in the beds surveyed in 2022 in the King Island (top) and Flinders Island (bottom) regions. Graduated symbols show the midpoint tow positions and mean size of scallops in each tow. Also shown are the 20m, 40m, 100m and 200m depth contours.

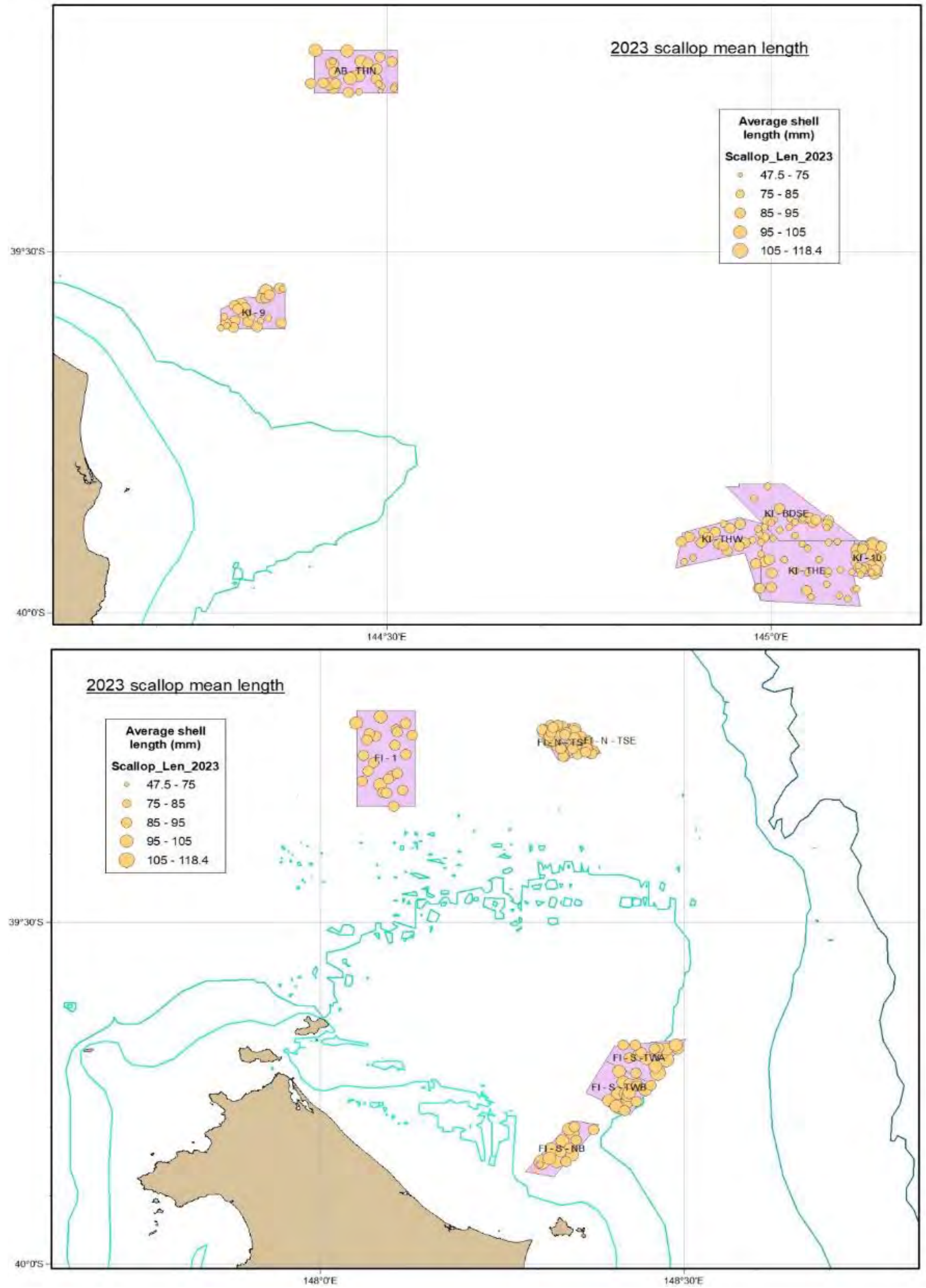

Map 8-8. Maps showing the mean size of scallops (shell length, mm) by tow in the beds surveyed in 2023 in the King Island (top) and Flinders Island (bottom) regions. Graduated symbols show the midpoint tow positions and mean size of scallops in each tow. Also shown are the 20m, 40m, 100m and 200m depth contours.

8.3. Maps of proportion of scallops < 85mm length by bed and year

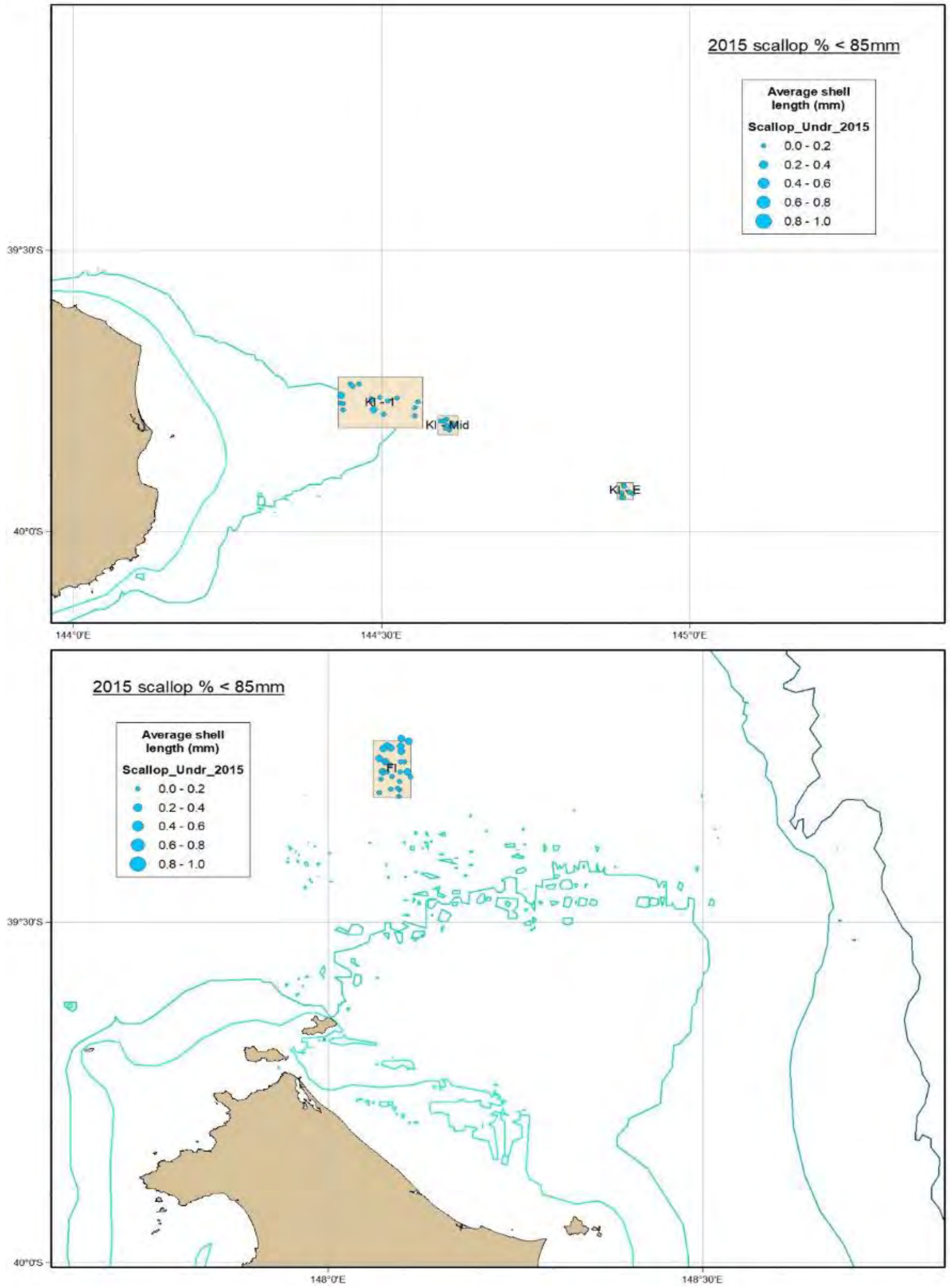

Map 8-9. Maps showing the proportion of undersize (< 85 mm shell length) of scallops by tow in the beds surveyed in 2015 in the King Island (top) and Flinders Island (bottom) regions. Graduated symbols show the midpoint tow positions and proportion undersize scallops in each tow. Also shown are the 20m, 40m, 100m and 200m depth contours.

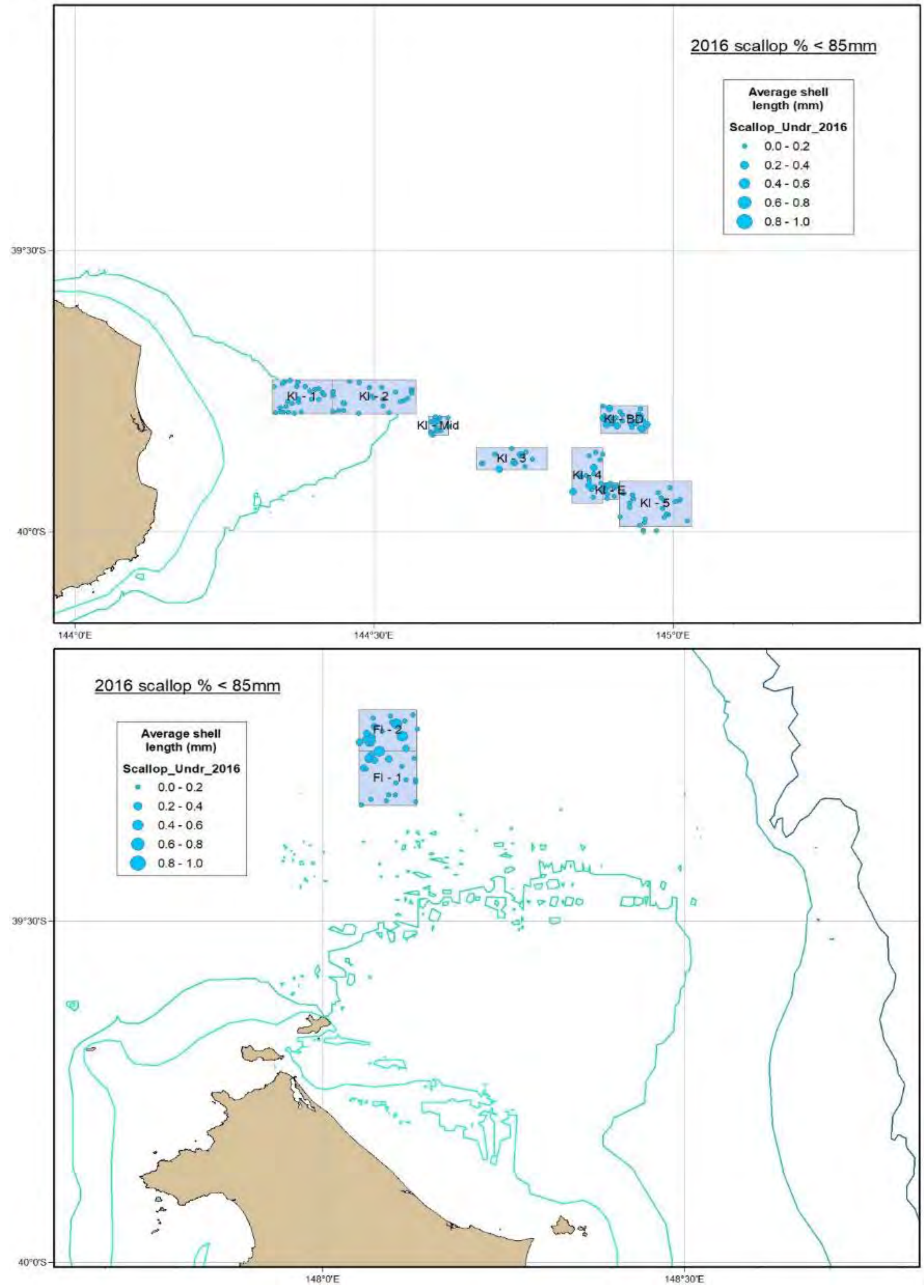

Map 8-10. Maps showing the proportion of undersize (< 85 mm shell length) scallops by tow in the beds surveyed in 2016 in the King Island (top) and Flinders Island (bottom) regions. Graduated symbols show the midpoint tow positions and proportion undersize scallops in each tow. Also shown are the 20m, 40m, 100m and 200m depth contours.

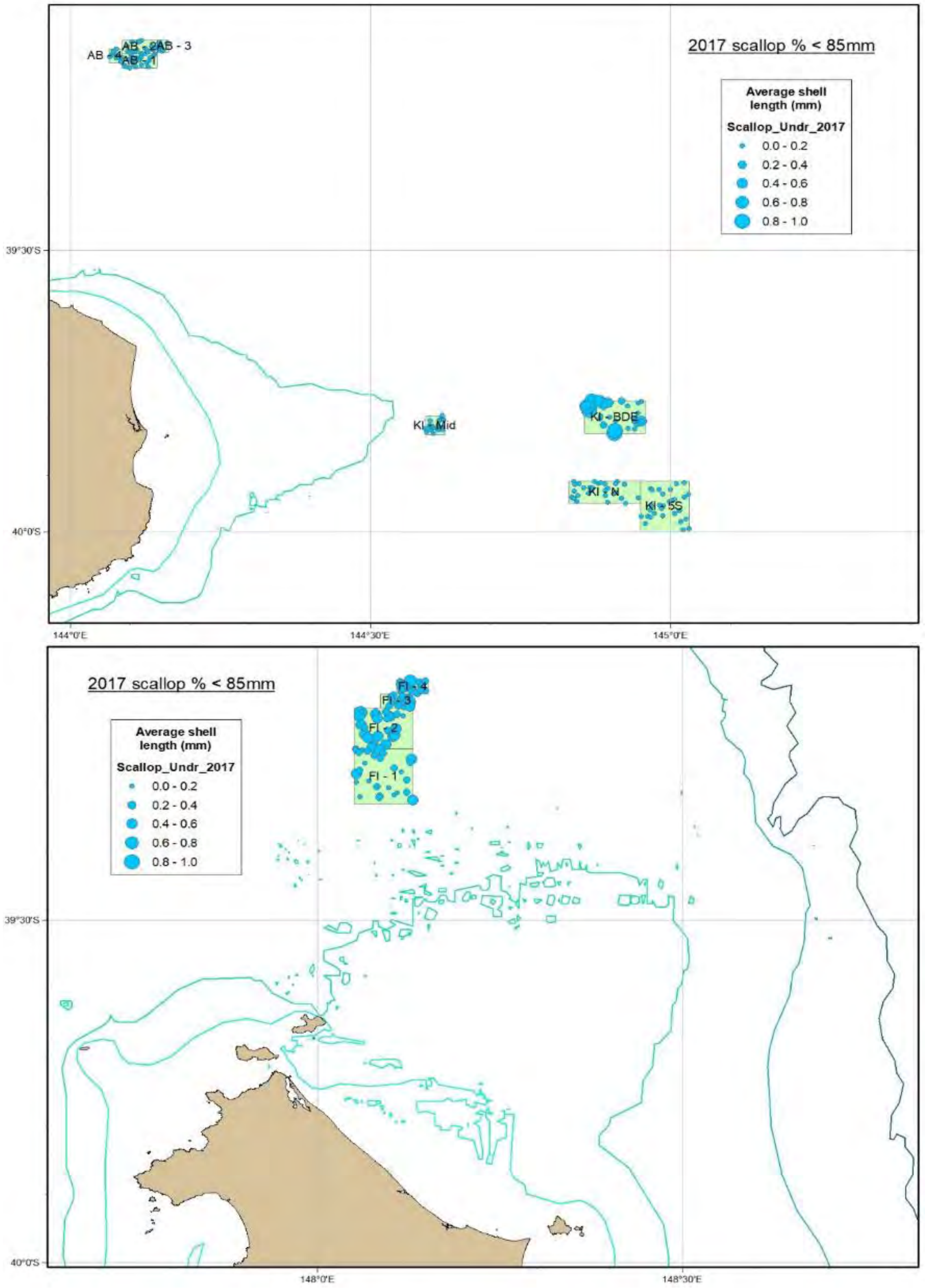

Map 8-11. Maps showing the proportion of undersize (< 85 mm shell length) scallops by tow in the beds surveyed in 2017 in the King Island (top) and Flinders Island (bottom) regions. Graduated symbols show the midpoint tow positions and proportion undersize scallops in each tow. Also shown are the 20m, 40m, 100m and 200m depth contours.

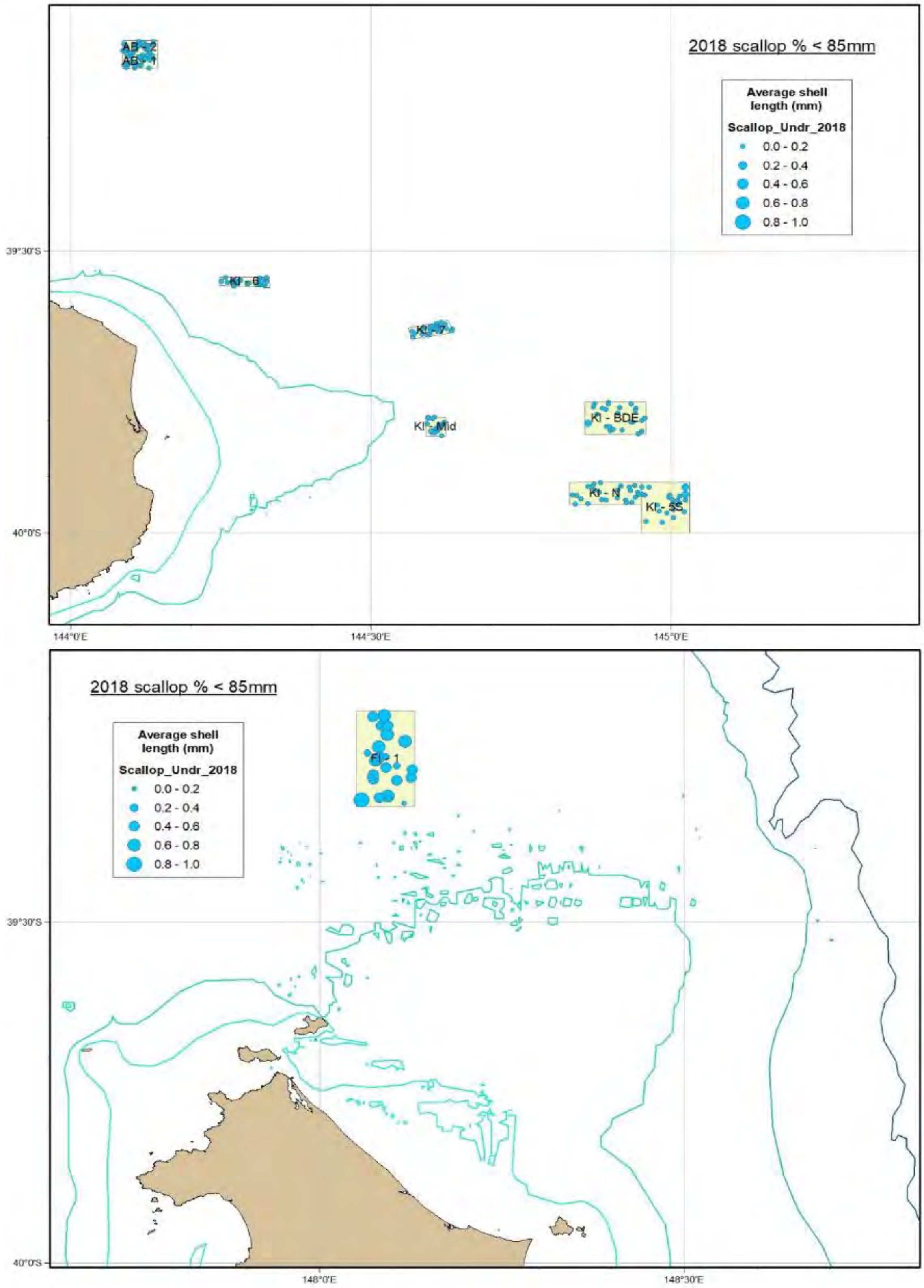

Map 8-12. Maps showing the proportion of undersize (< 85 mm shell length) scallops by tow in the beds surveyed in 2018 in the King Island (top) and Flinders Island (bottom) regions. Graduated symbols show the midpoint tow positions and proportion undersize scallops in each tow. Also shown are the 20m, 40m, 100m and 200m depth contours.

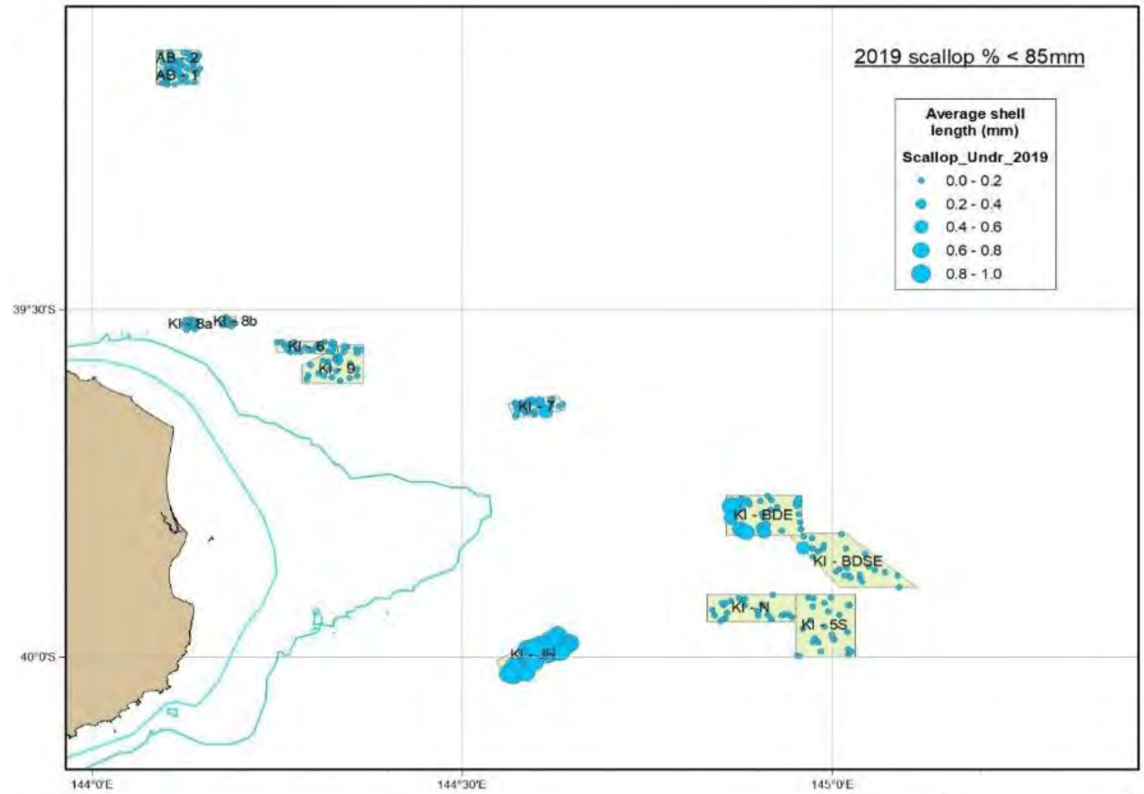

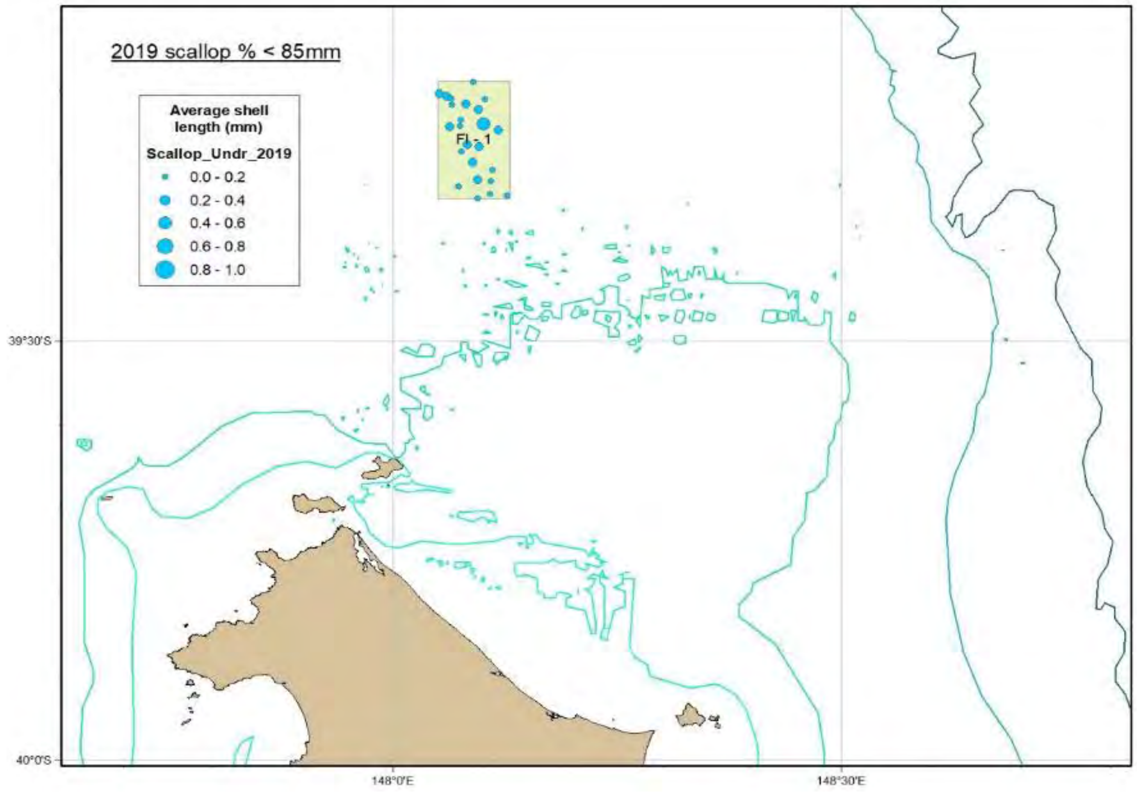

Map 8-13. Maps showing the proportion of undersize (< 85 mm shell length) scallops by tow in the beds surveyed in 2019 in the King Island (top) and Flinders Island (bottom) regions. Graduated symbols show the midpoint tow positions and proportion undersize scallops in each tow. Also shown are the 20m, 40m, 100m and 200m depth contours.

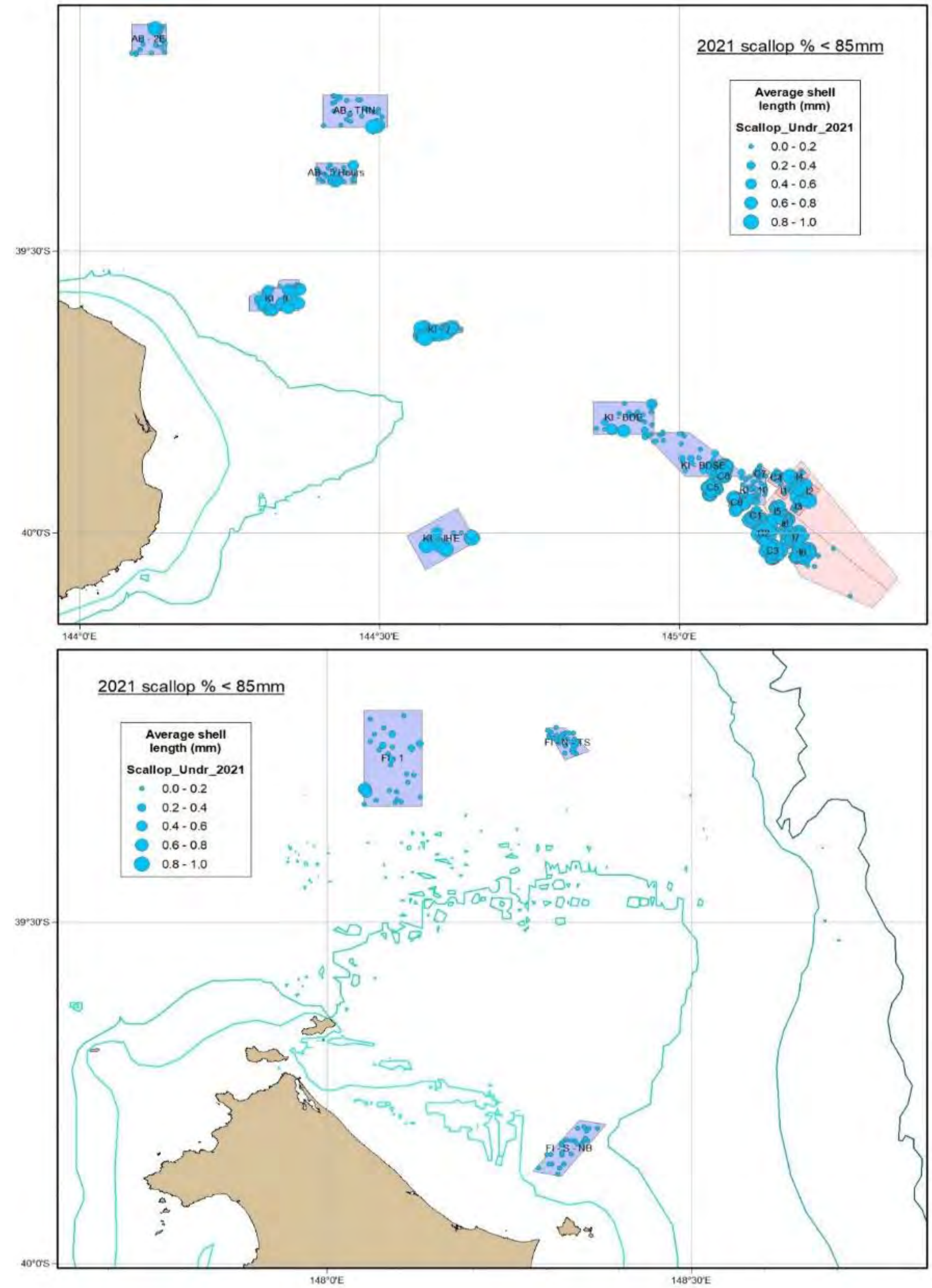

Map 8-14. Maps showing the proportion of undersize (< 85 mm shell length) scallops by tow in the beds surveyed in 2021 in the King Island (top) and Flinders Island (bottom) regions. Additional beds surveyed in the Beach Energy control/impact survey are shown to the southeast of the King Island East beds. Graduated symbols show the midpoint tow positions and proportion undersize scallops in each tow. Also shown are the 20m, 40m, 100m and 200m depth contours.

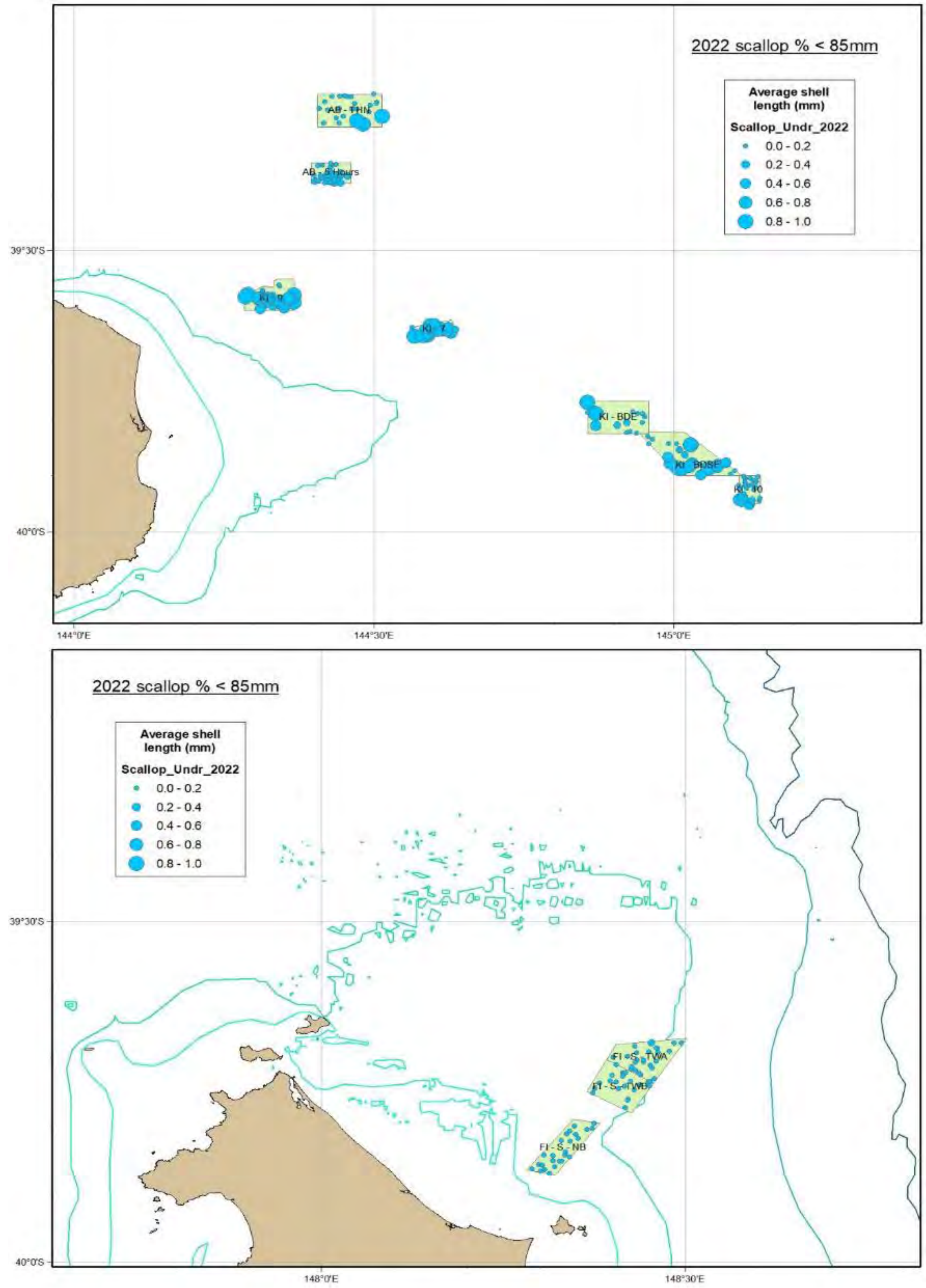

Map 8-15. Maps showing the proportion of undersize (< 85 mm shell length) scallops by tow in the beds surveyed in 2022 in the King Island (top) and Flinders Island (bottom) regions. Graduated symbols show the midpoint tow positions and proportion undersize scallops in each tow. Also shown are the 20m, 40m, 100m and 200m depth contours.

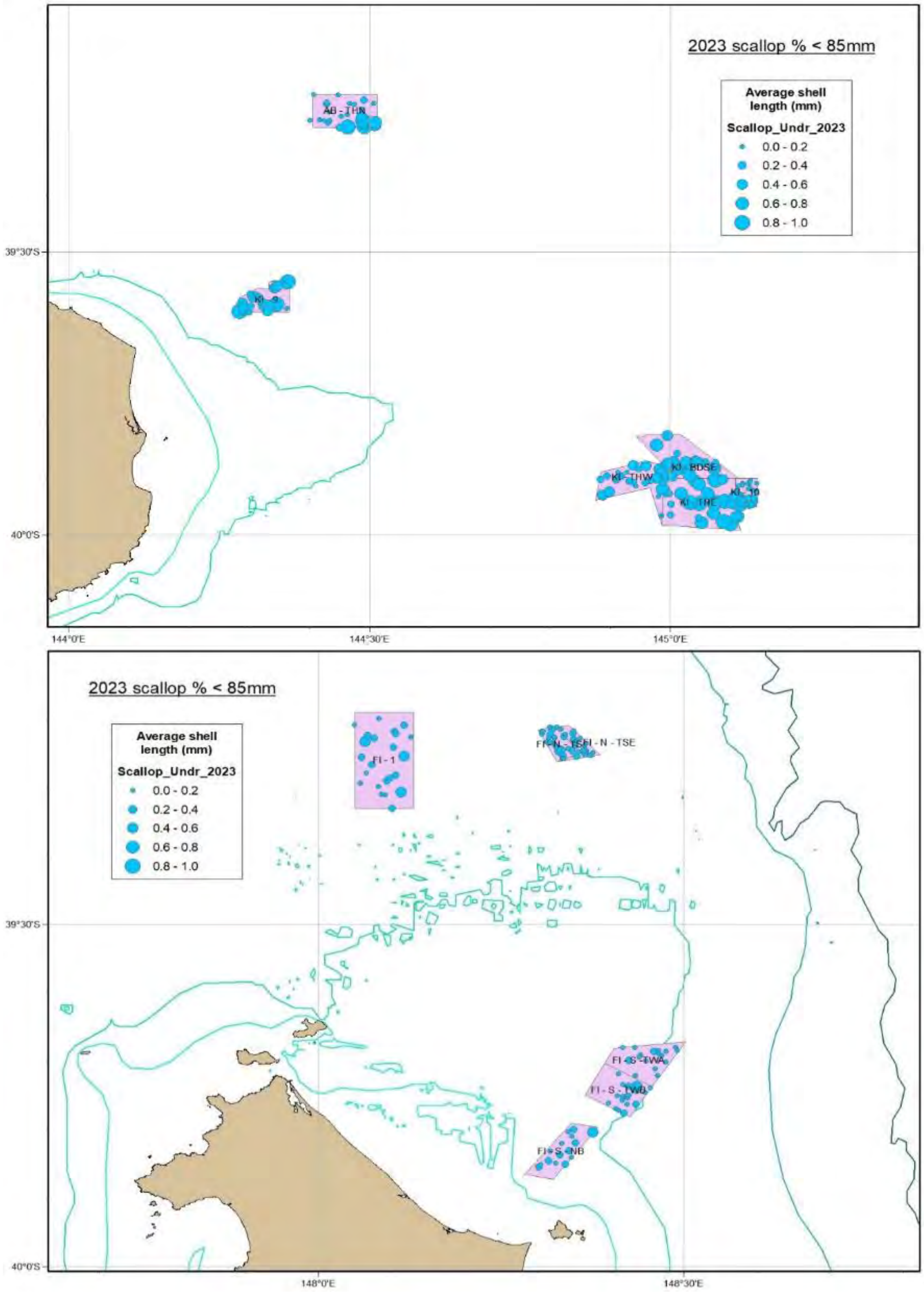

Map 8-16. Maps showing the proportion of undersize (< 85 mm shell length) scallops by tow in the beds surveyed in 2023 in the King Island (top) and Flinders Island (bottom) regions. Graduated symbols show the midpoint tow positions and proportion undersize scallops in each tow. Also shown are the 20m, 40m, 100m and 200m depth contours.

8.4. Trends in scallop biomass, mean size and proportion undersize by bed

Figure 8-2. Trends in survey estimates of scallop biomass in individual survey beds across years (from previous annual survey reports) with standard deviations. The bed codes and region names are shown for each bed, which are arranged in relative geographic position from N – S and E – W. (Note y-axis scale differs between beds.) KI – JH 2019 survey biomass estimated from the uncovered half of dredge only.

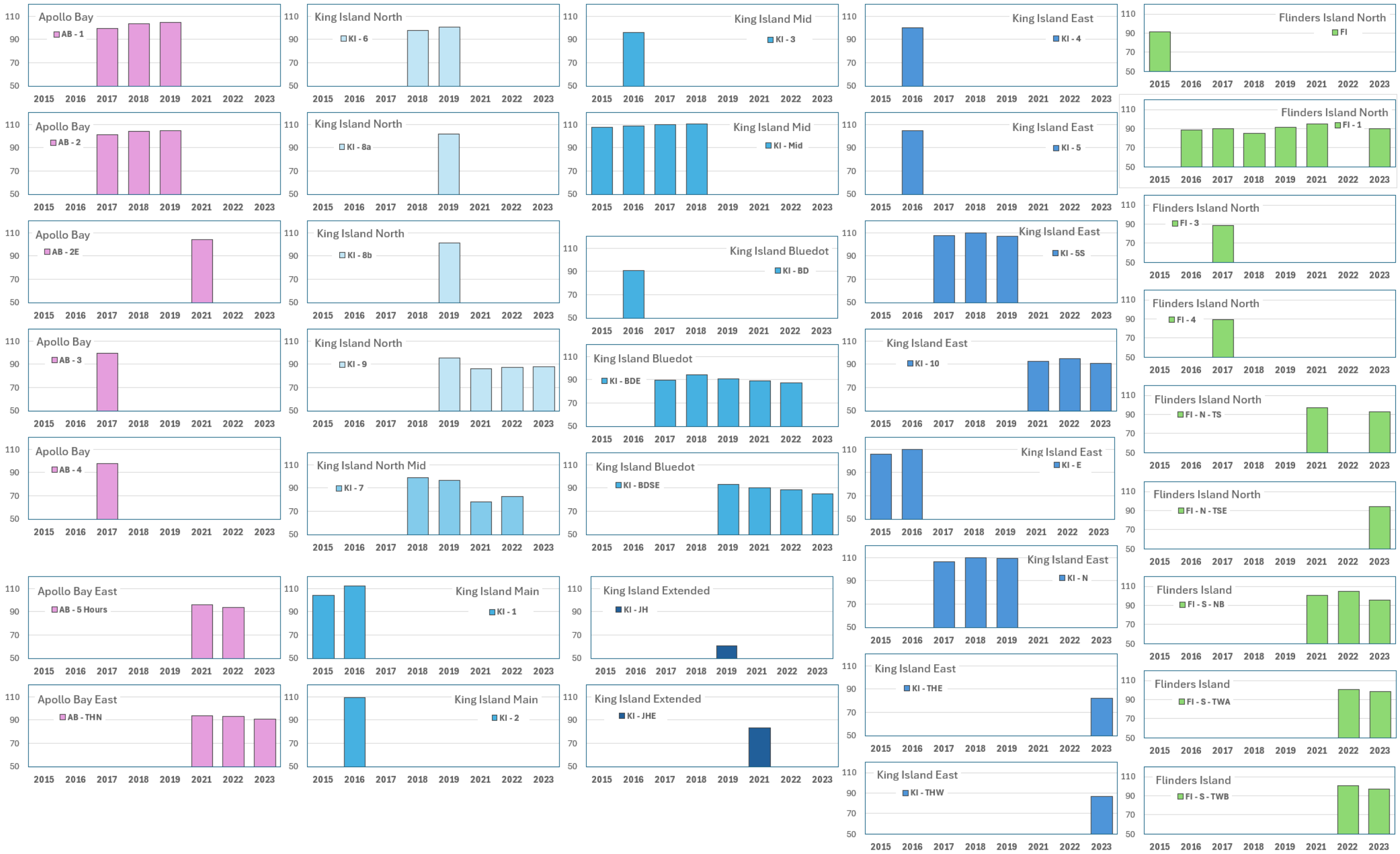

Figure 8-3. Trends in mean length of scallops in individual survey beds across years. The bed codes and region names are shown for each bed, which are arranged in relative geographic position from N – S and E – W. The y-axis is set to the maximum size of scallop caught of 119 mm shell length. KI – JH 2019 estimates from the covered and uncovered parts of the dredge combined.

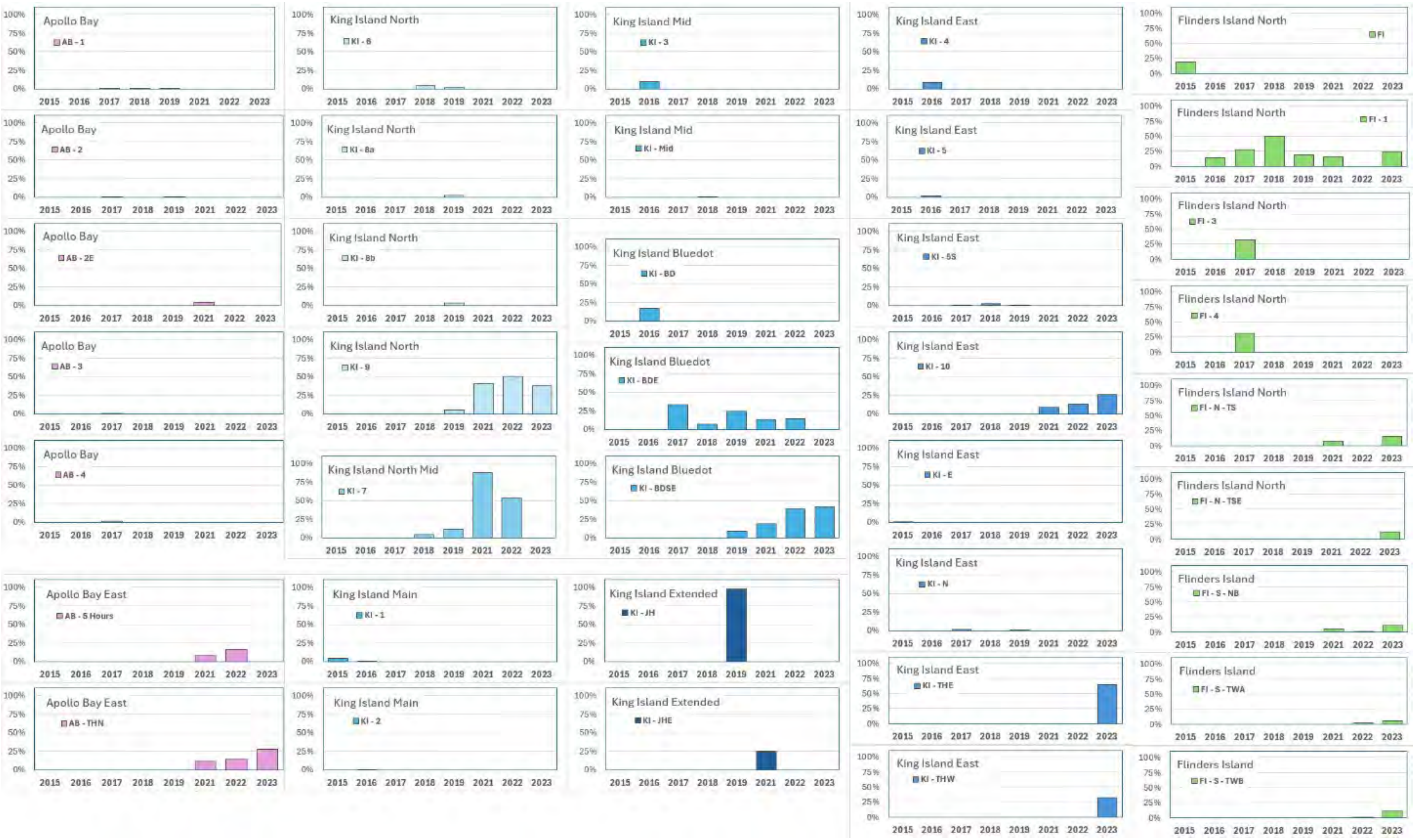

Figure 8-4. Trends in the percentage of undersize scallops (< 85mm shell length) in individual survey beds across years. The bed codes and region names are shown for each bed, which are arranged in relative geographic position from N – S and E – W. KI – JH 2019 estimates from the covered and uncovered parts of the dredge combined.

8.5. Length-frequency distributions by bed

Length-frequency distributions by survey bed, summed across tows in each bed, are shown below. This initial analysis by bed was used to inspect size frequency distribution to evaluate similarity between beds in a proposed summary region, to justify the inclusion of beds in a particular region.

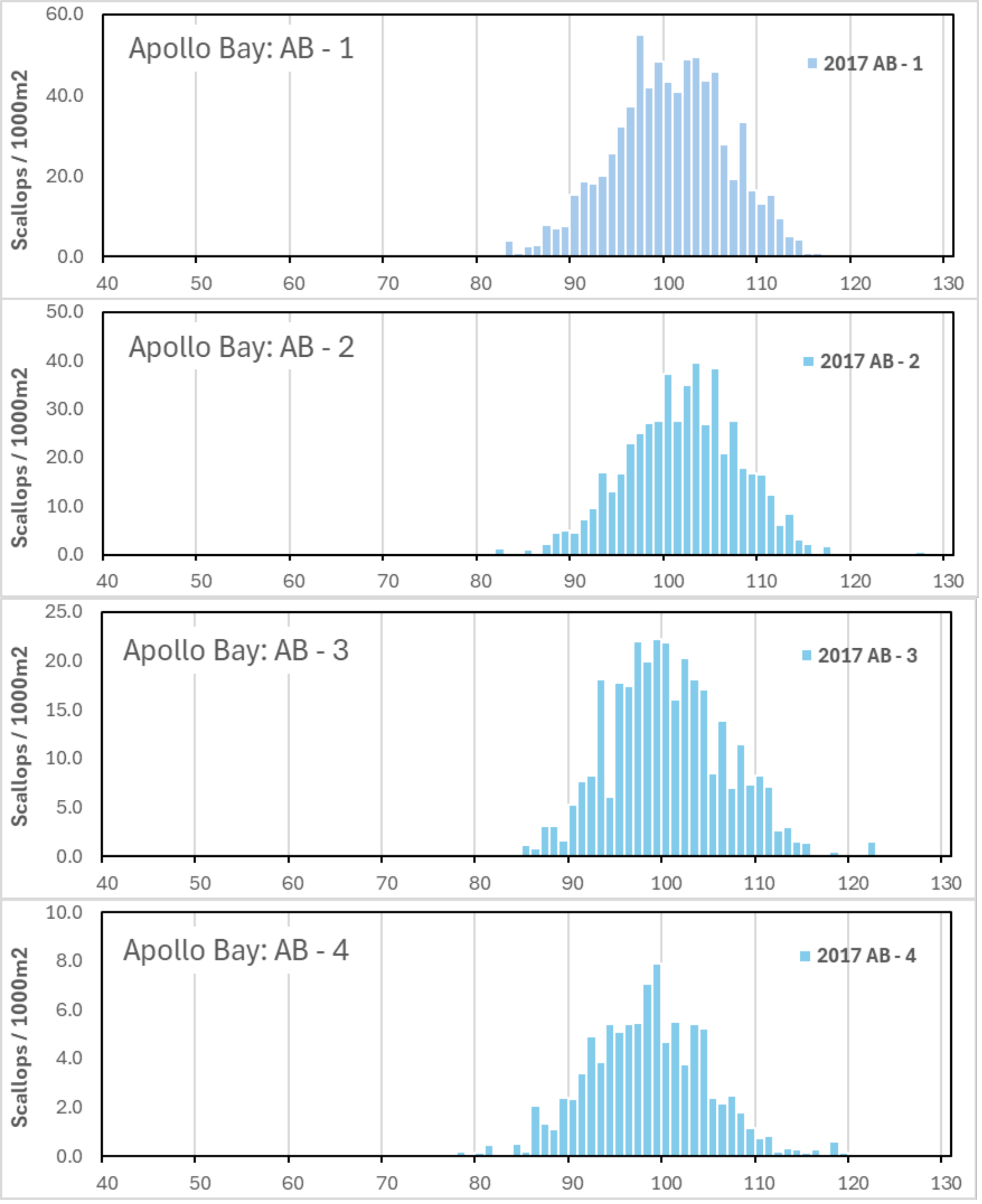

Figure 8-5. Comparative Length-frequency distributions (1 mm size classes) of scallops by individual bed in the Apollo Bay region in 2017.

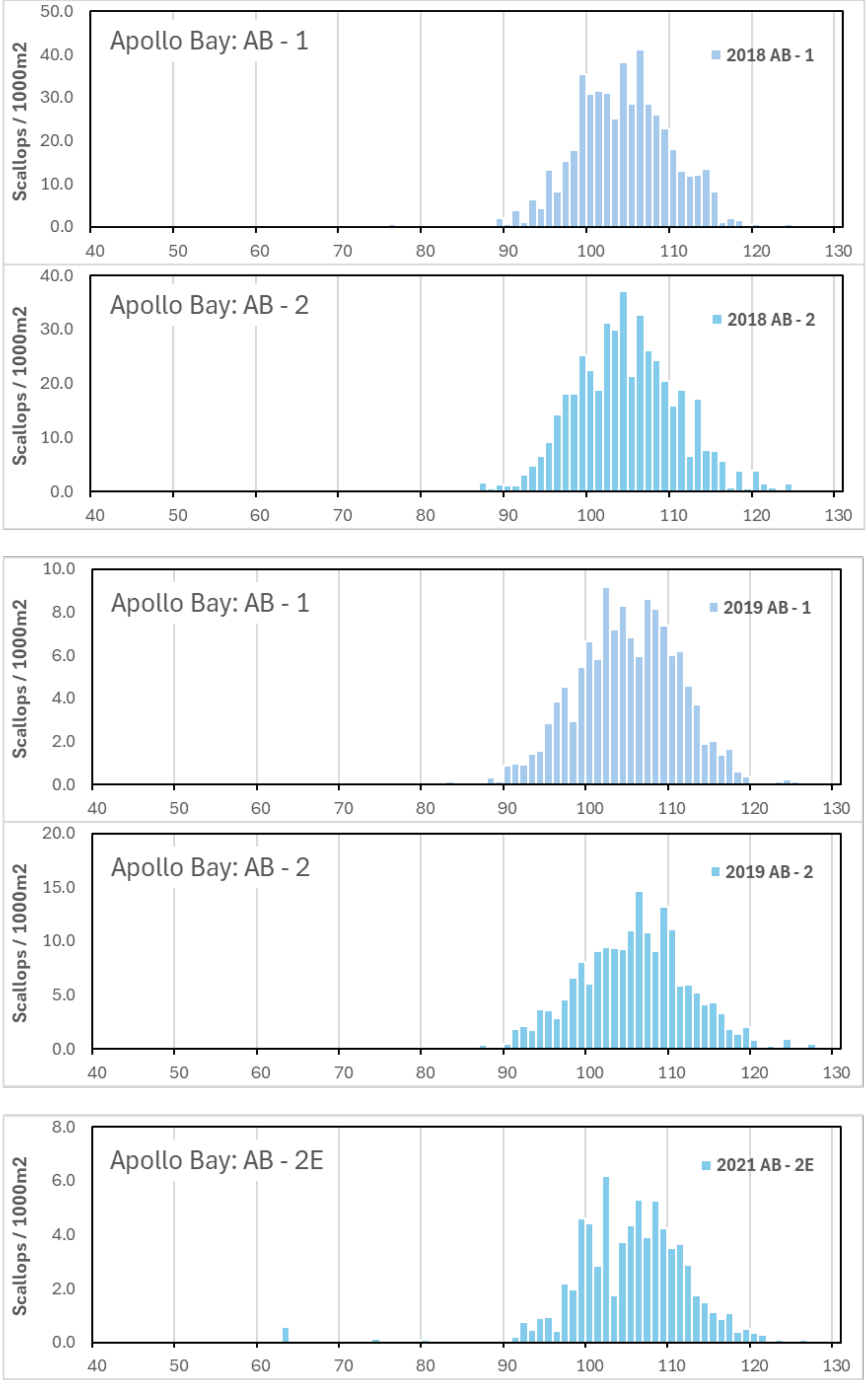

Figure 8-6. Comparative length-frequency distributions (1 mm size classes) of scallops by individual bed in the Apollo Bay region from 2018 - 2021.

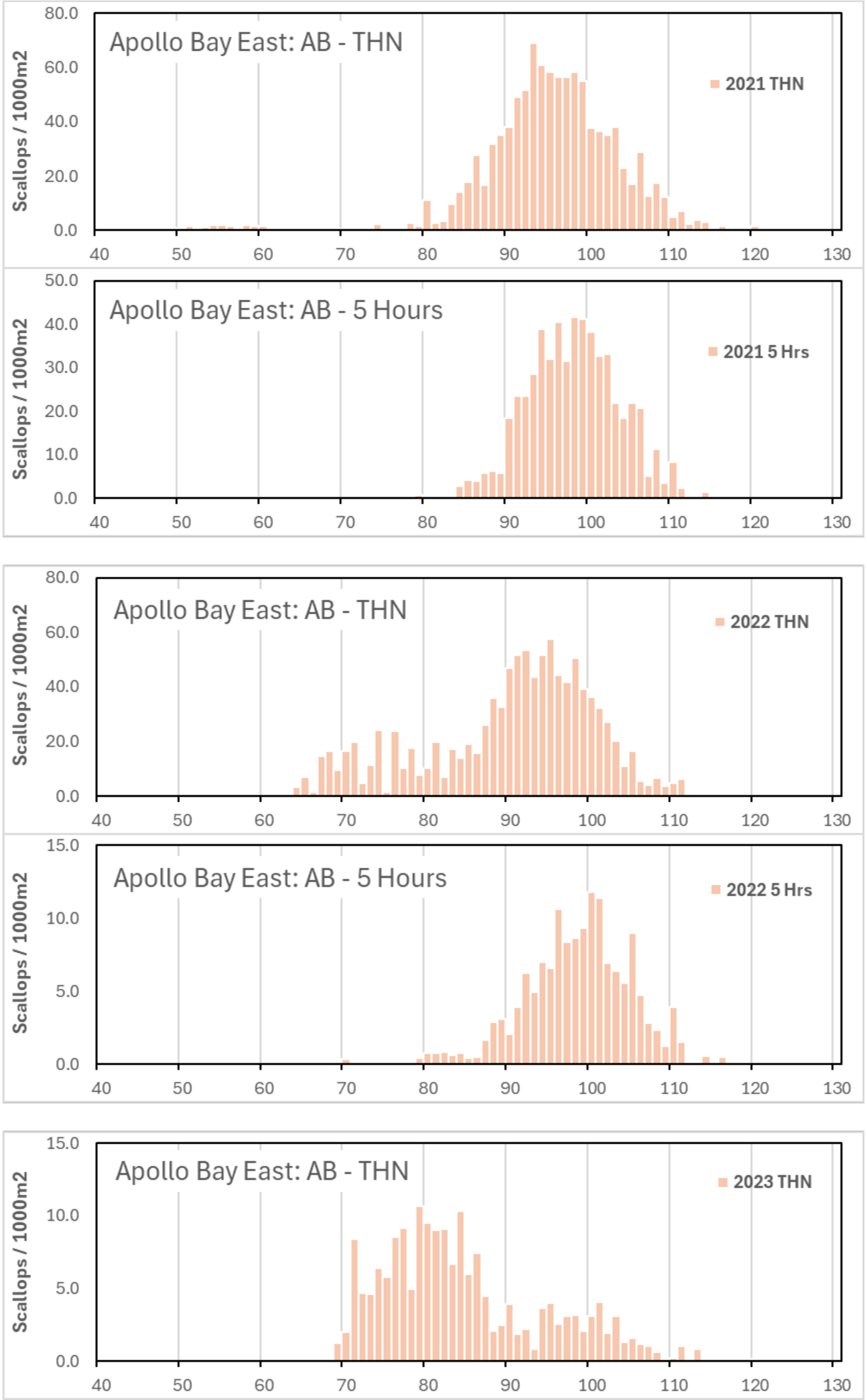

Figure 8-7. Comparative length-frequency distributions (1 mm size classes) of scallops by individual bed in the Apollo Bay East region from 2021 - 2023.

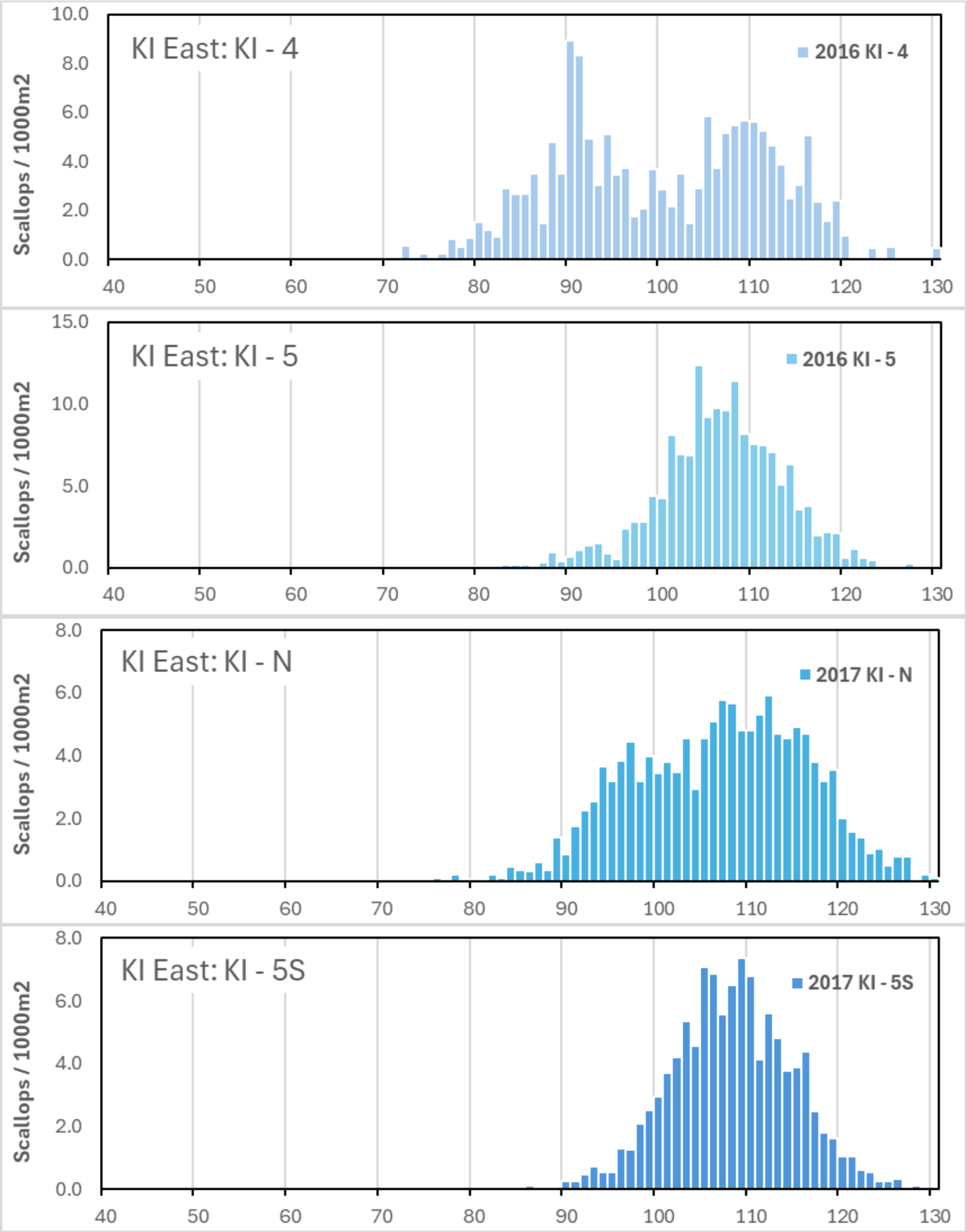

Figure 8-8. Comparative length-frequency distributions (1 mm size classes) of scallops by individual bed in the King Island East region from in 2016 and 2017.

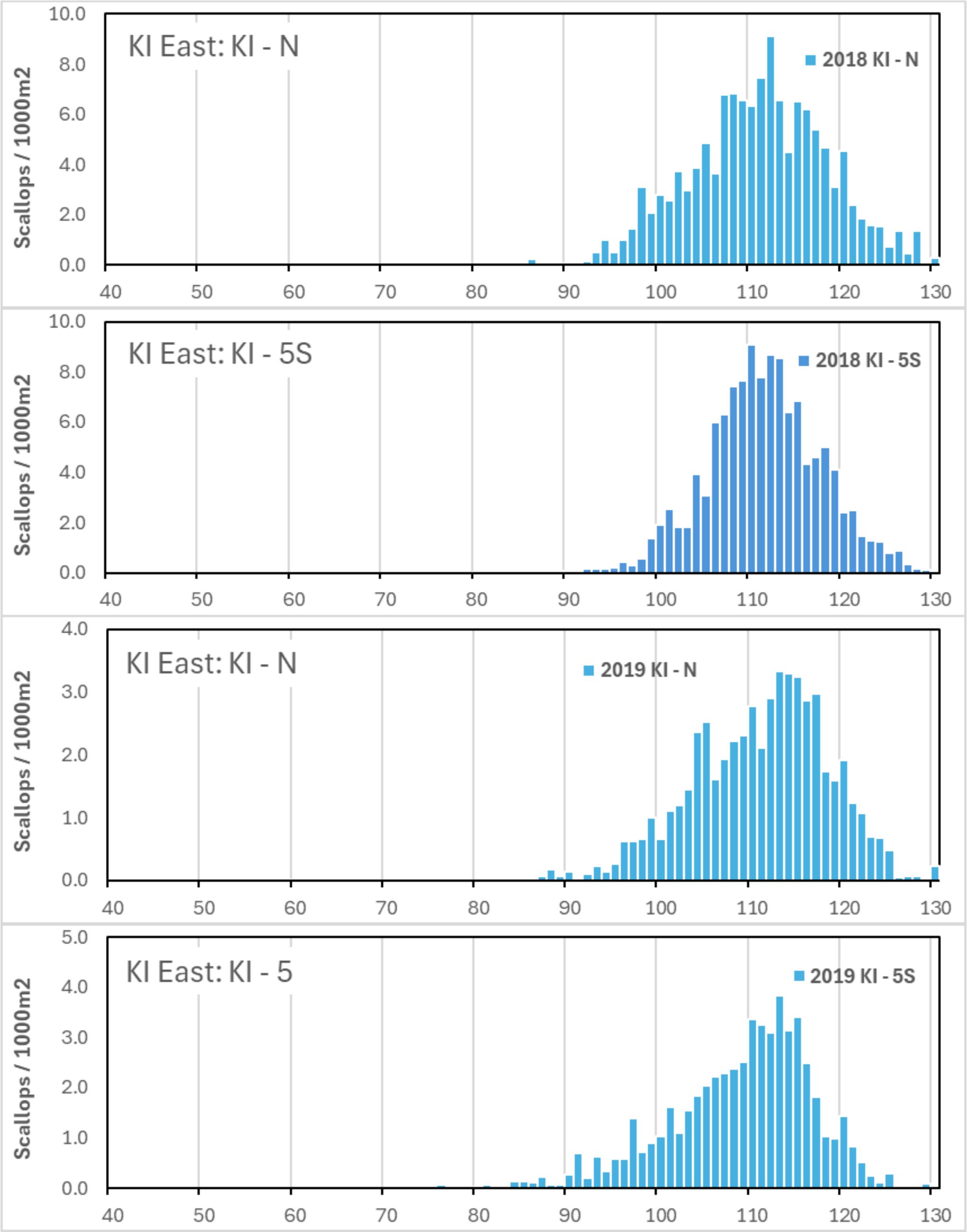

Figure 8-9. Comparative length-frequency distributions (1 mm size classes) of scallops by individual bed in the King Island East region in 2018 and 2019.

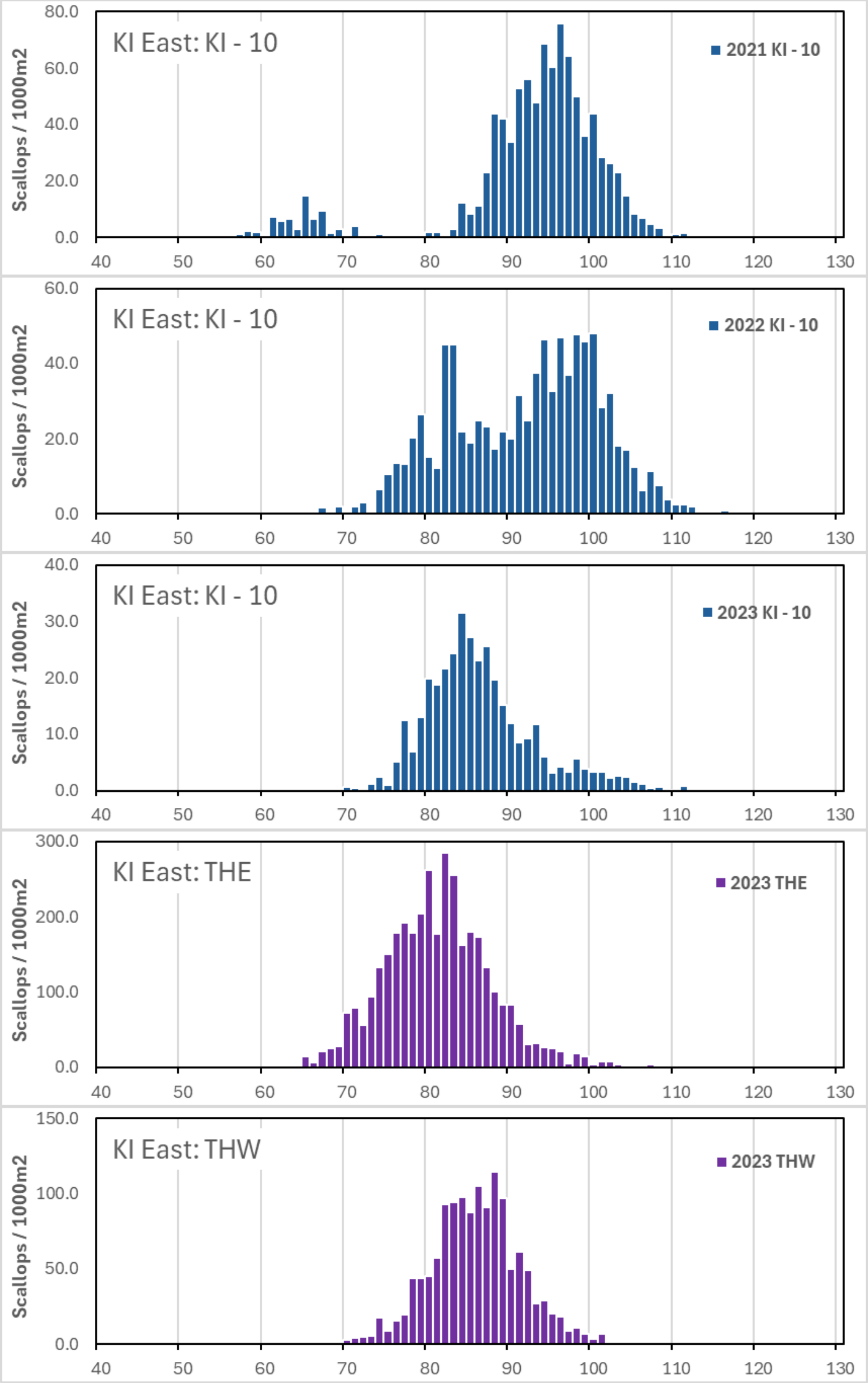

Figure 8-10. Comparative length-frequency distributions (1 mm size classes) of scallops by individual bed in the King Island East The Hill region from 2021 to 2023.

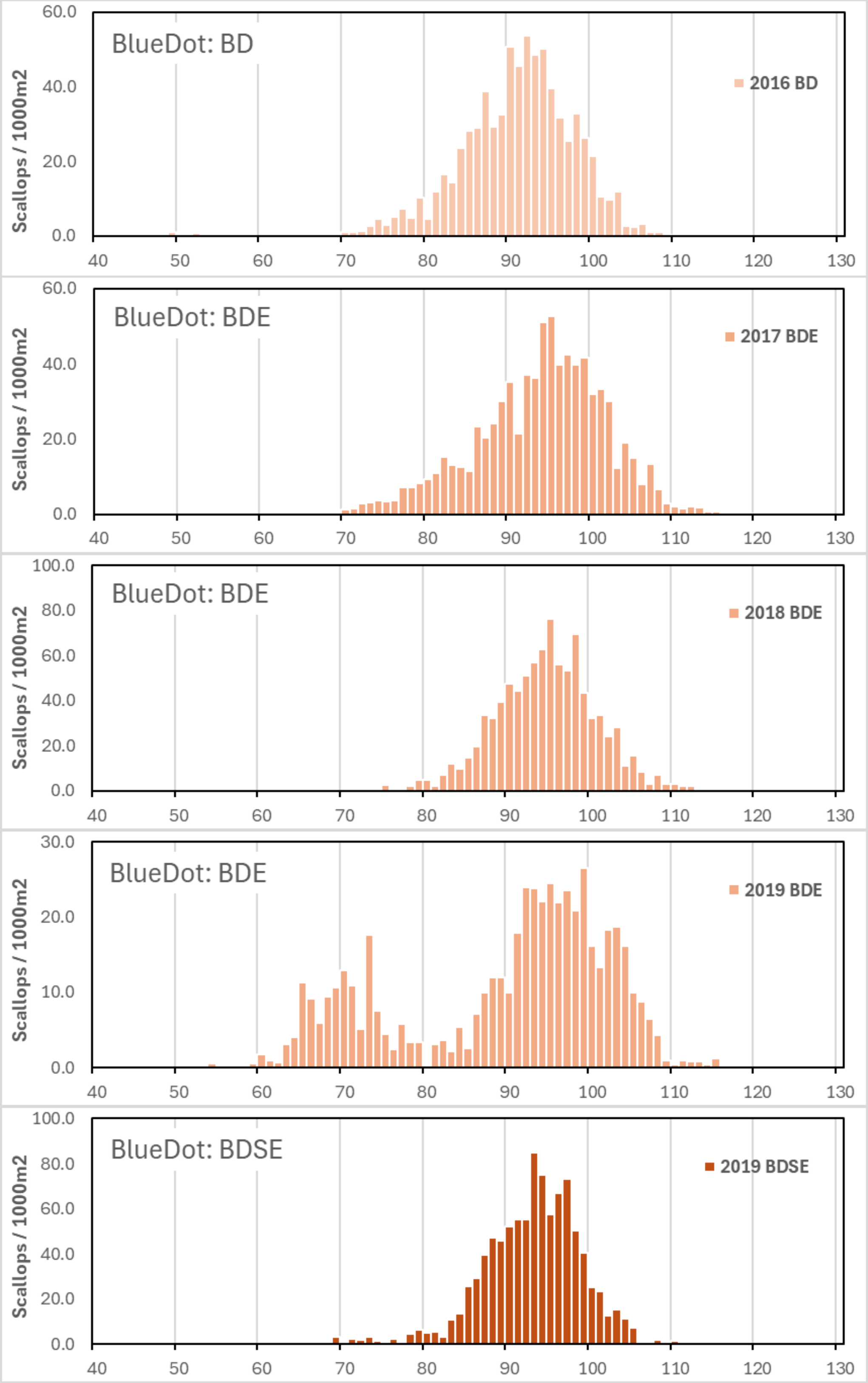

Figure 8-11. Comparative length-frequency distributions (1 mm size classes) of scallops by individual bed in the King Island BlueDot region from 2016 to 2019.

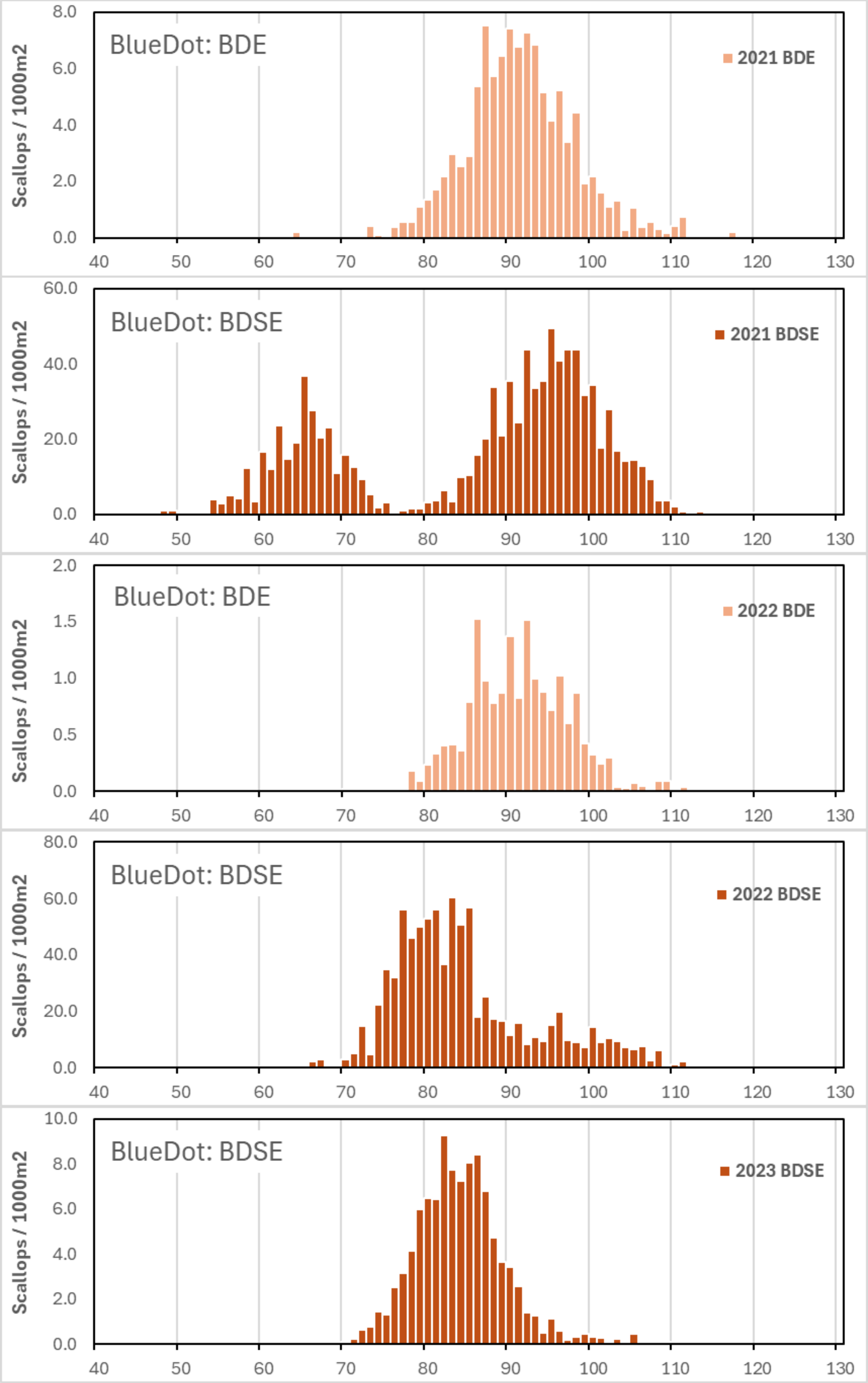

Figure 8-12. Comparative length-frequency distributions (1 mm size classes) of scallops by individual bed in the King Island BlueDot region from 2021 to 2023.

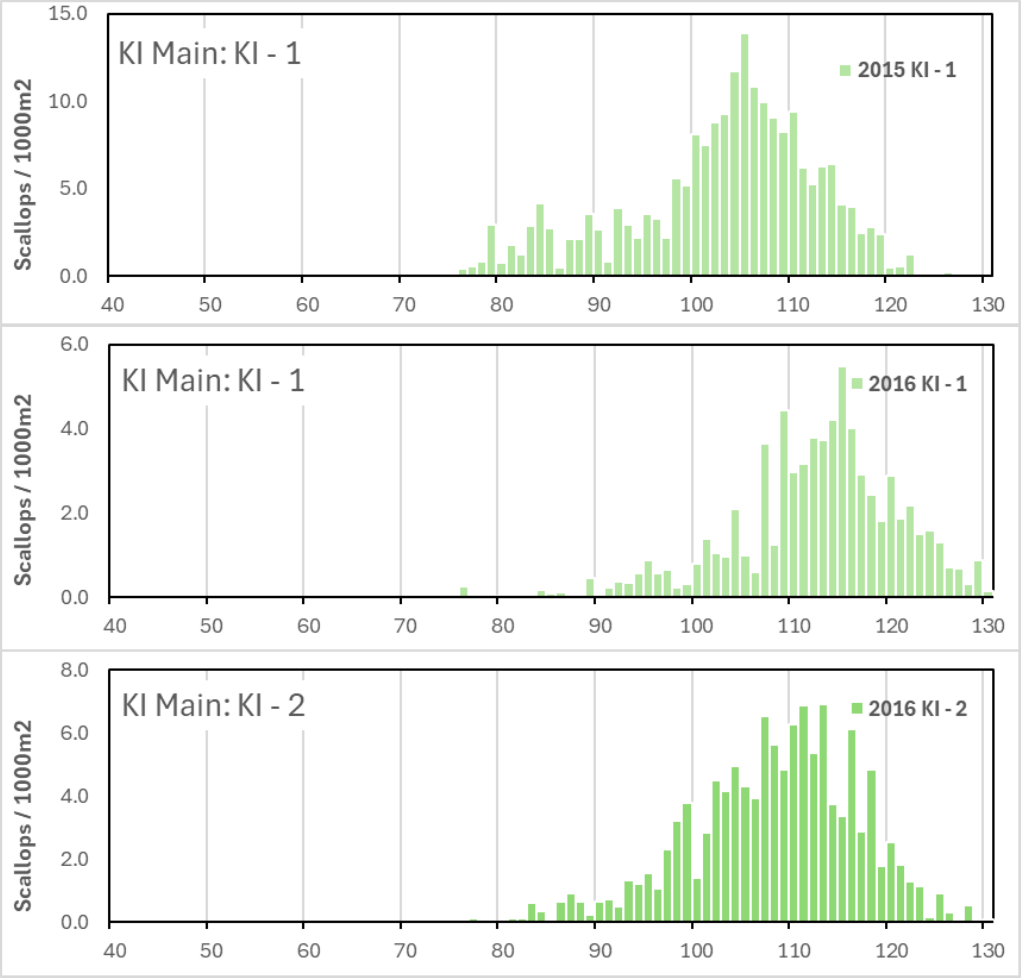

Figure 8-13. Comparative length-frequency distributions (1 mm size classes) of scallops by individual bed in the King Island Main region in 2015 and 2016.

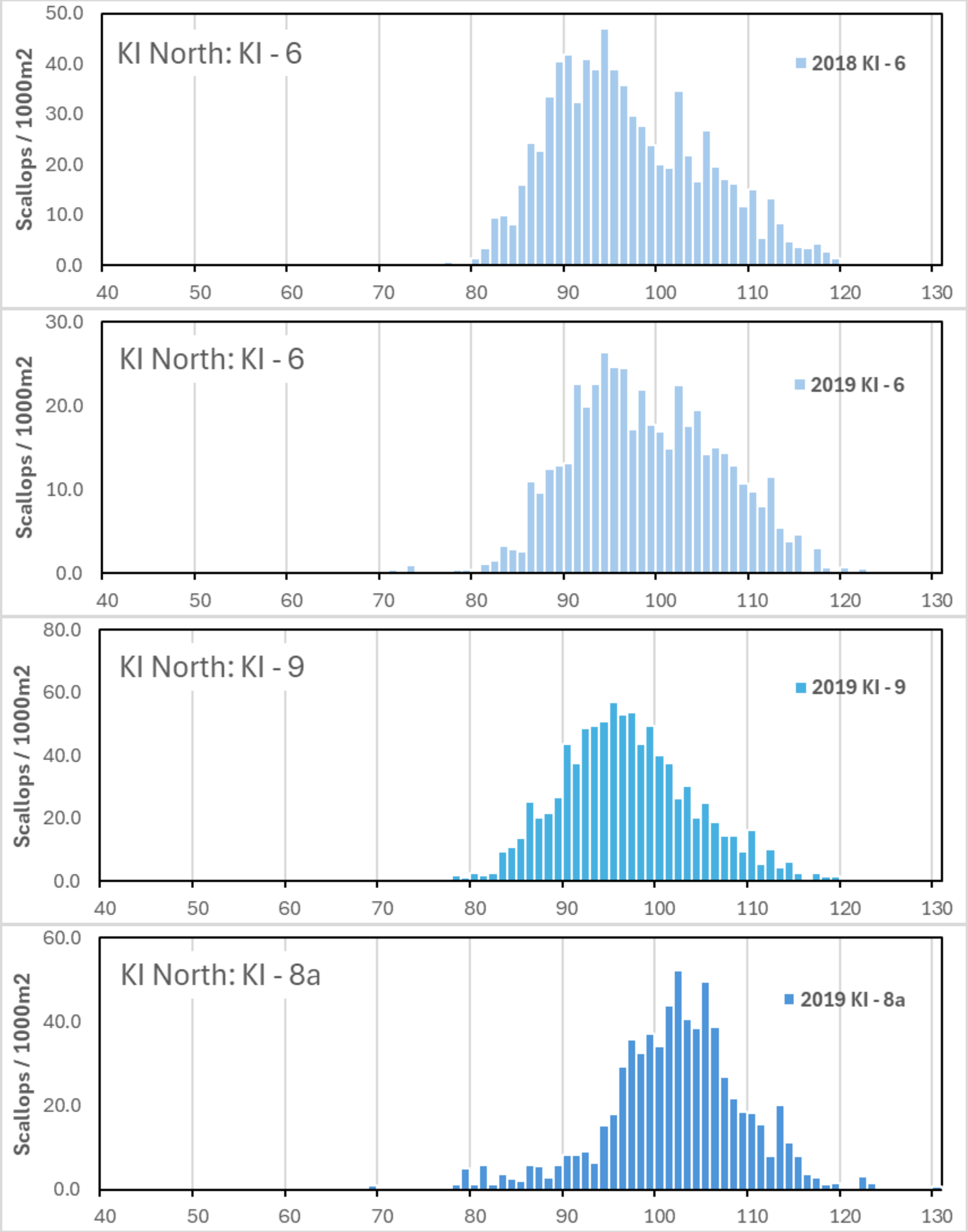

Figure 8-14. Comparative length-frequency distributions (1 mm size classes) of scallops by individual bed in the King Island North region in 2018 and 2019.

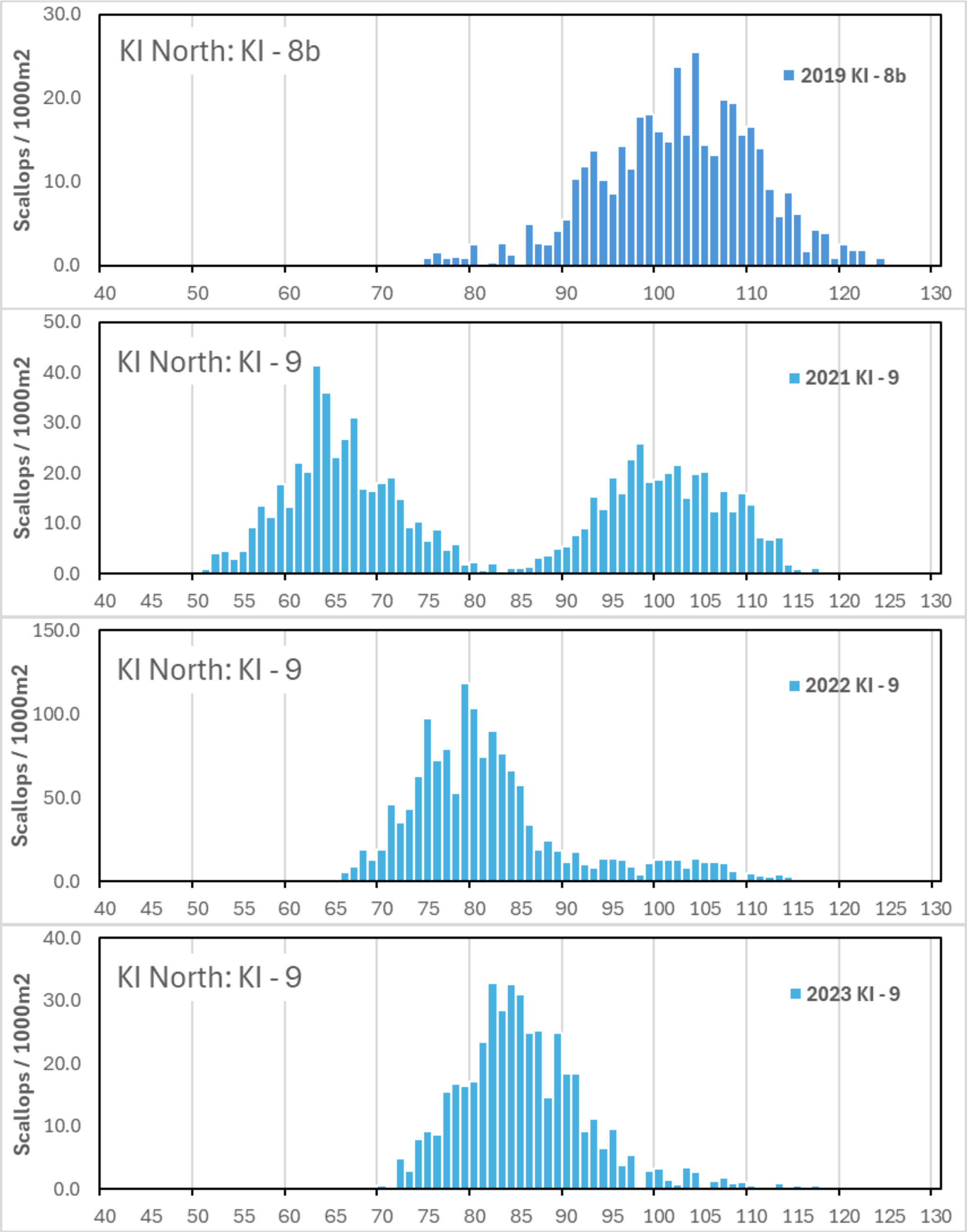

Figure 8-15. Comparative length-frequency distributions (1 mm size classes) of scallops by individual bed in the King Island North region from 2019 - 2023.

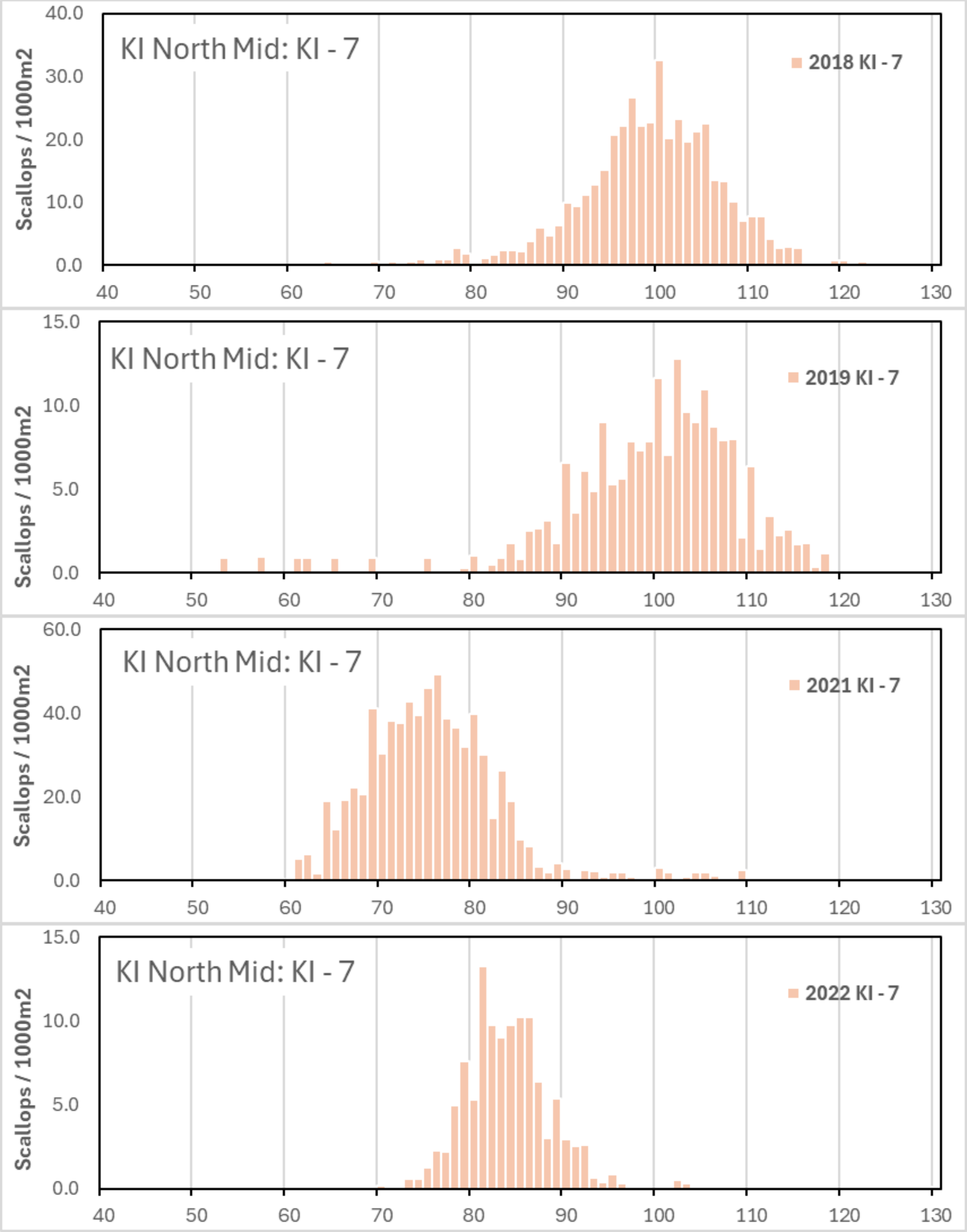

Figure 8-16. Comparative length-frequency distributions (1 mm size classes) of scallops by individual bed in the King Island North Mid region from 2018 - 2022.

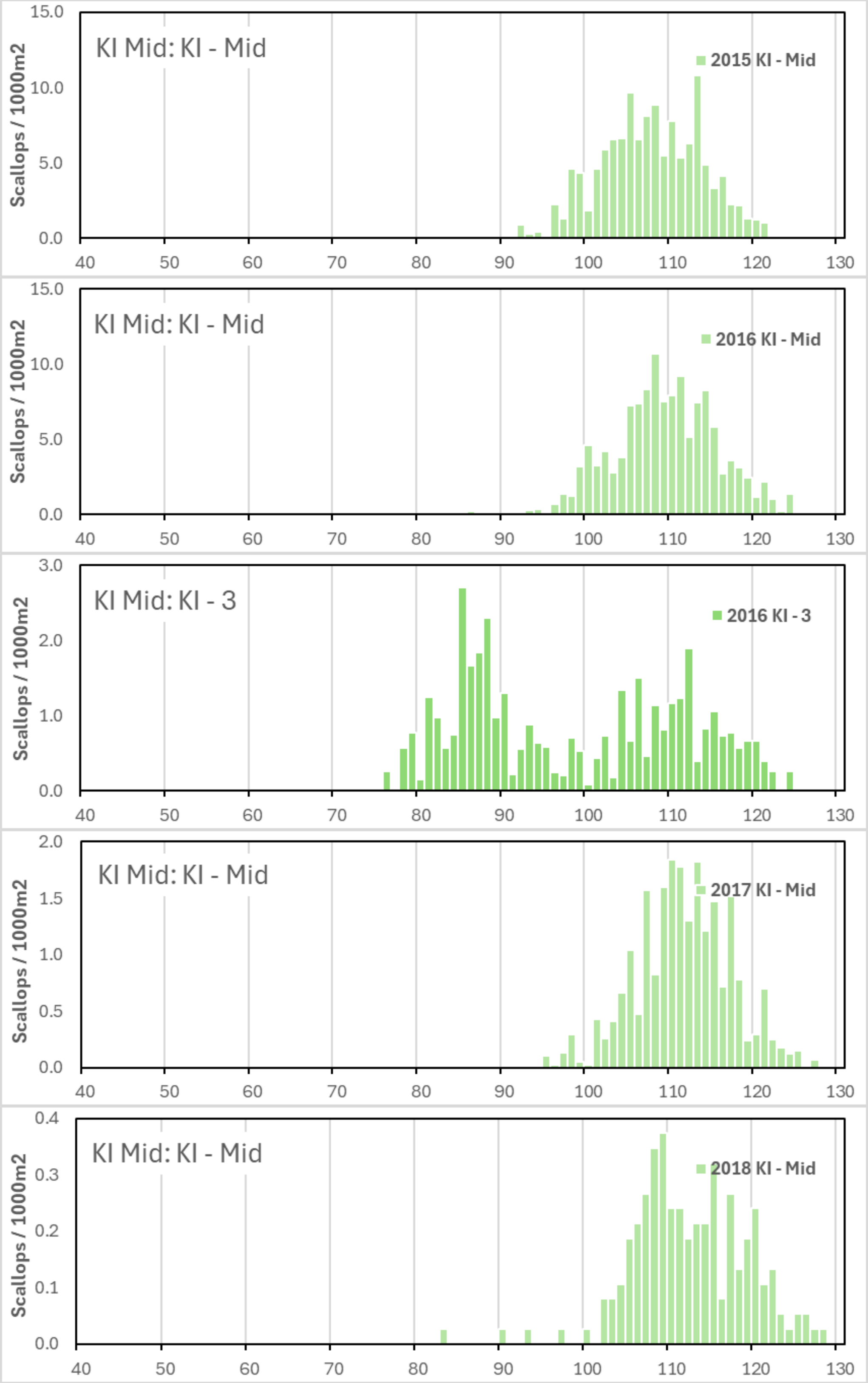

Figure 8-17. Comparative length-frequency distributions (1 mm size classes) of scallops by individual bed in the King Island Mid region from 2015 - 2018.

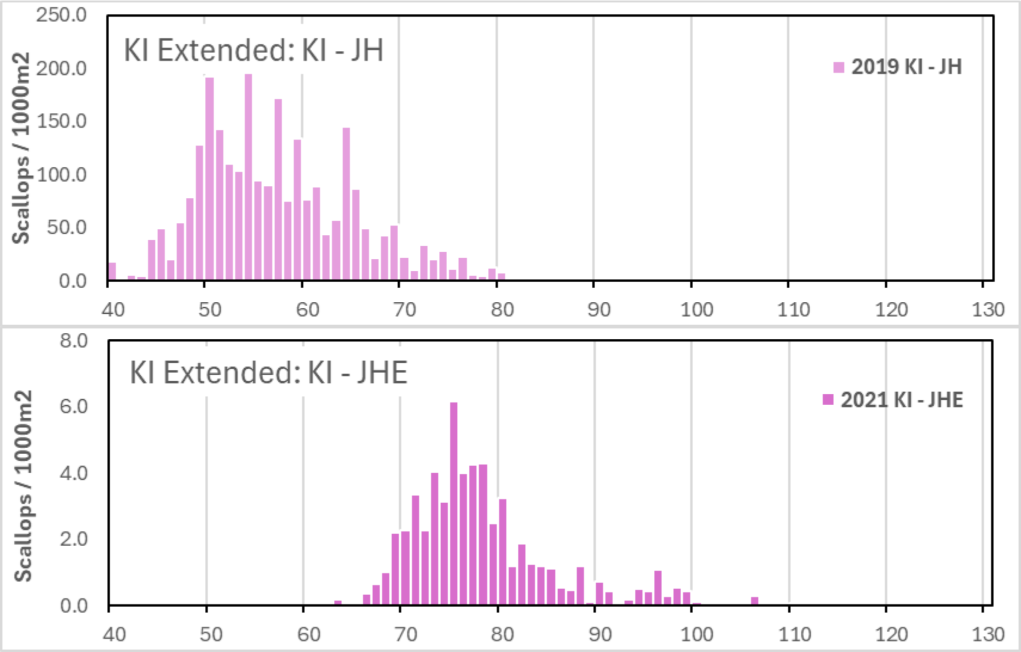

Figure 8-18. Comparative length-frequency distributions (1 mm size classes) of scallops by individual bed in the King Island JH Extended region in 2019 and 2021.

The JH-Extended bed was added to the 2019 and 2021 surveys in response to observations of high concentrations of juvenile scallops in the area, possibly justifying closure to protect these apparent new recruits until they reach legal size. In 2019, half of the dredge was covered with a finer mesh netting, resulting in high catches of smaller scallops than the dredge could usually catch. The 2019 length-frequency distributions are therefore not comparable to other areas, using a dredge with substantially smaller selectivity.

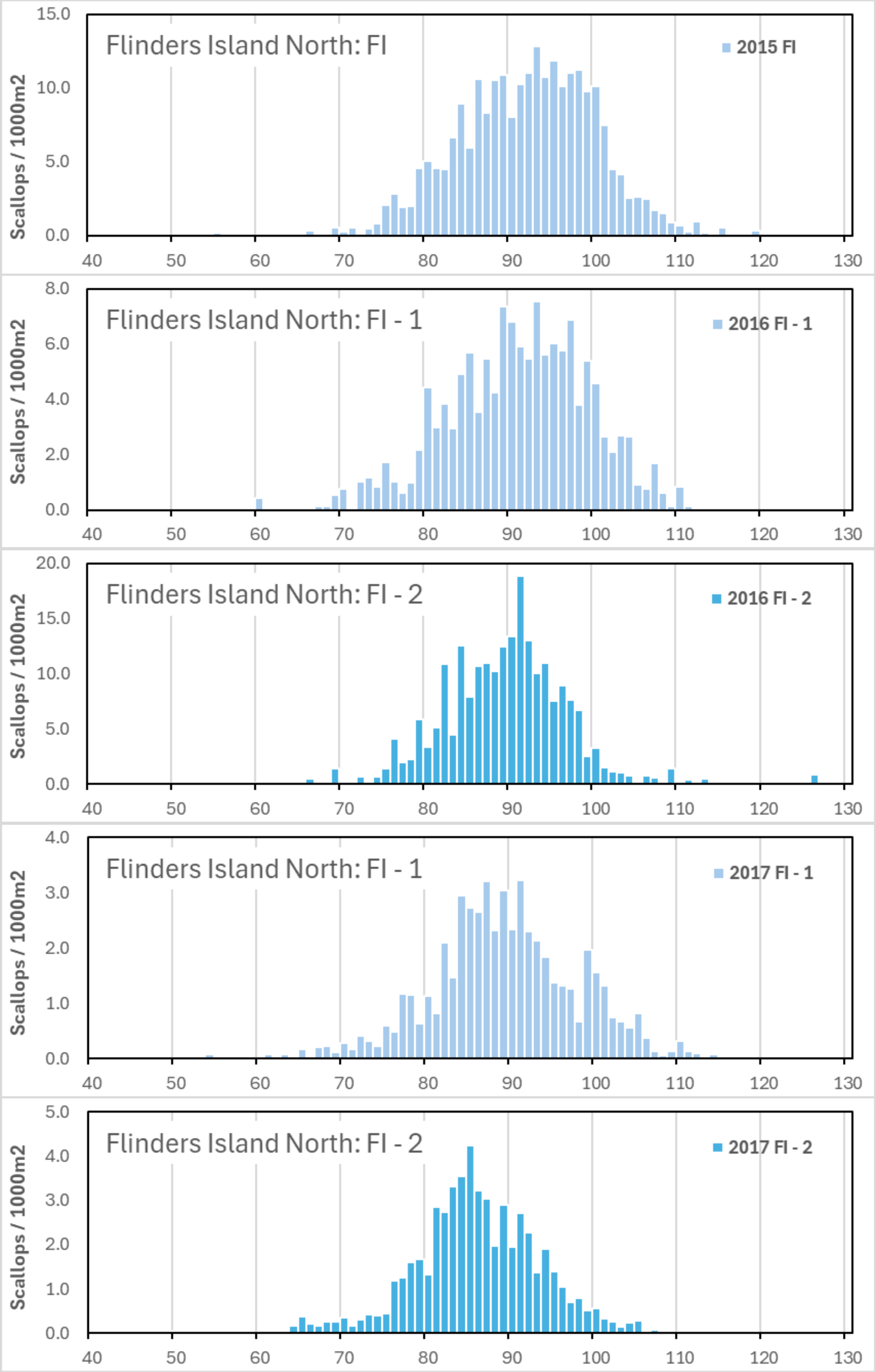

Figure 8-19. Comparative length-frequency distributions (1 mm size classes) of scallops by individual bed in the Flinders Island North region from 2015 - 2017.

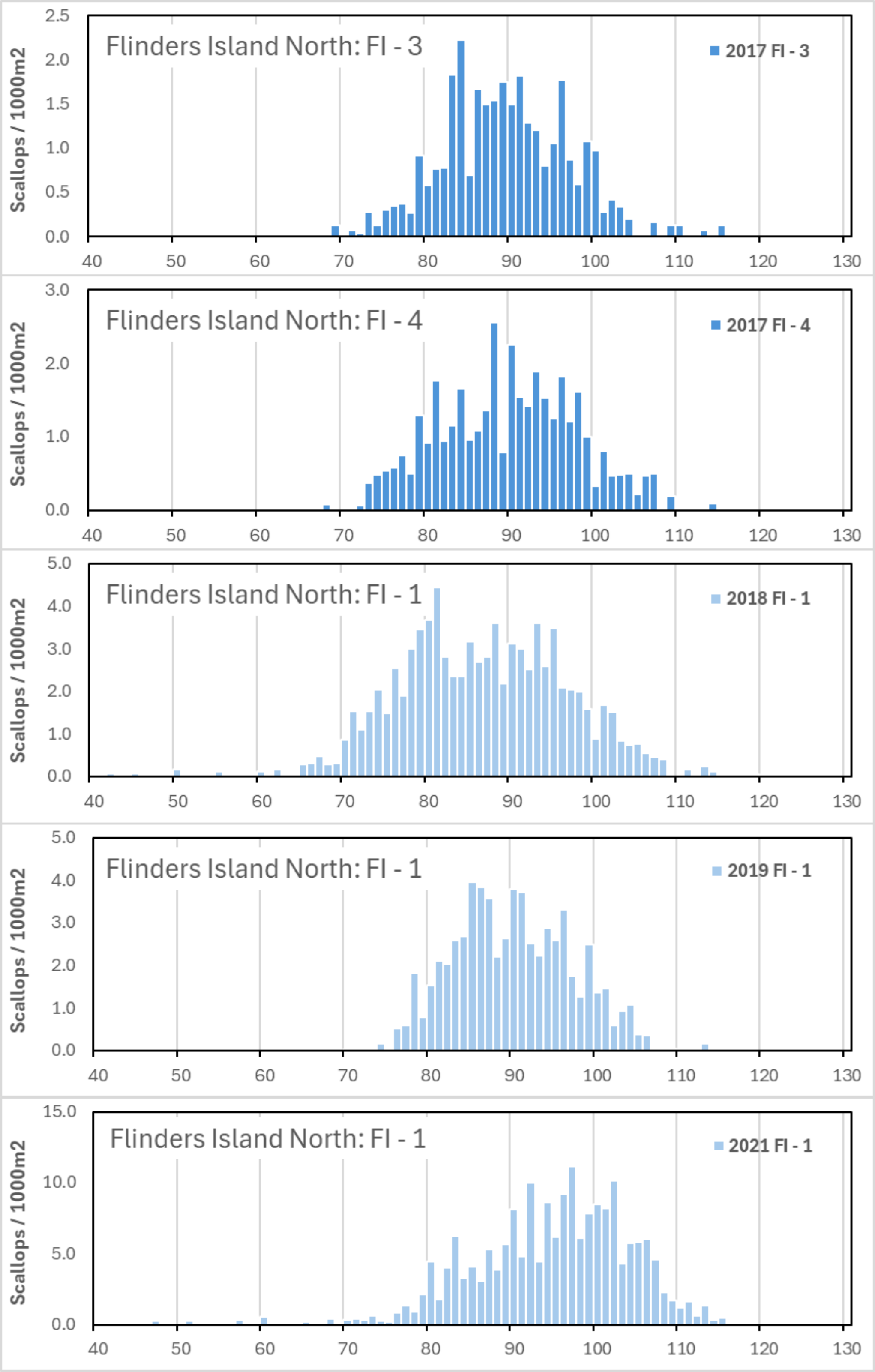

Figure 8-20. Comparative length-frequency distributions (1 mm size classes) of scallops by individual bed in the Flinders Island North region from 2017 - 2021.

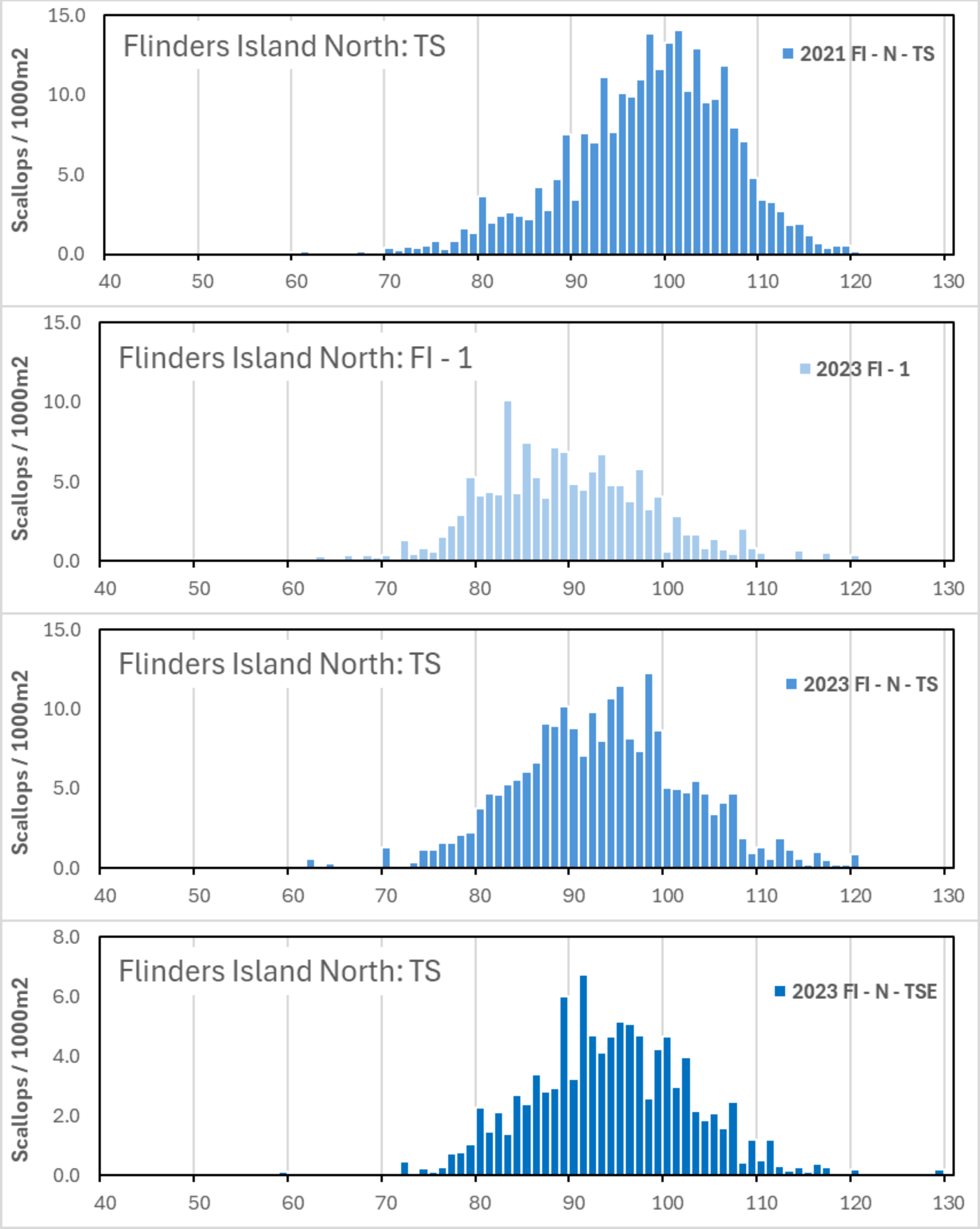

Figure 8-21. Comparative length-frequency distributions (1 mm size classes) of scallops by individual bed in the Flinders Island North region from 2021 - 2023.

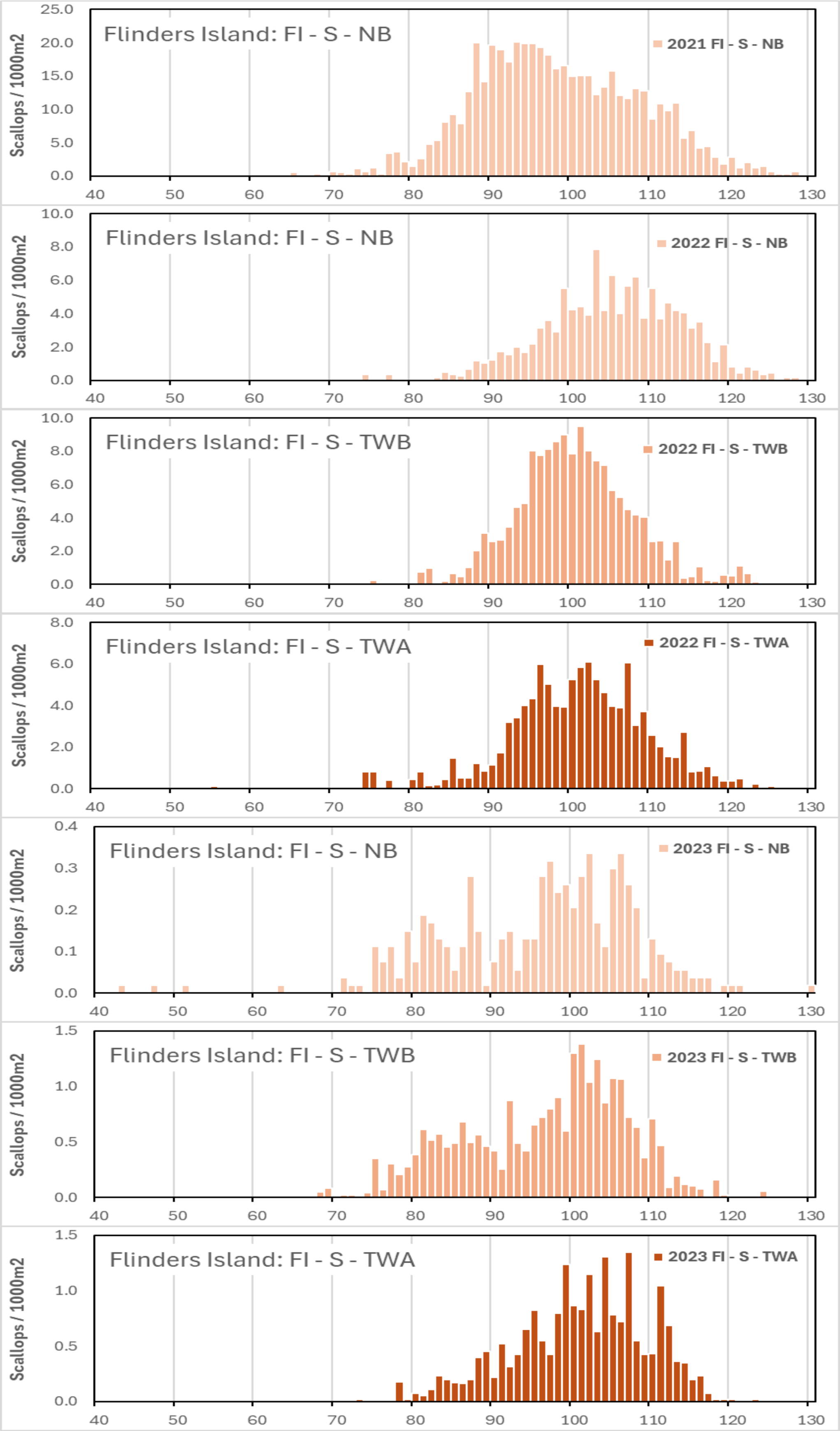

Figure 8-22. Comparative length-frequency distributions (1 mm size classes) of scallops by individual bed in the Flinders Island (south) region from 2021 - 2023.

8.6. Paired comparison of length-frequency distributions in scallop beds in each Region by year

The Tables below show paired comparisons of length-frequency distribution and cumulative density functions for beds in proposed regions for which data are available for both beds in a year. The overlaid length-frequency plots are chosen from those in Appendix 8.5. To these have been added overlaid paired eCDF plots, with calculated maximum Kolmogorov-Smirnov D separation differences. Table 8-2 provides a summary of the $Dmax$ and $Dsum$ scores obtained for each paired bed comparison.

Table 8-2. Summary of $Dmax$ and $Dsum$ scores for all bed comparisons conducted on the pairs of beds by Region shown in the tables below.

Region		*Dmax*	*Dsum*
Apollo Bay			
AB_1_2018	AB_2_2018	0.034	0.561
AB_1_2017	AB_3_2017	0.040	0.480
AB_1_2019	AB_2_2019	0.060	0.698
AB_1_2017	AB_2_2017	0.099	1.341
AB_2_2017	AB_3_2017	0.128	1.480
AB_3_2017	AB_4_2017	0.128	2.115
AB_1_2017	AB_4_2017	0.157	2.244
AB_THN_2021	AB_5H_2021	0.172	3.016
AB_2_2017	AB_4_2017	0.256	3.558
AB_THN_2022	AB_5H_2022	0.367	8.122
AB_2E_2021	AB_5H_2021	0.459	7.504
AB_2E_2021	AB_THN_2021	0.553	10.005
King Island North, NorthMid			
KI_8a_2019	KI_8b_2019	0.097	1.187
KI_6_2019	KI_7_2019	0.125	2.178
KI_8b_2019	KI_7_2019	0.129	3.131
KI_6_2019	KI_9_2019	0.137	1.990
KI_8a_2019	KI_7_2019	0.141	2.763
KI_6_2018	KI_7_2018	0.237	2.953
KI_9_2019	KI_7_2019	0.241	3.919
KI_9_2022	KI_7_2022	0.306	4.464
KI_6_2019	KI_8b_2019	0.321	5.703
KI_9_2019	KI_8b_2019	0.326	5.605
KI_9_2019	KI_8a_2019	0.337	5.208
KI_6_2019	KI_8a_2019	0.364	5.305
KI_9_2021	KI_7_2021	0.415	11.854
KI_7_2018	KI_Mid_2018	0.697	13.140
KI_6_2018	KI_Mid_2018	0.721	15.641
King Island Main, Mid			
KI_2_2016	KI_Mid_2016	0.114	1.932
KI_1_2016	KI_2_2016	0.231	4.320
KI_1_2016	KI_Mid_2016	0.251	3.918
KI_2_2016	KI_3_2016	0.406	9.606
KI_1_2016	KI_3_2016	0.471	13.887
KI_Mid_2016	KI_3_2016	0.484	10.777
King Island East			
KI_N_2018	KI_5S_2018	0.084	1.109
KI_N_2019	KI_5S_2019	0.110	2.130
KI_N_2017	KI_5S_2017	0.161	2.567
KI_4_2016	KI_5_2016	0.367	6.390
King Island FarEast			

KI_10_2023	KI_THW_2023	0.060	0.992
KI_BDSE_2023	KI_10_2023	0.133	2.269
KI_BDSE_2023	KI_THW_2023	0.165	1.902
KI_BDE_2022	KI_10_2022	0.177	3.119
KI_BDSE_2023	KI_THE_2023	0.211	2.849
KI_BDE_2019	KI_BDSE_2019	0.223	5.431
KI_BDE_2021	KI_10_2021	0.227	3.631
KI_BDSE_2021	KI_10_2021	0.237	6.639
KI_BDE_2021	KI_BDSE_2021	0.291	7.043
KI_10_2023	KI_THE_2023	0.315	5.118
KI_THW_2023	KI_THE_2023	0.334	4.655
KI_BDSE_2022	KI_10_2022	0.401	7.443
KI_BDE_2022	KI_BDSE_2022	0.523	6.921
Flinders Island North			
FI_1_2017	FI_3_2017	0.045	0.841
FI_1_2017	FI_4_2017	0.061	0.923
FI_3_2017	FI_4_2017	0.062	1.003
FI_N_TS_2023	FI_N_TSE_2023	0.065	0.982
FI_1_2016	FI_2_2016	0.143	1.985
FI_1_2021	FI_N_TS_2021	0.164	3.380
FI_1_2017	FI_2_2017	0.181	3.300
FI_1_2023	FI_N_TS_2023	0.187	3.844
FI_2_2017	FI_3_2017	0.193	3.519
FI_2_2017	FI_4_2017	0.222	3.772
FI_1_2023	FI_N_TSE_2023	0.247	4.782
Flinders Island South			
FI_S_NB_2023	FI_S_TWB_2023	0.043	1.199
FI_S_TWB_2022	FI_S_TWA_2023	0.074	1.326
FI_S_TWB_2023	FI_S_TWA_2023	0.172	4.443
FI_S_NB_2023	FI_S_TWA_2023	0.202	5.255
FI_S_NB_2022	FI_S_TWA_2022	0.216	4.330
FI_S_NB_2022	FI_S_TWB_2022	0.280	4.727

Region: Apollo Bay

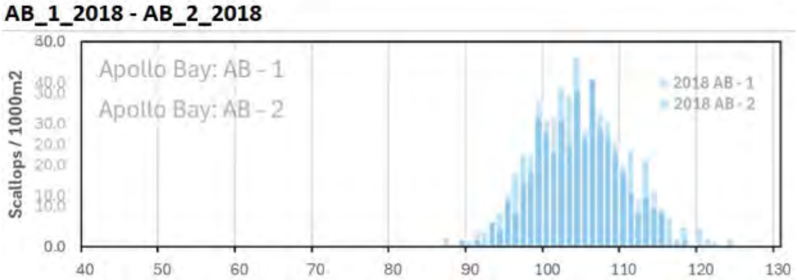

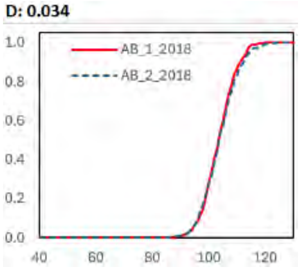

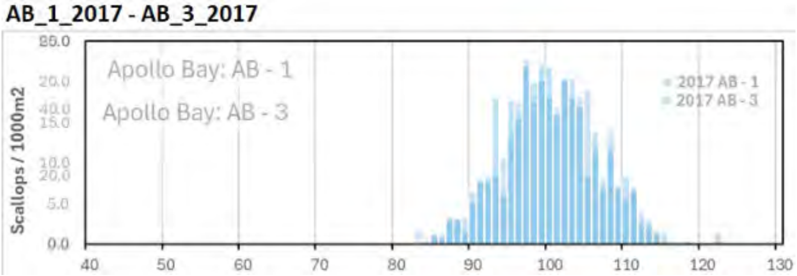

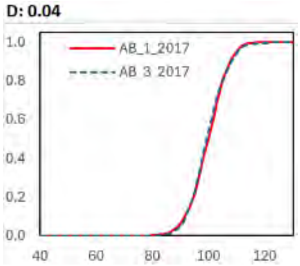

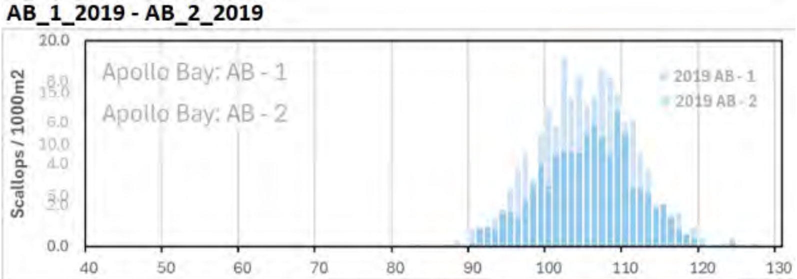

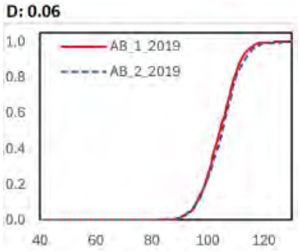

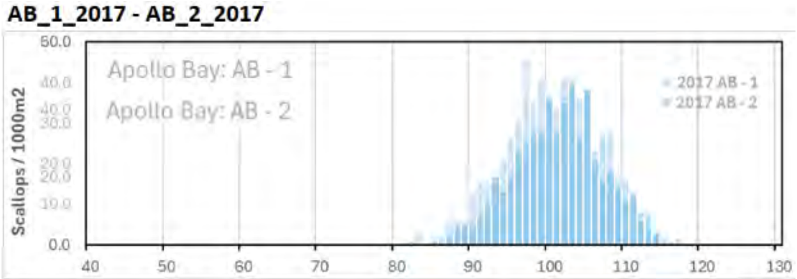

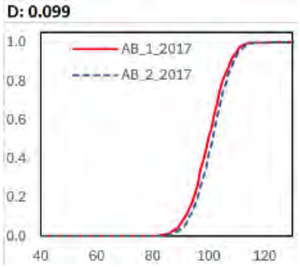

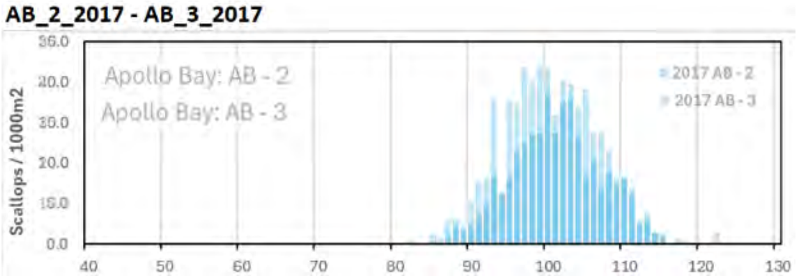

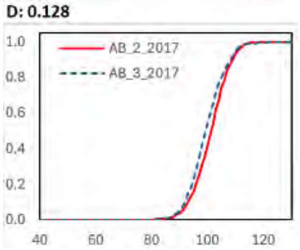

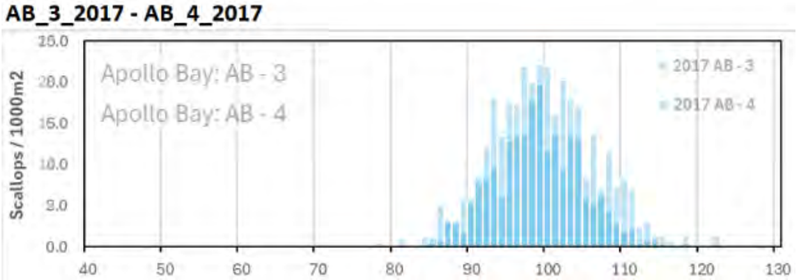

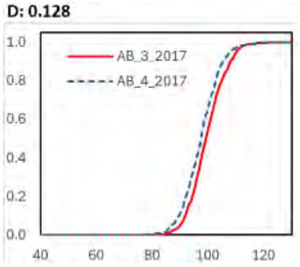

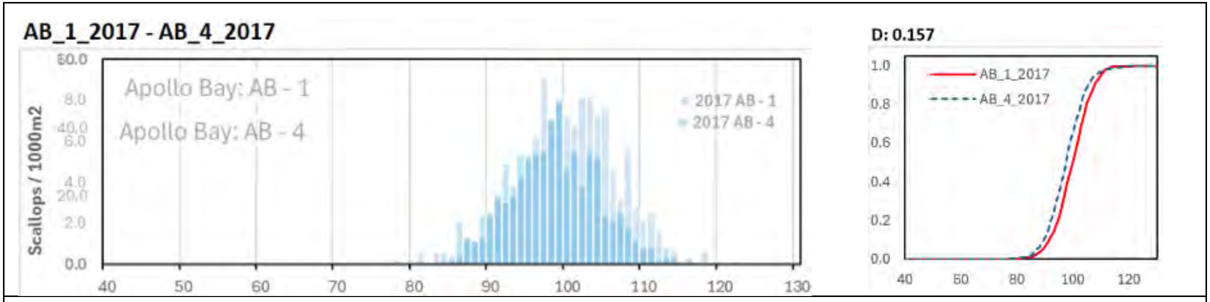
AB_1_2017 - AB_4_2017

D: 0.157

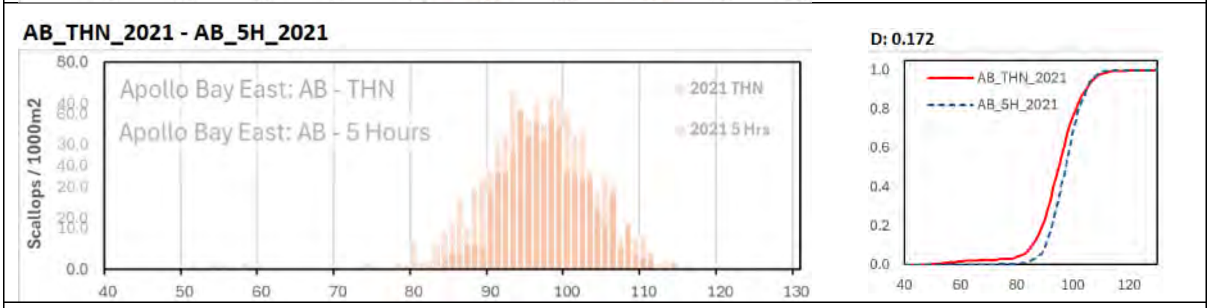
AB_THN_2021 - AB_5H_2021

D: 0.172

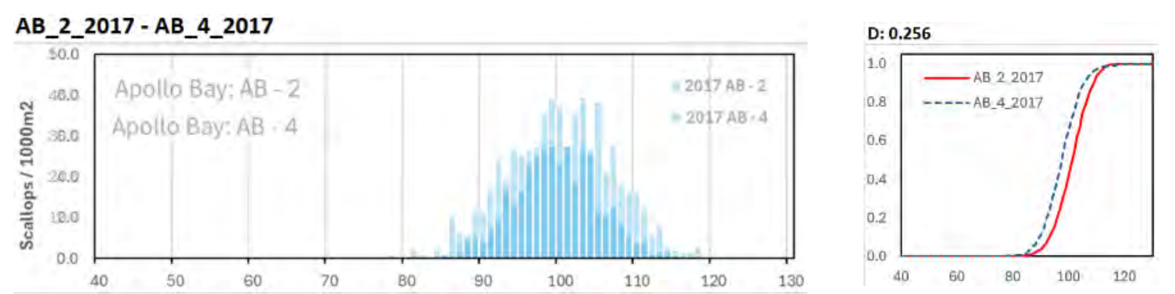
AB_2_2017 - AB_4_2017

D: 0.256

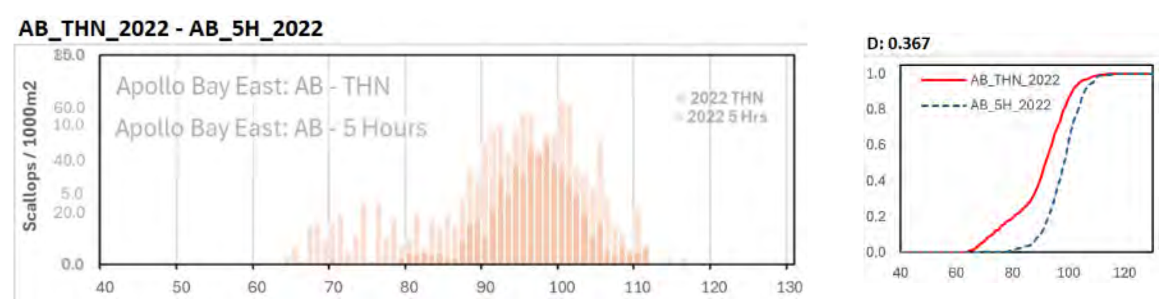
AB_THN_2022 - AB_5H_2022

D: 0.367

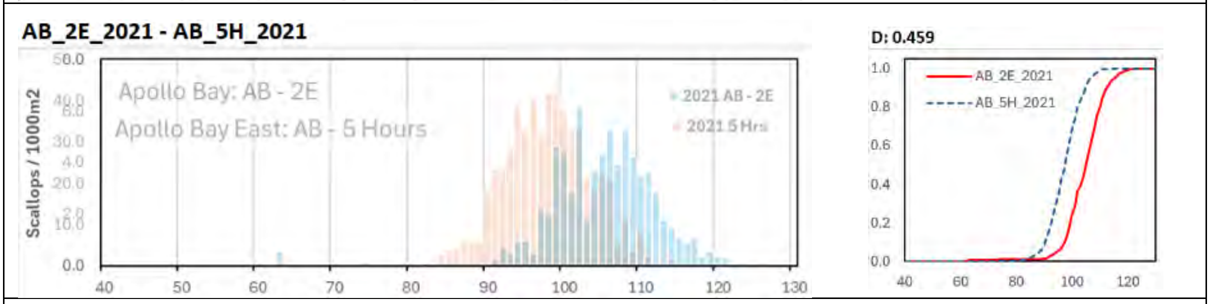
AB_2E_2021 - AB_5H_2021

D: 0.459

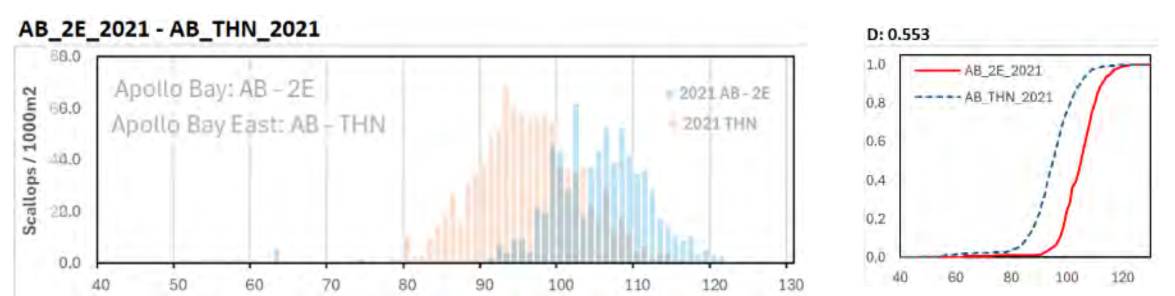
AB_2E_2021 - AB_THN_2021

D: 0.553

Region: King Island North, NorthMid, Mid

KI_8a_2019 - KI_8b_2019

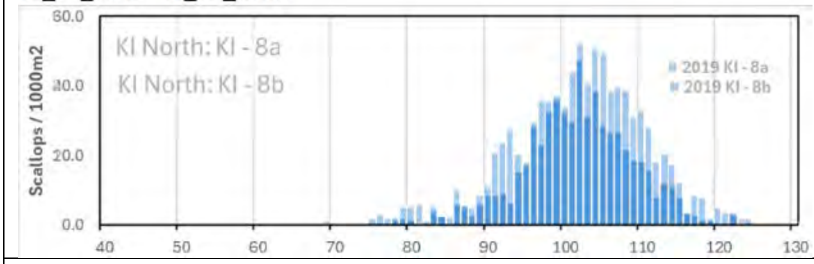

D: 0.097

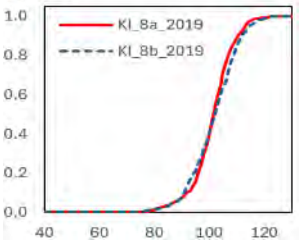

KI_6_2019 - KI_7_2019

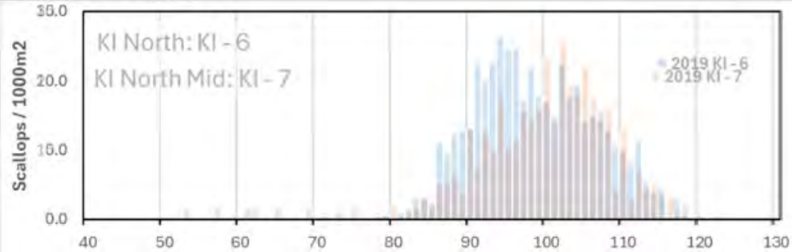

D: 0.125

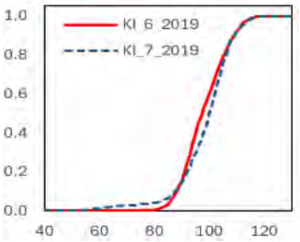

KI_8b_2019 - KI_7_2019

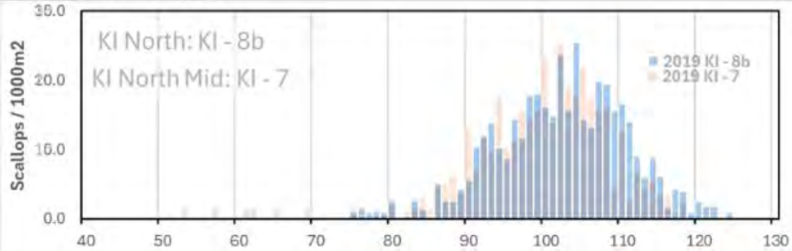

D: 0.129

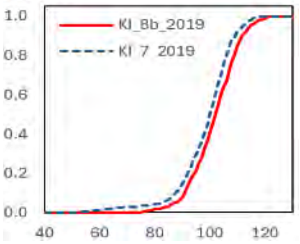

KI_6_2019 - KI_9_2019

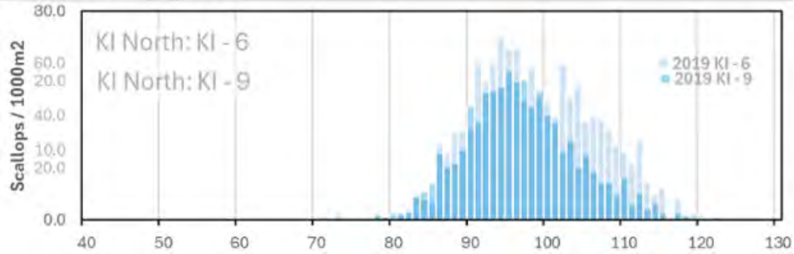

D: 0.137

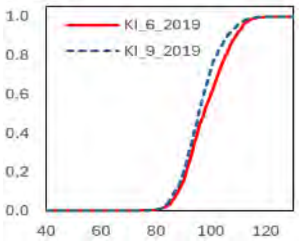

KI_8a_2019 - KI_7_2019

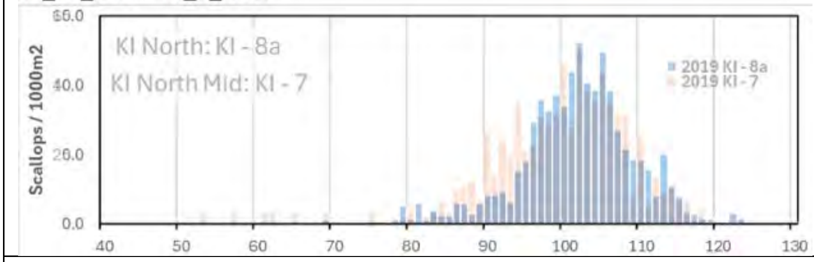

D: 0.141

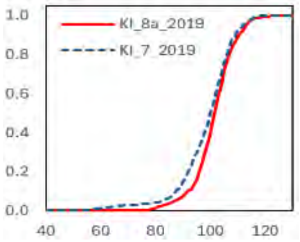

KI_6_2019 - KI_8b_2019

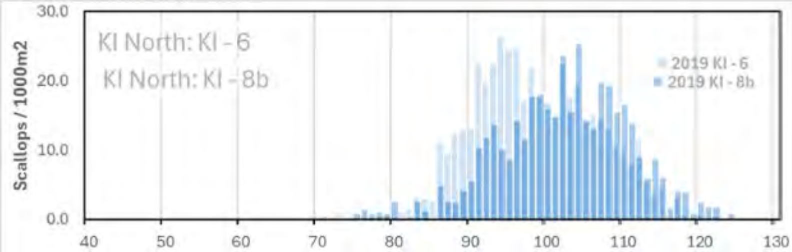

D: 0.207

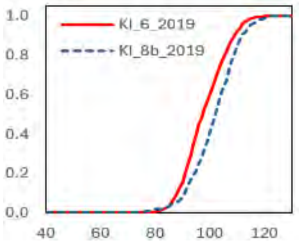

KI_6_2018 - KI_7_2018

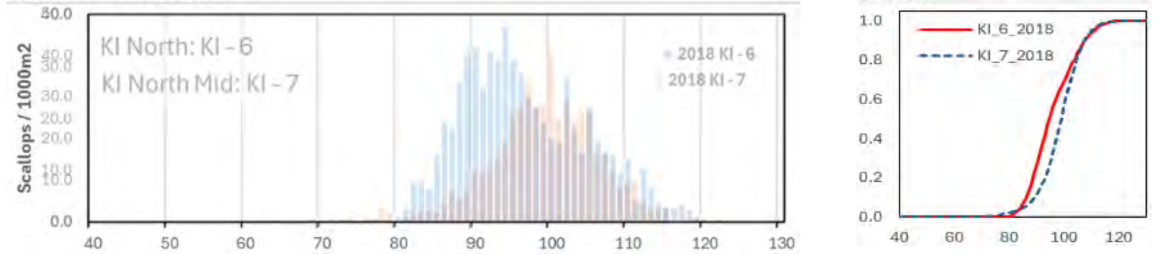

KI_9_2019 - KI_7_2019

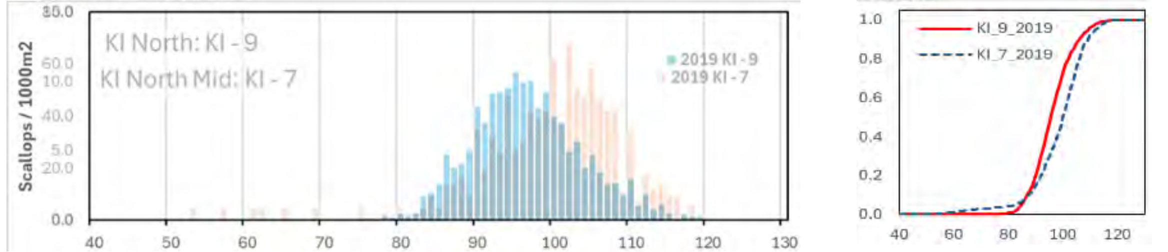

KI_6_2019 - KI_8a_2019

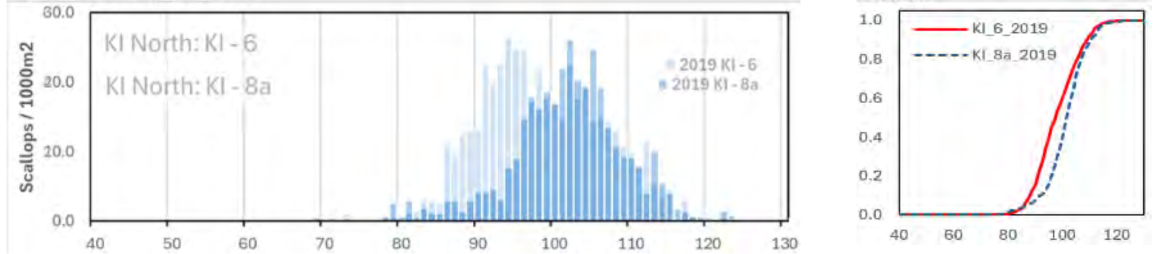

KI_9_2022 - KI_7_2022

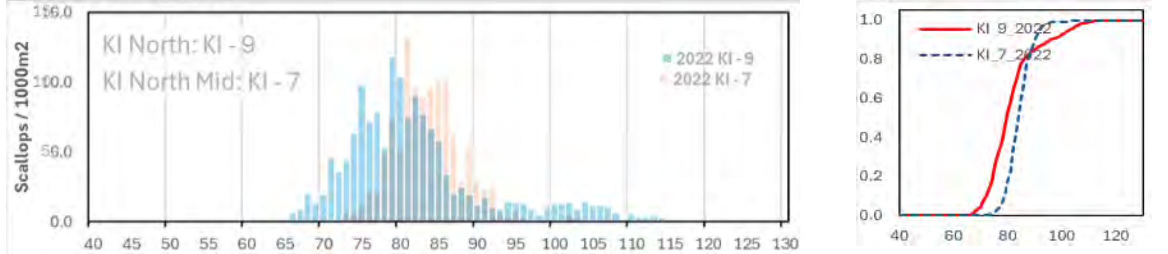

KI_9_2019 - KI_8b_2019

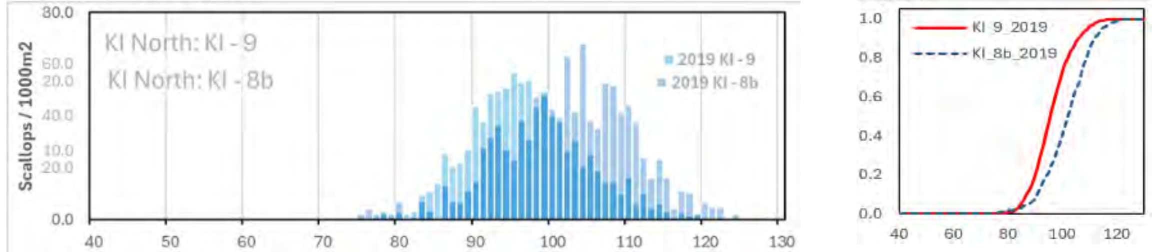

KI_9_2019 - KI_8a_2019

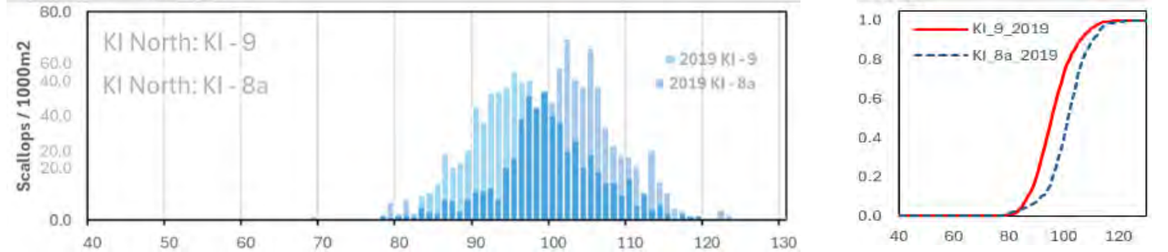

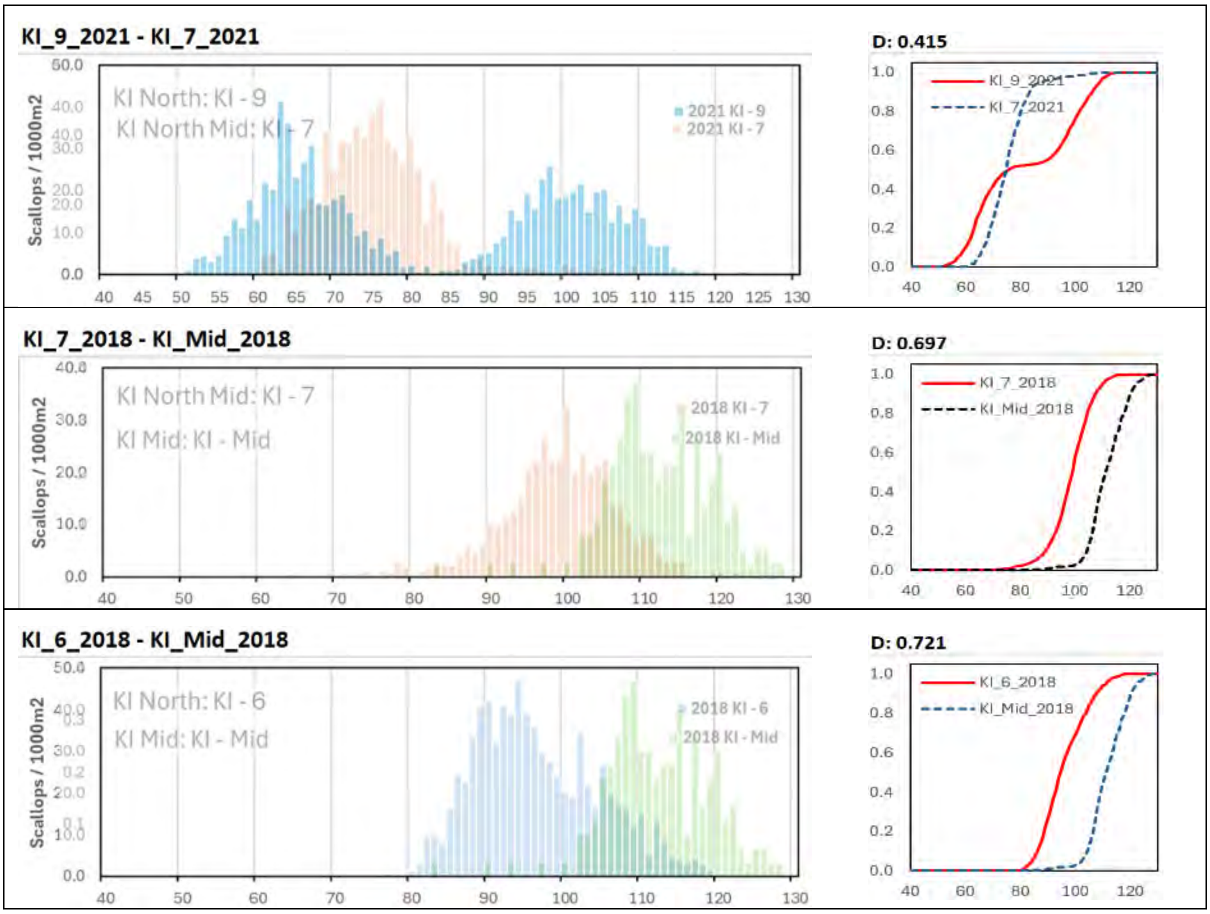
KI_9_2021 - KI_7_2021
KI North: KI - 9
KI North Mid: KI - 7
2021 KI - 9
2021 KI - 7
Scallops / 1000m2
D: 0.415
KI_9_2021
KI_7_2021
KI_7_2018 - KI_Mid_2018
KI North Mid: KI - 7
KI Mid: KI - Mid
2018 KI - 7
2018 KI - Mid
Scallops / 1000m2
D: 0.697
KI_7_2018
KI_Mid_2018
KI_6_2018 - KI_Mid_2018
KI North: KI - 6
KI Mid: KI - Mid
2018 KI - 6
2018 KI - Mid
Scallops / 1000m2
D: 0.721
KI_6_2018
KI_Mid_2018

Region: King Island Main, Mid

KI_2_2016 - KI_Mid_2016

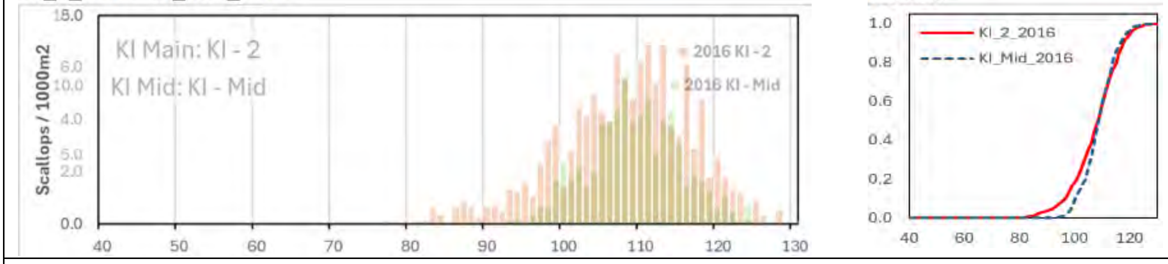

KI_1_2016 - KI_2_2016

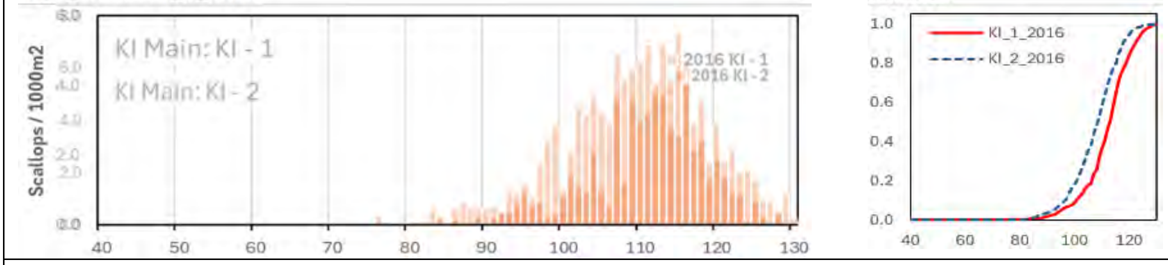

KI_1_2016 - KI_Mid_2016

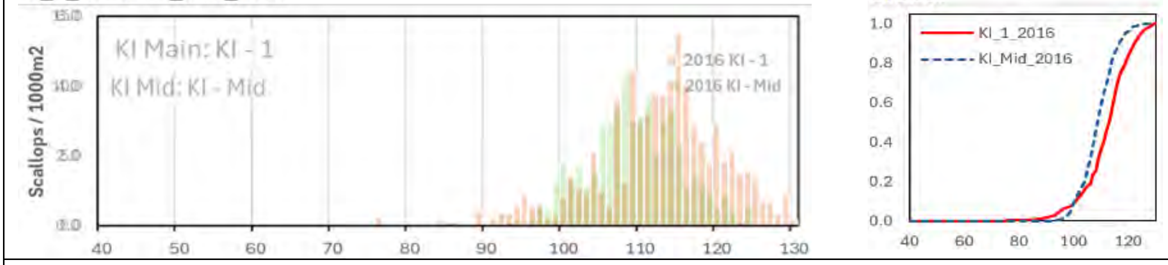

KI_2_2016 - KI_3_2016

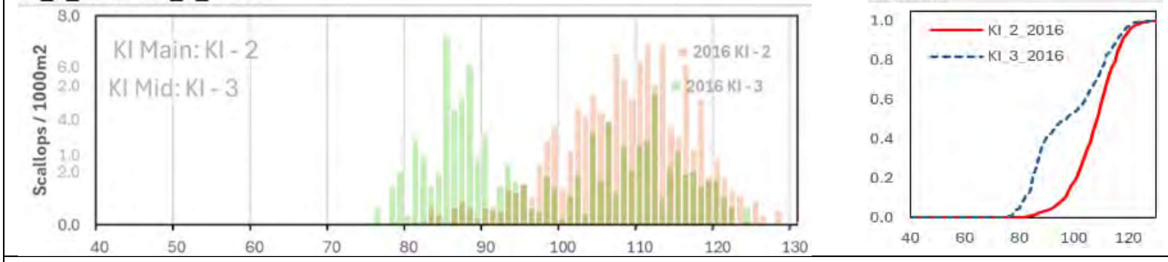

KI_1_2016 - KI_3_2016

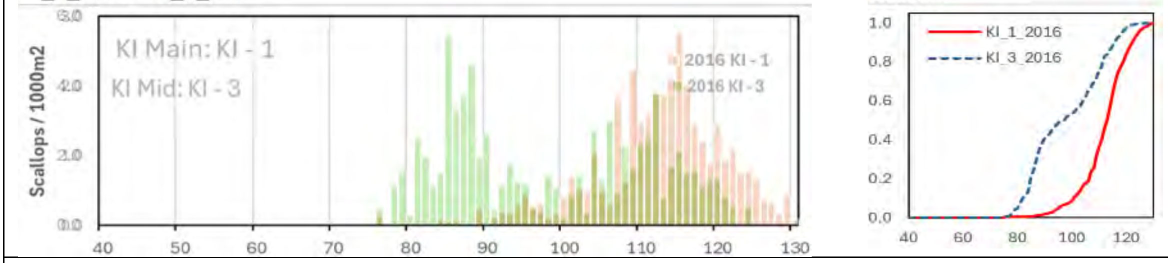

KI_Mid_2016 - KI_3_2016

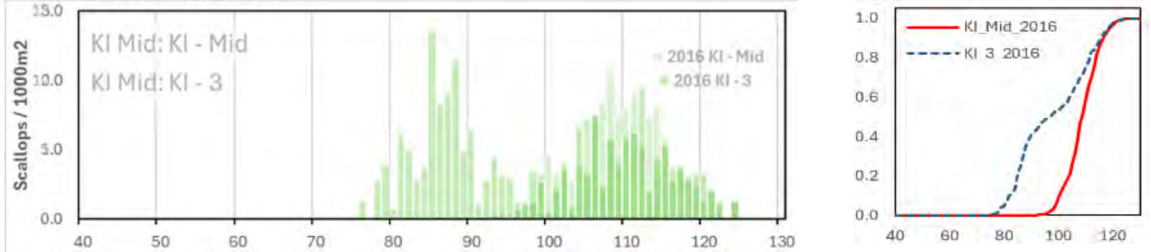

Region: King Island East

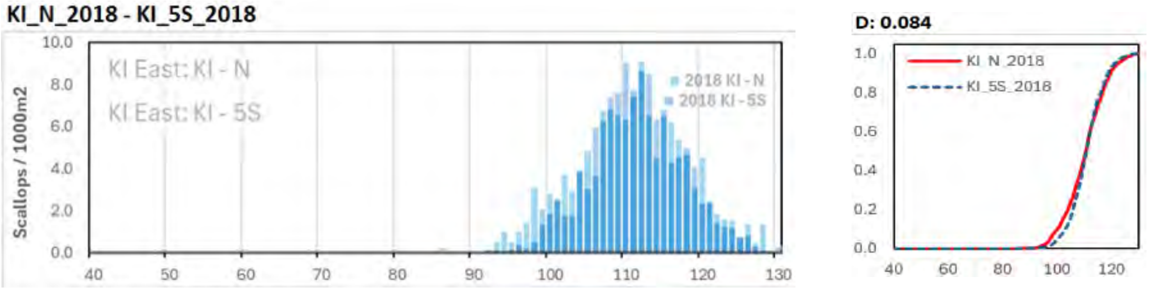

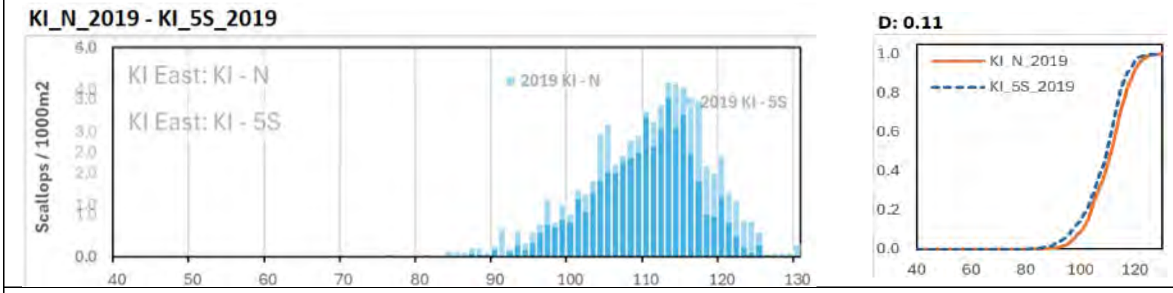

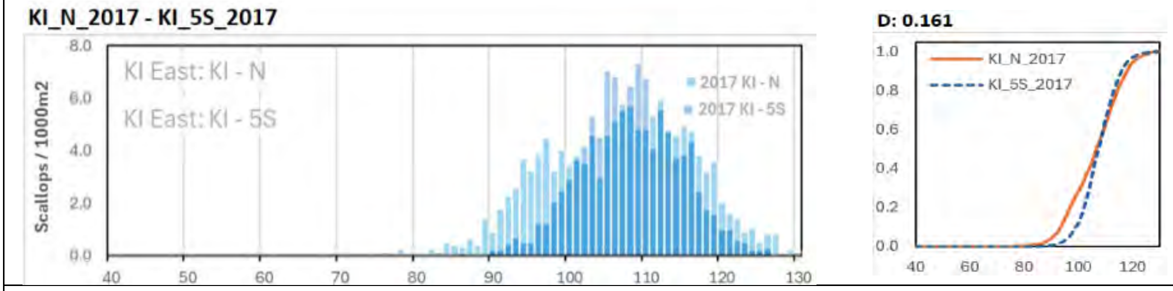

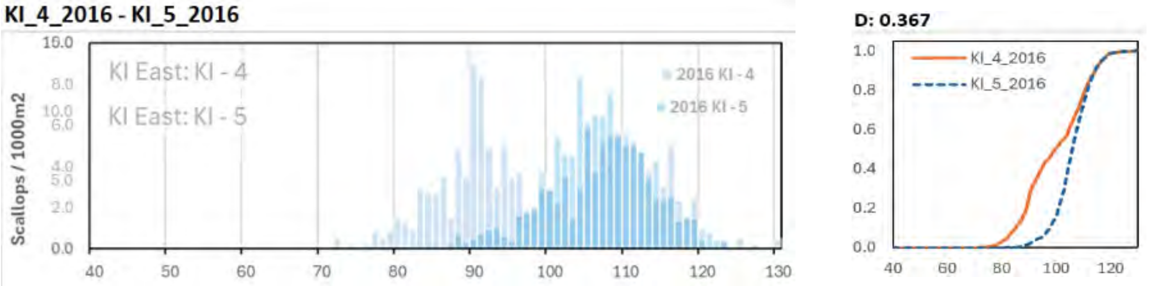

Region: King Island FarEast

KI_10_2023 - KI_THW_2023

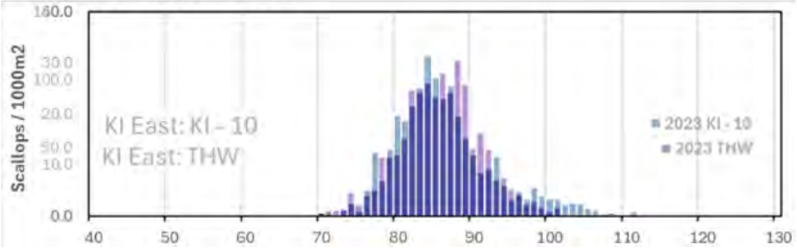

D: 0.06

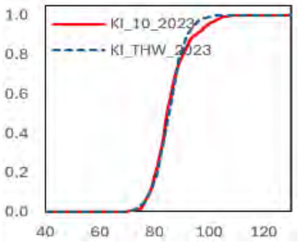

KI_BDSE_2023 - KI_10_2023

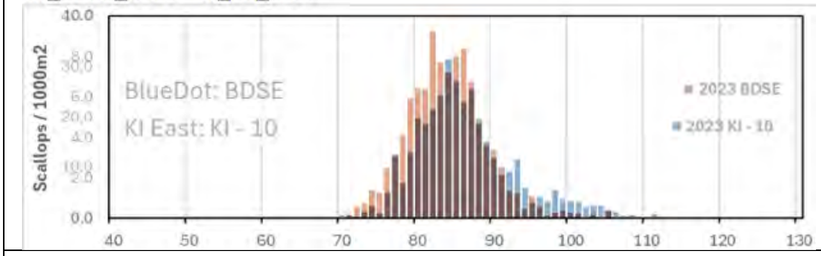

D: 0.133

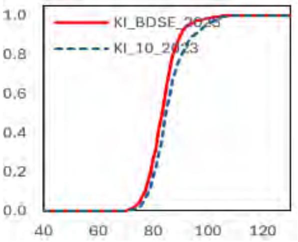

KI_BDSE_2023 - KI_THW_2023

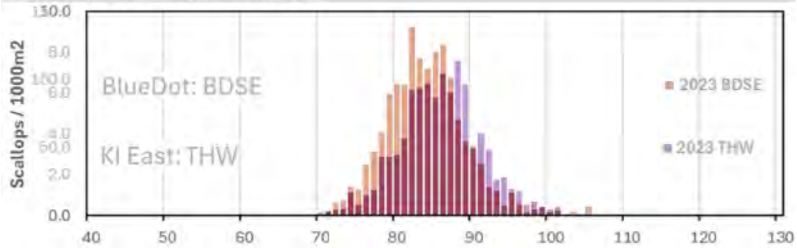

D: 0.165

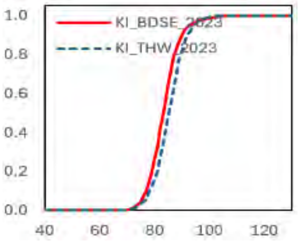

KI_BDE_2022 - KI_10_2022

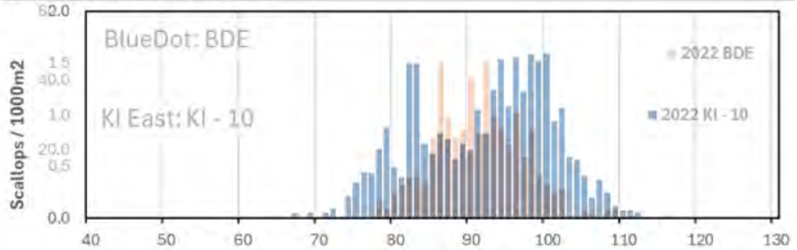

D: 0.177

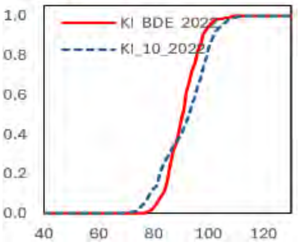

KI_BDSE_2023 - KI_THE_2023

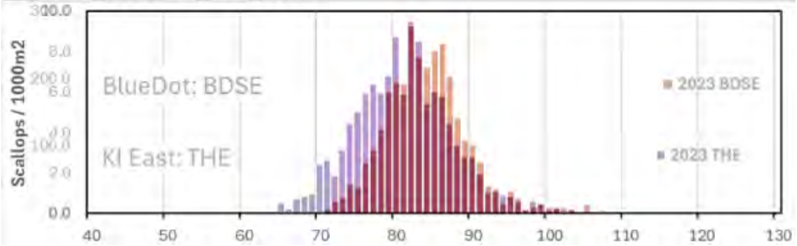

D: 0.211

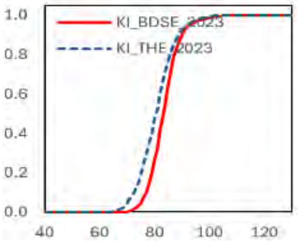

KI_BDE_2019 - KI_BDSE_2019

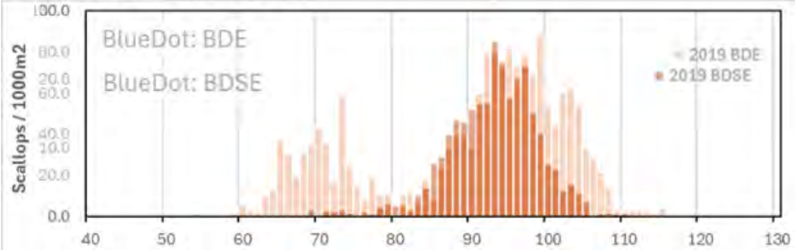

D: 0.223

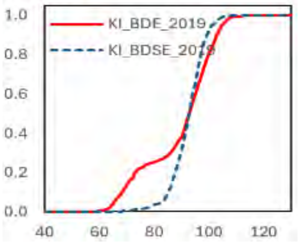

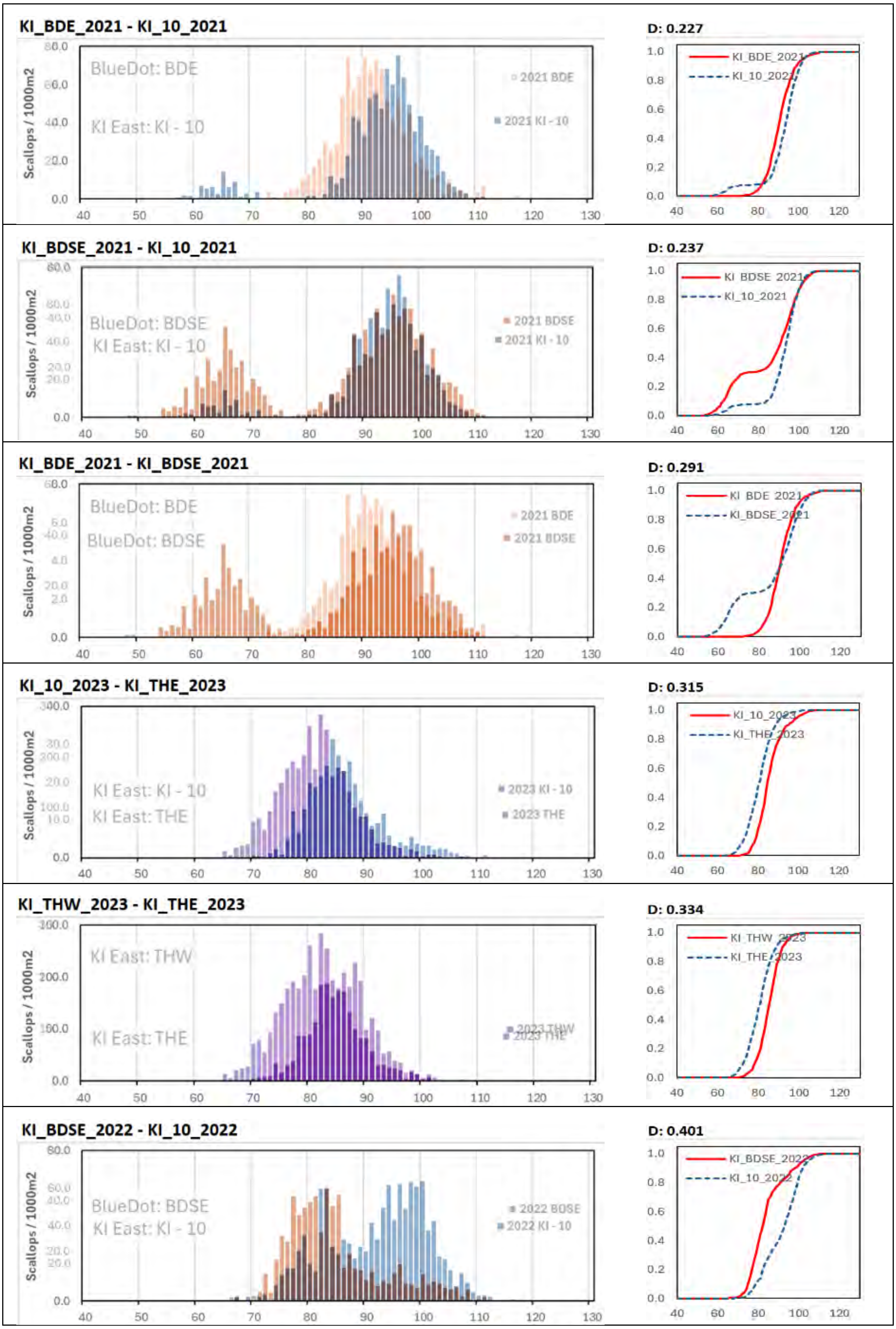
KI_BDE_2021 - KI_10_2021
BlueDot: BDE
KI East: KI - 10
2021 BDE
2021 KI - 10
D: 0.227
KI_BDE_2021
KI_10_2021
KI_BDSE_2021 - KI_10_2021
BlueDot: BDSE
KI East: KI - 10
2021 BDSE
2021 KI - 10
D: 0.237
KI_BDSE_2021
KI_10_2021
KI_BDE_2021 - KI_BDSE_2021
BlueDot: BDE
BlueDot: BDSE
2021 BDE
2021 BDSE
D: 0.291
KI_BDE_2021
KI_BDSE_2021
KI_10_2023 - KI_THE_2023
KI East: KI - 10
KI East: THE
2023 KI - 10
2023 THE
D: 0.315
KI_10_2023
KI_THE_2023
KI_THW_2023 - KI_THE_2023
KI East: THW
KI East: THE
2023 THW
2023 THE
D: 0.334
KI_THW_2023
KI_THE_2023
KI_BDSE_2022 - KI_10_2022
BlueDot: BDSE
KI East: KI - 10
2022 BDSE
2022 KI - 10
D: 0.401
KI_BDSE_2022
KI_10_2022
Scallops / 1000m2
0.0
20.0
40.0
60.0
80.0
100.0
200.0
300.0
40
50
60
70
80
90
100
110
120
130
0.2
0.4
0.6
0.8
1.0

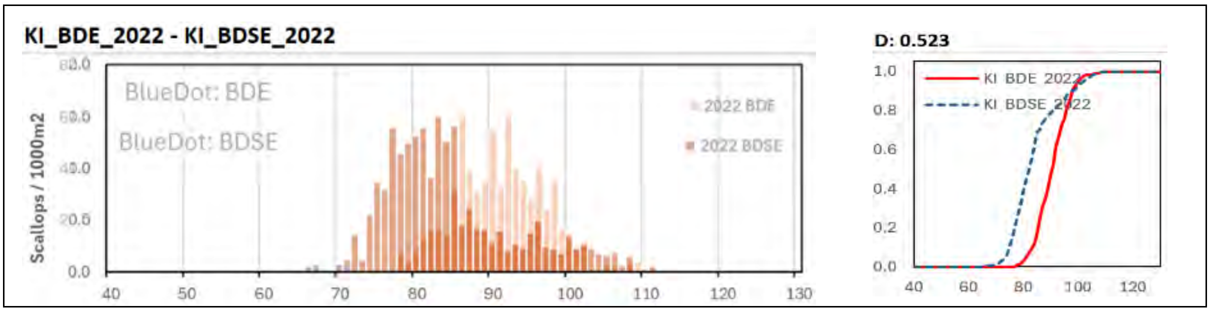
KI_BDE_2022 - KI_BDSE_2022
Scallops / 1000m2
80.0
60.0
40.0
20.0
0.0
BlueDot: BDE
BlueDot: BDSE
2022 BDE
2022 BDSE
40
50
60
70
80
90
100
110
120
130
D: 0.523
1.0
0.8
0.6
0.4
0.2
0.0
KI BDE 2022
KI BDSE 2022
40
60
80
100
120

Region: Flinders Island North

FI_1_2017 - FI_3_2017

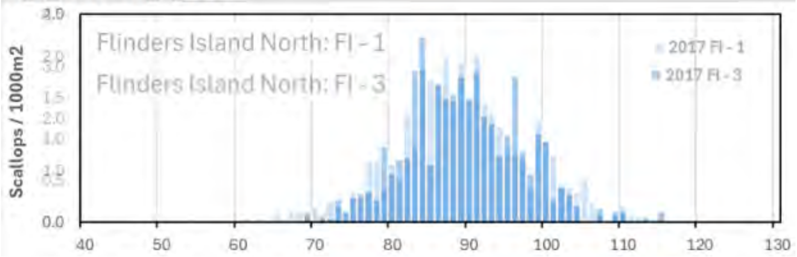

D: 0.045

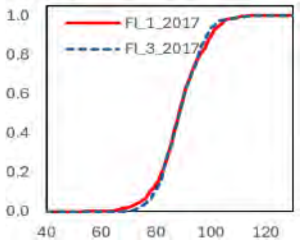

FI_1_2017 - FI_4_2017

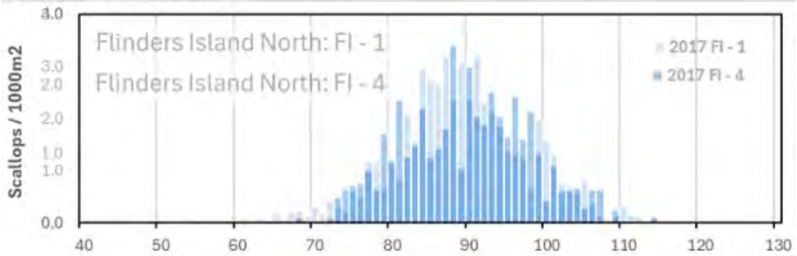

D: 0.061

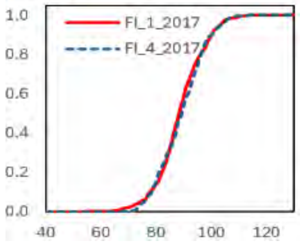

FI_3_2017 - FI_4_2017

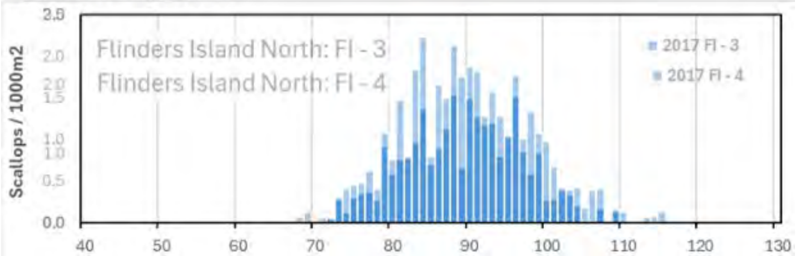

D: 0.062

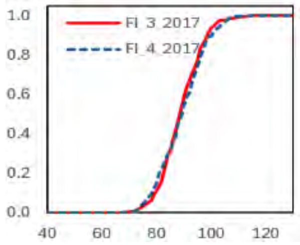

FI_N_TS_2023 - FI_N_TSE_2023

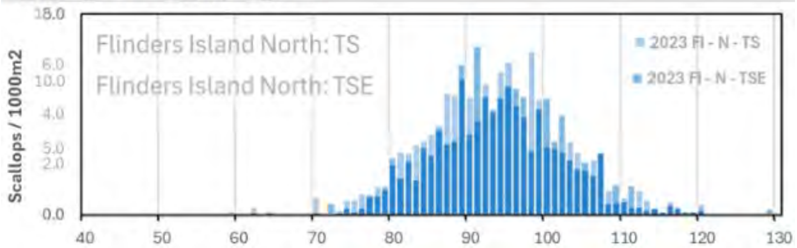

D: 0.065

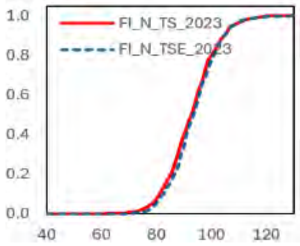

FI_1_2016 - FI_2_2016

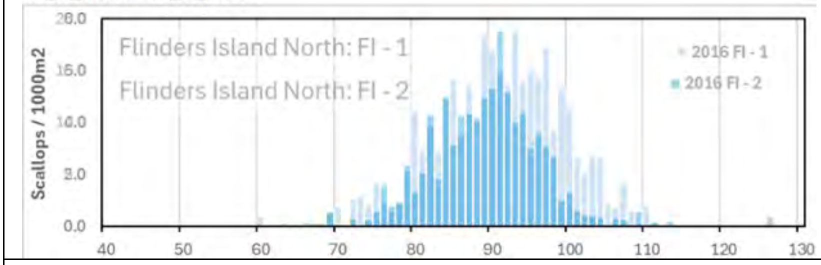

D: 0.143

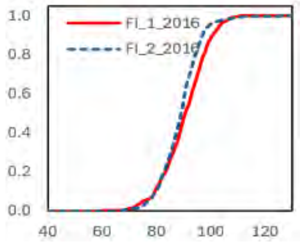

FI_1_2021 - FI_N_TS_2021

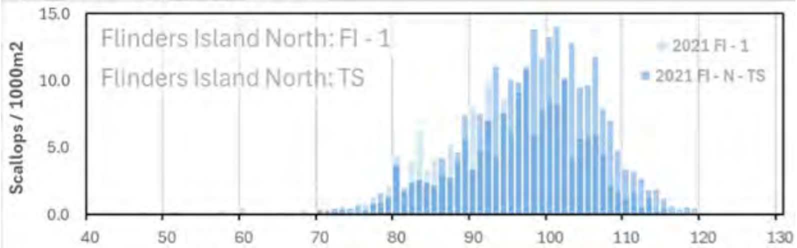

D: 0.164

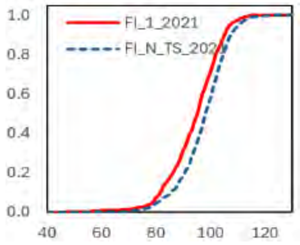

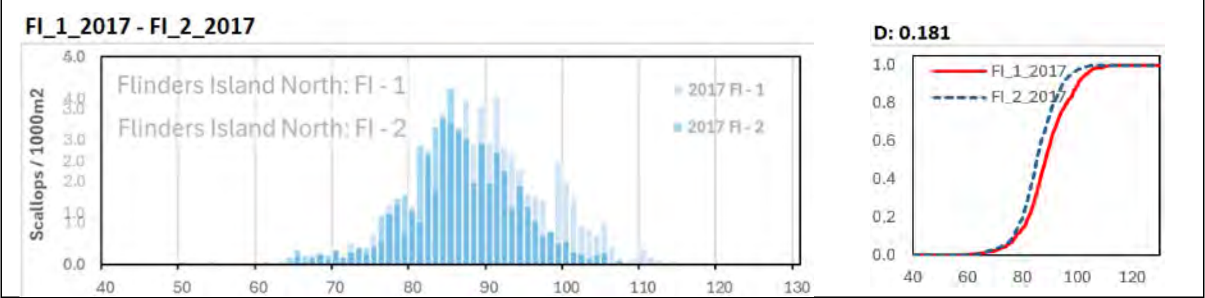

FI_1_2017 - FI_2_2017

D: 0.181

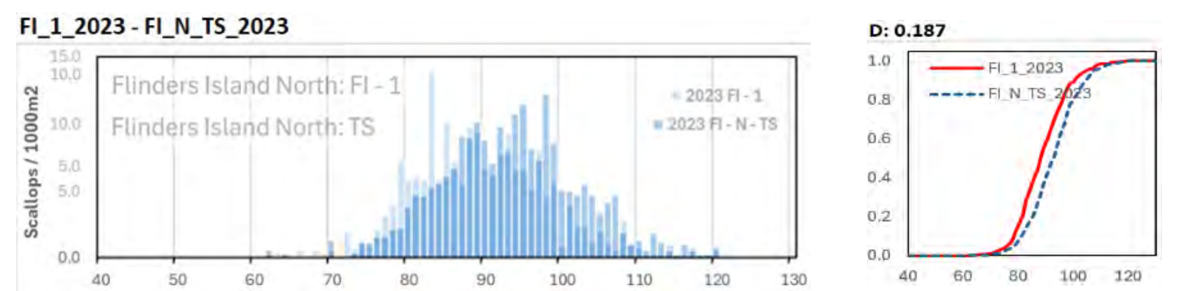

FI_1_2023 - FI_N_TS_2023

D: 0.187

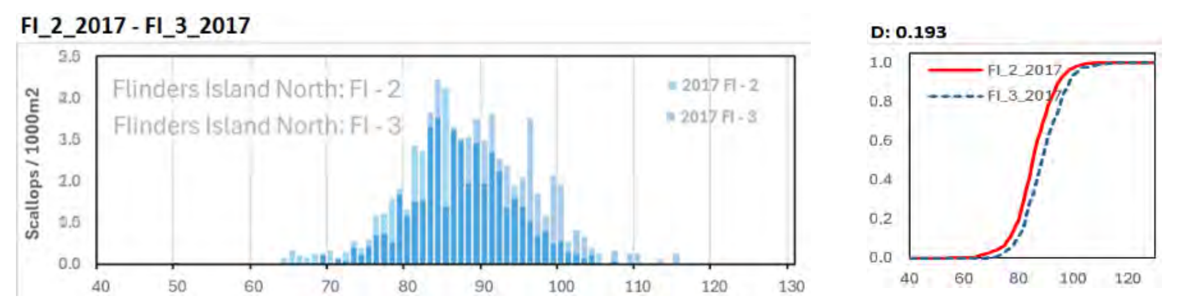

FI_2_2017 - FI_3_2017

D: 0.193

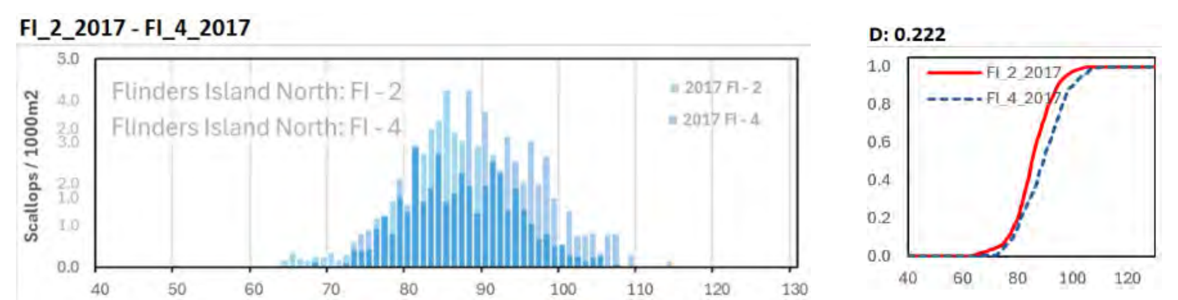

FI_2_2017 - FI_4_2017

D: 0.222

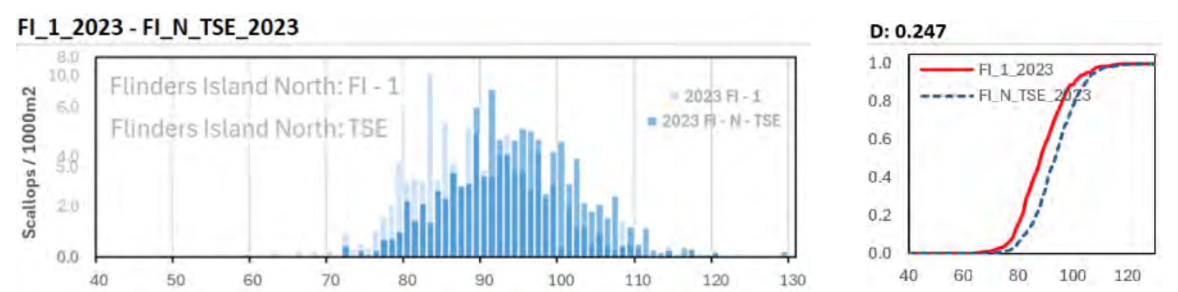

FI_1_2023 - FI_N_TSE_2023

D: 0.247

Region: Flinders Island South

FI_S_NB_2023 - FI_S_TWB_2023

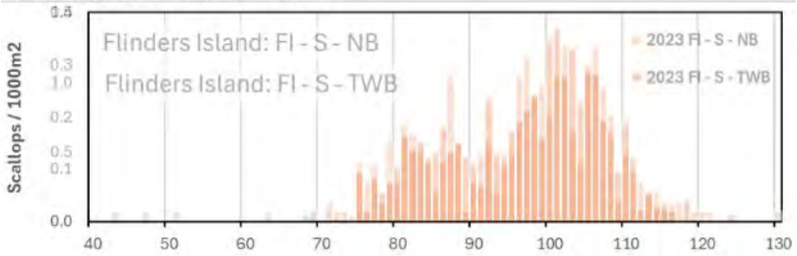

D: 0.043

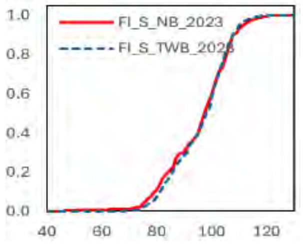

FI_S_TWB_2022 - FI_S_TWA_2023

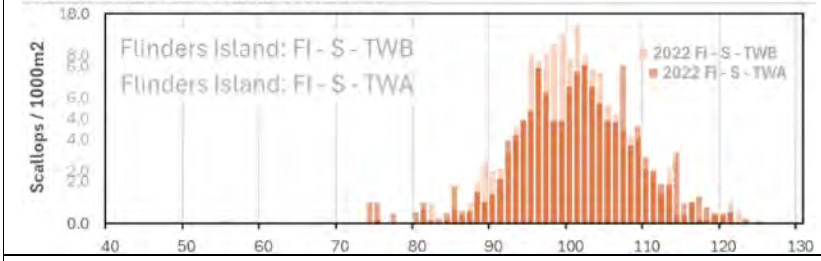

D: 0.074

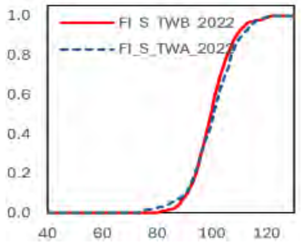

FI_S_TWB_2023 - FI_S_TWA_2023

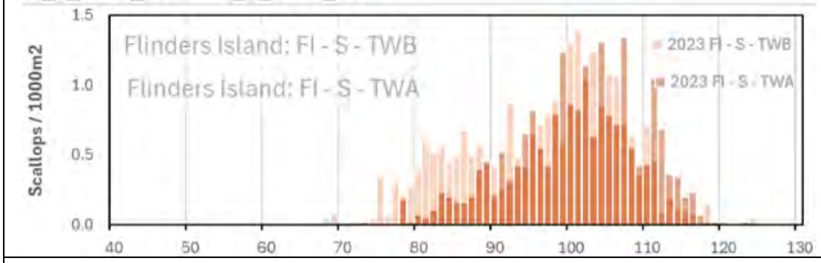

D: 0.172

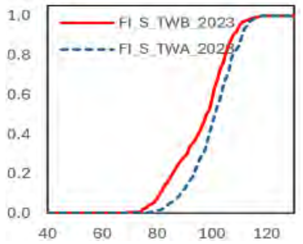

FI_S_NB_2023 - FI_S_TWA_2023

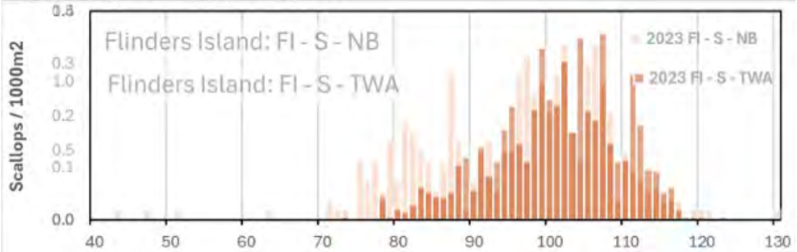

D: 0.202

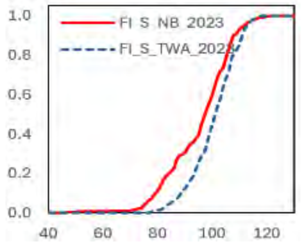

FI_S_NB_2022 - FI_S_TWA_2022

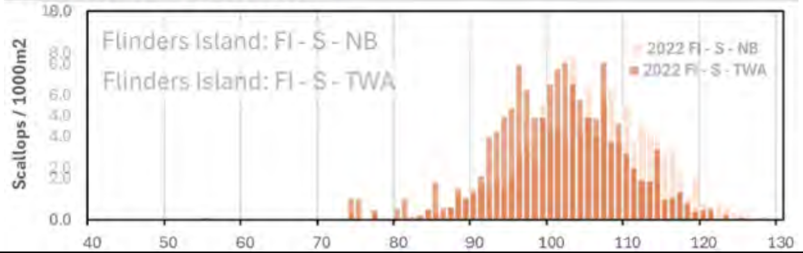

D: 0.216

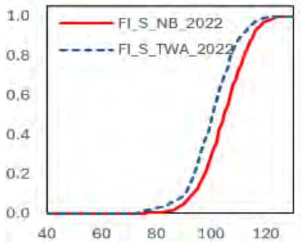

FI_S_NB_2022 - FI_S_TWB_2022

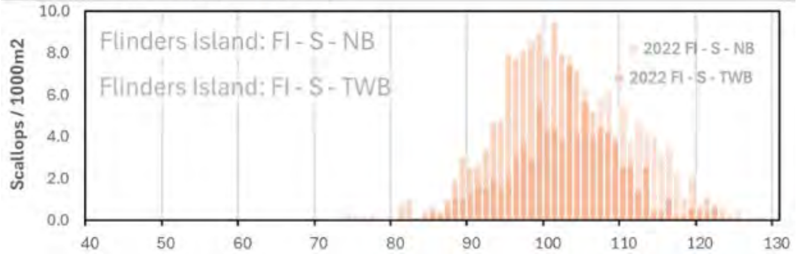

D: 0.28